EDITORIAL: CURRENT ASPECTS IN CHEMOPREVENTIVE STRATEGIES

EDITED BY: Hardeep Singh Tuli, Mukerrem Betul Yerer Aycan and Katrin Sak

PUBLISHED IN: Frontiers in Pharmacology and Frontiers in Oncology

frontiers Research Topics

ISSN 1664-8714
ISBN 978-2-88966-462-7
DOI 10.3389/978-2-88966-462-7

About Frontiers

Frontiers is more than just an open-access publisher of scholarly articles: it is a pioneering approach to the world of academia, radically improving the way scholarly research is managed. The grand vision of Frontiers is a world where all people have an equal opportunity to seek, share and generate knowledge. Frontiers provides immediate and permanent online open access to all its publications, but this alone is not enough to realize our grand goals.

Frontiers Journal Series

The Frontiers Journal Series is a multi-tier and interdisciplinary set of open-access, online journals, promising a paradigm shift from the current review, selection and dissemination processes in academic publishing. All Frontiers journals are driven by researchers for researchers; therefore, they constitute a service to the scholarly community. At the same time, the Frontiers Journal Series operates on a revolutionary invention, the tiered publishing system, initially addressing specific communities of scholars, and gradually climbing up to broader public understanding, thus serving the interests of the lay society, too.

Dedication to Quality

Each Frontiers article is a landmark of the highest quality, thanks to genuinely collaborative interactions between authors and review editors, who include some of the world's best academicians. Research must be certified by peers before entering a stream of knowledge that may eventually reach the public - and shape society; therefore, Frontiers only applies the most rigorous and unbiased reviews.
Frontiers revolutionizes research publishing by freely delivering the most outstanding research, evaluated with no bias from both the academic and social point of view. By applying the most advanced information technologies, Frontiers is catapulting scholarly publishing into a new generation.

What are Frontiers Research Topics?

Frontiers Research Topics are very popular trademarks of the Frontiers Journals Series: they are collections of at least ten articles, all centered on a particular subject. With their unique mix of varied contributions from Original Research to Review Articles, Frontiers Research Topics unify the most influential researchers, the latest key findings and historical advances in a hot research area! Find out more on how to host your own Frontiers Research Topic or contribute to one as an author by contacting the Frontiers Editorial Office: frontiersin.org/about/contact

EDITORIAL: CURRENT ASPECTS IN CHEMOPREVENTIVE STRATEGIES

Topic Editors:
Hardeep Singh Tuli, Maharishi Markandeshwar University, Mullana, India
Mukerrem Betul Yerer Aycan, Erciyes University, Turkey
Katrin Sak, Independent researcher, Estonia

Citation: Tuli, H. S., Aycan, M. B. Y., Sak, K., eds. (2021). Editorial: Current Aspects in Chemopreventive Strategies. Lausanne: Frontiers Media SA.
doi: 10.3389/978-2-88966-462-7

Table of Contents

frontiers in Pharmacology

EDITORIAL
published: 04 January 2021
doi: 10.3389/fphar.2020.607503

Editorial: Current Aspects in Chemopreventive Strategies

Hardeep Singh Tuli[1]*, *Mukerrem Betul Yerer*[2] *and Katrin Sak*[3]

[1]Department of Biotechnology, Maharishi Markandeshwar (Deemed to be University), Ambala, India, [2]Faculty of Pharmacy Department of Pharmacology, Erciyes University Drug Application and Research Center, Erciyes University, Kayseri, Turkey, [3]NGO Praeventio, Tartu, Estonia

Keywords: chemopreventive agents, targeted therapies, personalized medicine, antimutagenic, neoadjuvant therapy

Editorial on the Research Topic

Current Aspects in Chemopreventive Strategies

Despite extensive studies, cancer remains one of the most dreadful diagnoses and biggest challenges for human health all over the world, representing a leading cause of death in the industrialized countries. Various chemotherapeutic drugs, such as Doxorubicin, Tamoxifen and Paclitaxel, have been used for the treatment of tumours for more than half a century; however, there are still no curative options currently available in clinical settings and the severe adverse effects of these drugs threaten the well-being of the patients seriously. Current evidence suggests that further knowledge is urgently needed to clarify the unknown properties and molecular mechanisms of action of various chemopreventive molecules. This special issue attempts to highlight the ongoing advancement in chemopreventive and therapeutical approaches, in the context of cancer prevention and therapy. In particular, the specific objective of this collection was to gather the results of well-designed *in silico*, *in vitro* and *in vivo* preclinical studies, to draw scientists' attention towards precision and personalized medicine in cancer patients by performing targeted therapies. This issue is a collection of eleven articles that have beautifully described chemopreventive approaches with strong therapeutic applications. In this special issue you can find some papers on novel drugs such as a new class of magnetite (Fe3O4) particles, coined as "Single Crystalline Micrometric Iron Oxide Particles" (SCMIOPs), which is obtained by hydrothermal synthesis and were tested for their cytotoxic effects on different melanoma types. Furthermore, you can find the results of *in vitro* antitumor activity of some novel styryllactones, a class of compounds obtained from the genus Goniothalamus (Annonaceae). In addition to these novel compound studies with anticancer activity, on the basis of personalized medicine applications Liu et al has conducted a meta-analyses to determine the association between genetic polymorphisms and platinum-induced toxicity which summarizes the pharmacogenomic reports that focused on commonly reported platinum.

Additionally, our Italian colleagues supervised by Dr. Lenzi clearly demonstrated the antimutagenic activities of a natural bioactive compound, 6-MITC, on human lymphoblastic cells. An interesting paper of Calcabrini et al reported the chemopotentiation of two frequently used conventional drugs, Doxorubicin and Cisplatin, by a well-known phytochemical sulforaphane, presenting a possibility to mitigate the toxicity associated with the use of these chemotherapeutics. Moreover, the team of Yu et al demonstrated the antimetastatic effects of metapristone on breast cancer cells co-incubated with HPMEC, by interfering with the adhesion-invasion processes. With prospects to be translated in clinical practice in the future, Desai et al thoroughly summarized the recent advancements of nanotechnology-based chemopreventive strategies. Last but not least, the Indian clinical oncologists presented in their contribution a strong basis for further developing the Indian guidelines to prevent and manage chemotherapy-induced nausea and

OPEN ACCESS

Edited and reviewed by:
Heike Wulff,
University of California, Davis,
United States

****Correspondence:***
Hardeep Singh Tuli
hardeep.biotech@gmail.com

Specialty section:
This article was submitted to Pharmacology of Anti-Cancer Drugs, a section of the journal Frontiers in Pharmacology

Received: *17 September 2020*
Accepted: *30 November 2020*
Published: *04 January 2021*

Citation:
Tuli HS, Yerer MB and Sak K (2021) Editorial: Current Aspects in Chemopreventive Strategies. Front. Pharmacol. 11:607503. doi: 10.3389/fphar.2020.607503

vomiting. Bhatia et al. conducted a study to reveal the antioxidant potential and DNA protective abilities of *R. cinerea*. In addition, antiproliferative and apoptosis induction potential against immortalized L6 cell line have also discussed by the authors. In another study, Chan et al. suggested the potential of HLJDD as a neoadjuvant therapy to minimize chemo toxicity effects by reducing diarrhoea and improving tumour response. A review on anticancer potential of BC and its components to treat gastrointestinal diseases and distinctive cancer types, is another highlight of this special issue. We hope that you all will enjoy the reading of this thematic issue on **"Current Aspects in Chemopreventive Strategies"** from Frontiers in Pharmacology.

AUTHOR CONTRIBUTIONS

All authors listed have made a substantial, direct, and intellectual contribution to the work and approved it for publication.

Conflict of Interest: The authors declare that the research was conducted in the absence of any commercial or financial relationships that could be construed as a potential conflict of interest.

frontiers in Pharmacology

ORIGINAL RESEARCH
published: 20 November 2019
doi: 10.3389/fphar.2019.01296

RU486 Metabolite Inhibits CCN1/Cyr61 Secretion by MDA-MB-231-Endothelial Adhesion

Suhong Yu[1†], Cuicui Yan[1†], Wenjing Wu[1], Sudan He[1], Min Liu[1], Jian Liu[1], Xingtian Yang[1], Ji Ma[1], Yusheng Lu[2] and Lee Jia[1,2]*

[1] Cancer Metastasis Alert and Prevention Center, and Biopharmaceutical Photocatalysis of State Key Laboratory of Photocatalysis on Energy and Environment, College of Chemistry, Fujian Provincial Key Laboratory of Cancer Metastasis Chemoprevention and Chemotherapy, Fuzhou University, Fuzhou, China, [2] Institute of Oceanography, Minjiang University, Fuzhou, China

Successful adhesion of circulating tumor cells (CTCs) to microvascular endothelium of distant metastatic tissue is the key starting step of metastatic cascade that could be effectively chemoprevented as we demonstrated previously. Here, we hypothesize that the hetero-adhesion may produce secretory biomarkers that may be important for both premetastatic diagnosis and chemoprevention. We show that co-incubation of triple-negative breast cancer (TNBC) cell line MDA-MB-231 with human pulmonary microvascular endothelial monolayers (HPMEC) secretes Cyr61 (CCN1), primarily from MDA-MB-231. However, addition of metapristone (RU486 metabolite) to the co-incubation system inhibits Cyr61 secretion probably *via* the Cyr61/integrin $\alpha v\beta 1$ signaling pathway without significant cytotoxicity on both MDA-MB-231 and HPMEC. Transfection of MDA-MB-231 with Cyr61-related recombinant plasmid or siRNA enhances or reduces Cyr61 expression, accordingly. The transfection significantly changes hetero-adhesion and migration of MDA-MB-231, and the changed bioactivities by overexpressed CYR61 could be antagonized by metapristone *in vitro*. Moreover, the circulating MDA-MB-231 develops lung metastasis in mice, which could be effectively prevented by oral metapristone without significant toxicity. The present study, for the first time, demonstrates that co-incubation of MDA-MB-231 with HPMEC secrets CYR61 probably *via* the CYR61/integrin $\alpha_v\beta_1$ signaling pathway to promote adhesion-invasion of TNBC (early metastatic step). Metapristone, by interfering the adhesion-invasion process, prevents metastasis from happening.

Keywords: MDA-MB-231/HPMEC co-culture, metapristone, CYR61, integrin $\alpha_v\beta_1$, metastasis chemoprevention

OPEN ACCESS

Edited by:
Katrin Sak,
NGO Praeventio, Estonia

Reviewed by:
Srinivas V. Koduru,
Penn State Milton S. Hershey Medical Center, United States
Qiyang Shou,
Zhejiang Chinese Medical University, China

****Correspondence:***
Lee Jia
cmapcjia1234@163.com

†These authors have contributed equally to this work

Specialty section:
This article was submitted to Pharmacology of Anti-Cancer Drugs, a section of the journal Frontiers in Pharmacology

Received: *01 August 2019*
Accepted: *10 October 2019*
Published: *20 November 2019*

Citation:
Yu S, Yan C, Wu W, He S, Liu M, Liu J, Yang X, Ma J, Lu Y and Jia L (2019) RU486 Metabolite Inhibits CCN1/Cyr61 Secretion by MDA-MB-231-Endothelial Adhesion. Front. Pharmacol. 10:1296. doi: 10.3389/fphar.2019.01296

INTRODUCTION

Breast cancer is the most common cancer and the leading cause of related death among females worldwide (Akram et al., 2017; Barrios et al., 2018). Triple-negative breast cancer (TNBC) represents about 15% of all breast cancers and is largely refractory to current available therapies (Wein and Loi, 2017). Therefore, identifying biomarkers responsible for TNBC, and developing a novel cancer metastasis chemopreventive agent is critical for alternative breast cancer treatment approaches. Metastasis is a frequent occurrence in TNBC. The most important step in metastasis

is the migration of cancer cells away from the primary tumor, and then adhesion to the endothelial cells, a process called tumor invasion (Valastyan and Weinberg, 2011). Studies indicate that the migration and invasion of pathogenesis of tumor cells depend on cross-communications between tumor cells and various endothelial cells residing in their microenvironment (Rodvold and Zanetti, 2016; Lambert et al., 2017). For example, several growth factors signaling pathways, secreted proteins or micro RNAs (miRNAs) and exosomes are functional mediators of tumor-endothelial interactions in metastasis (Miller and Grunewald, 2015; Yu et al., 2015a; Yu et al., 2015b; Zeng et al., 2018). However, the way invasive cancer cells diminish the endothelial barrier function still remains elusive.

Cysteine-rich protein 61 (CCN1/Cyr61), cysteine-rich, heparin-binding extracellular matrix-associated protein, is the first cloned member of cysteine-rich protein (CCN) family which includes connective tissue growth factor (CTGF, CCN2), nephroblastoma over-expressed protein (Nov, CCN3), Wnt-1-induced secreted protein 1 (WISP-1, CCN4), WISP-2 (CCN5) and WISP-3 (CCN6) (Lin et al., 2012; Jandova et al., 2012). As a secreted protein, Cyr61 connects with the extracellular matrix and the cell surface (Grzeszkiewicz et al., 2002) and is a communication media between cancer cells and the host which can reflect the changes arising due to cancer treatment (Bonin-Debs et al., 2004; Mbeunkui et al., 2006). The Cyr61 protein has been reported to mediate cell adhesion, stimulate chemostasis, augment growth factor-induced DNA synthesis, foster cell survival, and enhance angiogenesis (Hou et al., 2014). Overexpression of Cyr61 enhanced the growth and migration of glioma cells through activation of the ILK-mediated-catenin-TCF/Lef and the Akt signaling pathways (Wu et al., 2017). Silencing Cyr61 in invasive breast cancer cells caused a major loss of MMP-1 induction from stromal fibroblasts and inhibited the tumorigenicity of breast cancer cells (Nguyen et al., 2006). Researchers showed that Cyr61 can activate biochemical signal transduction through interacting with various integrins (Crockett et al., 2007; Su et al., 2010). While binding of integrin $\alpha_v\beta_3$ triggered cell adhesion and apoptosis, binding of integrin $\alpha_6\beta_1$ induced senescence, and binding of integrin $\alpha_v\beta_5$ affected migration (Crockett et al., 2010; Lau, 2011). These reports indicated that the conformation of Cyr61 and integrins may play a vital role in metastasis.

Metapristone is the most predominant biological active metabolite of mifepristone (Heikinheimo et al., 1989; Teng et al., 2011), which has received considerable attention due to its anticancer activity in the recent years. Metapristone was developed as a novel cancer metastasis chemopreventive agent by us for its per-metastatic chemoprevention. In our previous studies, metapristone induced dose-dependent apoptosis, and interfered with adhesion of HT-29 cells to human umbilical vein endothelial cells (HUVECs) *in vitro* (Wang et al., 2014). Moreover, our studies demonstrated that metapristone inhibited TNBC cells migration and adhesion to endothelial cells through intervening the EMT-related signaling pathways (Yu et al., 2016). Inspired by our previous studies, we hypothesize that the anti-metastasis potential of metapristone is related with the bidirectional cross-talk between endothelial and tumor cells.

To test the hypothesis, we examined the effects of endothelial cells (HPMEC) on the aggressive phenotype of breast cancer cells (MDA-MB-231) using an *in vitro* co-culture system. We observed that the co-culture of HPMEC with MDA-MB-231 increased the expression of Cyr61 (CCN1), and the formation of Cyr61/integrin $\alpha_v\beta_1$ complex. This highlights an important contact in cell communication between malignant breast epithelial cells and the endothelium. This study also supports our hypothesis and reveals a novel function for metapristone in the prevention of breast cancer metastasis by intervening Cyr61/integrin $\alpha_v\beta_1$ signaling pathways. The study report is as follows.

MATERIALS AND METHODS

Materials

Anti-Cyr61, Anti-ITGAV, Anti-ITGB1, and goat Anti-Rabbit lgG H&L were from Abcam. Human recombinant Cyr61 was obtained from GeneTex. SiRNA-Cyr61 and negative control siRNA were purchased from Sangon Biotech (Shanghai). Pierce Co-Immunoprecipitation (Co-IP) Kit (26149) was purchased from Thermo scientific. The recombinant plasmid of pcDNA3.1-Cyr61 was constructed by our lab.

Cell Culture

MDA-MB-231 cells were obtained from American Type Culture Collection (ATCC, Manassas, VA), and were incubated with Leibovitz's L-15 medium (Catalog No. 30-2008) containing 10% FBS, 100 U/ml penicillin and 100 μg/ml streptomycin at 37 °C in a free gas exchange with atmospheric air. MCF-7 cells were purchased from the national experimental cell resource sharing service platform (Beijing) and cultured in RPMI-1640 medium with 10% FBS, 100 U/ml penicillin, and 100 μg/ml streptomycin. Human pulmonary microvascular endothelial cells (HPMEC) were purchased from PromoCell, and cultured in ECM with 10% FBS, 100 U/ml penicillin, and 100 μg/ml streptomycin at 37 °C in 5% CO_2 atmosphere.

In Vitro Cytotoxicity Studies

The *in vitro* cytotoxicity was determined as what we described previously (Lau, 2011; Shi et al., 1993). MDA-MB-231 cells were trypsinized and seeded on 96-well plates at 8×10^3 cells/well. After adhering of 24 h, doses of metapristone (0,10,25,50,75,100 μM) were added and incubated for another 12 and 24 h respectively. Then, 100 μl/well MTT (5 mg/ml) was added and incubated for 4 h in incubator. The MTT solution was aspirated and replaced with 100 μl/well dimethyl sulfoxide solution (DMSO). After shaking 10 to 30 min, the plates were measured at 570 nm using an infinite M200 Pro microplate reader (Tecan, Switzerland).

Co-Culture Model and iTRAQ Analysis

Metastasis, a process that cancer cells invade surrounding tissues and migrate to distal organs including lung, liver, brain, bone, and lymph nodes, is a major cause of mortality in breast cancer patients (Torre et al., 2015), and adhering to the vascular

endothelium is a key step when this process starts (Dotan et al., 2009). Thus, in this study, we used *co-culture* model to stimulate the tumor microenvironment *in vitro*. HPMEC cells were seeded in 75 cm flasks with complete ECM culture. After overnight adhesion, MDA-MB-231 cells (1:2) were plated into the same flasks with serum-free and metapristone (50 μM). Then the flasks were incubated another 24 h. Each group of serum-free ECM culture media was incubated for iTRAQ analysis. The procedures for iTRAQ and further analysis are described as these labs previously (Adav et al., 2010; Yu et al., 2015a; Yu et al., 2015b).

Elisa Assay

Enzyme-linked immunosorbent assay (ELISA) was used to investigate the secretion levels of Cyr61 at different conditions. Concentrations of Cyr61 from each group were measured quantitatively using a sandwich ELISA as described (Adav et al., 2010). Briefly, 96-Well ELISA plates were coated with mouse anti-human Cyr61 (ab80112) and stored overnight at 4°C. After three washes in PBST, wells were blocked with 1% BSA in PBS-T for 2 h at room temperature. Next, the serum-free medium was added to duplicate wells and human recombination Cyr61 (GTX48189-PRO) protein was diluted into different concentrations with PBS as the standard. Simultaneously, an additional set of wells were coated with blank buffer to serve as a control. Then plates were incubated at 37°C for 2 h and followed by three washed in PBS-T, respectively. A rabbit anti-human Cyr61 mAb (Santa Cruz Biotechnology, sc-13100) was added and incubated at 37°C for 2 additional h. After washing, alkaline phosphatase-conjugated goat anti-rabbit IgG antibodies were added for 2 additional h, then 2 M sodium hydroxide solution were used for color development. Concentrations of Cyr61 were determined by detecting the absorbance at 405 nm using an infinite M200 Pro microquant plate reader (Tecan, Switzerland). Each test was repeated at least three times.

Cell Morphology Assay

5×10^4 HPMEC cells were cultured in a 35 mm cell culture dish (NEST, GBD-35-20) for 12 h and then co-cultured with 2.5×10^4 MDA-MB-231 cells with or without metapristone (50 μM). This system was taken for a time-lapse photography by the Leica TCS SP8 confocal microscope.

Plasmid Construction, siRNAs Synthesis, and Transient Transfection

The ORF of the human Cyr61 cDNA was amplified by RT-PCR using specific primers (sense, 5`-taa aag ctt atg agc tcc cgc atc gcc ag-3` and antisense, 5`-ccc ctc gag tta gtc cct aaa ttt gtg aat gtc-3`) that were designed based on the Cyr61 gene (GenBank ID: CR536519.1) by Takara (Shiga, Japan). The gel-purified PCR products were digested with the restriction enzymes, HindIII and XhoI (Takara, Dalian, China), and cloned into the eukaryotic expression vector, pcDNA3.1 (Invitrogen, American). The inserted sequence was confirmed by DNA sequencing.

According to the design rule for RNAi (Laganà et al., 2015), a fragment of Cyr61 gene (5`-AACAUCAGUGCACAUGTAUUG-3`) was used as the target siRNA (Cyr61-siRNA). As control, the sequence of Cyr61 siRNA was rearranged at random (5`-CAAUACAUGUGCACUGAUGUU-3`) to yield the corresponding random-siRNA (ram-siRNA). siRNAs were synthesized by Sangon Biotech Corporation (Shanghai, China).

Transient transfection of MDA-MB-231 cells with siRNA oligos (100 pmol) and recombinant plasmid pcDNA3.1-Cyr61 (4 μg/well) was carried out using Lipofectamineeq \o\ac(○,R)3000 Transfection Reagent Protocol (life technologies), according to the manufacturer's instructions. Both of nontargeting siRNA and empty pcDNA3.1 vector were served as negative controls, respectively. These cells were harvested 24 h after transfection and used for further analysis.

Cell Adhesion Assay

The adhesion assay of MDA-MB-231 cells to the HPMECs was assessed according to the method described previously by this lab (Yu et al., 2015; Yu et al., 2016). Briefly, HPMECs were seeded in 24-well plates and grown to 90% confluence in the ECM medium. Then, TNF-α (final concentration: 10 ng/ml) was used to activate HPMECs for 4 h. Rhodamine 123-labled MDA-MB-231 cells were washed twice using PBS and resuspended by ECM medium with a dose of metapristone, and co-cultured with the HPMEC monlayers (1:8) in each well for 2 h. DMSO (0.1%) was used as the vehicle control. Then, nonadherent cells were removed by PBS and ten visual fields for each well were selected randomly and taken pictures using a fluorescence microscope (Zeiss, Germany). Mean inhibition of adhesion for 10 visual fields was calculated by using the equation: % of control adhesion = [the number of adhered cells in treated group/the number of adhered cells in the control group] × 100%.

Wound Healing Assay

MDA-MB-231 cells were seeded in 24-well plates with 5×10^4/ml cells in complete medium and were reached over 90% confluence. The scratch wound was generated by using a pipette tip, and the floating cells were removed through washing with PBS. Then the PBS was instead by L-15 with different concentrations of metapristone (0, 10, 50, 75 μM) and the wound healing was recorded by using a fluorescence microscope (Zeiss, Germany) at 0 and 24 h. DMSO (final concentration: 0.1%) as vehicle control was added after wounding. At indicated time points, motility was quantified by measuring the average extent of wound closure. Each sample was assayed in triplicate in three independent experiments.

RNA Extraction and Real-Time PCR

MDA-MB-231 cells (6×10^5) were seeded in complete L-15 medium in 6-well plates and incubated over 24 h. Then, the medium was renewed with L-15 in the presence of metapristone (0, 10, 50, 75 μM). After incubation of 24 h, total RNA was exacted with Trizol reagent (Invitrogen, American) according to the manufacturer's protocol and 4 μg RNA was converted to cDNA using PrimeScript™ RT reagent kit (TaKaRa, Dalian, China). The housekeeping gene, β-actin served as the internal control. Each

real-time PCR reaction contained SYBRR) Premx Ex Taq II (Tli RNaseH Plus), PCR Forward/Reverse Primer, cDNA solution and dH_2O. All PCR reactions were performed in triplicate using the mean value being used to determine mRNA levels. Relative mRNA expression levels for each gene were analyzed using the $2^{-\Delta\Delta Ct}$ method and normalized to the endogenous reference gene β-actin.

The main primers were as follows:

β-actin:
F: 5`-TGGCACCCAGCACAATGAA-3`
R: 5`-CTAAGTCATAGTCCGCCTAGAAGCA-3`
integrin αv
F: 5`-TTGTAAGTTGGCAGATCTTCCTAAGTT-3`
R: 5`-GATGGGTAGTGGCTGCACATAG-3`
integrin β1:
F: 5`-AATTGTGGGTGGTGCACAAAT-3`
R: 5`-TGGAGGGCAACCCTTCTTTT-3`
Cyr61:
F: 5`-TCT CGT TGC TCA TGA AATT-3`
R: 5`-TAG AGT GGG TAC ATC AAA GCT TCAG-3`

Western Blot Analysis

MDA-MB-231 cells cultured in the present of metapristone (0, 10, 50, 75 μM) were lysed by RIPA. Then, the lysates were supplemented with HALT protease and phosphatase inhibitor cocktail (Thermo Scientific). Antibodies used for western blot analysis include Cyr61, integrin α_v, integrin β_1, and β-actin. Immunodetection of electrophoresis-resolved proteins was accomplished using enhanced chemiluminescence based on standard protocols, and signals were quantified with a quantitative digital imaging system (Quantity One, Bio-Rad) based on at least five replicates.

Co-Immunoprecipitation

The formation of the Cyr61/integrin $\alpha_v\beta_1$ complex in MDA-MB-231 cells was analyzed by co-immunoprecipitation and western blot according to the manufacturer's instructions. Briefly, cells were lysed with IP Lysis/Wash Buffer (0.025 M Tris, 0.15 M NaCl, 0.001 M EDTA, 1% NP-40, 5% glycerol; pH7.4, containing 10 mM protease inhibitors (PMSF). Cell lysates (500 μl/15 × 10^5 cells) were incubated with mouse anti-Cyr61 monoclonal antibody binding to aminolink plus coupling resin in pierce spin columns. Purified mouse IgG (Beyotime Biotechnology) was used as the negative control. The pierce spin columns were washed four times, and the bound proteins were released by Elution Buffer for western blot analysis with rabbi anti-integrin α_v and rabbit anti-integrin β_1.

Immunofluorescence Microscopy

MDA-MB-231 cells (1.0×10^5) grown on 35 mm cell culture dish (NEST, GBD-35-20) were rinsed three times using PBS, and fixed in 4% paraformaldehyde for 30 min. Cells were then washed three times with PBS, and permeabilized with 0.2% Triton x-100 for 10 min. After washed three times with PBS again, the cells were blocked with 10% BSA for 30 min, then were incubated with mouse anti-Cyr61 (1:100) and rabbit anti-integrin α_v (1:500)/anti-integrin β_1 (1:250) for 1–2 h in room temperature, rewashed, and incubated with FITC-conjugated goat anti-mouse IgG and CY3-conjugated goat anti-rabbit for 1 h. Finally, the cells were washed, and examined using a Leica TCS SP8 Spectral Confocal System.

In Vivo Tumor Xenograft Study

Four or six-week-old female BALB/C nude mice were purchased from the Shanghai Laboratory Animal Center (Shanghai, China) and maintained under clean conditions. Then they were divided into experimental group and control group randomly, eight animals per group. Cells (5 × 10^6) were resuspended in 200 μl of PBS, and injected into the lateral tail veins of mice, which had been orally gavaged with vegetable oil in the present of a dose of metapristone, 0 mg/kg (control), 2.5 mg/kg and 50 mg/kg for 3–4 days, respectively. After 5–7 weeks gavage, the lungs were removed, washed with PBS and fixed in 10% neutral buffered formalin. The number of lung tumor nodules was counted by visual inspection using a magnifying glass, then were paraffin embedded and stained with hematoxylin and eosin (H&E). The further study was to test the expression of Cyr61 and integrin $\alpha_v\beta_1$ in lung tissue using immunohistochemical analysis assay. All of the animal experiments were performed in accordance with animal protocol procedures, approved by the Institutional Animal Care and Use Committee of Fuzhou University.

Statistical Analysis

Data are presented as the mean ± standard error of the mean (SEM) or means ± standard deviations (SD). Statistical analysis was performed using the student's *t*-test and one-way analysis of variance. A P-value less than 0.05 was considered statistically significant.

Results

The Cytotoxicity Effect of Metapristone on the Growth of MDA-MB-231 and HPMEC Cells.

We evaluated the effect of various concentrations of metapristone on the viability of MDA-MB-231, MCF-7, and HPMEC cells for 12 and 24 h by MTT assay. As shown in **Figures 1A–C**, the viability of each group cells decreased in a dose- and time-dependent manner following metapristone treatment. Their IC_{50} values for metapristone (24 h) were 88.1 ± 3.2 (MDA-MB-231), 87.0 ± 2.7 (MCF-7), and 91.2± 2.5(HPMEC) μM, respectively.

Overview of Quantitative Proteomics and ELISA Validation

iTRAQ analysis was performed on the purified proteins extracted from the supernatant of co-culture system with or without metapristone (50 μM) treatment to find the metapristone-mediated anti-metastasis proteins. As represented by the flow chart in **Figure 1**. In total, 105 secreted proteins showed significant differences in metapristone-treated co-culture system (*P*-value < 0.05). Among these differentially expressed proteins (DEPs), 77 were up-regulated (**Table 1**) and 28 were down-regulated (**Table 2**). Pharmacoproteomic study showed that the expression

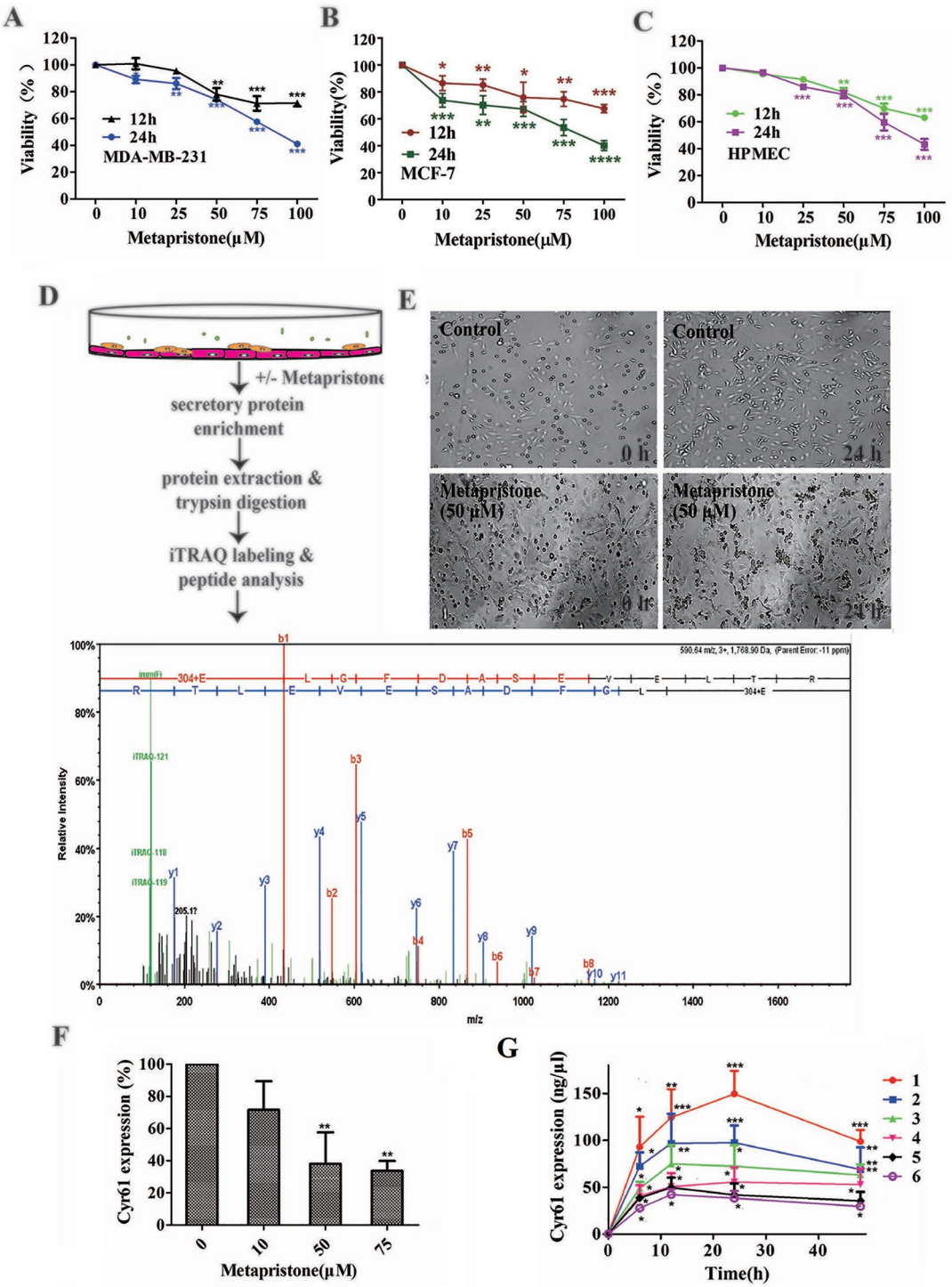

FIGURE 1 | Secretion of Cyr61 from MDA-MB-231 and human pulmonary microvascular endothelial cells co-culture system and inhibition by metapristone of the secretion. **(A)** Effect of metapristone on MDA-MB-231 viability. **(B)** Effect of metapristone on MCF-7 viability. **(C)** Effect of metapristone on HPMEC viability. **(D)** Flow chart showing that MDA-MB-231 and HPMEC were co-cultured in the presence and absence of metapristone for 24 h followed by trypsin digestion and iTRAQ pharmacoproteomic analysis; The Cyr61 proteomic signal was shown at its corresponding m/z. **(E)** Confocal microscopy images showing the morphological changes by metapristone (50 μM) in the same spots where the two cell lines were co-cultured. **(F)** inhibition by metapristone of Cyr61 secretion. **(G)** time course of Cyr61 secretion (ELISA assay) under different conditions: 1) MDA-MB-231+ HPMEC; 2) MDA-MB-231+ HPMEC+ metapristone (50 μM); 3) MDA-MB-231; 4) MDA-MB-231+ metapristone (50 μM); 5) HPMEC; 6) HPMEC+ metapristone (50 μM). The data represent the mean± SEM (n = 3). *, $P < 0.05$, **, $P < 0.01$ and ***, $P < 0.001$ *vs.* the untreated control.

TABLE 1 | Up-regulated proteins expressed in the conditioned media of MDA-MB-231 co-cultured with HPMECs.

No.	Score	%Cov	Accession number	Protein name	Peptides	Regulation (fold change)[a]
1	126	27.1	NP_003510.1	Cluster of Histone H2B type 1-L	7	1.59*
2	237	17.2	NP_001274523.1	Chloride intracellular channel protein 1	5	2.33*
3	218	26.1	NP_003290.1	Endoplasmin	5	1.77*
4	106	20.8	AAB59514.1	Apolipoprotein A-I	6	3.51*
5	552	29.8	NP_001596.2	Alanine–tRNA ligase, cytoplasmic	9	1.69*
6	267	30.0	NP_001245204.1	Sterile alpha motif domain-containing protein 3	5	3.15*
7	341	53.9	NP_001032752.1	Elongation factor 1-beta	11	6.51**
8	441	60.7	NP_005057.1	Splicing factor, proline- and glutamine-rich	10	1.75*
9	261	56.2	AAA58420.1	Caldesmon	5	7.50*
10	403	36.7	NP_004699.1	Programmed cell death protein 5	7	2.33*
11	230	51.4	NP_945189.1	Protein-glutamine gamma-glutamyltransferase 2	7	2.11*
12	137	24.2	NP_005491.1	SUMO-activating enzyme subunit 1	6	11.50**
13	1135	34.9	NP_001191020.1	40S ribosomal protein S10	5	3.55**
14	1123	43.9	NP_006127.1	F-actin-capping protein subunit alpha-2	10	5.24**
15	651	35.4	NP_060705.2	Cytosolic non-specific dipeptidase	7	7.21**
16	434	22.8	NP_057406.2	Ras-related protein Rab-14	7	10.15**
17	1019	58.2	NP_061819.2	Sialic acid synthase	9	1.85*
18	501	28.9	NP_001020092.1	60S ribosomal protein L9	5	3.26*
19	1101	33.9	NP_001304672.1	Elongation factor 1-delta	6	17.25**
20	348	29.0	NP_006005.2	EKC/KEOPS complex subunit LAGE3	6	1.87*
21	228	45.3	NP_001139699.1	40S ribosomal protein S20	9	6.56**
22	301	23.5	NP_001276978.1	General vesicular transport factor p115	8	2.76*
23	504	48.9	NP_001020.2	40S ribosomal protein S26	6	5.57**
24	216	24.1	NP_001306011.1	High mobility group protein HMG-I/HMG-Y	7	6.36**
25	259	22.4	NP_006704.3	Activated RNA polymerase II transcriptional coactivator p15	6	3.57**
26	133	45.6	NP_001339771.1	Suppression of tumorigenicity 18 protein	4	2.26*
27	1132	33.0	NP_001308414.1	40S ribosomal protein S19	11	3.69**
28	333	53.7	NP_002789.1	Proteasome subunit beta type-6	7	7.96**
29	309	44.2	NP_000966.2	60S ribosomal protein L11	5	4.23**
30	116	34.3	NP_001007.2	40S ribosomal protein S12	7	8.55**
31	243	35.1	NP_001034891.1	Cell division control protein 42 homolog	4	5.16**
32	634	44.3	NP_055277.1	U6 snRNA-associated Sm-like protein LSm1	10	6.33**
33	1005	30.7	CAA45860.1	Tetranectin	11	4.22**
34	1223	44.6	NP_996756.1	Serine/threonine-protein phosphatase PP1-alpha catalytic subunit	7	2.16*
35	164	17.1	NP_001186273.1	60S ribosomal protein L17	8	1.77*
36	422	20.6	NP_001254628.1	40S ribosomal protein S3a	11	2.89*
37	1117	52.3	NP_002892.1	Reticulocalbin-1	10	1.87*
38	311	22.1	NP_001135757.1	40S ribosomal protein S24	6	4.70**
39	118	28.3	BAB20429.1	Dihydropteridine reductase	5	11.33**
40	336	19.8	NP_006395.2	Endothelial protein C receptor	5	21.70**
41	559	43.7	NP_001001.2	40S ribosomal protein S6	7	9.18**
42	1224	29.4	NP_000963.1	60S ribosomal protein L7a	9	5.43*
43	406	23.4	NP_004517.2	DNA replication licensing factor MCM2	4	1.78*
44	518	24.5	NP_057215.3	Ras-related protein Rab-10	6	2.18*
45	217	33.8	NP_006560.3	Cell growth regulator with EF hand domain protein 1	5	3.54**
46	342	23.5	NP_001247436.1	40S ribosomal protein S3	6	1.90*
47	986	66.9	NP_072045.1	40S ribosomal protein S18	8	2.13*
48	1033	42.8	NP_006764.3	ATP-dependent RNA helicase DDX18	10	1.91*
49	557	67.9	NP_000509.1	Hemoglobin subunit beta	5	3.59**
50	1107	65.4	NP_001265308.1	ADP-ribosylation factor-like protein 6-interacting protein 4	6	3.22**
51	1091	21.6	NP_000508.1	Hemoglobin subunit alpha	6	11.90**
52	664	55.7	NP_789839.1	Proteasome activator complex subunit 3	5	13.27**
53	348	33.9	NP_001277255.1	Ubiquitin carboxyl-terminal hydrolase 38	7	5.93**
54	648	70.1	NP_001093163.1	60S ribosomal protein L31	8	2.77*
55	990	52.9	NP_001093256.1	Intercellular adhesion molecule 2	9	12.51**
56	115	19.5	NP_000345.2	Thyroxine-binding globulin	5	20.03**
57	667	33.5	NP_958845.1	Transcription elongation factor A protein 1	6	2.10*
58	1006	66.3	NP_001006.1	40S ribosomal protein S11	7	12.36**
59	852	44.4	NP_631908.1	Probable tRNA pseudouridine synthase 1	15	5.16**
60	223	66.1	NP_000306.1	Parathyroid hormone	9	2.53*
61	109	17.7	NP_001290555.1	60S ribosomal protein L10	11	6.26**
62	310	54.4	NP_000981.1	60S ribosomal protein L27a	8	11.15**

(*Continued*)

TABLE 1 | Continued

No.	Score	%Cov	Accession number	Protein name	Peptides	Regulation (fold change)[a]
63	339	32.8	AAA51683.1	Alpha-2-HS-glycoprotein	9	2.23*
64	398	42.5	NP_808760.1	Histone H2A.J	7	2.57*
65	671	54.8	NP_001030168.1	60S ribosomal protein L14	12	9.31**
66	245	25.9	AAA02852.1	Aminoacylase-1	8	2.90*
67	279	45.9	NP_000959.2	60S ribosomal protein L4	6	12.14**
68	1013	56.2	NP_001022.1	40S ribosomal protein S28	5	7.42**
69	1102	63.6	NP_001230060.1	60S ribosomal protein L13	6	7.01**
70	686	73.0	NP_001307070.1	60S ribosomal protein L6	9	13.43**
71	354	55.4	NP_057018.1	Nucleolar protein 58	10	9.64**
72	1224	21.1	NP_001257907.1	IST1 homolog	10	2.66*
73	556	43.2	NP_001002.1	40S ribosomal protein S7	7	8.81**
74	352	26.1	NP_778224.1	Histone H4	4	2.90*
75	1039	79.4	NP_113584.3	E3 ubiquitin-protein ligase HUWE1	4	14.31**
76	601	29.6	NP_037377.1	Vacuolar protein sorting-associated protein 4A	7	16.37**
77	1096	58.4	NP_001307930.1	Translation initiation factor IF-2, mitochondrial	4	61.25**

[a]*Regulations (fold-changes) of differentially expressed proteins in MDA-MB-231 cells (metapristone-treatment versus control). *P < 0.05; **P < 0.01.*

TABLE 2 | Down-regulated proteins expressed in the conditioned media of MDA-MB-231 co-cultured with HPMECs.

No.	Score	%Cov	Accession number	Protein name	Peptides	Regulation (fold change)[a]
1	699	23.3	P08779.4	Cluster of Keratin, type I cytoskeletal 16	11	0.47*
2	237	51.2	NP_001633.1	Amyloid-like protein 2	7	0.42*
3	1051	35.1	NP_000217.2	Keratin, type I cytoskeletal 9	7	0.51*
4	158	28.5	NP_004039.1	Beta-2-microglobulin	5	0.52*
5	435	17.3	NP_003245.1	Metalloproteinase inhibitor 1	5	0.35**
6	763	33.7	NP_004930.1	ATP-dependent RNA helicase DDX1	4	0.41**
7	501	19.1	NP_003013.1	SH3 domain-binding glutamic acid-rich-like protein	4	0.65*
8	722	61.4	NP_055635.3	Mitochondrial import receptor subunit TOM70	7	0.36**
9	1015	26.9	NP_001159506.1	Suprabasin	5	0.61*
10	238	47.2	NP_001339702.1	Junction plakoglobin	6	0.44**
11	122	23.4	NP_059118.2	Calmodulin-like protein 5	14	0.49*
12	633	61.1	NP_060275.2	Ras-interacting protein 1	6	0.57*
13	814	36.9	NP_003109.1	SPARC	16	0.40**
14	1226	19.7	NP_055463.1	E3 ubiquitin-protein ligase DZIP3	5	0.63*
15	1104	20.3	NP_005520.4	Basement membrane-specific heparan sulfate proteoglycan core protein	8	0.54*
16	439	21.7	NP_000349.1	Transforming growth factor-beta-induced protein ig-h3	8	0.59*
17	1615	36.3	NP_009016.1	Follistatin-related protein 1	4	0.63*
18	1532	34.1	NP_001545.2	Protein CYR61	8	0.39**
19	716	27.5	NP_001308350.1	Rho GDP-dissociation inhibitor 2	6	0.49**
20	374	34.5	NP_116020.1	Hepatoma-derived growth factor-related protein 2	10	0.56*
21	715	46.9	NP_000511.2	Beta-hexosaminidase subunit alpha	4	0.45**
22	1227	52.3	NP_002895.3	Negative elongation factor E	9	0.57*
23	1032	36.3	NP_079472.1	GrpE protein homolog 1, mitochondrial	7	0.61*
24	760	35.1	NP_002169.1	Insulin-like growth factor-binding protein 6	7	0.52*
25	1069	37.3	NP_001340245.1	Protein FAM49B	8	0.47**
26	419	29.1	NP_115729.1	Vacuolar protein-sorting-associated protein 25	12	0.56*
27	512	36.6	NP_004809.2	Probable ATP-dependent RNA helicase DDX23	6	0.53*
28	405	23.9	NP_001136155.1	Coiled-coil domain-containing protein 121	5	0.60*

[a]*Regulations (fold-changes) of differentially expressed proteins in MDA-MB-231 cells (metapristone-treatment versus control). *P < 0.05; **P < 0.01.*

of Cyr61 was significantly down-regulated by metapristone by 60%, which was one of the most significantly changed proteins. To validate this, ELISA was performed. Compared with the control, the expression level of Cyr61 secreted from co-culture was down-regulated to 72%, 39%, and 36%, respectively, at 10, 50, and 75 μM of metapristone (**Figure 1F**), confirming that the proteomic data was reliable.

The Origins of Cyr61 Secreted

To explore whether MDA-MB-231/HPMEC co-culture increases Cyr61 secretion, we tested the concentrations of Cyr61 in different groups at 0, 6, 12, 24, and 48 h by ELISA. As shown in **Figure 1G**, the secretion of Cyr61 increased at the beginning, then saturated or decreased progressively. Cyr61 expression in co-culture group was higher than that in MDA-MB-231 or

HPMEC monocultures. Both MDA-MB-231 cells and HPMECs could secrete Cyr61, but the former secreted more. The secretions of Cyr61 in metapristone groups were lower than that in non-treatment groups. These results indicated that the co-culture system provided a better microenvironment for expression and secretion of Cyr61 compared with monoculture.

To further investigate the relationship between metapristone and co-culture model, a time-lapse photography was taken, which showed that MDA-MB-231 cells suspended in culture tended to adhere to HPMECs on the dish, but this tendency was interfered by metapristone. The co-culture system in the presence and absence of metapristone showed almost 0% adhesion. At 24 h after co-culture, the control group reached 45% adhesion, whereas the metapristone-treated group reached only 20% adhesion (**Figure 1E**).

Metapristone Inhibits Cyr61-Mediated Cell Migration and Adhesion

First, we constructed the "pcDNA3.1-Cyr61" plasmid and synthesized the "Cyr61-siRNA" (see **Supplementary Information**, **Figure S1** and **S2**) to test the function of Cyr61 in metapristone-related anti-metastasis mechanics. Then, would healing assay was used to examine the effects of endogenous Cyr61 protein and metapristone on MDA-MB-231 cell motility. As shown in **Figure 2A**, the overexpression of Cyr61 enhanced cellular migration (170%) and the down-regulation of Cyr61 expression inhibited cellular migration (53%). MDA-MB-231 cells migration was inhibited by metapristone in a concentration-dependent manner by 74% (10 μM), 52% (50 μM), and 45% (75 μM), respectively (**Figure 2**). These results suggested that metapristone significantly inhibited Cyr61-mediated cell motility and wound closure at concentrations lowering than its IC_{50}.

It is well known that tumor cells adhesion to the ECM is a fundamental step in cancer metastasis (Gilkes et al., 2014; Conlon and Murray, 2019). The adhesion of MDA-MB-231 cells to HPMECs was examined to determine whether metapristone can regulate cell adhesion at a non-cytotoxic concentration by Cyr61 pathway. Compared with the control, the adhesion rate of MDA-MB-231 cells was 218%, 48%, 63%, 44%, and 41%, respectively, for transfection groups (pcDNA3.1-Cyr61,

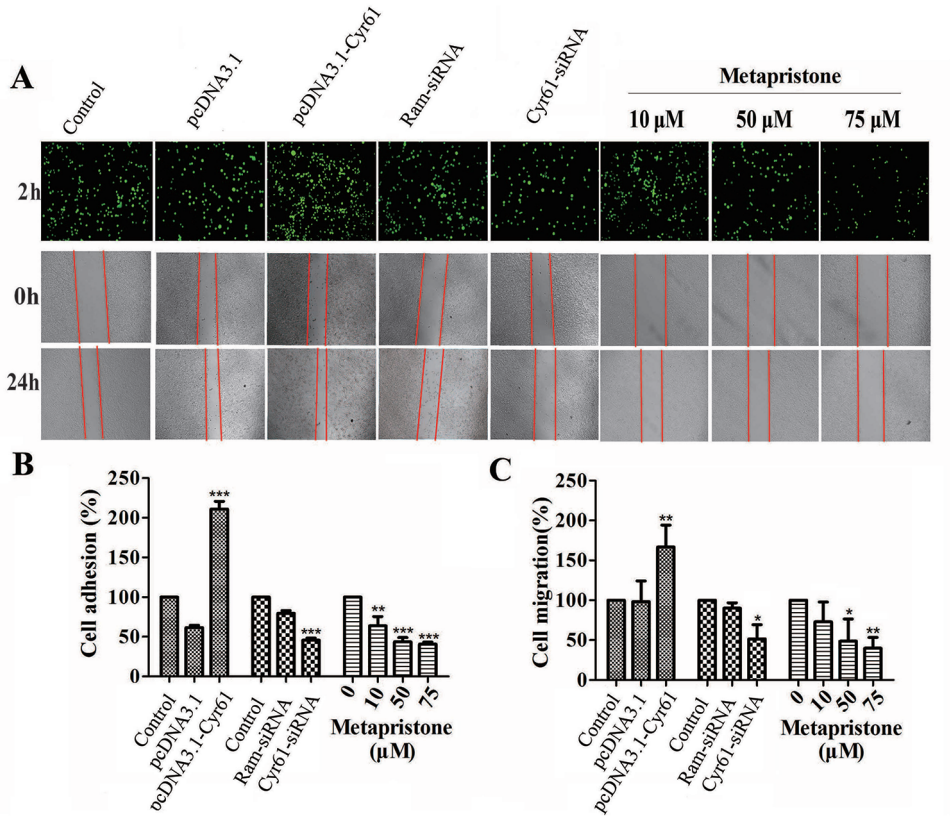

FIGURE 2 | Cyr61-related cell adhesion and migration were mediated by metapristone. MDA-MB-231 cells were transfected with pcDNA3.1, pcDNA3.1-Cyr61 recombinant plasmid, or Ram-siRNA, Cyr61-siRNA for 36–48 h. **(A)** Upper panel: inhibition by metapristone of MDA-MB-231 cell adhesion to human pulmonary microvascular endothelial cells; note, the adhesion between pcDNA3.1-Cyr61 cancer cells and HPMECs was significantly enhanced. Whereas, the adhesion between Cyr-61-siRNA cancer cells and HPMECs was reduced in comparison with their controls. Metapristone caused concentration-dependent inhibition of the adhesion. Middle and lower panels: changes by metapristone in cell migration rate following the scratch assay. **(B)** Quantitative analysis of the adhesion between Cyr61-transfected cancer cells and HPMECs. **(C)** The MDA-MB-231 cells were transfected and treated differently, and the migration rate following the scratch assay was quantitatively determined; The data represent mean± SEM (n = 3), *, $P < 0.05$; **, $P < 0.01$; and ***, $P < 0.001$ *vs*. the controls.

Cyr61-siRNA) and metapristone treatment groups (10, 50 and 75 μM) (**Figures 2A, B**). Metapristone markedly inhibited the adhesion of MDA-MB-231 cells to endothelial monolayers in a concentration-dependent manner through the Cyr61-dependent mechanism.

Metapristone Inhibits Adhesion and Migration of MDA-MB-231 Cells *via the* Cyr61/Integrin $\alpha_v\beta_1$ Signaling Pathway

Previous reports have indicated that the CCN family interacts with integrin receptors to modulate cell biological functions (Holbourn et al., 2008). Therefore, we sought to identify the cellular adhesion receptor(s) through which Cyr61 may function. By using co-immunoprecipitation assay, as shown in **Figure 3**, integrin $\alpha_v\beta_1$, as a new receptor for Cyr61 in the MDA-MB-231/HPMEC co-cultures was identified by immunoprecipitation combined with western blot analysis. We found that MDA-MB-231/HPMEC co-cultures promoted the formation of Cyr61/integrin $\alpha_v\beta_1$ complex, which was inhibited by metapristone significantly. The results were further confirmed by confocal microscopy co-localized methods using immunofluorescent staining of the CYR1, integrin α_v, and integrin β_1 proteins in MDA-MB-231 cells (**Figure 3B**).

Furthermore, the effects of metapristone on the expressions of Cyr61, integrin α_v, and integrin β_1 on the protein and mRNA levels were determined using qRT-PCR and western blot analysis. The results showed that when the MDA-MB-231 cells were treated with different doses of metapristone, the expressions of Cyr61 and integrin $\alpha_v\beta_1$ were dose-dependently decreased (**Figures 4A, B, D**). As the secreted protein, the expression of Cyr61 in cell culture was detected by ELISA assay. As shown in **Figure 4**, the significantly reduced expression of the Cyr61 was observed in the presence of metapristone. The metapristone might regulate cell adhesion and migration through Cyr61/integrin $\alpha_v\beta_1$ pathway in MDA-MB-231 cells.

Effect of Metapristone on Experimental Lung Metastasis *in Vivo*

The lungs are a frequent target of metastatic breast cancer cells (Landemaine et al., 2008; Oskarsson et al., 2011). Therefore, we further examined the anti-metastatic efficacy of metapristone on MDA-MB-231 cells using a xenograft mice model. **Figure 5** showed representative images of pulmonary metastases of MDA-MB-231 breast cancer in each group. We obviously observed that pulmonary metastatic nodules and the rate of lung tumor-metastasis from the mice treated with the metapristone were less than those of mice in control group (**Figures 5B, C**). In addition, the histological examinations (hematoxylin-eosin staining of various lung sections) showed the metastatic nodules colonized in the lungs of metapristone treatment groups were smaller than that of non-treated group with lower density (**Figure 5**). Furthermore, there was obvious effect on the expressions of Cyr61 and integrin $\alpha_v\beta_1$ in these lung tissues (**Figure 5**) at different dose levels. By comparison, the positive areas of Cyr61 and integrin $\alpha_v\beta_1$ were decreased with high dose metapristone.

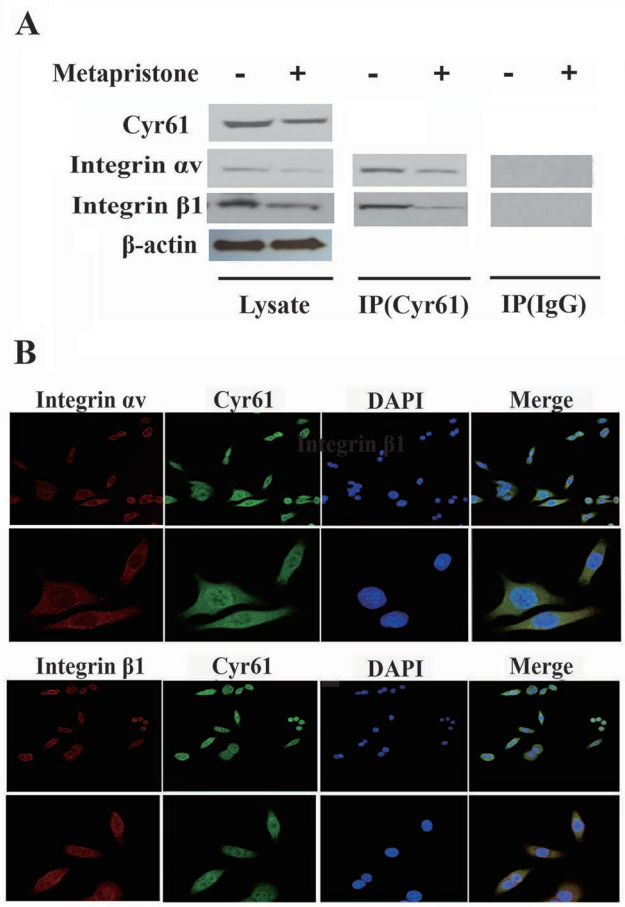

FIGURE 3 | Formation of Cyr61/integrin αvβ1 complex in MDA-MB-231 cells. **(A)** Co-immunoprecipitation evidence: MDA-MB-231 cell lysates were added to aminolink-coupling resin columns that were individually coupled with anti-Cyr61 antibody (land 1 and 3), anti-integrin αv antibody (land 2), or anti-integrin β1 antibody (land 4). The bound complexes were eluted with the washing buffer and tested by western blotting with anti-integrin αv antibody (land 1), anti-Cyr61 antibody (land 2 and 4), or anti-integrin β1 antibody, individually. Samples of Lysis (before column; left), IgG, and Target (column elutes; right) after western blotting showed that the anti-Cyr61 antibody elute was integrin αv positive (land 1), integrin β1 positive (land 3), and Cyr61 positive (land 2 and 4). **(B)** Cyr61/integrin αvβ1 co-localization evidence: MDA-MB-231 cells were immunofluorescent-stained with Cyr61 (green), integrin αv (the upper two panels), or integrin β1 (the lower two panels; both in dark red) and DAPI (in blue for nuclear) dyes followed by confocal microscopic examination at amplification×20 (top panel) or ×40 (bottom panel). The merged images showed co-localization of Cyr61 with integrin αv and β1.

DISCUSSION

Tumor microenvironment plays an important role in directly stimulating malignant cell metastasis. For example, normal endothelial and tumor cells usually communicate indirectly before or directly after adhesion, through a complex network of interactions to drive cellular differentiation, tissue structures

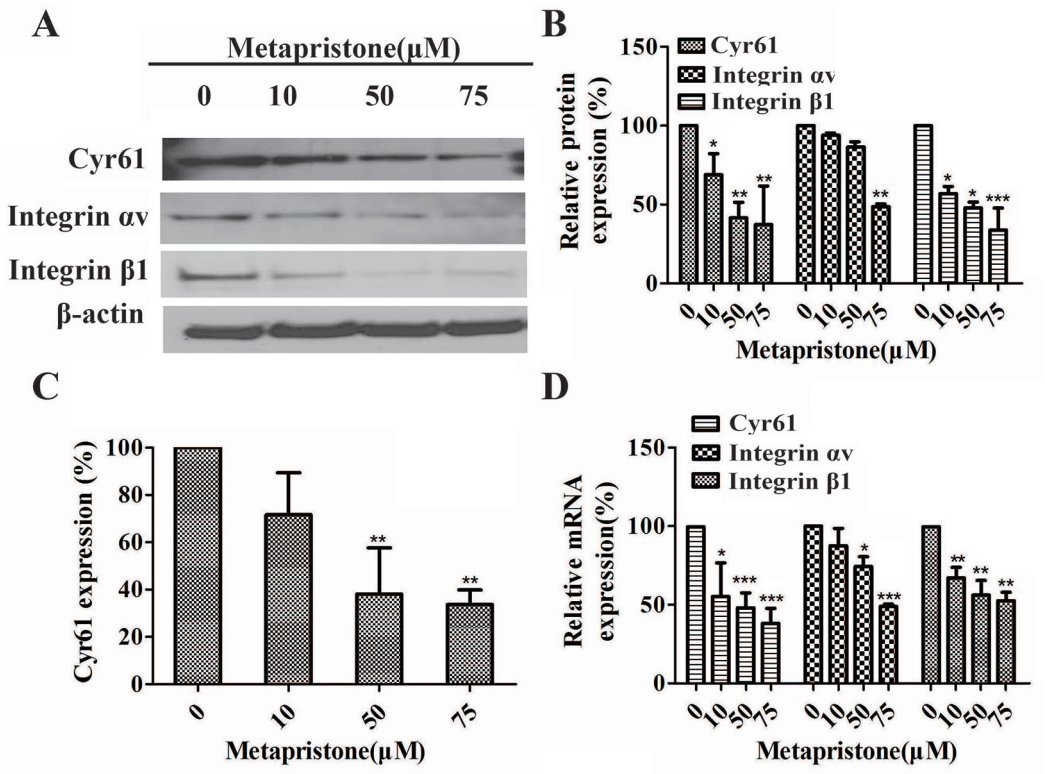

FIGURE 4 | Inhibition by metapristone of expressions of Cyr61 and integrin αvβ1 in MDA-MB-231 cells. Western blot images **(A)** and the related quantitative analysis, **(B)** and quantitative ELISA analysis **(C)** of inhibition by metapristone of expressions of Cyr61 and integrin αvβ1 in MDA-MB-231 cells. **(D)** mRNA expression of Cyr61, integrin αv and β1 was inhibited by metapristone in a concentration-dependent manner. The data are expressed as the mean± SEM (n = 3). *, $P < 0.05$; **, $P < 0.01$, and ***, $P < 0.001$ *vs*. the untreated controls.

formation, cancer invasion, and metastasis. One function of this communication is to exchange both soluble and insoluble signaling molecules, such as secreted proteins, miRNAs and exosomes. However, the underlying mechanism is not well understood.

In this study, we used a MDA-MB-231/HPMEC co-culture model to investigate the secreted proteins involved in cell adhesion/invasion, the crucial procedures of cancer early metastasis (Devis et al., 2017). iTRAQ technology exhibited superb performance in the quantitative proteomic study (Astier, 2010). Using iTRAQ-based proteomic approach, we identified 105 secreted proteins, showing significant differences in metapristone (a potential cancer metastasis chemopreventives)-treated co-culture secretome compared to the control group (P-value < 0.05) (**Figure 1** and **Table 1**). In particular, we found that MDA-MB-231/HPMEC co-cultures promoted the secretion levels of Cyr61 relative to MDA-MB-231 or HPMEC monocultures. In contrast, metapristone not only inhibited the Cyr61 secretion, but also prevented adhesion of MDA-MB-231 cells to HPMECs in morphology (**Figure 1** and **Figure 2**).

Cyr61 (CCN1), as the first cloned member of cysteine-rich protein (CCN) family, is a secreted, cysteine-rich, heparin binding extracellular matrix-associated protein (Planque and Perbal, 2003; D'Antonio et al., 2010). To date, a number of reports describe that Cyr61 is involved in many cell biological functions. For example, Cyr61 has been identified to mediate cell adhesion, migration, proliferation, apoptosis, and angiogenesis. Cyr61 is highly expressed in breast cancer (Sánchez-Bailón et al., 2015; Mayer et al., 2017; Yang et al., 2018), and is without a doubt associated with expression stage, tumor size, positive lymph nodes and age (Xie et al., 2001). The analysis indicated that blocking Cyr61 might be a potent method for TNBC breast cancer treatment. We previously reported how metapristone inhibited the adhesion and migration of MDA-MB-231 breast cancer cells through EMT-related pathway (Yu et al., 2016). However, the other mechanism remains largely unknown. In the present study, the effect of metapristone induction on Cyr61 activity to interfere cell adhesion and migration was examined by the transfection of siRNA-Cyr61/pcDNA3.1-Cyr61 into MDA-MB-231 (see **Supplementary Information**). Our results showed that overexpression/knockdown of Cyr61 significantly increase/decrease adhesion and migration of MDA-MB-231 cells, respectively (**Figure 2**).

A number of the activities of Cyr61 can be attributed to its interaction with integrin receptors (Kireeva, 1998; Jedsadayanmata et al., 1999; Chen et al., 2000; Grzeszkiewicz et al., 2001; Schober et al., 2002). For example, primary human skin fibroblasts adhesion to Cyr61 is dependent on integrin $\alpha_6\beta_1$ (Leu et al., 2003), and

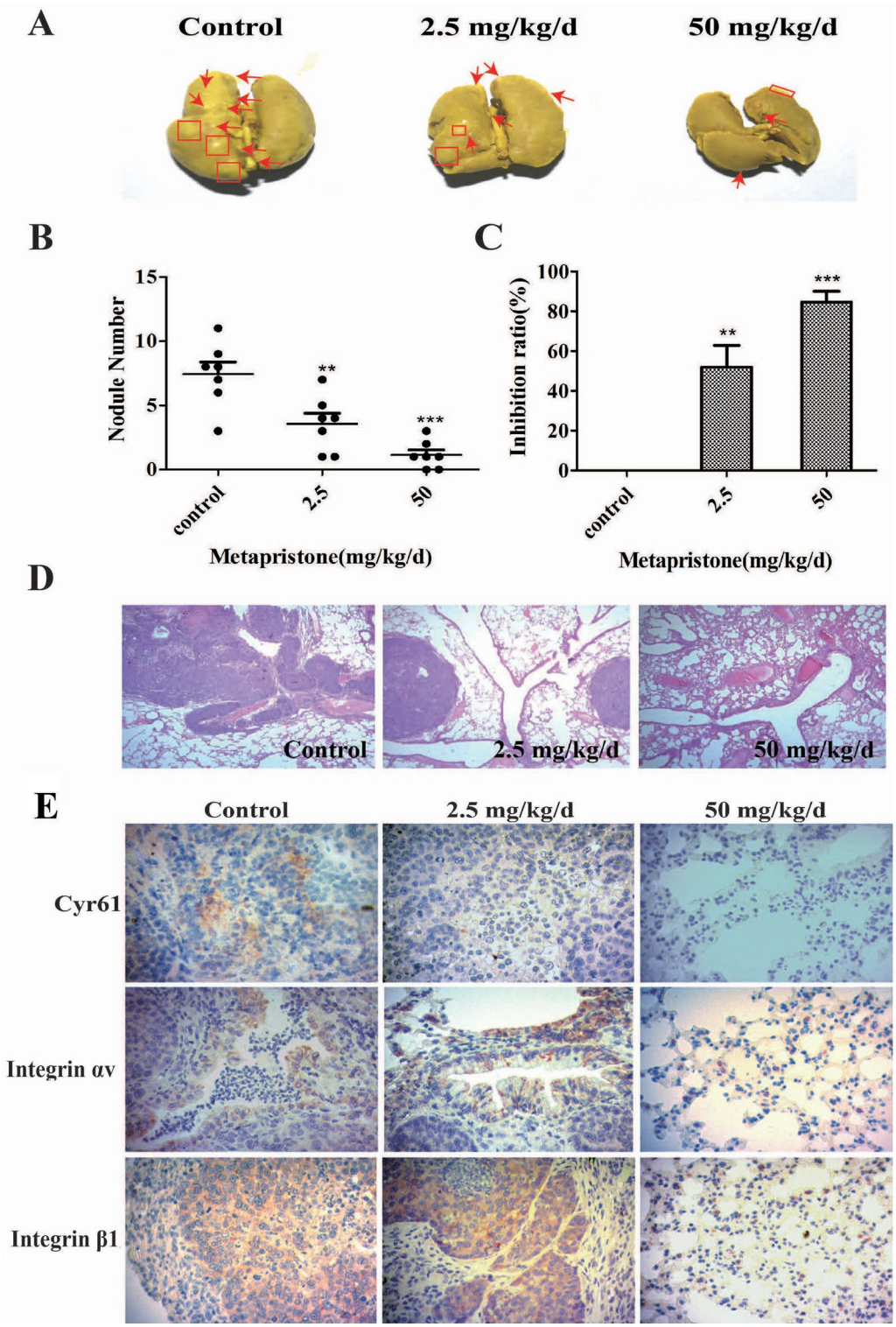

FIGURE 5 | Metapristone inhibits lung metastasis of MDA-MB-231 cells *via* decreasing levels of Cyr61 and integrin αvβ1. **(A)** photography of mouse lung metastasis after six weeks of MDA-MB-231 inoculation *via* tail vein injection. The mice were pretreated with oral metapristone for three days before the inoculation followed by 6-week oral administration of metapristone. Control, drug vehicle; **(B)** quantitative comparison in mouse lung tumor nodules between the control and metapristone groups (n = 5/group); **P < 0.01, ***P < 0.001. **(C)** inhibition rate of mouse lung tumor metastasis after metapristone treatment; **(D)** hematoxylin–eosin staining of the lungs (amplification× 5); the arrows indicate metastatic foci that were significantly reduced by metapristone; **(E)** lung immunostaining with antibodies against Cyr61, integrin αv and integrin β1; the staining showed reduction in Cyr61/integrin avβ1 formation by metapristone.

activation-dependent adhesion of blood platelets to Cyr61 is mediated through interaction with integrin $\alpha_2\beta_3$ (Jedsadayanmata et al., 1999). To understand Cyr61's action in MDA-MB-231/HPMEC co-cultures, we sought to identify the cellular adhesion receptor(s) through which Cyr61 may function. We provided the first demonstration of the identification integrin $\alpha_v\beta_1$ as a novel receptor for Cyr61 in MDA-MB-231/HPMEC co-cultures by immunoprecipitation combined with western blot analysis (**Figure 3**). The expressions of Cyr61, integrin α_v, and integrin β_1 on the protein and mRNA levels were all down-regulated by metapristone in a dose-dependent manner. Furthermore, metapristone inhibited the formation of Cyr61/integrin $\alpha_v\beta_1$ complex, which are correlated with cell adhesion and migration (**Figure 4**). Moreover, the circulating MDA-MB-231, developing lung metastasis in mice, could be effectively prevented by oral metapristone without significant toxicity (**Figure 5**). Also, our studies demonstrated the obvious inhibition effect on the expressions of Cyr61 and integrin $\alpha_v\beta_1$ in lung tissues after metapristone treatment.

Taken together, we have demonstrated for the first time that co-incubation of triple-negative breast cancer cell line MDA-MB-231 with HPMEC promotes the secretion of Cyr61 (CCN1), primarily from MDA-MB-231, which forms Cyr61/integrin $\alpha_v\beta_1$ complex. Moreover, our data show that metapristone, a new chemopreventive, has the ability to inhibit TNBC cells adhesion and migration through down-regulation of Cyr61 and the formation of Cyr61/integrin $\alpha_v\beta_1$ complex (**Figure 6**).

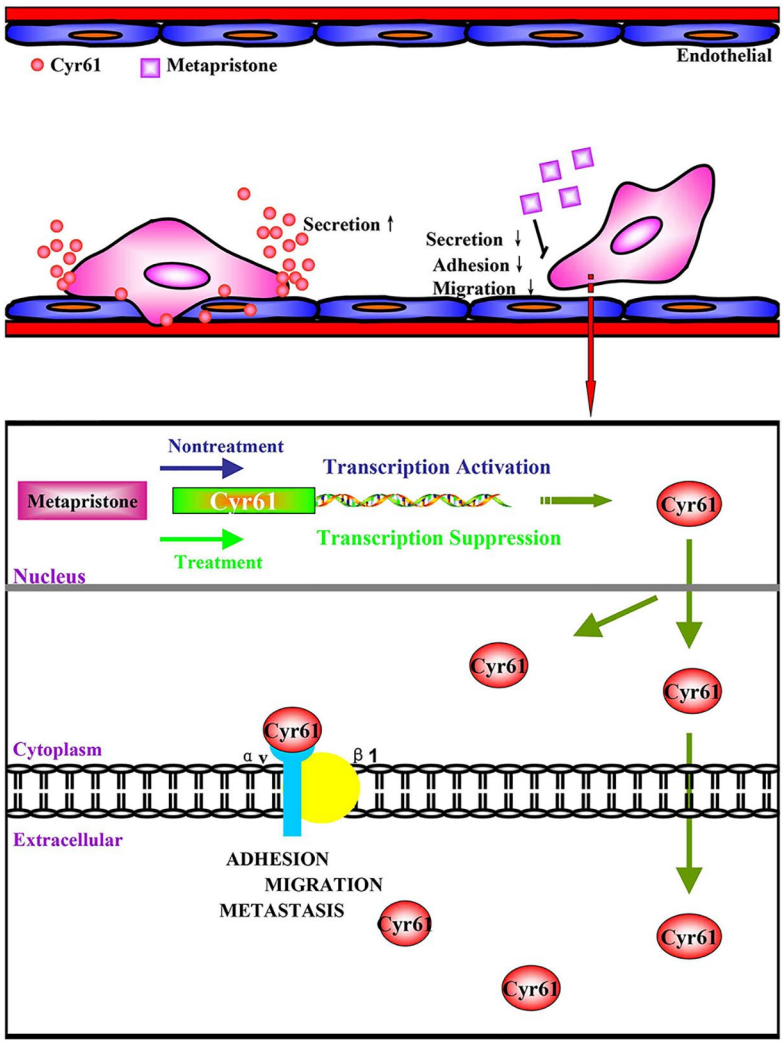

FIGURE 6 | (A) possible mechanism of Cyr61 secretion and its inhibition by metapristone. Activated CTCs adhere to endothelial cells in the metastatic microenvironment, and the adhesion induces hetero-cellular communication and the resultant secretion of Cyr61 from CTCs, which forms Cyr61/integrin avβ1 complex to advance the adhesion/invasion metastasis. Metapristone inhibits the Cyr61 secretion, and the related adhesion/invasion process; **(B)** quantitative comparison in mouse lung tumor nodules between the control and metapristone groups (n = 5/group); **(C)** inhibition rate of mouse lung tumor metastasis after metapristone treatment; **(D)** hematoxylin–eosin staining of the lungs (amplification× 5); the arrows indicate metastatic foci that were significantly reduced by metapristone; **(E)** lung immunostaining with antibodies against Cyr61, integrin αv and integrin β1; the staining showed reduction in Cyr61/integrin avβ1 formation by metapristone.

Our data provide more details in understanding metastasis mechanism of microenvironment of tumor, especially under the tumor cells/endothelial cells co-culture condition, offer a cache of potential therapeutic targets, and more importantly, provide a molecular framework for clinical evaluation of metapristone as a potential cancer metastatic chemopreventive agent.

DATA AVAILABILITY STATEMENT

All datasets generated for this study are included in the article/ **Supplementary Material**.

ETHICS STATEMENT

The animal study was reviewed and approved by The Experimental animal ethics committee, Fuzhou University.

AUTHOR CONTRIBUTIONS

LJ and SY conceived and designed the experiments. SY and CY performed the pharmacoproteomic analysis. WW, SH, ML, JL, and YL carried out the cell biology experiments. XY and JM performed the animal experiments. CY and WW acquired and drew the pictures. LJ and SY wrote the manuscript. All authors read and approved the final manuscript.

ACKNOWLEDGMENTS

This work was supported by grants from National Natural Science Foundation of China (NSFC) U1505225, 81502617, 81273548; the grant from Ministry of Science and Technology of China (MOST 2015CB931804); the grant from Fujian Development and Reform Commission (project#829054, 2014/168), Fujian Science and Technology plan project (2015Y0071), the financial support from the program of China Scholarships Council (No. 201706655014), and China Postdoctoral Science Foundation (2015M582027).

The authors thank the Department of Chemistry and the Institute of Biomedical Science, Fudan University, Peoples Republic of China, for technical support.

SUPPLEMENTARY MATERIAL

The Supplementary Material for this article can be found online at: https://www.frontiersin.org/articles/10.3389/fphar.2019.01296/full#supplementary-material

REFERENCES

Adav, S. S., Li, A. A., Manavalan, A., Punt, P., and Sze, S. K. (2010). Quantitative iTRAQ secretome analysis of Aspergillus niger reveals novel hydrolytic enzymes. *J. Proteome Res.* 9, 3932–3940. doi: 10.1021/pr100148j

Akram, M., Iqbal, M., Daniyal, M., and Khan, A. U. (2017). Awareness and current knowledge of breast cancer. *Biol. Res.* 50, 33. doi: 10.1186/s40659-017-0140-9

Astier, A. (2010). Recent developments of pharmacogenomics in the treatment of colorectal cancers. *Annales Pharmaceutiques Françaises.* 68, 233–253. doi: 10.1016/j.pharma.2010.04.001

Barrios, C. H., Reinert, T., and Werutsky, G. (2018). Global breast cancer research: moving forward. *Am. Soc. Clin. Oncol. Educ. Book.* 38, 441–450. doi: 10.1200/EDBK_209183

Bonin-Debs, A. L., Boche, I., Gille, H., and Brinkmann, U. (2004). Development of secreted proteins as biotherapeutic agents. *Expert Opin. Biol. Therapy.* 4, 551–558. doi: 10.1517/14712598.4.4.551

Chen, N., Chen, C. C., and Lau, L. F. (2000). Adhesion of human skin fibroblasts to Cyr61 is mediated through integrin alpha 6beta 1 and cell surface heparan sulfate proteoglycans. *J. Biol. Chem.* 275, 24953–24961. doi: 10.1074/jbc.M003040200

Conlon, G. A., and Murray, G. I. (2019). Recent advances in understanding the roles of matrix metalloproteinases in tumour invasion and metastasis. *J. Pathol.* 247, 629–640. doi: 10.1002/path.5225

Crockett, J. C., Schütze, N., Tosh, D., Jatzke, S., Duthie, A., Jakob, F., et al. (2007). The matricellular protein CYR61 inhibits osteoclastogenesis by a mechanism independent of alphavbeta3 and alphavbeta5. *Endocrinology.* 148, 5761–5768. doi: 10.1210/en.2007-0473

Crockett, J. C., Schütze, N., Tosh, D., Jatzke, S., Duthie, A., and Jakob, F. (2010). Matricellular protein CCN1 activates a proinflammatory genetic program in murine macrophages. *J. Immunol.* 184, 3223–3232. doi: 10.4049/jimmunol.0902792

D'Antonio, K. B., Schultz, L., Albadine, R., Mondul, A. M., Platz, E. A., Netto, G. J., et al. (2010). Decreased expression of Cyr61 is associated with prostate cancer recurrence after surgical treatment. *Clin. Cancer Res. Official J. Am. Assoc. Cancer Res.* 16, 5908–5913. doi: 10.1158/1078-0432.CCR-10-1200

Devis, L., Moiola, C. P., Masia, N., Martinez-Garcia, E., Santacana, M., Stirbat, T. V., et al. (2017). Activated leukocyte cell adhesion molecule (ALCAM) is a marker of recurrence and promotes cell migration, invasion, and metastasis in early-stage endometrioid endometrial cancer. *J. Pathol.* 241, 475–487. doi: 10.1002/path.4851

Dotan, E., Cohen, S. J., Alpaugh, K. R., and Meropol, N. J. (2009). Circulating tumor cells: evolving evidence and future challenges. *Oncologist.* 14, 1070–1082. doi: 10.1634/theoncologist.2009-0094

Gilkes, D. M., Semenza, G. L., and Wirtz, D. (2014). Hypoxia and the extracellular matrix: drivers of tumour metastasis. *Nat. Rev. Cancer.* 14 (6), 430–439. doi: 10.1038/nrc3726

Grzeszkiewicz, T. M., Kirschling, D. J., Chen, N., and Lau, L. F. (2001). CYR61 stimulates human skin fibroblast migration through integrin αvβ5 and enhances mitogenesis through integrin αvβ3, independent of its carboxyl-terminal Domain. *J. Biol. Chem.* 276, 21943–21950. doi: 10.1074/jbc.M100978200

Grzeszkiewicz, T. M., Lindner, V., Chen, N., Lam, S. C., and Lau, L. F. (2002). The Angiogenic factor cysteine-rich 61 (CYR61, CCN1) supports vascular smooth muscle cell adhesion and stimulates chemotaxis through integrin alpha(6) beta(1) and cell surface heparan sulfate proteoglycans. *Endocrinology.* 143, 1441–1450. doi: 10.1210/endo.143.4.8731

Heikinheimo, O., Haukkamaa, M., and Lähteenmäki, P. (1989). Distribution of RU486 and its demethylated metabolites in humans. *J. Clin. Endocrinol. Metabolism* 68, 270. doi: 10.1210/jcem-68-2-270

Holbourn, K. P., Acharya, K. R., and Perbal, B. (2008). The CCN family of proteins: structure–function relationships. *Trends Biochem. Sci.* 33, 461–473. doi: 10.1016/j.tibs.2008.07.006

Hou, C. H., Lin, F. L., Hou, S. M., and Liu, J. F. (2014). Cyr61 promotes epithelial-mesenchymal transition and tumor metastasis of osteosarcoma by Raf-1/MEK/ERK/Elk-1/TWIST-1 signaling pathway. *Mol. Cancer* 13, 236. doi: 10.1186/1476-4598-13-236

Jandova, J., Beyer, T. E., Meuillet, E. J., and Watts, G. S. (2012). The matrix protein CCN1/CYR61 is required for αVβ5-mediated cancer cell migration. *Cell Biochem. Function.* 30, 687–695. doi: 10.1002/cbf.2853

Jedsadayanmata, A., Chen, C. C., Kireeva, M. L., Lau, L. F., and Lam, S. C. (1999). Activation-dependent adhesion of human platelets to Cyr61 and Fisp12/mouse connective tissue growth factor is mediated through integrin alpha(IIb)beta(3). *J. Biol. Chem.* 274, 24321–24327. doi: 10.1074/jbc.274.34.24321

Kireeva, M. L. (1998). Adhesion of human umbilical vein endothelial cells to the immediate-early gene product Cyr61 is nediated through integrin alpha v beta 3. *J. Biol. Chem.* 273, 3090–3096. doi: 10.1074/jbc.273.5.3090

Laganà, A., Veneziano, D., Russo, F., Pulvirenti, A., Giugno, R., Croce, C. M., et al. (2015). Computational design of artificial RNA molecules for gene regulation. *Methods Mol. Biol.* 1269, 393–412. doi: 10.1007/978-1-4939-2291-8_25

Lambert, A. W., Pattabiraman, D. R., and Weinberg, R. A. (2017). Emerging biological principles of metastasis. *Cell.* 168, 670–691. doi: 10.1016/j.cell.2016.11.037

Landemaine, T., Jackson, A., Bellahcène, A., Rucci, N., Sin, S., Abad, B. M., et al. (2008). A six-gene signature predicting breast cancer lung metastasis. *Cancer Res.* 68, 6092–6099. doi: 10.1158/0008-5472.CAN-08-0436

Lau, L. F. (2011). CCN1/CYR61: the very model of a modern matricellular protein. *Cell. Mol. Life Sci.* 68, 3149–3163. doi: 10.1007/s00018-011-0778-3

Leu, S. J., Liu, Y., Chen, N., Chen, C. C., Lam, S. C., and Lau, L. F. (2003). Identification of a novel integrin α6β1 binding site in the angiogenic inducer CCN1 (CYR61). *J. Biol. Chem.* 278, 33801–33808. doi: 10.1074/jbc.M305862200

Lin, J., Huo, R., Wang, L., Zhou, Z., Sun, Y., Shen, B., et al. (2012). A novel anti-Cyr61 antibody inhibits breast cancer growth and metastasis *in vivo. Cancer Immunol. Immunotherapy.* 61, 677–687. doi: 10.1007/s00262-011-1135-y

Mayer, S., Erbes, T., Timme-Bronsert, S., Jaeger, M., Rücker, G., Kuf, F., et al. (2017). Clinical relevance of Cyr61 expression in patients with hormone-dependent breast cancer. *Oncol. Lett.* 14, 2334–2340. doi: 10.3892/ol.2017.6406

Mbeunkui, F., Fodstad, O., and Pannell, L. K. (2006). Secretory protein enrichment and analysis: an optimized approach applied on cancer cell lines using 2D LC-MS/MS. *J. Proteome Res.* 5, 899–906. doi: 10.1021/pr050375p

Miller, I. V., and Grunewald, T. G. P. (2015). Tumour-derived exosomes: tiny envelopes for big stories. *Biol. Cell.* 107, 287–305. doi: 10.1111/boc.201400095

Nguyen, N., Kuliopulos, A., Graham, R. A., and Covic, L. (2006). Tumor-derived Cyr61(CCN1) promotes stromal matrix metalloproteinase-1 production and protease-activated receptor 1-dependent migration of breast cancer cells. *Cancer Research.* 66, 2658–2665. doi: 10.1158/0008-5472.CAN-05-2082

Oskarsson, T., Acharyya, S., Zhang, X. H., Vanharanta, S., Tavazoie, S. F., Morris, P. G., et al. (2011). Breast cancer cells produce tenascin C as a metastatic niche component to colonize the lungs. *Nat. Med.* 17, 867–874. doi: 10.1038/nm.2379

Planque, N., and Perbal, B. (2003). A structural approach to the role of CCN (CYR61/CTGF/NOV) proteins in tumourigenesis. *Cancer Cell International.* 3, 15. doi: 10.1186/1475-2867-3-15

Rodvold, J. J., and Zanetti, M. (2016). Tumor microenvironment on the move and the Aselli connection. *Sci. Signaling.* 9, fs13. doi: 10.1126/scisignal.aag2279

Sánchez-Bailón, M. P., Calcabrini, A., Mayoral-Varo, V., Molinari, A., Wagner, K. U., Losada, J. P., et al. (2015). Cyr61 as mediator of Src signaling in triple negative breast cancer cells. *Oncotarget* 6, 13520–13538. doi: 10.18632/oncotarget.3760

Schober, J. M., Chen, N., Grzeszkiewicz, T. M., Jovanovic, I., Emeson, E. E., Ugarova, T. P., et al. (2002). Identification of integrin alpha(M)beta(2) as an adhesion receptor on peripheral blood monocytes for Cyr61 (CCN1) and connective tissue growth factor (CCN2): immediate-early gene products expressed in atherosclerotic lesions. *Blood.* 99, 4457–4465. doi: 10.1182/blood.v99.12.4457

Su, J. L., Chiou, J., Tang, C. H., Zhao, M., Tsai, C. H., and Chen, P. S. (2010). CYR61 regulates BMP-2-dependent osteoblast differentiation through the {alphav}{beta3}integrin/integrin-linked kinase/ERK pathway. *J. Biol. Chem.* 285, 31325–31336. doi: 10.1074/jbc.M109.087122

Teng, Y. N., Dong, R. Q., Wang, B. J., Liu, H. J., Jiang, Z. M., Wei, C. M., et al. (2011). Determinations of mifepristone and its metabolites and their pharmacokinetics in healthy female Chinese subjects. *Acta Pharmaceutica Sinica* 46, 1241–1245. doi: 10.1210/jcem-68-2-270

Torre, L. A., Bray, F., Siegel, R. L., Ferlay, J., Lortet-Tieulent, J., and Jemal, A. (2015). Global cancer statistics. *CA Cancer J. Clin.* 65, 87–108. doi: 10.3322/caac.21262

Valastyan, S., and Weinberg, R. A. (2011). Tumor metastasis: molecular insights and evolving paradigms. *Cell.* 147, 275–292. doi: 10.1016/j.cell.2011.09.024

Wang, J., Chen, J., Wan, L., Shao, J., Lu, Y., Zhu, Y., et al. (2014). Synthesis, spectral characterization, and in vitro cellular activities of metapristone, a potential cancer metastatic chemopreventive agent derived from mifepristone (RU486). *Aaps Journal.* 16 (2), 289–298. doi: 10.1208/s12248-013-9559-2

Wein, L., and Loi, S. (2017). Mechanisms of resistance of chemotherapy in early-stage triple negative breast cancer (TNBC). *Breast.* 34 Suppl 1, S27–S30. doi: 10.1016/j.breast.2017.06.023

Wu, P., Ma, G., Zhu, X., Gu, T., Zhang, J., Sun, Y., et al. (2017). Cyr61/CCN1 is involved in the pathogenesis of psoriasis vulgaris *via* promoting IL-8 production by keratinocytes in a JNK/NF-κB pathway. *Clin. Immunol.* 174, 53–62. doi: 10.1016/j.clim.2016

Xie, D., Miller, C. W., O'Kelly, J., Nakachi, K., Sakashita, A., Said, J. W., et al. (2001). Breast cancer. Cyr61 is overexpressed, estrogen-inducible, and associated with more advanced disease. *J. Biol. Chem.* 276, 14187–14194. doi: 10.1074/jbc.M009755200

Yang, R., Chen, Y., and Chen, D. (2018). Biological functions and role of CCN1/Cyr61 in embryogenesis and tumorigenesis in the female reproductive system (Review). *Mol. Med. Rep.* 17, 3–10. doi: 10.3892/mmr.2017.7880

Yu, S., Yang, X., Zhu, Y., Xie, F., Lu, Y., Yu, T., et al. (2015a). Systems pharmacology of mifepristone (RU486) reveals its 47 hub targets and network: Comprehensive analysis and pharmacological focus on FAK-Src-Paxillin complex. *Sci. Rep.* 5, 7830. doi: 10.1038/srep07830

Yu, S., Cao, H., Shen, B., and Feng, J. (2015b). Tumor-derived exosomes in cancer progression and treatment failure. *Oncotarget.* 6, 37151–37168. doi: 10.18632/oncotarget.6022

Yu, S., Yan, C., Yang, X., He, S., Liu, J., Qin, C., et al. (2016). Pharmacoproteomic analysis reveals that metapristone (RU486 metabolite) intervenes E-cadherin and vimentin to realize cancer metastasis chemoprevention. *Sci. Rep.* 6, 22388. doi: 10.1038/srep22388

Zeng, X., Zhang, Y., Xu, H., Zhang, T., Xue, Y., and An, R. (2018). Secreted frizzled related protein 2 modulates epithelial-mesenchymal transition and stemness *via* Wnt/β-Catenin signaling in choriocarcinoma. *Cell Physiol. Biochem.* 50, 1815–1831. doi: 10.1159/000494862

Conflict of Interest: The authors declare that the research was conducted in the absence of any commercial or financial relationships that could be construed as a potential conflict of interest.

frontiers in Pharmacology

ORIGINAL RESEARCH
published: 10 March 2020
doi: 10.3389/fphar.2020.00252

Ancient Chinese Medicine Herbal Formula Huanglian Jiedu Decoction as a Neoadjuvant Treatment of Chemotherapy by Improving Diarrhea and Tumor Response

*Yau-Tuen Chan[1], Fan Cheung[1], Cheng Zhang[1], Bowen Fu[1], Hor-Yue Tan[1], Hisayoshi Norimoto[2], Ning Wang[1] and Yibin Feng[1]**

[1] School of Chinese Medicine, Li Ka Shing Faculty of Medicine, The University of Hong Kong, Pokfulam, Hong Kong,
[2] PuraPharm International (H.K.) Ltd., Shatin, Hong Kong

Background: Diarrhea is a major gastrointestinal complication in cancer patients receiving chemotherapy. Prognosis and treatment of chemotherapy-induced diarrhea (CID) remain unsatisfactory. This study aims to explore the potential of an ancient Chinese Medicine herbal formula Huanglian Jiedu Decoction (HLJDD) as an adjuvant treatment on CID.

Method: HLJDD extract was prepared by GMP manufacturing standard with quality and stability being checked. 5-fluorouracil (5-Fu) and irinotecan (CPT-11)-induced diarrhea model in mice was established and pre-, co- and post-treatment of HLJDD was implemented. Mechanism of action was explored by detecting related protein expression. In addition, the effect of HLJDD on diarrhea and tumor response induced by clinical regimens FOLFOX and FOLFIRI was measured in murine orthotopic colorectal cancer model.

Results: HLJDD exhibited consistency in quality and stability after 24-month storage. Pre-treatment of HLJDD, but not co-treatment or post-treatment, could significantly improve the diarrhea score, body weight loss and intestinal damage in 5-Fu- and CPT-11-treated mice. Pre-treatment of HLJDD reduced cell apoptosis in the intestine of chemotherapy-treated mice, and promoted renewal of intestinal cell wall. CD44 was predicted as the potential target of HLJDD-containing compounds in CID. HLJDD pre-treatment induced presentation of CD44-postive cells in the intestine of chemotherapy-treated mice, and initiated expression of stemness-associated genes. Transcriptional products of the downstream Wnt signaling of CD44 were elevated. Furthermore, pre-treatment of HLJDD could significantly improve the tumor response of clinical chemotherapy regimens FOLFOX and FOLFIRI in orthotopic colorectal cancer, and reduce diarrhea and intestinal damage. Conclusion: Our study suggests the potential of HLJDD as a neoadjuvant treatment of chemotherapy by reducing diarrhea and improving tumor response.

Keywords: Huanglian Jiedu decoction, chemotherapy-induced diarrhea, 5-fluorouracil, irinotecan, tumor response

OPEN ACCESS

Edited by:
Hardeep Singh Tuli, Maharishi Markandeshwar University, India

Reviewed by:
Javad Sharifi-Rad, Shahid Beheshti University of Medical Sciences, Iran
Manoj Nepal, Sentara Norfolk General Hospital, United States

***Correspondence:**
Yibin Feng
yfeng@hku.hk

Specialty section:
This article was submitted to Pharmacology of Anti-Cancer Drugs, a section of the journal Frontiers in Pharmacology

Received: *17 December 2019*
Accepted: *24 February 2020*
Published: *10 March 2020*

Citation:
Chan Y-T, Cheung F, Zhang C, Fu B, Tan H-Y, Norimoto H, Wang N and Feng Y (2020) Ancient Chinese Medicine Herbal Formula Huanglian Jiedu Decoction as a Neoadjuvant Treatment of Chemotherapy by Improving Diarrhea and Tumor Response. Front. Pharmacol. 11:252. doi: 10.3389/fphar.2020.00252

INTRODUCTION

Cancer chemotherapy is one of the most common non-surgical cancer therapeutic approaches (Mishra et al., 2018; Ribas and Wolchok, 2018; Levine and Kroemer, 2019; Tang et al., 2019). It works specifically by damaging the cancer cells or slowing down their growth, yet it is accompanied with patient discontinuation problem due to the associated adverse events and drug resistance. Highly proliferative tissues such as gastrointestinal mucosa, skin and hematopoietic system may be the non-specific targets of chemotherapeutic agents leading to early stage of toxicities, and late adverse effects referring to the low proliferating tissues which further leads to fibrosis, neuronal, vascular and respiratory damage (Di Fiore and Van Cutsem, 2009). Gastrointestinal toxicity is often reported when the chemotherapy disrupts the colon permeability and intestinal mucosal structure. The most common symptoms of chemotherapy induced GI toxicity are diarrhea, vomiting, anorexia, and nausea (Mitchell, 2006). Chemotherapy induced diarrhea (CID) is a result of intestinal mucosa damage, which repeatedly triggers apoptotic and inflammatory events in intestinal epithelium and bowel wall. CID may be life threatening due to the continuous loss of electrolytes and fluids accompanied with malnutrition (Stein et al., 2010).

Accumulating studies have demonstrated that Chinese herbal medicines could be adjunct therapy for cancer patients, predominantly in reducing cancer therapy-associated adverse effects and thereby improving life quality (Chen et al., 2016; Gou et al., 2016). A recent double-blinded randomized study demonstrated that intervention of Chinese herbal medicine for breast or colon cancer patients significantly reduced chemotherapy associated GI toxicity, nausea in particular (Mok et al., 2007). Another Chinese herbal formulation, PHY906 which employed by practitioners for GI complications, showed promising outcome in reducing irinotecan induced GI toxicity. Previous clinical studies have shown intervention by PHY906 reduced the incidence of CPT-11 associated diarrhea (Kummar et al., 2011) and phase II clinical trial is currently conducted at U.S. on metastatic colorectal cancer patients who undergoing chemotherapy (Health, 2019). As opposed to prevention of the intestinal damage incurred by CPT-11, PHY906 recovers the functions of intestinal cells through increased progenitor cells regeneration and blocked CPT-11 induced inflammation (Lam et al., 2010).

HLJDD is composed of four Chinese herbal species, which includes *Coptis chinensis* Franch, *Phellodendron amurense* Rupr, *Gardenia jasminoides* J. Ellis and *Scutellaria baicalensis* Georgi and constructed by a total of 29 major single constituents. It has been reported to associate with various pharmacological activities such as arthritis, type II diabetes and ischemic stroke (Hu et al., 2013; Wang et al., 2013; Zhang et al., 2014). Our recent work has also demonstrated the inhibitory effect of HLJDD in cancer growth and angiogenesis in xenograft murine model through inactivation of eEF2 activity (Wang et al., 2015). Furthermore, previous studies postulated that HLJDD exerts protective effect on indomethacin-triggered intestinal damage by reducing inflammation related adenosine deaminase activity (Watanabe-Fukuda et al., 2009). In this study, we for the first time evaluated the possibility of using HLJDD for the treatment of CID. We chose 5-fluororacial (5-Fu) and irinotecan (CPT-11), which were commonly used as first-line chemotherapy in cancer treatment but were frequently reported to induce diarrhea in patients, to establish the animal model of CID. Effects on different treatments of HLJDD were systemically evaluated while its mechanism of action was proposed by computational prediction and validated by experimental approaches. Notably, the combination of HLJDD with clinical used chemotherapy regimens to improve tumor regression and reduce CID was studied in an orthotopic colorectal cancer model.

MATERIALS AND METHODS

Chemicals, Reagents and Antibodies

5-Fu (Sigma-Aldrich, United States), oxaliplatin (Selleckchem, United States), Folinic acid (Sigma-Aldrich, United States), CPT-11 (Selleckchem, United States) and loperamide were obtained by purchase.

Preparation of HLJDD and Quality Control

Preparation of HLJDD was performed in Good Manufacturing Practice according to our previous studies (Wang et al., 2015). 0.1 g powdered extract of HLJDD was precisely weighed by analytical balance, and then dissolved in 10 mL 50% Methanol-H_2O. Samples were then sonicated for 30 min to get completely dissolved followed by centrifugation at 4,000 rpm for 10 min. 1 ml of supernatant was filtered with 0.45 μm filter. Preparation was conducted in triplicate. 2.0 mg of reference chemicals, including berberine, baicalin and geniposide, were precisely weighed and dissolved in 10 mL 50% Methanol-H_2O. Samples and reference chemicals were analyzed with rapid separation liquid chromatography-combined diode array detector (RSLC-DAD, UltiMate^{TM} 3000, Thermofisher, United States). Separation was performed on C18 HPLC/UHPLC column provided by ACE (100 × 2.1 mm) with mobile phase shown in **Table 1**. The flow rate is 0.5 mL/min. The amounts of berberine, baicalin, phellodendrine and geniposide in HLJDD extracts at 1-, 3-, 6-, 12-, and 24-storage were quantified.

Chemotherapy-Induced Diarrhea Model in Mice

Study protocol has been approved by the Committee on the Use of Live Animals in Teaching and Research (CULATR) of the University of Hong Kong (Ref. No: 4433-17). Chemotherapeutic treatment was designed to closely imitate the clinical regimens. To establish the 5-Fu-induced CID model, mice were given intraperitoneal injection of 50 mg/kg 5-Fu solution for the first 4 days and had a 3-day rest. The 5-Fu treatment cycle was repeated once. To establish the CPT-11-induced CID model, mice were given intraperitoneal injection of 125 mg/kg CPT-11 solution for the first 3 days and had a 4-day rest. The CPT-11 treatment cycle was repeated once. In both models, pre-, co-, and post-treatment of HLJDD would be tested. In each treatment,

TABLE 1 | Chromatography separation program.

Time (min)	Acetonitrile (%)	0.05% KH_2PO_4, 0.05% TEA in H_2O, pH2.5 (%)
0	5	95
1	5	95
3	6	94
7	6	94
10	10	90
15	15	85
19	15	85
20	16	84
25	16	84
28	23	77
35	65	35

daily oral gavages of 50, 100, 200 mg/kg HLJDD for 2 weeks were tested (**Figures 2A**, **3A**).

Orthotopic Colorectal Cancer Model in Mice

Study protocol has been approved by the CULATR of the University of Hong Kong (Ref. No.: 4505-17). The orthotopic implantation of colorectal cancer mice model was established according to literature report (Tseng et al., 2007). In brief, colon cancer cell HT-29 transfected with luciferase reporter was subcutaneously injected to the left flank of athymic nude mice. When the cells formed around 1-cm^3 tumors, mice were sacrificed by overdose of pentobarbital (200 mg/kg, intraperitoneally). Tumor was dissected out and cut into 2-mm^3 pieces. A small cube of tumor was then implanted into the cecum of mice. One week after implantation, mice were screened under live animal imager to confirm formation of orthotopic tumor. Qualified mice were randomized and given treatment for 4 weeks. Mice received either 200 mg/kg/day HLJDD or same volume of water via oral gavage for the first weeks, then were given FOLFOX or FOLFIRI chemotherapy regimens for another 2 weeks. Treatment frequency and doses of the chemotherapeutic regimen were set accordingly to the clinical usage and literature report of the particular regimen. Loperamide in the positive control group was given during chemotherapy.

Measurement of Diarrhea and Intestinal Damage

A grading system for diarrhea will be used to score the diarrhea severity every 3 days. The scoring system can be interpreted as follows, (0) (no diarrhea): solid stool with no sign of soiling around the anus. The stool is very firm when subjected to pressure with tweezers; (1) (very mild diarrhea): formed stools that appear moist on the outside, and no sign of soiling around the anus. Stool is less firm when considerable pressure applied with tweezers; (2) (mild diarrhea): formed stools that appear moist on the outside, and some signs of soiling around anus. Stools will easily submit to pressure applied with tweezers; (3) (diarrhea): no formed stools with a mucous-like appearance. Considerable soiling around the anus and the fur around tail. Mouse takes a long time to pass stool; (4) (severe, watery diarrhea): mostly clear or mucous-like liquid stool with very minimal solid present and considerable soiling around anus (Pearson et al., 2013).

1.0 cm samples of jejunum will be collected and fixed in 4% paraformaldehyde. And samples will be processed for hematoxylin-eosin (H&E) staining and analyzed by two independent trained histologists. Patho-morphological changes in intestinal sections will be scored as: 4: Severe; 3: Markedly abnormal; 2: Moderate; 1: Mild; or 0: Normal (Kojouharov et al., 2014).

Immunofluroscence

Paraffin-embedded sections were rehydrated and antigens on the sections were retrieved with citric buffer (10 mM Sodium Citrate, 0.05% Tween 20, pH 6.0) via at 100°C for 5 min. After washing, the tissues were blocked with 10% normal goat serum in PBS supplemented with 0.5% Tween 20. Primary antibodies (1:100 v/v dilution in blocking buffer) were then applied and incubated overnight at 4°C. Then appropriate secondary antibodies were added. Expression of related protein targets were then examined under confocal microscope (LSM780, Carl Zeiss, Germany). 4′,6-diamidino-2-phenylindole (DAPI) was used to stain the cell nuclei. TUNEL assay was performed with ApoBrdU DNA Fragmentation Assay (Biovision, United States).

Quantitative Real-Time PCR

Total RNA from tissue was extracted with Trizol method (Invitrogen, United States). cDNA was prepared with first strand synthesis kit (Takara, Japan). Quantitative real-time PCR was performed with SYBR master mix (Takara, Japan) on the LC480 platform (Roche, United States). Primers used in this study were listed in **Table 2**.

Data Mining

The interaction between components from HLJDD and protein targets was retrieved from the Comparative Toxicogenomics Database (CTD[1]). Meanwhile, the sequencing data in Gene Expression Omnibus (GEO) database GSE28873 and GSE11722 was accessed to retrieved genes of intestine cells being regulated

[1]http://ctdbase.org/

TABLE 2 | Primer list.

Gene	Forward primer	Reverse primer
Lgr5	TCTTCACCTCCTACC TGGACCT	GGCGTAGTCTGCTATG TGGTGT
Olfm4	CCAGCTGGAGGTGG AGATAA	GCTGATGTTCACCA CACCAC
Wnt3	CAAGCACAACAATGA AGCAGG	TCGGGACTCACGGTG TTTCTC
Axin2	GAGTAGCGCCGTGTTA GTGACT	CCAGGAAAGTCCGGAAGA GGTATG
Fzd5	CTTGTTTCCAAAGTCCAAT CAAGTG	GCCTACTCTTCACCCTTC TTTAACG
Pygo2	GTTTGGGCTGTCCTGAA AGTCTG	ATAAGGGCGCCGAA AGTTGA

commonly by 5-Fu and CPT-11. Venn analysis was performed to gain a group of a common gene of the three lists[2].

Statistical Analysis

Data was present as Mean ± SD. Differences were measured with an ordinary two-way ANOVA with LSD multiple comparisons, with $p < 0.05$ was considered statistically significant.

RESULTS

HLJDD Is Consistent in Quality and Suitable for Long-Time Storage

To ensure the quality of HLJDD used in this study, we established a chromatographic fingerprint (**Figure 1A**) of the formula. Three major components, berberine from Coptidis Rhizoma and Phellodendri Chinensis Cortex., baicalin from Scutellaria baicalensis Georgi and geniposide from Gardenia jasminoides Ellis, were selected as chemical markers for the quality control. We first of all tested the inter-batch consistence of HLJDD produced by GMP manufacturer via quantifying berberine, baicalin and geniposide in three batches of the extracts, and found no significant difference in amount of each compound among three batches of HLJDD (**Figure 1B**). Then the stability of HLJDD kept at ordinary indoor environment for 1, 3, 6, 12, and 24 months was measured. The amounts of berberine, baicalin and geniposide remained unchanged after 24-month storage (**Figure 1C**). These data suggest that production of HLJDD in GMP manufacturing is reproducible in batches and the extracts are suitable for up to 2 years storage under ordinary indoor condition.

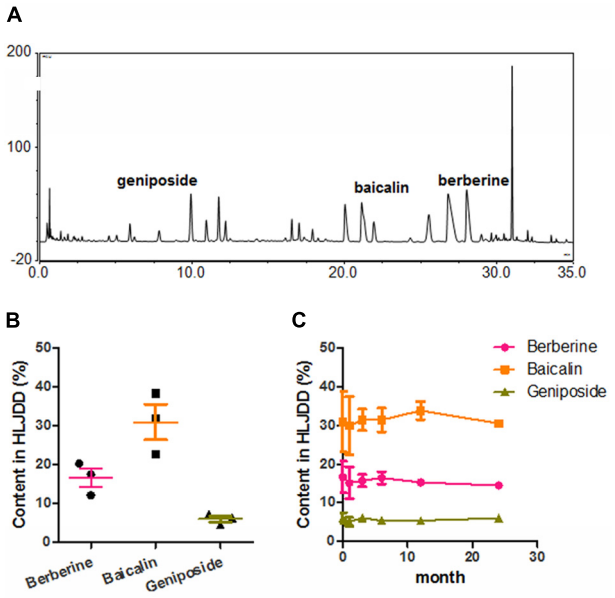

FIGURE 1 | Quality control of HLJDD. **(A)** Showed the representative chromatogram of HLJDD extracts. Three major compounds, berberine, baicalin and geniposide, were identified on the chromatogram by matching the retention time and UV spectrum with those of reference compounds; **(B)** showed the inter-batches quality of HLJDD as represented by the relative contents of berberine, baicalin and geniposide; **(C)** showed that stability of HLJDD over 24-month storage as represented by the relative contents of berberine, baicalin, and geniposide.

Pre-treatment of HLJDD Improved 5-Fu-Induced Diarrhea and in Mice

HLJDD has been reported to possess various biological activities and was proposed to potentially treat diseases such as diabetes (Chen et al., 2018), hepatic damage (Wei et al., 2018), ischemic stroke (Zhang et al., 2017), and cancer (Wang et al., 2015). To determine if oral administration of HLJDD can relieve CID, we established 5-Fu-induced intestine damage model with some modification on previous published protocol (Sakai et al., 2013). Pre-treatment, co-treatment and post-treatment of HLJDD with 5-Fu were tested and the scheme was shown in **Figure 2A**. Significant reduction in body weight of mice treated with 5-Fu was observed. We also observed a significant increase of diarrhea. Two-week pre-treatment of HLJDD potently prevented 5-Fu-induced body weight loss as well as diarrhea in mice in a dose-dependent manner, and 200 mg/kg HLJDD pretreatment for 2 weeks showed optimal effect. The diarrhea scores dropped to below 2 in the high-dose group, which signified a very mild to mild diarrhea condition in that group. In comparison to the model groups that were having a condition of score 4, which represented very severe diarrhea symptoms. Co-treatment or post-treatment of HLJDD did not show significant effect on 5-Fu-induced body weight loss nor diarrhea in mice (**Figures 2B,C**).

[2]http://bioinformatics.psb.ugent.be/webtools/Venn/

The protective effect of pre-treatment of HLJDD was further proven by the histological analysis on intestine structure, which revealed that mice with HLJDD pre-treatment exhibited more normal and intact microscopic intestine structure, while co-treatment or post-treatment of HLJDD can minimally protect intestine tissue from 5-Fu-induced damage (**Figure 2D** and **Table 3**). These observations suggested that pre-treatment of HLJDD before using chemotherapeutic agent 5-Fu could reduce undesired side effects.

Pre-treatment of HLJDD Improved CPT-11-Induced Diarrhea in Mice

CPT-11 is clinically observed to induce frequent diarrhea in patients undergoing chemotherapy of CPT-11-containing regimens. To test if HLJDD can prevent diarrhea induced by CPT-11, we established the CPT-11-induced diarrhea model of mice with some modifications on previously published protocol (Xue et al., 2007). Pre-treatment, co-treatment and post-treatment of HLJDD with CPT-11 were tested and the regimen was illustrated as in **Figure 3A**. Consistent with 5-Fu, CPT-11 could significantly induce body weight loss in mice. Pre-treatment of HLJDD exhibited potent improvement on the loss of body weight and diarrhea control induced by CPT-11 in a dose dependent manner. Similar to its action in 5-Fu-induced diarrhea model, co-treatment and post-treatment of HLJDD could not achieve body weight gain of CPT-11-treated mice

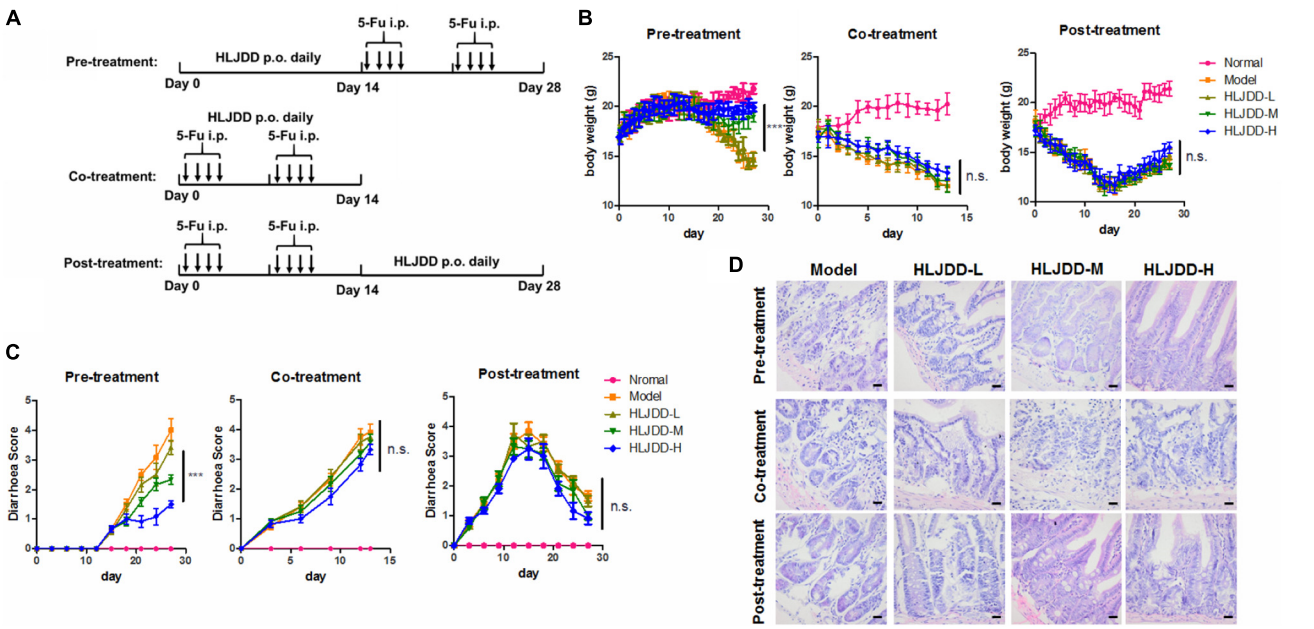

FIGURE 2 | Pre-treatment but not co-treatment or post-treatment of HLJDD improved 5-Fu-induced diarrhea. **(A)** Showed the treatment scheme; **(B)** showed that pre-treatment but not co-treatment or post-treatment of HLJDD improved body weight loss induced by 5-Fu; **(C)** showed that pre-treatment but not co-treatment or post-treatment of HLJDD improved diarrhea score induced by 5-Fu; **(D)** showed that pre-treatment but not co-treatment or post-treatment of HLJDD improved the histological structure of jejunum damaged by 5-Fu. ***$p < 0.001$ when compared with the model group.

(**Figure 3B**), nor reverse the situation in CPT-11-induced mice diarrhea (**Figure 3C**). Histological analysis suggested that pre-treatment but not co-treatment or post-treatment of HLJDD can preserve the microscopic intestine structure of CPT-11-treated mice (**Figure 3D** and **Table 4**). These observations suggested that pre-treatment of HLJDD could prevent diarrhea induced by chemotherapeutic agent CPT-11.

HLJDD Accelerated Intestine Cell Proliferation and Renewal During Chemotherapy-Induced Diarrhea

To further understand the action of pre-treated HLJDD on CID, we applied TUNEL to measure the DNA damage in intestine segments. It was found that both 5-Fu and CPT-11 could significantly induce DNA damage of intestinal cells, as indicated by the presence of TUNEL-positive cells in the intestine segments, while pre-treatment of HLJDD dose-dependently reduce the number of TUNEL-positive cells, suggesting pre-treatment of HLJDD may accelerate the disappearance of damaged cells (**Figure 4A**). The clearance of damage cells was further evidenced by the observation that less expression of apoptotic marker caspase-3 (**Figure 4B**). As HLJDD did not directly contact with chemotherapy, we then supposed that the disappearance of apoptotic cells in the intestine segments was possibly attributed by the accelerated replacement of dead cells by newly proliferative cells in the intestine of HLJDD-treated mice. Ki67 was used to stain the newly proliferative cells in the intestine segments. It was shown that pre-treatment of HLJDD could increase the presence of Ki67-positive proliferative cells in the intestine of 5-Fu and CPT-11-treated mice (**Figure 4C**). These findings suggest that pre-treatment of HLJDD could recover crypt cells in the intestine segments by accelerating its proliferation and renewal, which may contribute to its prevention on CID.

TABLE 3 | Overall histological score of jejunum of 5-Fu-treated mice.

Group	Pre-treatment	Co-treatment	Post-treatment
Normal	0.000 ± 0.000	0.000 ± 0.000	0.000 ± 0.000
Model	3.400 ± 0.2828	3.350 ± 0.3536	2.350 ± 0.3536
HLJDD-L	3.450 ± 0.2121	3.350 ± 0.2121	2.250 ± 0.6364
HLJDD-M	2.600 ± 0.2828*	3.000 ± 0.2828	2.050 ± 0.4950
HLJDD-H	1.600 ± 0.1414**	3.050 ± 0.3536	1.900 ± 0.5657

*$p < 0.05$, **$p < 0.01$ when compared with the model group.*

HLJDD Promoted the Expression of Intestinal Progenitor Cell Markers After Chemotherapy

To further understand the mechanism of action, we first identified the genes of intestine cells being regulated commonly by 5-Fu and CPT-11 by accessing the sequencing data in Gene Expression Omnibus (GEO) database. Expression of genes with significant changes after 5-Fu (GSE28873) and CPT-11 (GSE11722) treatment were analyzed and common genes were highlighted (**Figure 5A**). Prediction of genes being regulated by compounds within HLJDD was extracted from the Comparative

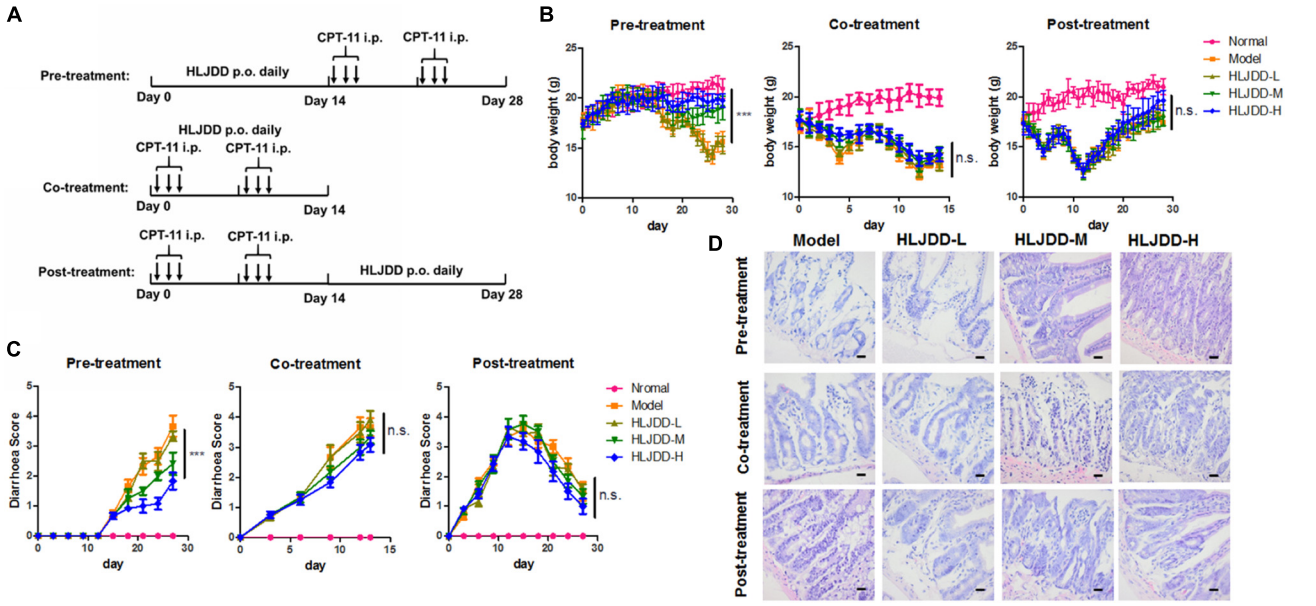

FIGURE 3 | Pre-treatment but not co-treatment or post-treatment of HLJDD improved CPT-11-induced diarrhea. **(A)** Showed the treatment scheme; **(B)** showed that pre-treatment but not co-treatment or post-treatment of HLJDD improved body weight loss induced by CPT-11; **(C)** showed that pre-treatment but not co-treatment or post-treatment of HLJDD improved diarrhea score induced by CPT-11; **(D)** showed that pre-treatment but not co-treatment or post-treatment of HLJDD improved the histological structure of jejunum damaged by CPT-11. ***$p < 0.001$ when compared with the model group.

Toxicogenomics Database (CTD)[3]. By overlapping the gene lists, we found that CD44 and CAV1 are HLJDD-regulated common genes in 5-Fu and CPT-11-treated intestine. CD44-postive cells in the intestine represent a group of progenitor cells that keeps self-renewal activity and could rapidly differentiate into crypt cells (**Figure 5B**). We then stained the intestine with antibody to CD44, and observed that pre-treatment of HLJDD could significantly increase the CD44-positive cells at the bottoms of the crypts when mice were exposed to 5-Fu and CPT-11, suggesting that HLJDD pre-treatment may potentiate the progenitor cells in the intestine segments in 5-Fu/CPT-11-treated mice (**Figure 5C**). This was further proven by the observation that the mRNA expression of stem cell makers such as Lgr5, Ascl2 and Olfm4 were significantly induced in the intestine of HLJDD pre-treated mice (**Figure 5D**). As CD44 and Lgr5 were reported as the upstream molecules of Wnt/β-catenin signaling (Su et al., 2016; Zhang et al., 2018), we then measured if pre-treatment of HLJDD resulted in activation of Wnt/β-catenin pathway in the intestine segments of 5-Fu/CPT-11-treated mice. Interestingly, in mice without 5-Fu/CPT-11 treatment, HLJDD pre-treatment had no potential effect in elevating the Wnt/β-catenin signaling, but it could significantly induce mRNA expression of Wnt/β-catenin signaling products including Wnt3, Fzd5, Axin2 and Pygo2 (**Figure 5E**). Our data suggests that HLJDD could promote the repopulation of intestine progenitor cells after chemotherapy probably through activating Wnt/β-catenin signaling.

[3]http://ctdbase.org/

HLJDD Improved Tumor Inhibition of Clinical 5-Fu/CPT-11-Containing Chemotherapy Regimens in Colorectal Cancer Model

5-Fu and CPT-11 are chemotherapeutic agents commonly used in a combing regimen in the clinical treatment of colorectal cancer. Clinical oncologists and physicians designed some common combinations based on the condition of cancer patients, which include FOLFOX and FOLFIRI. To examine if pre-treatment of HLJDD benefits chemotherapy of colorectal cancer in terms of improving treatment outcomes and reducing diarrhea, we established an orthotopic colorectal cancer model in athymic nude mice followed by HLJDD plus FOLFOX/FOLFIRI treatment (**Figure 6A**). Loperamide, which was a clinically first-line treatment of chemotherapy-induced diarrhea, was introduced as positive control (Andreyev et al., 2014). Significant increase of luciferase signal intensity was observed in control group, indicating that tumor grew fast in the absence of

TABLE 4 | Overall histological score of jejunum of CPT-11-treated mice.

Group	Pre-treatment	Co-treatment	Post-treatment
Normal	0.000 ± 0.000	0.000 ± 0.000	0.000 ± 0.000
Model	3.650 ± 0.3536	3.450 ± 0.3536	2.450 ± 0.0707
HLJDD-L	0.3450 ± 0.2121	3.500 ± 0.1414	2.600 ± 0.288
HLJDD-M	2.220 ± 0.2828**	3.350 ± 0.2121	2.050 ± 0.2121
HLJDD-H	1.850 ± 0.0707**	3.650 ± 0.3536	2.000 ± 0.1414

**$p < 0.01$ when compared with the model group.

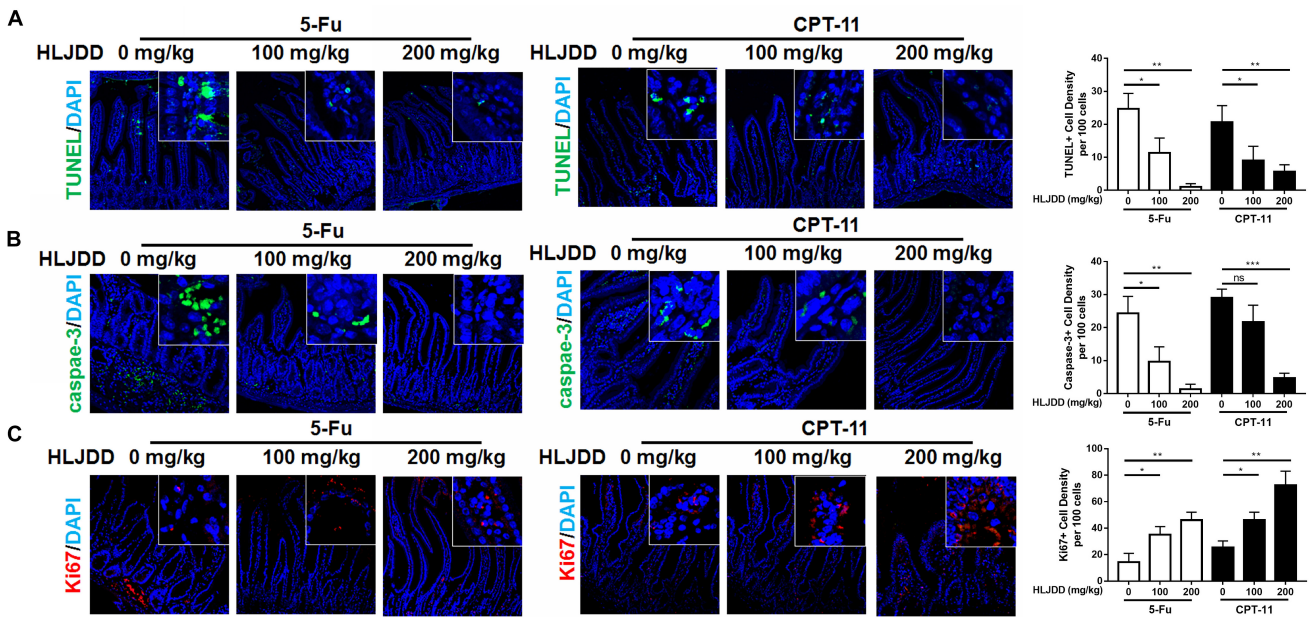

FIGURE 4 | Pre-treatment of HLJDD reduced intestinal cell apoptosis and improved renewal in chemotherapy-treated mice. **(A)** Showed that pre-treatment of HLJDD could significantly reduce the positive TUNEL signal in the intestinal section of chemotherapy-treated mice; **(B)** showed that pre-treatment of HLJDD could significantly reduce the expression of cleaved caspases-3 in the intestinal section of chemotherapy-treated mice; **(C)** showed that pre-treatment of HLJDD could significantly improve the renewal-associated Ki67 expression in the intestinal section of chemotherapy-treated mice. $^{*}p < 0.05$, $^{**}p < 0.01$, $^{***}p < 0.001$ when compared with the model group.

any treatment. FOLFOX or FOLFIRI treatment may reduce the tumor signal in some extent. Loperamide co-treatment have no significant effect on further reducing tumor growth rate in the presence of chemotherapy regimen, while pre-treatment of HLJDD showed further suppression to tumor growth (**Figures 6B,C**). In addition, Moderate-to-severe diarrhea was observed 3 days after chemotherapeutic regimens started. As the FOLFIRI regimen contains more diarrhea-inducing chemotherapeutic agents (especially CPT-11) than FOLFOX, the earlier initiation of diarrhea was predictable. Co-treatment of loperamide can significantly reduce the diarrhea caused by chemotherapy. Pre-treatment of HLJDD exhibited compatible effect in reducing diarrhea to loperamide, suggesting the potential of HLJDD as a prophylactic treatment to FOLFIRI-induced diarrhea (**Figure 6D**). Intestine damage was observed in mice of treatment group. While loperamide cannot significantly improve the intestine damage, Mice with HLJDD pre-treatment exhibited improved intestine integrity (**Figure 6E** and **Table 5**). These data suggest that HLJDD could enhance the clinical 5-Fu/CPT-11-containing chemotherapy regimens in the treatment of colorectal cancer model via improving treatment outcomes and reducing diarrhea.

DISCUSSION

Chemotherapy-induced diarrhea is common in cancer patients under treatment. According to a recent review, the frequency of serious CID (with grading at 3–4) is 5–47% in clinical trials. Grade 1-2 diarrhea is more commonly observed in patients receiving chemotherapeutic agents. Furthermore, some target therapeutic agents and monoclonal antibodies are reported with frequent incidences of diarrhea in patients (Andreyev et al., 2014). Economic burden of CID was estimated to be US$6,600 for every outpatients care of grade 4 diarrhea, according to a recent review based on 22 published articles (Tarricone et al., 2016). CID was observed in 50–80% of patients receiving chemotherapy, which may result in deviation from the planned chemotherapy schedule, leading to chemotherapy failure. Severe CID may be life-threatening (Stein et al., 2010). The diarrhea condition represented by the diarrhea score was significantly alleviated in the HLJDD treated groups, especially in the 200 mg/kg group, from 4 to below 2 ($p < 0.01$). Very promising anti-CID effect was observed by HLJDD in mice model, and it is believed that the same effect could be reproduced with amended dose in human population.

Although CID is frequently observed as an established gastrointestinal side effect of cancer chemotherapy, there is few studies trying to understand its pathological mechanisms. It was suggested that changes of gut microbiota and secretion of mucin would result in CID (Stringer et al., 2007; Li et al., 2017). It was also claimed that CID could be a result of intestinal mucosa damage, which repeatedly trigger apoptotic and inflammatory events in intestinal epithelium and bowel wall (Lee et al., 2014). Notably, some recent studies have highlighted the role of intestinal progenitor cells in the crypts in the regeneration and integrity of intestinal epithelium. Due to the rapid renewal property, intestinal progenitor cells are easily but

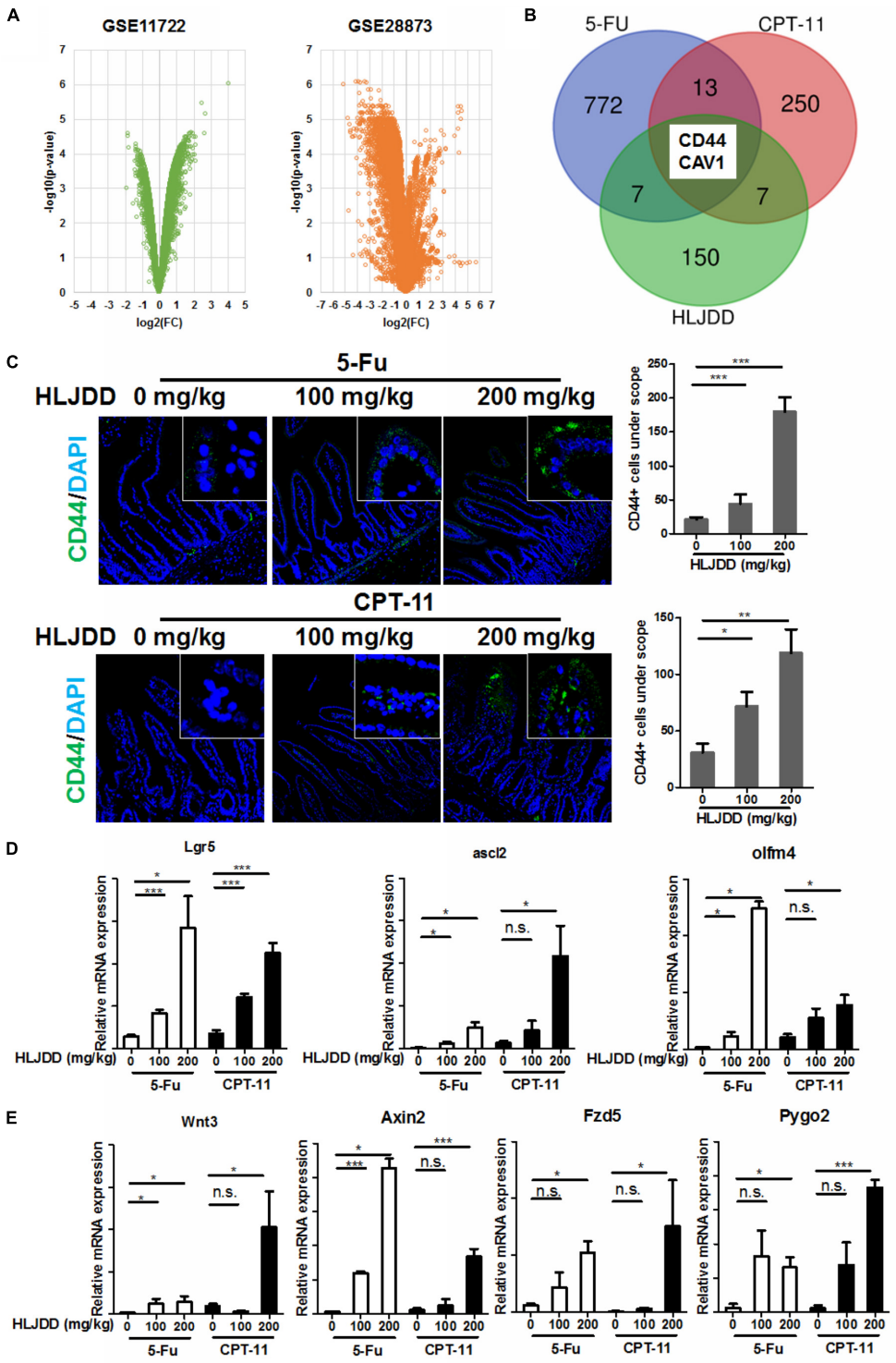

FIGURE 5 | Pre-treatment induced CD44 expression and activation of its downstream Wnt signaling in the intestinal cell of chemotherapy-treated mice. **(A)** showed the volcano plots of gene expression in the intestine challenged by 5-Fu (GSE28873) and CPT-11 (GSE11722). Genes with relative expression of log2(fold change) > 1 and log10(*p*-value) > 2 were shortlisted; **(B)** showed overlapped of genes with significant expression change after 5-Fu and CPT-11 treatment, and genes with expression affected by compounds in HLJDD. Tow genes, CD44 and CAV1, were the common genes among the three populations; **(C)** showed that pre-treatment of HLJDD could significantly improve the CD44 expression in the intestinal section of chemotherapy-treated mice; **(D)** showed that expression of stemness-related gene, including lgr5, ascl2 and oflm4 in the intestine cells in the intestine of chemotherapy-treated mice was induced by pre-treatment of HLJDD; **(E)** showed that expression of Wnt pathway-related genes, including Wnt3, Axin2, Fzd5 and Pygo2, in the intestine cells in the intestine of chemotherapy-treated mice was induced by pre-treatment of HLJDD; $^{*}p < 0.05$, $^{**}p < 0.01$, $^{***}p < 0.001$ when compared with the model group.

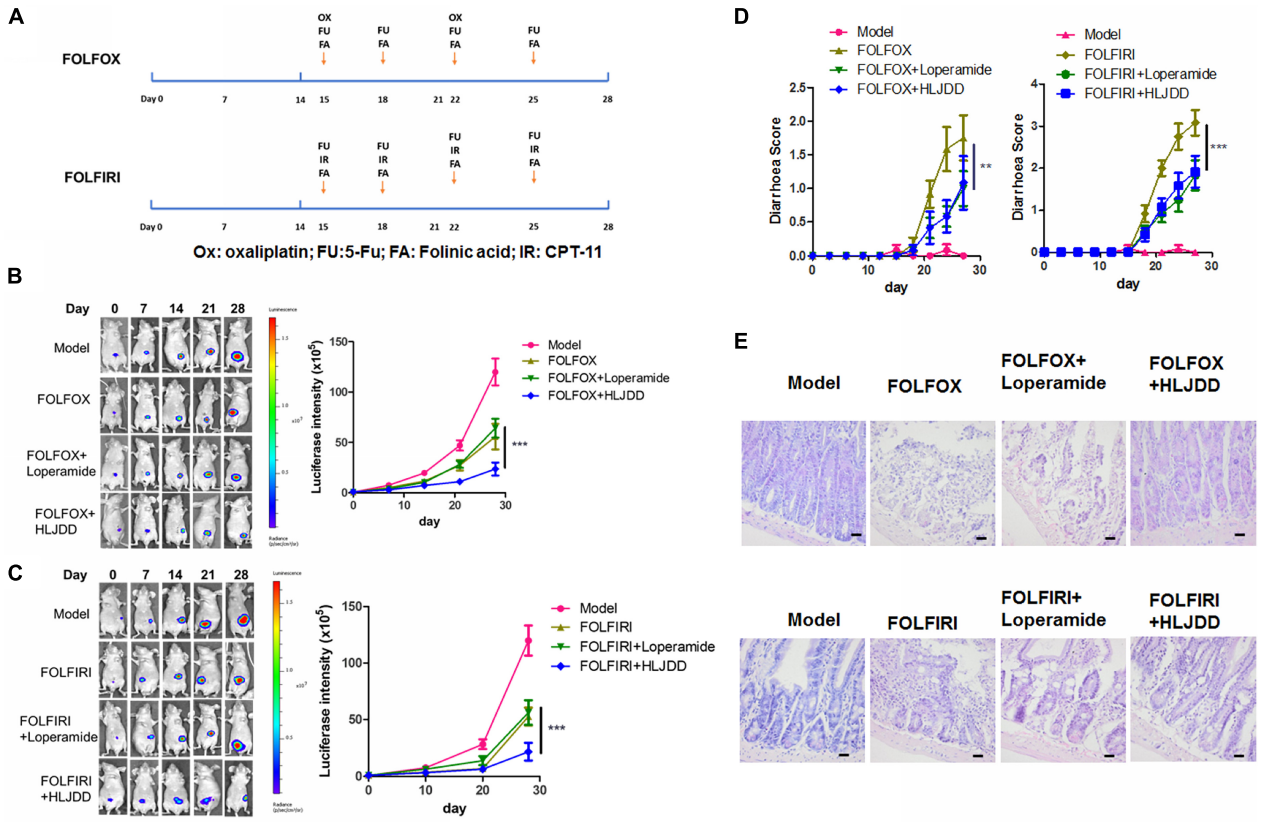

FIGURE 6 | Pre-treatment of HLJDD improved tumor response and diarrhea in clinical chemotherapy regimens FOLFOX- and FOLFIRI-treated colon cancer in mice. **(A)** Showed the regimen plan of FOLFOX and FOLFIRI; **(B,C)** showed that 2-week pretreatment of HLJDD at 200 mg/kg could significantly potentiate the tumor suppressive effect FOLFOX and FOLFIRI on orthotopic colon cancer; **(D)** showed that 2-week pretreatment of HLJDD at 200 mg/kg could significantly improve the diarrhea induced by FOLFOX and FOLFIRI; **(E)** showed that 2-week pretreatment of HLJDD at 200 mg/kg could improve the histological structure of jejunum in FOLFOX- and FOLFIRI-treated colon cancer in mice. $^{**}p < 0.01$, $^{***}p < 0.001$ when compared with the respective chemotherapy regimen group.

non-specifically targeted by the chemotherapeutic agents that aim to kill fast growing cancer cells. Previous studies have suggested that chemotherapeutic agents could induce apoptosis and inhibit proliferation of intestinal progenitor cells (Dekaney et al., 2009; Zhan et al., 2014). In our study, we observed that pre-treatment of HLJDD could significantly preserve intestinal progenitor cells in crypts of mice receiving chemotherapy by a notable increase in CD44+ cells under scope ($p < 0.01$). Given that HLJDD was not given simultaneously with chemotherapeutic agents, it is not possible that HLJDD renders any reduced absorption or abortion from the cells. Instead, HLJDD recovered the Wnt/β-catenin signaling activity in the CD44+ intestinal progenitor cells in the crypts of mice receiving chemotherapy ($p < 0.05$). Interestingly, HLJDD did not elevate the basic level of Wnt/β-catenin signaling in mice without chemotherapy but can sustain its activity during chemotherapy. Considering the continuous activation of Wnt/β-catenin signaling would be a risk of tumorigenesis (Joosten et al., 2017), HLJDD might not likely to expose the patients who are going to receive chemotherapy under a high risk of tumorigenesis. An unenviable confounding variable here was that the pre-treatment of HLJDD was given at the early stage of tumor development, while the co-treatment and post-treatment were given at relatively later stages. There could be possibly differences in action of HLJDD on the intestine.

5-Fu and CPT-11 are given systemically for anal, breast, colorectal, oesophageal, stomach, pancreatic and skin cancers. An early study of the efficacy and toxicity of irinotecan for patients with metastatic colorectal cancer reported that, approximately 56% of patients receiving CPT-11 demonstrated symptoms of diarrhea (grade 3-4) (Conti et al., 1996). Lenfers et al. (1999) even postulated as high as 86% of grade 3-4 diarrhea in patients receiving CPT-11 and 57% in patients with 5-FU. Combination treatment of leucovorin, 5-FU and CPT-11 showed improvement

TABLE 5 | Overall histological score of jejunum of FOLFOX- and FOLFIRI-treated mice.

Group	FOLFOX	FOLFIRI
Model	0.5500 ± 0.3536	0.4000 ± 0.1414
Chemotherapy regimen	4.350 ± 0.7778	4.850 ± 0.2121
Loperamide	4.550 ± 0.2121	4.400 ± 0.7071
HLJDD	2.300 ± 0.7071*	2.800 ± 0.4243*

$p < 0.05$ when compared with the respective chemotherapy regimen group.

in survival and response rate of metastatic colorectal cancer patients, however, the incidence rate of grade 3 diarrhea is 13.2% and grade 4 diarrhea is approximately 7% (Saltz et al., 2000). There are not many publications directly studying the chemo-regimens FOLFOX and FOLFIRI in animal model. According to the few papers regarding the use of chemotherapeutic regimens in animal (Robinson et al., 2013a,b), we designed and adjusted the dose and treatment frequency of chemotherapeutic agents. Using the orthotopic colorectal cancer model, we validated that the modified FOLFOX and FOLFIRI can well mimic the clinical efficacy and intestine toxicity in patients. The successful translation of FOLFOX and FOLFIRI regimen from clinical setting to animal model would offer a good reference for the further studies of strategies in improving chemotherapy in colorectal cancers.

Official guideline of management of CID is yet available, though some tentative protocols have been recommended based on literature review by multidisciplinary team (Andreyev et al., 2014). Current clinical treatment of CID includes loperamide and octreotide. Administration of loperamide remains to be the first line treatment and subcutaneous injection of octreotide together with antibiotics will be intervened for patients who failed high doses of loperamide and developed grade 3-4 symptoms (Benson et al., 2004). In our study, we tested loperamide as a positive control to stop diarrhea in colorectal cancer mice treated with chemotherapy regimens. Although it could significantly prevent the occurrence of diarrhea during chemotherapy, loperamide is not likely beneficial to the tumor regression by FOLFOX or FOLFIRI given its mechanism of antidiarrheal effect. Interestingly, the tumor growth was restricted during HLJDD treatment, indicating that the synergistic effect of HLJDD may be the result of its prophylactic control before patients go into chemotherapeutic regimen. In addition, pre-treatment of HLJDD can significantly alleviate diarrhea and intestine damage induced by chemotherapeutic regimens. Considering its efficacy and safety, HLJDD may be potentially an adjuvant treatment to chemically relevant treatments of colorectal cancer.

With regards to the long history of HLJDD usage in traditional Chinese medicine for thousands of years, the safety of this prescription on patient is unquestionably assured. Before the clinical application of HLJDD to reduce the side effects as well as enhance tumor response with chemotherapy such as 5FU and CPT-11, its efficacy on human population should be justified in human clinical trial. A randomized double-blind controlled study to compare the effect of HLJDD to a placebo could be an option. Notably, although HLJDD was experimentally demonstrated to be effective on reducing CID, more clinical data reporting benefits in future study are needed before application as adjuvant to cancer treatment in patients. Every action of intaking medicine should be consulted by practitioners.

CONCLUSION

We systemically evaluated the potential of a Chinese herbal formula HLJDD as prophylactic treatment of CID. Quality and stability of the herbal extract of HLJDD was assessed by chemical fingerprinting, and no apparent degradation of major active compounds in the decoction after 24-month storage was shown. Pre-treatment but not co- or post-treatment of HLJDD could dose-dependently prevent body weight loss, diarrhea and intestinal damage induced by chemotherapeutic agents 5-Fu and CPT-11. This effect of HLJDD has been correlated with reduced intestinal cell apoptosis and improvement of cell renewal. Target identification suggested that CD44 level in renewing crypt cells could be maintained by HLJDD pre-treatment, and restoration of CD44 improved certain level of Wnt-signaling pathway activity to maintain the rapid cell renewal for repairing the intestinal wall during chemotherapy. In addition, pre-treatment of HLJDD improved the efficacy of 5-Fu and CPT-11-containing chemotherapeutic regimens FOLFOX and FOLFIRI in suppressing orthotopic tumor growth of human colorectal cancer. Our study sheds light on the potential of HLJDD as a neoadjuvant treatment for chemotherapy by improving diarrhea and tumor response.

DATA AVAILABILITY STATEMENT

Publicly available datasets were analyzed in this study, these can be found in the Comparative Toxicogenomics Database (CTD, http://ctdbase.org/); the NCBI Gene Expression Omnibus (GEO) database (GSE28873 and GSE11722).

ETHICS STATEMENT

The animal study was reviewed and approved by Committee on the Use of Live Animals in Teaching and Research (CULATR) of the University of Hong Kong.

AUTHOR CONTRIBUTIONS

YF and NW designed and conceived the study. Y-TC, CZ, H-YT, BF, and NW did experiments and analyzed the data. HN provided standardized extract of HLJDD. Y-TC, FC, NW, and YF drafted the manuscript. All authors revised and confirmed the manuscript.

FUNDING

This study was supported by Research Grant Council, HKSAR (Project code: RGC GRF 17152116), Commissioner for Innovation Technology, HKSAR (Project code: ITS/091/16FX), and Health and Medical Research Fund (HMRF, project code: 15162961 and 16172751).

REFERENCES

Andreyev, J., Ross, P., Donnellan, C., Lennan, E., Leonard, P., Waters, C., et al. (2014). Guidance on the management of diarrhoea during cancer chemotherapy. *Lancet Oncol.* 15, e447–e460. doi: 10.1016/S1470-2045(14)70006-3

Benson, A. B. III, Ajani, J. A., Catalano, R. B., Engelking, C., Kornblau, S. M., Martenson, J. A., et al. (2004). Recommended guidelines for the treatment of cancer treatment-induced diarrhea. *J. Clin. Oncol.* 22, 2918–2926. doi: 10.1200/jco.2004.04.132

Chen, M., Liao, Z., Lu, B., Wang, M., Lin, L., Zhang, S., et al. (2018). Huang-Lian-Jie-Du-Decoction ameliorates hyperglycemia and insulin resistant in association with gut microbiota modulation. *Front. Microbiol.* 9:2380. doi: 10.3389/fmicb.2018.02380

Chen, X., Deng, L., Jiang, X., and Wu, T. (2016). Chinese herbal medicine for oesophageal cancer. *Cochrane Database. Syst. Rev.* 1:Cd004520. doi: 10.1002/14651858.CD004520.pub7

Conti, J. A., Kemeny, N. E., Saltz, L. B., Huang, Y., Tong, W. P., Chou, T. C., et al. (1996). Irinotecan is an active agent in untreated patients with metastatic colorectal cancer. *J. Clin. Oncol.* 14, 709–715. doi: 10.1200/jco.1996.14.3.709

Dekaney, C. M., Gulati, A. S., Garrison, A. P., Helmrath, M. A., and Henning, S. J. (2009). Regeneration of intestinal stem/progenitor cells following doxorubicin treatment of mice. *Am. J. Physiol. Gastrointest. Liver Physiol.* 297, G461–G470. doi: 10.1152/ajpgi.90446.2008

Di Fiore, F., and Van Cutsem, E. (2009). Acute and long-term gastrointestinal consequences of chemotherapy. *Best Pract. Res. Clin. Gastroenterol.* 23, 113–124. doi: 10.1016/j.bpg.2008.11.016

Gou, H., Gu, L. Y., Shang, B. Z., Xiong, Y., and Wang, C. (2016). Protective effect of Bu-Zhong-Yi-Qi decoction, the water extract of Chinese traditional herbal medicine, on 5-fluorouracil-induced intestinal mucositis in mice. *Hum Exp Toxicol.* 35, 1243–1251. doi: 10.1177/0960327115627686

Health (2019). A Phase II Multicenter, Randomized, Placebo Controlled, Double Blinded Clinical Study of KD018 as. (a)Modulator of Irinotecan Chemotherapy in Patients With Metastatic Colorectal Cancer [Online]. Available at: https://clinicaltrials.gov/ct2/show/NCT00730158 (accesed May 22, 2019).

Hu, Y., Hu, Z., Wang, S., Dong, X., Xiao, C., Jiang, M., et al. (2013). Protective effects of Huang-Lian-Jie-Du-Tang and its component group on collagen-induced arthritis in rats. *J. Ethnopharmacol.* 150, 1137–1144. doi: 10.1016/j.jep.2013.10.038

Joosten, S. P. J., Zeilstra, J., van Andel, H., Mijnals, R. C., Zaunbrecher, J., Duivenvoorden, A. A. M., et al. (2017). MET signaling mediates intestinal crypt-villus development, regeneration, and adenoma formation and is promoted by stem cell CD44 isoforms. *Gastroenterology* 153:1040-1053e44. doi: 10.1053/j.gastro.2017.07.008

Kojouharov, B. M., Brackett, C. M., Veith, J. M., Johnson, C. P., Gitlin, I. I., Toshkov, I. A., et al. (2014). Toll-like receptor-5 agonist Entolimod broadens the therapeutic window of 5-fluorouracil by reducing its toxicity to normal tissues in mice. *Oncotarget* 5, 802–814. doi: 10.18632/oncotarget.1773

Kummar, S., Copur, M. S., Rose, M., Wadler, S., Stephenson, J., O'Rourke, M., et al. (2011). A phase I study of the chinese herbal medicine PHY906 as a modulator of irinotecan-based chemotherapy in patients with advanced colorectal cancer. *Clin. Colorectal Cancer* 10, 85–96. doi: 10.1016/j.clcc.2011.03.003

Lam, W., Bussom, S., Guan, F., Jiang, Z., Zhang, W., Gullen, E. A., et al. (2010). The four-herb Chinese medicine PHY906 reduces chemotherapy-induced gastrointestinal toxicity. *Sci. Transl. Med.* 2:45ra59. doi: 10.1126/scitranslmed.3001270

Lee, C. S., Ryan, E. J., and Doherty, G. A. (2014). Gastro-intestinal toxicity of chemotherapeutics in colorectal cancer: the role of inflammation. *World J. Gastroenterol.* 20, 3751–3761. doi: 10.3748/wjg.v20.i14.3751

Lenfers, B. H., Loeffler, T. M., Droege, C. M., and Hausamen, T. U. (1999). Substantial activity of budesonide in patients with irinotecan (CPT-11) and 5-fluorouracil induced diarrhea and failure of loperamide treatment. *Ann. Oncol.* 10, 1251–1253. doi: 10.1023/a:1008390308416

Levine, B., and Kroemer, G. (2019). Biological functions of autophagy genes: a disease perspective. *Cell* 176, 11–42. doi: 10.1016/j.cell.2018.09.048

Li, H. L., Lu, L., Wang, X. S., Qin, L. Y., Wang, P., Qiu, S. P., et al. (2017). Alteration of gut microbiota and inflammatory cytokine/chemokine profiles in 5-fluorouracil induced intestinal mucositis. *Front. Cell Infect. Microbiol.* 7:455. doi: 10.3389/fcimb.2017.00455

Mishra, A. P., Salehi, B., Sharifi-Rad, M., Pezzani, R., Kobarfard, F., Sharifi-Rad, J., et al. (2018). Programmed cell death, from a cancer perspective: an overview. *Mol. Diagnosis Ther.* 22, 281–295. doi: 10.1007/s40291-018-0329-9

Mitchell, E. P. (2006). Gastrointestinal toxicity of chemotherapeutic agents. *Semin. Oncol.* 33, 106–120. doi: 10.1053/j.seminoncol.2005.12.001

Mok, T. S., Yeo, W., Johnson, P. J., Hui, P., Ho, W. M., Lam, K. C., et al. (2007). A double-blind placebo-controlled randomized study of Chinese herbal medicine as complementary therapy for reduction of chemotherapy-induced toxicity. *Ann. Oncol.* 18, 768–774. doi: 10.1093/annonc/mdl465

Pearson, J. S., Giogha, C., Ong, S. Y., Kennedy, C. L., Kelly, M., Robinson, K. S., et al. (2013). A type III effector antagonizes death receptor signalling during bacterial gut infection. *Nature* 501, 247–251. doi: 10.1038/nature12524

Ribas, A., and Wolchok, J. D. (2018). Cancer immunotherapy using checkpoint blockade. *Science* 359:1350. doi: 10.1126/science.aar4060

Robinson, S. M., Mann, D. A., Manas, D. M., Oakley, F., Mann, J., and White, S. A. (2013a). The potential contribution of tumour-related factors to the development of FOLFOX-induced sinusoidal obstruction syndrome. *Br. J. Cancer* 109, 2396–2403. doi: 10.1038/bjc.2013.604

Robinson, S. M., Mann, J., Vasilaki, A., Mathers, J., Burt, A. D., Oakley, F., et al. (2013b). Pathogenesis of FOLFOX induced sinusoidal obstruction syndrome in a murine chemotherapy model. *J. Hepatol.* 59, 318–326. doi: 10.1016/j.jhep.2013.04.014

Sakai, H., Sagara, A., Matsumoto, K., Hasegawa, S., Sato, K., Nishizaki, M., et al. (2013). 5-Fluorouracil induces diarrhea with changes in the expression of inflammatory cytokines and aquaporins in mouse intestines. *PLoS One* 8:e54788. doi: 10.1371/journal.pone.0054788

Saltz, L. B., Cox, J. V., Blanke, C., Rosen, L. S., Fehrenbacher, L., Moore, M. J., et al. (2000). Irinotecan plus fluorouracil and leucovorin for metastatic colorectal cancer. Irinotecan study group. *N. Engl. J. Med.* 343, 905–914. doi: 10.1056/NEJM200009283431302

Stein, A., Voigt, W., and Jordan, K. (2010). Chemotherapy-induced diarrhea: pathophysiology, frequency and guideline-based management. *Ther. Adv. Med. Oncol.* 2, 51–63. doi: 10.1177/1758834009355164

Stringer, A. M., Gibson, R. J., Bowen, J. M., Logan, R. M., Yeoh, A. S., and Keefe, D. M. (2007). Chemotherapy-induced mucositis: the role of gastrointestinal microflora and mucins in the luminal environment. *J. Support Oncol.* 5, 259–267.

Su, J., Wu, S., Wu, H., Li, L., and Guo, T. (2016). CD44 is functionally crucial for driving lung cancer stem cells metastasis through Wnt/beta-catenin-FoxM1-Twist signaling. *Mol. Carcinog.* 55, 1962–1973. doi: 10.1002/mc.22443

Tang, Z. M., Liu, Y. Y., He, M. Y., and Bu, W. B. (2019). Chemodynamic therapy: tumour microenvironment-mediated fenton and fenton-like reactions. *Angewandte Chem. Int. Ed.* 58, 946–956. doi: 10.1002/anie.201805664

Tarricone, R., Abu Koush, D., Nyanzi-Wakholi, B., and Medina-Lara, A. (2016). A systematic literature review of the economic implications of chemotherapy-induced diarrhea and its impact on quality of life. *Crit. Rev. Oncol. Hematol.* 99, 37–48. doi: 10.1016/j.critrevonc.2015.12.012

Tseng, W., Leong, X., and Engleman, E. (2007). Orthotopic mouse model of colorectal cancer. *J. Vis. Exp.* 10:484. doi: 10.3791/484

Wang, N., Feng, Y., Tan, H. Y., Cheung, F., Hong, M., Lao, L., et al. (2015). Inhibition of eukaryotic elongation factor-2 confers to tumor suppression by a herbal formulation Huanglian-Jiedu decoction in human hepatocellular carcinoma. *J. Ethnopharmacol.* 164, 309–318. doi: 10.1016/j.jep.2015.02.025

Wang, P. R., Wang, J. S., Zhang, C., Song, X. F., Tian, N., and Kong, L. Y. (2013). Huang-Lian-Jie-Du-Decotion induced protective autophagy against the injury of cerebral ischemia/reperfusion via MAPK-mTOR signaling pathway. *J. Ethnopharmacol.* 149, 270–280. doi: 10.1016/j.jep.2013.06.035

Watanabe-Fukuda, Y., Yamamoto, M., Miura, N., Fukutake, M., Ishige, A., Yamaguchi, R., et al. (2009). Orengedokuto and berberine improve indomethacin-induced small intestinal injury via adenosine. *J. Gastroenterol.* 44, 380–389. doi: 10.1007/s00535-009-0005-2

Wei, D. D., Wang, J. S., Duan, J. A., and Kong, L. Y. (2018). Metabolomic assessment of acute cholestatic injuries induced by thioacetamide and by bile duct ligation, and the protective effects of Huang-Lian-Jie-Du-decoction. *Front Pharmacol* 9:458. doi: 10.3389/fphar.2018.00458

Xue, H., Sawyer, M. B., Field, C. J., Dieleman, L. A., and Baracos, V. E. (2007). Nutritional modulation of antitumor efficacy and diarrhea toxicity

related to irinotecan chemotherapy in rats bearing the ward colon tumor. *Clin. Cancer Res.* 13, 7146–7154. doi: 10.1158/1078-0432.CCR-07-0823

Zhan, Y. S., Tan, S. W., Mao, W., Jiang, J., Liu, H. L., and Wu, B. (2014). Chemotherapy mediates intestinal injury via p53/p53 upregulated modulator of apoptosis (PUMA) signaling pathway. *J. Dig. Dis.* 15, 425–434. doi: 10.1111/1751-2980.12157

Zhang, J., Cai, H., Sun, L., Zhan, P., Chen, M., Zhang, F., et al. (2018). LGR5, a novel functional glioma stem cell marker, promotes EMT by activating the Wnt/beta-catenin pathway and predicts poor survival of glioma patients. *J. Exp. Clin. Cancer Res.* 37:225. doi: 10.1186/s13046-018-0864-6

Zhang, Q., Wang, J., Liao, S., Li, P., Xu, D., Lv, Y., et al. (2017). Optimization of Huang-Lian-Jie-Du-decoction for ischemic stroke treatment and mechanistic study by metabolomic profiling and network analysis. *Front. Pharmacol.* 8:165. doi: 10.3389/fphar.2017.00165

Zhang, X. J., Deng, Y. X., Shi, Q. Z., He, M. Y., Chen, B., and Qiu, X. M. (2014). Hypolipidemic effect of the Chinese polyherbal Huanglian Jiedu decoction in type 2 diabetic rats and its possible mechanism. *Phytomedicine* 21, 615–623. doi: 10.1016/j.phymed.2013.11.004

Conflict of Interest: HN was employed by the company PuraPharm International (H.K.) Ltd.

The remaining authors declare that the research was conducted in the absence of any commercial or financial relationships that could be construed as a potential conflict of interest.

frontiers in Pharmacology

ORIGINAL RESEARCH
published: 13 March 2020
doi: 10.3389/fphar.2020.00322

Antiproliferative Effects of *Roylea cinerea* (D. Don) Baillon Leaves in Immortalized L6 Rat Skeletal Muscle Cell Line: Role of Reactive Oxygen Species Mediated Pathway

Astha Bhatia[1], Harpal Singh Buttar[2], Rohit Arora[3], Balbir Singh[4], Amritpal Singh[4], Sarabjit Kaur[4] and Saroj Arora[1]*

[1] Department of Botanical and Environmental Sciences, Guru Nanak Dev University, Amritsar, Punjab, India, [2] Department of Pathology and Laboratory Medicine, Faculty of Medicine, University of Ottawa, Ottawa, ON, Canada, [3] Department of Biochemistry, Sri Guru Ram Das University of Health Sciences, Amritsar, Punjab, India, [4] Department of Pharmaceutical Sciences, Guru Nanak Dev University, Amritsar, Punjab, India

OPEN ACCESS

Edited by:
Hardeep Singh Tuli, Maharishi Markandeshwar University, Mullana, India

Reviewed by:
Pradeep Kumar Singh Visen, Independent Researcher, Scarborough, ON, Canada
Munish Garg, Maharshi Dayanand University, India
Harpreet Walia, DAV University, India

***Correspondence:**
Saroj Arora
sarojarora.gndu@gmail.com

Specialty section:
This article was submitted to Pharmacology of Anti-Cancer Drugs, a section of the journal Frontiers in Pharmacology

Received: *28 December 2019*
Accepted: *05 March 2020*
Published: *13 March 2020*

Citation:
Bhatia A, Singh Buttar H, Arora R, Singh B, Singh A, Kaur S and Arora S (2020) Antiproliferative Effects of Roylea cinerea (D. Don) Baillon Leaves in Immortalized L6 Rat Skeletal Muscle Cell Line: Role of Reactive Oxygen Species Mediated Pathway. Front. Pharmacol. 11:322. doi: 10.3389/fphar.2020.00322

Roylea cinerea (D. Don) Baill. (Lamiaceae) is an indigenous plant of Western Himalayas, and has been used by the native population for the treatment of various diseases such as fever, malaria, diabetes, jaundice, and skin ailments. However, limited proportion of pharmacological and toxicological information is available on the bioactive properties of this plant. Therefore, the present study was designed to explore the anti-oxidant and anti-proliferative activities of *Roylea cinerea*. Methanolic extracts of leaves and stem of *Roylea cinerea* were prepared through maceration procedure and evaluated for the antioxidant activity using hydrogen/electron donating and hydroxyl radical scavenging assay. Significant antioxidant activity was observed for the methanolic extract of leaves in DPPH (EC_{50} 239 μg/ml), molybdate ion reduction assay (29.73 μg ascorbic acid equivalent/mg dry weight of extract) as well as in plasmid nicking assay. Anti-proliferative and apoptotic activity in L6 rat skeletal muscle cell line was done using *in vitro* assays, i.e., MTT, Lactate dehydrogenase, mitochondrial membrane potential assay along with phase contrast, confocal, and scanning electron microscopy. The methanol extract of leaves and stem inhibited the growth of L6 cells with IC_{50} value of 69.41μg/ml and 124.93 μg/ml, respectively, and the lactate dehydrogenase activity was 20.29% and 0.3%, respectively. Cell cycle analysis by flow cytometry exhibited the arrest of cells in G1 and sub-G1 phase by methanolic leaves extract. Furthermore, the results of microscopic and docking analysis strengthened the observation made in the present study regarding the apoptotic mode of cell death in the L6 cell line. The *in vitro* findings of our studies revealed that the bioactive ingredients present in the methanolic extract of leaves and stem of *Roylea cinerea* have the anticancer potential. Further *in vivo* studies are needed to verify the *in vitro* results.

Keywords: ***Roylea cinerea* (D. Don) Baill., antioxidant, L6, confocal, cell cycle, apoptosis**

INTRODUCTION

Reactive oxygen species (ROS) are normally produced in the body from the mitochondria and are often termed as 'redox messengers'. The ROS form an integral part of various intracellular signaling pathways. However, enhanced exposure to xenobiotics and oxidative stress generate prodigious levels of ROS, which in the absence of antioxidant defense pathways can attack cell membrane and alter the structure of cellular macromolecules, protein functioning and may also cause mutations in cellular DNA. Several studies have confirmed the relationship between elevated levels of ROS and carcinogenesis (Weinberg, 1989). The multistep process of carcinogenesis commences through disturbed homeostasis between deviant proto-oncogenes activation and suppression of tumor suppressor genes with critical pathways and biomarkers (Rashid, 2017). Cancer chemoprevention edges on unraveling the potent cost-effective anticancer agents that can specifically influence cellular transformations in the early stages. Despite numerous beneficial effects of synthetic drugs, naturally occurring phytochemicals are preferred as potential anticancer therapies considering the lesser toxicity and fewer side effects.

Naturally occurring phytochemicals have been used in the management of numerous chronic and non-communicable diseases, including cancer and cardiometabolic disorders, and have currently become an important area of research and drug discovery programmes. Basic studies have shown that initiation of cancer is a multistep process that involves tumor initiation, and promotion followed by its progression (Basu, 2018). Extensive efforts are required to unravel the complete mechanism of anti-cancer agents which involves several underlying intracellular signaling cascades. In this context, tailored supplementation of phytochemicals can target these unregulated pathways to inhibit such cellular complications or induce programmed cell death or apoptosis including cyclin dependent kinases and many growth factors. Phytochemicals based anticancer therapies can act as an effective alternative to healthcare costs and side effects in the treatment of cancer with synthetic drugs with an advantage of being inexpensive and accessible. For example, phytochemicals may prevent the carcinogenic effect by capturing the free radicals, and by detoxifying the carcinogen and preventing them to reach the target sites. These natural products may also influence tumor suppressor genes and stimulate the innate immune system, including apoptosis, thereby inhibiting the cellular proliferation pathways and activating various targets such as mitogen-activated protein kinases (MAPKs) and ICE/Ced-3 family proteases (caspases, Singh et al., 2016; Chikara et al., 2018).

Roylea cinerea (D. Don) Baillon belongs to the family Lamiaceae. It is an indigenous herb, native to India and grows at an altitude of 1200-3700 m in the Western Himalayas and at the foothills of Nepal. This phytomedicinal plant has been used as a febrifuge, tonic for contusions as well as for treating diabetes mellitus, malaria, and skin diseases (Dobhal and Joshi, 1979; Khare, 2007; Rawat and Vashistha, 2013). The petroleum ether and the chloroform extracts from leaves of *Roylea cinerea* (D. Don) Baillon have been reported with antiplasmodial activity (Dua et al., 2011). The branches of the plant are found to be useful in the treatment of jaundice in infants. Its flowers are used in winters for snuffing to cure coughs (Parkash and Aggarwal, 2010). Several phytochemical compounds have been isolated from the aerial parts of the plant such as labdane-diterpenoids: calyenone, epicalyone, calyone, and precalyone, cinereanoid A, cinereanoid B (Prakash et al., 1979; Sharma et al., 2015); moronic acid (Majumder et al., 1979); cinereanoid C, cinereanoid D, β-lactam, flavonoid glycosides: rutin, isoquercetin, nicotiflorin, martynoside, undatuside A and 50-β-D-glucopyranosyloxyjasmonic acid (Sharma et al., 2017); from chloroform fraction: pilloin, 1-methylindole-3-carboxaldehyde, β-sitosterol, and stigmasterol (Sharma et al., 2015). The compound precalyone (a diterpene) isolated from *Roylea calycina* syn *cinerea* (aerial plant parts) showed anticancer activity up to 143% at concentration of 50 mg/kg in P-388 lymphocytic leukemia in mice in a study conducted (Rastogi and Dhawan, 1990; Pundir and Mahindroo, 2019). Moreover, in another study reported, a target oriented binding analysis to active binding site of Hsp90 and Hsp70 protein which showed potential dual binding affinity of cinereanoid D at 0.1 mg/ml and 1 mg/ml concentration respectively to both the proteins (Sharma et al., 2017).

To the best of our knowledge, no detailed study is available regarding aerial parts of *Roylea cinerea* (D. Don) Baillon with anticancer and antiproliferative potential Thus, keeping in view the scanty literature and some preliminary studies available regarding anticancer potential of *Roylea cinerea* (D. Don) Baillon, the present study was conducted with an objective of unraveling the anticancer potential of methanolic extracts of *Roylea cinerea* (leaves and stem). Further, the mechanistic study was carried out to confirm antiproliferative and apoptotic activity of the methanolic leaves extract of *R. cinerea* in immortalized L6 rat skeletal muscle cell line *via in vitro* assays and microscopic analysis combined with docking analysis of phytoconstituents present in it with PI3K and antiapoptotic proteins (Bcl-2, Bcl-X_L).

METHODOLOGY

Plant Collection and Extraction

The plant material (leaves and stem) was collected from District Palampur, Himachal Pradesh, India during the month of May, 2016. The collected plant material was identified and submitted as a voucher specimen for authenticity in the Herbarium, Department of Botanical and Environmental Sciences, Amritsar, India (Accession no. 7376). The plant material (leaves and stem) was completely air dried, coarsely powdered and subjected to maceration procedure in methanol for 2–3 days with agitation at intervals. Literature studies support the use of alcoholic extracts for the extraction of secondary metabolites mainly for polyphenols from plant material as compared to water extracts due to higher extractive potential (Singh et al., 2019). After

maceration, the methanolic extracts were concentrated using rotary evaporator (IKA® RV 10) followed by air-drying and stored at −20°C until use.

Estimation of Total Phenolic Content

Total Phenolic Content was determined using Folin Ciocalteu method given by Yu et al. (2002) with slight modifications. The standard curve for gallic acid (12.5–1,600 μg/ml) was used to calculate the content and expressed as μg gallic acid equivalent/mg dry weight of the extract.

Estimation of Total Flavonoid Content

Total Flavonoid Content was determined using the method given by Kim et al. (2003) with slight modifications. The standard curve for rutin (12.5–1,600 μg/ml) was used to calculate the content and expressed as μg rutin equivalent/mg dry weight of the extract.

Antioxidant Activity

Hydrogen Donating Activity

Hydrogen donating activity was assessed *via* DPPH (2,2-diphenyl-1-picrylhydrazyl) free radical scavenging assay. The assay was performed as per the method given by Blois (1958) with minor modifications. The plant extracts (30 μl) with varying concentrations (25–1,000 μg/ml) was incubated with 200 μl of DPPH dissolved in methanol for 30 min at 37˚C. Following the incubation, the final absorbance was measured using Biotek multi-well plate reader at 517 nm against a blank solution. The % radical scavenging activity was calculated as:

$$(OD_{BLANK-}OD_{SAMPLE})/OD_{BLANK} \times 100$$

Gallic acid was used as standard and evaluated at a varying concentration (5–100 μg/ml)

Electron Donating Activity

Electron donating activity was assessed *via* molybdate ion reduction assay. Plant extracts were evaluated for their ability to reduce molybdate ion as per the method given by Prieto et al. (1999) with slight modifications. The extract (25 μl) was mixed with 250 μl reagent (0.6 M H_2SO_4, 28 mM sodium phosphate, and 4 mM ammonium molybdate). The final reaction mixture (300 μl) was heated at 95˚C for 1.5 h. The absorbance was read at 695 nm using Biotek multi-well plate reader. The antioxidant activity was calculated using a standard curve for ascorbic acid (20–200 μg/ml) and expressed in terms of ascorbic acid equivalents (**Supplementary Figure 6**).

Hydroxyl Scavenging Activity

The DNA nicking assay was performed according to Lee et al. (2002) with minor modifications. Fenton reagent (30 mM H_2O_2, 80 mM $FeCl_3$, 50 mM ascorbic acid) was used as a negative control. The plant extracts concentrations (12.5–400 μg/ml) were mixed with freshly prepared negative control and pBR 322 plasmid DNA. The final reaction mixture was made up to 20 μl using sterile distilled water. Electrophoresis was performed after loading different reaction mixtures into 1% agarose gel at 60 V for 1.5 h. Bands were visualized using the Gel Doc XR system (Bio-Rad, USA) and quantified using Gel Quant and Labimage Platform software (free version) software.

Antiproliferative Activity

MTT Assay

The plant extracts (leaves and stem) from *Roylea cinerea* (D. Don) Baill. were evaluated for their anti-proliferative activity in L6 skeletal muscle cell line using the method given by Liu et al. (2006) with minor modifications. The L6 cells were seeded in 96 well plate with a density of $10x10^3$ cells/well and incubated for 24 h. After incubation, cells were treated with varying concentration of plant extracts (25–1,600 μg/ml) for 24 h at 37°C and 5% CO_2. Following incubation, MTT (100 μl) was added to each well after carefully removing the media and further incubated for 4 h. Post-treatment, the solution was aspirated from each well and insoluble formazan was dissolved in DMSO (100 μl). The absorbance was recorded at 540 nm using Biotek Synergy HT multi-well plate reader against blank. The percentage inhibition was calculated as:

$$((OD_{BLANK-}OD_{SAMPLE})/OD_{BLANK} \times 100)$$

Growth inhibitory concentration (the concentration of the sample with 50% death of the cells, i.e., $G1_{50}$)

Lactate Dehydrogenase Assay

The cellular damage was assessed *via* the enzyme lactate dehydrogenase which is present in all cells and released rapidly during cell damage. The assay was performed according to the method given by Abe and Matsuki (2000) to evaluate cellular damage or cell death *via* necrosis. The cells were seeded with density $3x10^5$ in 24 well plate at 37˚C and 5% CO_2 for 24 h. After incubation, the cells were treated with GI_{50} and GI_{70} of plant extracts calculated from MTT assay for 24 h. Post-treatment, the supernatant (100 μl) was collected and transferred to 96 well plate followed by the addition of 100 μl LDH buffer (2.5 mg Lithium lactate, 2.5 mg NAD^+, Tris-HCl (pH 8.2) dissolved in 0.1% Triton-X; 100 μl MTT and 1 μl methoxyphenazine methosulfate). The reaction mixture was incubated for 30 min in dark followed by the addition of stop solution (100 μl) 1M acetic acid. Absorbance was read at 570 nm using Biotek Synergy HT multi-well plate reader against blank and % enzyme activity was calculated as:

$$((OD_{BLANK-}OD_{SAMPLE})/OD_{BLANK} \times 100)$$

Assesment of Cell Morphology Through Microscopic Studies

The morphological features of normal and apoptotic cells were examined through phase-contrast microscope as per the method given by Ramasamy et al. (2013). Nuclear morphology was analyzed by confocal microscopy using DAPI and Ethidium Bromide-acridine orange (EB/AO) to detect apoptotic cells (Kasibhatla et al., 2006). The cells were analyzed using the Nikon A1R Laser Scanning Confocal Microscope (Nikon

Corporation, Japan) with NIS-Elements AR analysis software (version 4.11.00). Scanning electron microscopy was performed as per the method given by Ye et al. (2012) to study the surface morphology of normal and apoptotic cells using scanning electron microscope (Carl Zeiss SUPRA55).

Intracellular Reactive Oxygen Species Content

ROS levels were determined in L6 rat skeletal muscle cells using DCFH-DA probe (Dichloro-dihydro-fluorescein diacetate) as per the method given by Deng et al., 2013 with slight modifications. Cells were cultured in a 6-well plate with density $5x10^5$ cells/well (2 ml) and incubated for 24 h. The cells were treated with IC_{30}, IC_{50}, and IC_{70} of *Roylea cinerea* (D. Don) Baill. methanolic leaves and stem extract for another 24 h. After treatment, cells were incubated for 30 min with the DCFH-DA probe (10 μg/ml) at 37°C in the CO_2 incubator. Following incubation, the cells were harvested and washed twice with 1x PBS (1 ml) and immediately observed for oxidative burst with Biotek multi-well plate reader for fluorescent intensity (485 nm excitation and 528 nm emission) as well as BD Accuri TM C6 Flow Cytometer (excitation 488 nm, emission 535 nm, FL-1 channel, events recorded 10,000 per sample), and the results obtained were expressed in terms of % intracellular ROS in cells.

Measurement of Mitochondrial Membrane Potential

MMP was determined in L6 rat skeletal muscle cells using Rhodamine-123 as per the method given by Deng et al. (2013) with slight modifications. Cells were cultured in a 6-well plate with density $5x10^5$cells/well (2 ml) and incubated for 24 h. The cells were treated for 24 h with IC_{30}, $IC_{50}$and IC_{70} of *Roylea cinerea* (D. Don) Baill. methanolic leaves and stem extract and incubated for 30 min with the Rhodamine-123 (10 μg/ml) at 37°C in the CO_2 incubator. Following incubation, cells were harvested and washed twice with 1x PBS (1 ml) and immediately observed with Biotek multi-well plate reader for fluorescent intensity (485 nm excitation and 528 nm emission) as well as BD AccuriTM C6 Flow Cytometer (excitation 511 nm, emission 535 nm, FL-1 channel, events recorded 10,000 per sample).

Cell Cycle Analysis

Cell cycle analysis was performed to analyze DNA content in different phases of cell cycle as per the method given by Jordan et al. (1996) with slight modifications. L6 cells plated in six well plate ($5x10^5$) were treated with various concentrations of *R. cinerea* leaves extract for 24 h. After treatment, cells were centrifuged to obtain a pellet and washed with chilled 500 μl of PBS. Further, the cells were fixed with 70% ethanol at 15°C for 30 min. After fixation, the cells were again centrifuged to obtain a pellet and washing step was repeated followed by incubation of cells with RNAase (10 μg/ml) and propidium iodide stain (10 μg/ml) for another 30 min. After incubation, cells were analyzed immediately for DNA content using BD AccuriTM C6 Cytometer (excitation 488 nm, emission 600 nm, FL2 channel, events recorded 10,000 per sample). The histogram obtained from cell cycle distribution was analyzed by BD AccuriTM C6 software and expressed in terms of % cells in each phase of cell cycle.

Molecular Docking Studies

The methanolic extract of leaves of *R. cinerea* exhibited substantial anti-proliferative activity, therefore the docking studies were carried out for the chemical constituents already reported in this plant (Sharma et al., 2015; Sharma et al., 2017). The chemical structure and molecules for which docking was carried out are provided in **Supplementary Figure 1**. Ligand structures were obtained from PubChem (https://pubchem.ncbi.nlm.nih.gov/search/search.cgi) and prepared using chemsketch tool. In this study, the protein structure of the target proteins PI3K (PDB ID: 1E8Z), Bcl2 (PDB ID: 4IEH), Bclxl (PDB ID: 4QNQ) and a binding pockets was obtained from the protein data bank (www.rcsb.org) (**Supplementary Figure 2**). The preparation of the target proteins was done using Swiss PDB viewer v4.1.0 involved energy minimization. Further, polar hydrogen atoms were added to target protein and for the computation of partial atomic charge using AutoDock4. Hetero-atoms present in the protein structures 1E8Z, 4IEH, and 4QNQ were removed prior to autodock analysis. The automated docking of specified ligands into protein binding pocket was done considering Gasteiger charges for each atom present in the target. Three-dimensional affinity grid size for 1E8Z was 51.201, 12.569, 28.184 (x, y, and z), for 4IEH was 14.216, 21.636, 11.709, and for 4QNQ was 52.232, 7.115, -11.211 used on the geometric center of the target protein. Docking algorithm was run using Cygwin software to obtain the binding energy data for each run. Visualization and analysis of the results were done using UCSF chimera 1.11rc.

Statistical Analysis

The data were analyzed using regression analysis and implemented by best-fit-model. The regression equation obtained was used for the calculation of TPC, TFC, EC_{50}, and GI_{50} values. In addition, one-way analysis of variances (ANOVA) and Tukey's test was employed for comparing means of different concentrations of the same extract assuming variances are equal using IBM SPSS version 16.0 software. The difference in % ROS and % depolarized cells between the control cells and treated cells was analyzed by Student's Independent t-test. The results were expressed as mean ± SE.

RESULTS AND DISCUSSION

Previous reports have confirmed the relation between the intake of natural phytochemicals and the low incidence of various diseases such as heart diseases, diabetes, cancer and the process of aging. Furthermore, medicinal plants demonstrating higher antioxidant activity have been reported to contain a high amount of phenolic compounds. Thus, such plants can act as a potential source of antioxidants to combat various diseases including cancer. A perusal of literature showed various medicinal

plants with high phenolic content associated with their chemopreventive as well as anticancer activity. Such reports include Lichochalcone A (LCA) from licorice, Cinnamtannin B1 from litchi, green tea (*Camellia sinensis*), ethanolic extract of *Tragopogon porrifolius*, blackberry, apples, *Prunus avium* (cherries), *Fagopyrum tataricum*, *Emblica officinalis,* etc (Wang et al., 2008; Serra et al., 2010; Lou et al., 2011; Zheng et al., 2012; Wen et al., 2015; Al-Rimawi et al., 2016; Chen et al., 2017). In the present study, total phenolic content (TPC) for methanolic extracts of leaves and stem of *R. cinerea* was obtained as 13.86 and 31.65 µg GAE/mg dry weight of the extract. The total flavonoid content (TFC) values for both the extracts was obtained as 111.87 and 37.91 µg RE/mg dry weight of the extract respectively (**Figure 1A**). Further, methanolic extracts of leaves and stem of *Roylea cinerea* (D. Don) Baill. were evaluated for their antioxidant potential in terms of their hydrogen donating capacity. Among leaves and stem extract, the former exhibited higher DPPH radical scavenging activity with IC_{50} of 239 µg/ml as compared to the latter exhibiting IC_{50} of 1,076.42 µg/ml (**Figure 1B**). Gallic acid was used as standard and it showed the IC_{50} of 8.56 µg/ml. The extracts were also evaluated for their electron-donating ability *via* molybdate ion reduction assay. The *R. cinerea* leaves extract exhibited 49.84 µg ascorbic acid equivalents/1.6 mg dry weight of extract and stem extract showed comparatively lower activity of 28.44 µg ascorbic acid equivalents/1.6 mg dry weight of extract (Y=0.0074x-0.1115, R^2 = 0.993)(**Figure 1A**).

The TPC and TFC values clearly indicated that the leaves extracts were rich in flavonoid content and the stem extract showed higher content of phenolic compounds. In the previous study, stem and leaves extract of *R. cinerea* were investigated for the presence of seven polyphenols including gallic acid, rutin, catechin, quercetin, umbelliferone, epicatechin, and kaempferol. The extracts showed the presence of high content of rutin leaves as compared to the stem (Bhatia et al., 2019). Rutin and its metabolites contain vicinyl dihydroxy groups which are mainly responsible for its free radical scavenging properties (Yang et al., 2008). The potential of polyphenols is affected by the position as well as the number of hydroxyl groups attached to the aromatic ring combined with their glycosylation or the presence of other hydrogen donating groups such as –SH, -NH (Cai et al., 2004). These functional groups have also been implicated in inhibiting oxidation progression *via* radical chain-breaking properties (Ghasemzadeh and Ghasemzadeh, 2011). The DNA protective ability against the OH radical was assessed through plasmid nicking assay with slight modifications. The leaves extract of *R. cinerea* were able to protect the native DNA (more or less), i.e., supercoiled DNA (form I) in a dose-dependent manner upto 72.6% (**Figure 2A**) as compared to the stem extract with 6.5% of Form I and 92.6% of Form II DNA (linear DNA) (**Figure 2B**). The antioxidant results in the case of leaves extract showed higher TFC content, DPPH radical scavenging activity and molybdate ion reduction ability which can be corroborated with the presence of rutin in high amount in leaves. These findings have been confirmed with the literature survey (Bhatia et al., 2019; Pundir and Mahindroo, 2019). The stem extract showed less antioxidant activity, as well as low TFC value but TPC value was higher as compared to leaf extract.

The extracts obtained from *R. cinerea* leaves and stem were also evaluated for anti-proliferative activity in the immortalized L6 skeletal muscle cell line by MTT assay. Both the extracts showed varying degrees of inhibitory potential against cell growth in dose-dependent manner (**Figure 3**). The leaves and stem extract explicited a considerable level of inhibitory potential with 83.06% and 81.14% inhibition at 400 µg/ml with GI_{50} of 69.41 µg/ml and 124.93 µg/ml respectively (**Figure 3**). The antiproliferative potential of both the extracts was substantially corroborated with the antioxidant potential. The majority of the

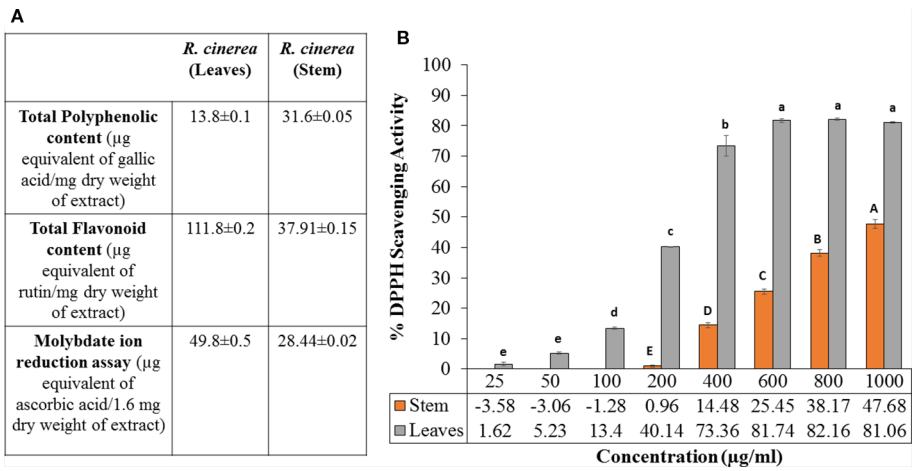

	R. cinerea (Leaves)	*R. cinerea* (Stem)
Total Polyphenolic content (µg equivalent of gallic acid/mg dry weight of extract)	13.8±0.1	31.6±0.05
Total Flavonoid content (µg equivalent of rutin/mg dry weight of extract)	111.8±0.2	37.91±0.15
Molybdate ion reduction assay (µg equivalent of ascorbic acid/1.6 mg dry weight of extract)	49.8±0.5	28.44±0.02

FIGURE 1 | (A) Molybdate ion reduction potential, total phenolic content (TPC) and total flavonoid content (TFC) values of leaves and stem extract of *R. cinerea*), **(B)** DPPH radical scavenging potential of leaves and stem extract of *R. cinerea.* (Values are mean ± S.E. of three parallel measurements. Different letters indicate significant differences between different concentrations of *R. cinerea* (leaves and stem) methanolic extracts ($p < 0.05$, Tukeys HSD test, (F-ratio- 381.283 (*R. cinerea* (stem)), 833.829 (*R. cinerea* (leaves))).

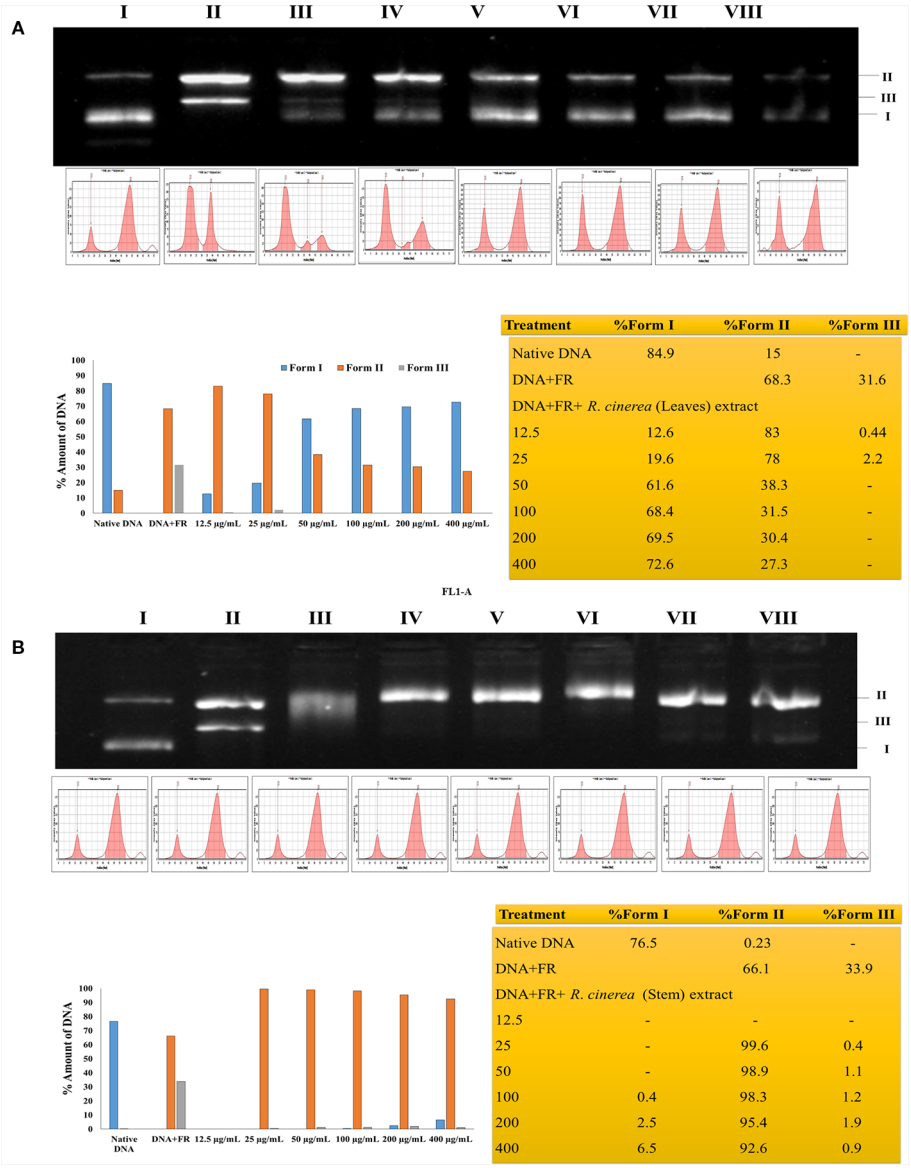

Treatment	%Form I	%Form II	%Form III
Native DNA	84.9	15	-
DNA+FR		68.3	31.6
DNA+FR+ *R. cinerea* (Leaves) extract			
12.5	12.6	83	0.44
25	19.6	78	2.2
50	61.6	38.3	-
100	68.4	31.5	-
200	69.5	30.4	-
400	72.6	27.3	-

Treatment	%Form I	%Form II	%Form III
Native DNA	76.5	0.23	-
DNA+FR		66.1	33.9
DNA+FR+ *R. cinerea* (Stem) extract			
12.5	-	-	-
25	-	99.6	0.4
50	-	98.9	1.1
100	0.4	98.3	1.2
200	2.5	95.4	1.9
400	6.5	92.6	0.9

FIGURE 2 | (A) Protective effects of leaf extract obtained from *R. cinerea* against Fenton's reagent (FR) induced DNA damage (nicking) in pBR322. Lane I: native DNA, Lane II: DNA+FR, Lane III-VIII: DNA+FR+leaf extract (12.5–400 µg/ml). **Form I**: Supercoiled DNA, **Form II**: Linear (nicked) DNA and **Form III**: Relaxed circular DNA. **(B)** Protective effects of stem extract obtained from *R. cinerea* against Fenton's reagent (FR) induced DNA damage (nicking) in pBR322. Lane I: native DNA, Lane II: DNA+FR, Lane III-VIII: DNA+FR+stem extract (12.5–400 µg/ml). **Form I**: Supercoiled DNA, **Form II**: Linear (nicked) DNA and **Form III**: Relaxed circular DNA.

reported anticancer herbal medicines have been proved to be efficient in several clinical reports and experimental research for the prevention as well as treatment of cancer to a better extent (Konkimalla and Efferth, 2008; Reuben et al., 2012). In a previous study, *Roylea cinerea* (D.Don) Baill. showed anticancer activity against SK-Mel 41, U-87 MG, Hela, MDA-MBA-231 cell line with GI_{50} 131.8 µg/ml, 275.4 µg/ml, and 302.0 µg/ml, respectively (Bahuguna et al., 2015). The mode of death (apoptosis) was confirmed by comparing the LDH activity of the treated L6 cells (GI_{50}, GI_{70}) which showed decreased LDH activity. Cancer cells have been reported with a high glycolysis rate for survival. Instead of entering further into citric acid cycle, pyruvate is converted into lactate *via* lactate dehydrogenase enzyme. This step consumes NADH and produces NAD^+, consequently inducing a decrease in mitochondrial membrane potential which ultimately causes apoptosis (Franco-Molina et al., 2010). The leaves and stem extract-treated cells caused 20.09% (GI_{50}), 39.32% (GI_{70}), and 0.3% (GI_{50}), 14.49% (GI_{70}) LDH activity respectively which confirmed the apoptotic mode of cell death.

Furthermore, the L6 cells were treated with the GI_{50} of leaves extract of *R. cinerea* for 24 h revealed significantly enhanced levels of intracellular ROS (**Figures 4B, D**). The elevated levels of

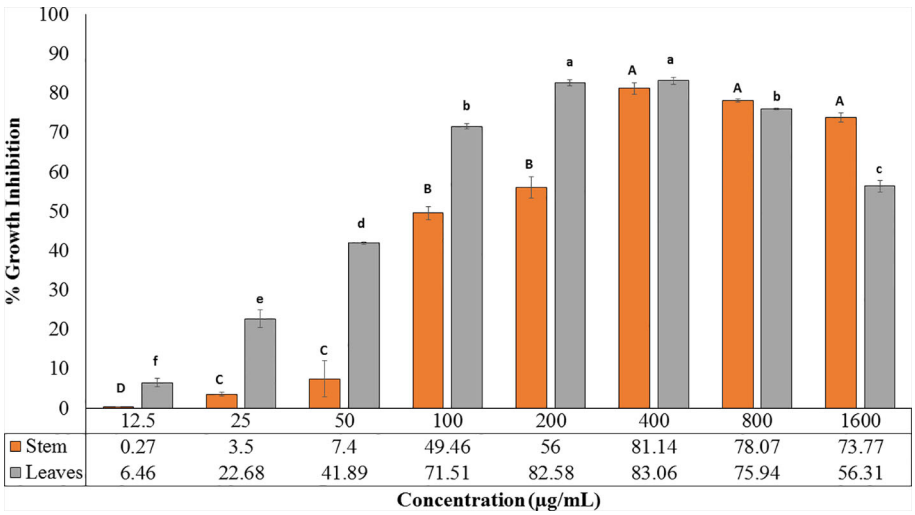

FIGURE 3 | Cytotoxic potential of leaves and stem extract of *R. cinerea* evaluated by MTT assay. (Values are mean ± S.E. of three parallel measurements. Different letters indicate significant differences between different concentrations of *R. cinerea* (leaves and stem) methanolic extracts ($p < 0.05$, Tukeys HSD test, (F-ratio-277.429 (*R. cinerea* (stem)), 663.915 (*R. cinerea* (leaves)).

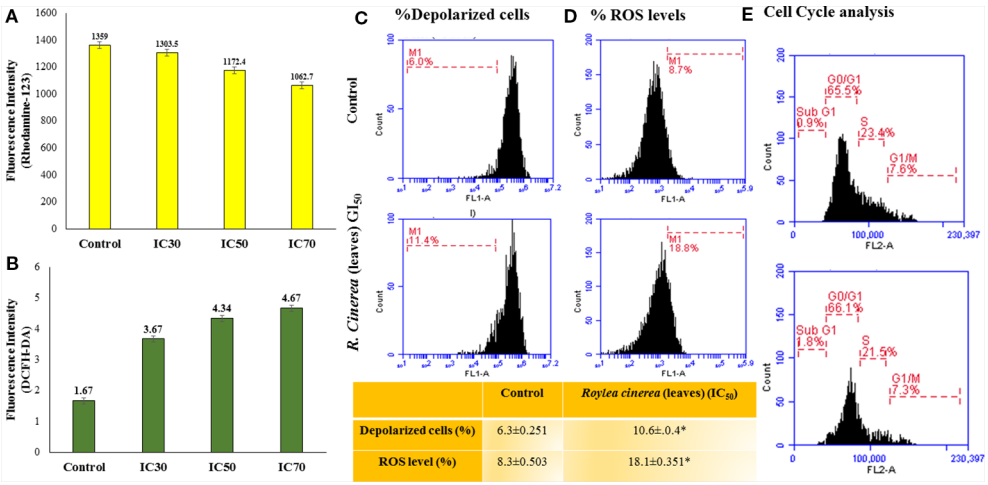

FIGURE 4 | (A) MMP status assessed by Rhodamine-123 staining for leaves extract of *R. cinerea* in L6 cell line analyzed with Biotek multi-well plate reader for fluorescent intensity (485 nm excitation and 528 nm emission). **(B)** Reactive oxygen species (ROS) status assessed by DCFH-DA staining for leaf extract of *R. cinerea* analyzed with Biotek multi-well plate reader for fluorescent intensity (485 nm excitation and 528 nm emission). **(C)** MMP status assessed by Rhodamine-123 staining for leaves extract of *R. cinerea* in L6 cell line analyzed with BD Accuri TM C6 Flow Cytometer (excitation 488 nm, emission 535 nm, FL-1 channel, events recorded 10,000 per sample). *Difference between % depolarized cells in control cells and treated cells (IC_{50} *R. cinerea* (leaves) extract) statistically significant (Independent Student's t-test, $p \leq 0.5$) **(D)** ROS status assessed by DCFH-DA staining for leaf extract of *R. cinerea* analyzed with BD AccuriTM C6 Flow Cytometer (excitation 511 nm, emission 535 nm, FL-1 channel, events recorded 10,000 per sample), *Difference between % ROS in control cells and treated cells (IC_{50} *R. cinerea* (leaves) extract) statistically significant (Independent Student's t-test, $p \leq 0.5$) **(E)** Effect of methanolic leaves extract of *R. cinerea* on cell cycle analysis compared with non-treated cells (control).

intracellular ROS in L6 cells demonstrated the apoptogenic efficiencies of both the extracts. ROS is generated continuously in the body as a consequence of mitochondrial bioenergetics mainly oxidative metabolism. But these radicals ($O_2^{\cdot -}$ superoxide anion, $OH^{\cdot}$ hydroxyl radical, $OOH^{\cdot}$ peroxide radical and H_2O_2, etc.) are balanced *via* an indigenous cellular system. These radicals form an integral part of a network of cellular signaling pathways including cell proliferation and programmed cell death (Hansen et al., 2006; Menon and Goswami, 2007). However, imbalanced intracellular redox can target various biomarkers

involved in cancer pathophysiology which includes CDK's (cyclin-dependent kinases), various transcriptional factors (Nrf2, FOXO3) and pro-apoptotic markers including MAPK's (Mates et al., 2012; Roleira et al., 2015). Phenolic compounds are known to show pleiotropic effects by acting as pro-oxidants in order to preserve normal cell cycle regulation *via* CDK's functions, suppress inflammation, tumor invasion combined with induction of apoptosis (Ziech et al., 2012). The active constituents present in *R. cinerea*, in spite of showing considerable *in vitro* antioxidant potential, might be stimulated to act as pro-oxidant in the state of imbalanced redox environment in L6 cells. Elevated levels of ROS also affects cell membrane, mitochondria, DNA, lipids, and proteins. Mitochondria play a crucial role in the process of induction of apoptosis as it contains various pro-apoptotic markers such as apoptotic proteases and cytochrome c. ROS can cause the opening of mitochondrial permeability transition pores and disruption of the electron transport chain which ultimately leads to apoptosis or cell death. The methanolic leaves extract (GI_{50}) also substantially altered the mitochondrial membrane potential which ultimately leads to the opening of mitochondrial pores followed by the release of pro-apoptotic markers that lead to cell death (Bortner and Cidlowski, 1999) (**Figures 4A, C**).

Mostly the anticancer drugs induce apoptosis through nuclease mediated destruction of DNA content in cells which leads to induction of cell cycle arrest. Thus, to elucidate the effects of methanolic leaves extract of *R. cinerea* on DNA content in L6 cells, cell cycle assay was performed using propidium iodide fluorescent dye. The membrane permeable PI dye intercalates with bases of DNA and represents the DNA content present in cells. In our experiment, the methanolic leaves extract of *R. cinerea* at GI_{50} concentration, showed the enhanced percentage of Sub-G1 phase from 0.9% to 1.8% which represents the apoptotic population when compared to control non treated cells. Further, cell population in G0/G1 phase was increased in treated cells from 65.5% to 66.1% with a decrease in S phase (23.4% to 21.5%) and G1/M phase (7.6% to 7.3%). The results indicated the increase in apoptotic cells and cell cycle arrest at G0/G1 phase in treated cells as compared to the non-treated cells which may be attributed to DNA damage mediated p53 activation to check further cell proliferation (**Figure 4E**) (Khan et al., 2019). The anticancer drugs specifically act by initiating various signaling pathways and ultimately inducing apoptosis. The mode of death induced by methanolic extract of leaves and stem of *R. cinerea* was confirmed through various *in vitro* experiments. Phase-contrast microscopy clearly depicted the presence of membrane blebbing, cell shrinkage, and apoptotic bodies in treated cells as compared to normal healthy cells in control. Confocal microscopy revealed various apoptotic features such as condensed nuclear material, flattened cytoplasmic borders, degradation of DNA into scattered masses in treated cells as compared to control L6 cells (**Figure 5**). AO/EB staining confirmed the presence of apoptotic cells (dark orange) in treated groups and live cells in control (green) (**Figure 5**). Furthermore, scanning electron microscopy studies clearly showed cell size reduction, blebbing of the membrane, rounding of cells, and apoptotic bodies. Thus, the results of the present study clearly corroborated with the association of phytochemicals (phenolics) in combating cancer *via*. pleiotropic effects and altering signaling pathways at the mitochondrial level.

The experimental results obtained paved the way to clarify the mechanism involved by which the leaves extract was able to activate caspase-3 activity in L6 cells. To obtain further information, docking studies were performed. Previously reported phyto-constituent present in *R. cinerea viz.,* 1-methyl-1-H-indole-3-carbaldehyde, β-lactam, β-sitosterol, calyone, cinereanoid A, cinereanoid B, cinereanoid C, cinereanoid D, pilloin, rutin, and stigmasterol were made to dock to the protein structure of PI3K (PDB ID: 1E8Z), Bcl2 (PDB ID: 4IEH), and Bclxl (PDB ID: 4QNQ). The docking pose with minimum binding energy was considered for further analysis through chimera software to get a clear picture of the ligand regarding its orientation, H-bonding, identification of residues and mode of interactions. It revealed that phytoconstituents present in the methanolic extract of leaves possessed a good binding affinity toward the protein targets (PI3K, Bcl2, and Bclxl). Docking confirmations were analyzed for each ligand which explicated interactions of different amino residues of protein targets with user-defined ligands through H-bond formation. Among various ligands, cinereanoid D showed minimum binding energy, i.e., -11.56 Kcal/mol and fits well in the binding cavity of PI3K protein target (1E8Z) (**Figures 6A1–A3**). However, for protein target 1E8Z, stigmasterol also showed H-bonding with minimum binding energy of -10.85 Kcal/mol (ASP 884 with bond length 3.016 Å) followed by calyone with binding energy -10.65 Kcal/mol (GLU 880 with bond length 2.730 Å), rutin with binding energy -10.10 Kcal/mol (GLU 814 and ALA 885 with bond length 2.881 Å and 2.835 Å), Cinereanoid C, Cinereanoid A (GLU 880 and ALA 885 with bond length 2.621 and 2.653 Å), β-sitosterol, Cinereanoid B (VAL 882 and LYS 883 with bond length 3.009 and 2.870 Å), pilloin (ALA 885 with bond length 2.899 Å) showed binding energy -10.00, -9.37, -9.16, -9.03, and -8.31 Kcal/mol, respectively (**Supplementary Figure 3**, **Table 1**). The PI3K pathway is one of the major pathway for cell growth and survival. Over-activation *via* PDGFR and EGFR families (oncogenic targets) of this preordained PI3K pathway can lead to frequent incidences of cancer. This assumption makes it an obvious target for cancer treatment *via* developing some promising isoform specific PI3K inhibitors such as class Ia PI3-kinases. Class Ia PI3 kinases have been well documented for transmitting signals for survival responses through PKB/AKT activation. ATP binding sites/pocket as a catalytic domain present on PI3Kinases can occur as a probable target of PI3K inhibitors to bind. Labdane diterpenoids are commonly found in family Lamiaceae. In cinereanoid D, butenolide side chain (furan) is present with a hydroxyl group at 16-C. Literature studies showed scarce scientific evidence regarding the structure activity relationship of novel labdane diterpenoids cinereanoid A-D. Labdane diterpenoids are reported to affect DNA synthesis facilitated by the presence of a double bond at its C7-C8 position (Dimas et al., 1998). However, stigmasterol have been well reported for its efficacy to inhibit cancer development and progression in both *in vitro* and *in vivo* system (Zhang et al., 2016).

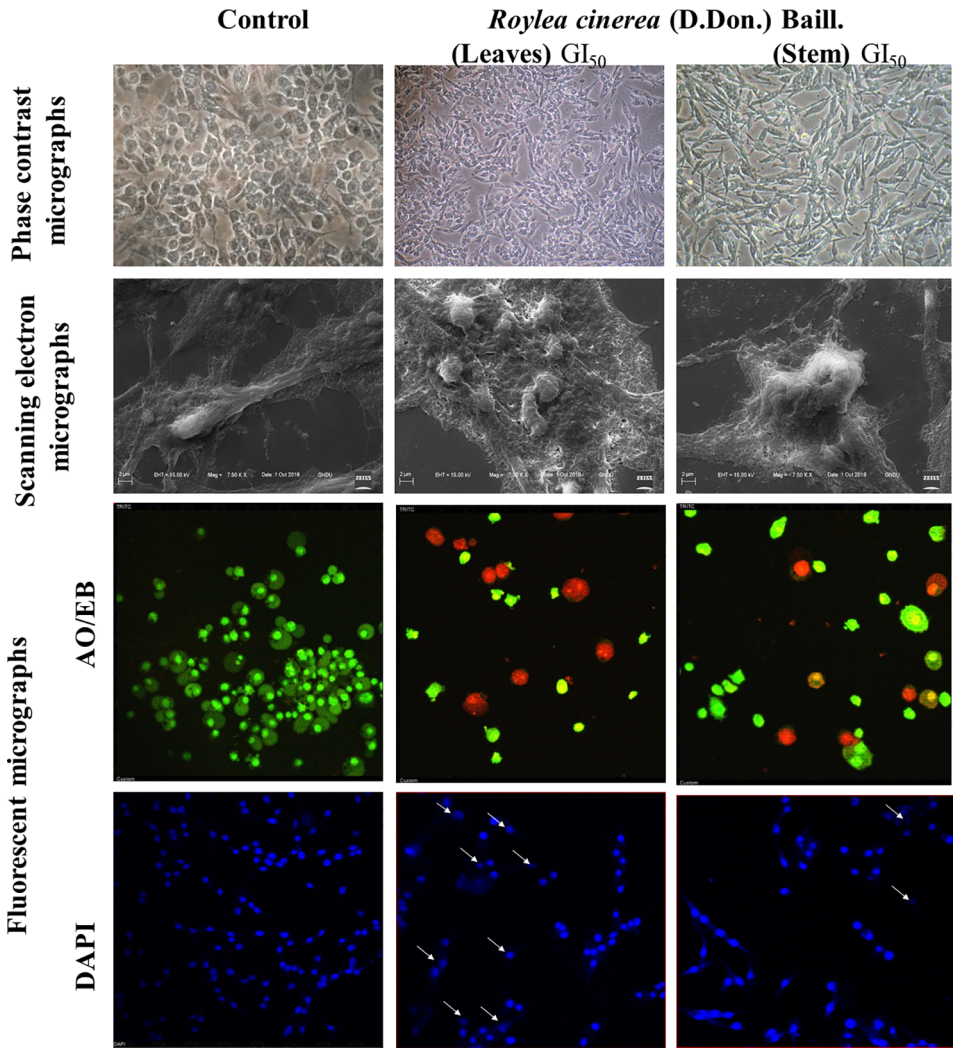

FIGURE 5 | L6 cells imaged by phase contrast for morphological changes (40x); Scanning electron microscopy for surface variations (7.50 KX); Confocal microscopy for nuclear with DAPI and AO/EB (40x).

PI3 Kinases through AKT activates Bcl2 family proteins. Protein targets Bcl2 and Bclxl are basically anti-apoptotic/pro-survival proteins with four conserved domains BH1, BH2, BH3, and BH4. In response to death signals, the BH3 domain is neutralized by pro-apoptotic proteins, i.e., Bad, Bmf which leads to the release of cytochrome c for apoptosis through disturbing the integrity of the mitochondrial membrane. Overexpression of Bcl2 family proteins may be responsible for the progression of cancer. For the protein target Bcl2 (4IEH), among selected ligands, stigmasterol showed minimum binding energy of -9.81 Kcal/mol (ARG 105 with bond length 3.079 Å) to binding cavity (**Figures 6B1–B3**) followed by cinereanoid A, rutin, calyone, β-sitosterol, cinereanoid D, cinereanoid C, cinereanoid B, pilloin with minimum binding energy -9.48, -9.09 (GLY 104 with bond length 2.772 Å), -8.77 (ARG 105 and TYR 67 with bond length 3.023 and 2.998 Å), -8.61 (TYR 161 with bond length 2.859 Å), -8.09, -8.05, -7.50, and -7.08 Kcal/mol (ARG 66 with bond length 3.097 Å), respectively.1-methyl-1-H-indole-3-carbaldehyde and β-lactam showed minimum binding energy -4.74 and -4.15 Kcal/mol (**Supplementary Figure 4**, **Table 1**).Furthermore, for the protein target Bclxl (4QNQ), maximum affinity to the binding cavity was shown by rutin -9.31 Kcal/mol with H-bond formation with amino acid residues GLN 183 (3.013 Å), TRP 188 (3.001 Å), SER 4 (3.005 Å) (**Figures 6C1–6C3**) followed by cinereanoid D, cinereanoid A, cinereanoid B, calyone, β-sitosterol, cinereanoid C, stigmasterol, pilloin, 1-methyl-1-H-indole-3-carbaldehyde and β-lactam with minimum binding energy -8.38, -8.36 (ALA 93 with bond length 2.660 Å), -8.14 (ALA 93 with bond length 2.512 Å), -8.08, -8.01, -7.78, -7.43, -7.28, -4.71, and -4.39, respectively. The ligands which did not show any H-bonding were still well fit into the binding cavity of the protein which may be attributed to electrostatic, Van der waal forces and hydrophobic interactions (**Supplementary Figure 5**, **Table 1**). Thus, the experimental findings confirming loss of mitochondrial membrane potential, generation of ROS and cell cycle arrest at G0/G1 phase by

TABLE 1 | Predicted binding energies for constituents present in *Roylea cinerea* (D.Don) Baill. docked with PI3K (PDB ID: 1E8Z), Bcl2 (PDB ID: 41EH), Bclxl (PDB ID: 4QNQ) obtained from www.rcsb.org.

S.No.	Molecules	PI3K (PDB:1E8Z)		Bcl2 (PDB:4IEH)		Bclxl (PDB ID: 4QNQ)	
		Minimum binding energy (Kcal/mol)	No. of H-bonds	Minimum binding energy (Kcal/mol)	No. of H-bonds	Minimum binding energy (Kcal/mol)	No. of H-bonds
1.	1-methyl-1-H-indole-3-carbaldehyde	-5.38		-4.74	0	-4.71	0
2.	β-lactam	-5.47	1	-4.15	0	-4.39	0
3.	β-sitosterol	-9.16	1	-8.61	1	-8.01	0
4.	Calyone	-10.65	0	-8.77	2	-8.08	0
5.	Cinereanoid A	-9.37	2	-9.48	0	-8.36	0
6.	Cinereanoid B	-9.03	2	-7.50	0	-8.14	0
7.	Cinereanoid C	-10.00	0	-8.05	0	-7.78	1
8.	Cinereanoid D	**-11.56**	1	-8.09	0	-8.38	1
9.	Pilloin	-8.31	1	-7.08	1	-7.28	0
10.	Rutin	-10.10	2	-9.09	1	**-9.31**	3
11.	Stigmasterol	-10.85	1	**-9.81**	1	-7.43	0

The bold values represent compounds with minimum binding energy.

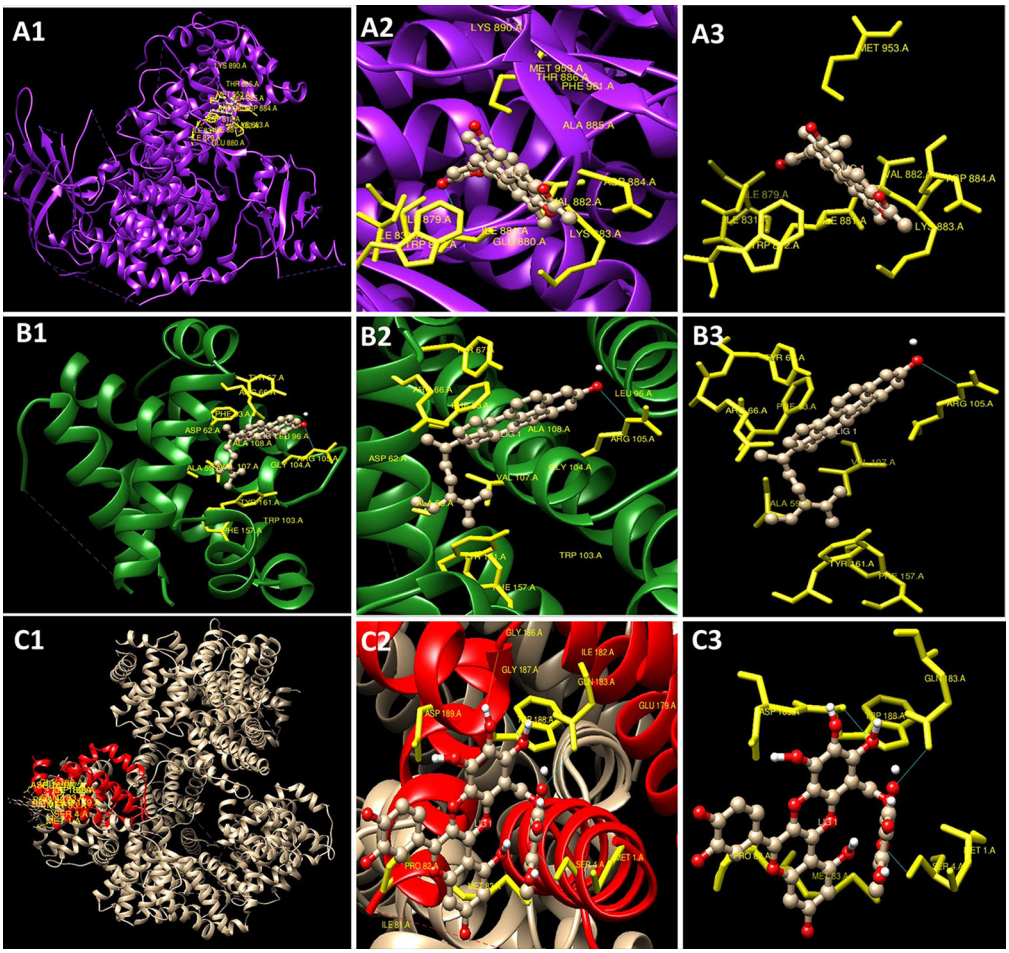

FIGURE 6 | Docking conformations (Chimaera software) showing interaction of compounds with minimum binding energy **(A1–A3)**. Cinereanoid D with PI3K (PDB ID: 1E8Z) **(B1–B3)** Stigmasterol with Bcl2 (PDB ID: 4IEH) **(C1–C3)** Rutin with Bclxl (PDB ID: 4QNQ).

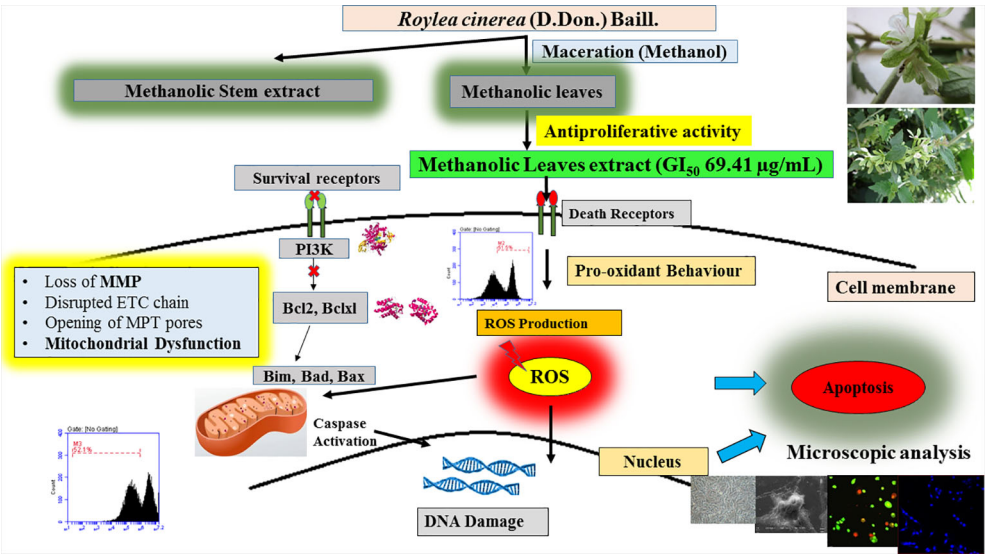

FIGURE 7 | Detailed proposed mechanism involved in the induction of apoptosis in L6 cells by *R.cinerea* leaves extract.

the methanolic extract of leaves of *R.cinerea* corroborated with the docking studies showing the synergistic potential of its phytoconstituents in the induction of apoptosis in immortalized L6 skeletal muscle cell line (**Figure 7**).

CONCLUSION

The present study revealed the antioxidant potential and DNA protective abilities of methanolic extracts of leaves and stem of *R. cinerea* along with antiproliferative and apoptosis induction potential against immortalized L6 cell line. However, the methanolic leaves extract of *R. cinerea* showed better activity as compared to stem extract. Furthermore, mechanistic analysis revealed that methanolic extracts of leaves of *R. cinerea* induced apoptosis basically through increasing intracellular ROS generation, decreasing mitochondrial membrane potential and ultimately lead to cell death *via* apoptosis. Further, the experimental findings were strengthened by docking with already reported phytoconstituents of *Roylea cinerea* in literature with PI3 kinase and anti-apoptotic/pro-survival proteins. The study provided partial evidence for a pharmacological basis regarding clinical applications of *Roylea cinerea* in the treatment of cancer and will add significant information to establish a strong base to conduct further research on this plant and its unexplored health benefits. However, further *in vivo* experiments are required to confirm the efficacy and mechanism of action regarding this plant.

DATA AVAILABILITY STATEMENT

All datasets generated for this study are included in the article/**Supplementary Material**.

AUTHOR CONTRIBUTIONS

AB: formal analysis, investigation, methodology, data curation, and writing—original draft. HS and RA: writing, reviewing, and editing. AS and SK: intellectual contribution and reviewing manuscript. SA: conceptualization, supervision and project administration, reviewing and editing, and resources. BS: conceptualization, methodology, reviewing and editing, and supervision. All authors read and approved the final manuscript.

FUNDING

The present study was supported by the University Grants Commission (UGC), New Delhi under the Rajiv Gandhi National Fellowship scheme to AB (vide grant no. 201415-RGNF-2014-15-SC-PUN-68052).

ACKNOWLEDGMENTS

The authors are grateful to the UGC (University Grants Commission) for financial assistance under Rajiv Gandhi National Fellowship scheme. The authors are thankful to Centre for Emerging Life Sciences (Instrumentation facility) and Head, Department of Botanical and Environmental Sciences, Guru Nanak Dev University, Amritsar, India for providing necessary facilities.

SUPPLEMENTARY MATERIAL

The Supplementary Material for this article can be found online at: https://www.frontiersin.org/articles/10.3389/fphar.2020.00322/full#supplementary-material

SUPPLEMENTARY FIGURE 1 | Structure of phyto-constituents (Ligands) present in *R. cinerea* prepared using Chemsketch software for docking analysis.

SUPPLEMENTARY FIGURE 2 | Structure of protein PI3K (1E8Z), Bcl2 (4IEH), Bclxl (4QNQ) and their binding sites obtained from www.rcsb.org.

SUPPLEMENTARY FIGURE 3 | Docking conformations of the phytoconstituents present in *R. cinerea viz*., a) 1-methyl-1-H-indole-3-carbaldehyde b) β-lactam c) β-sitosterol d) calyone e) cinereanoid A f) cinereanoid B g) cinereanoid C h) cinereanoid D i) pilloin j) rutin, and k) stigmasterol with PI3K (1E8Z).

SUPPLEMENTARY FIGURE 4 | Docking conformations of the phytoconstituents present in *R. cinerea viz*., a) 1-methyl-1-H-indole-3-carbaldehyde b) β-lactam c) β-sitosterol d) calyone e) cinereanoid A f) cinereanoid B g) cinereanoid C h) cinereanoid D i) pilloin j) rutin, and k) stigmasterol with Bcl2 (4IEH).

SUPPLEMENTARY FIGURE 5 | Docking conformations of the phytoconstituents present in *R. cinerea viz*., a) 1-methyl-1-H-indole-3-carbaldehyde b) β-lactam c) β-sitosterol d) calyone e) cinereanoid A f) cinereanoid B g) cinereanoid C h) cinereanoid D i) pilloin j) rutin, and k) stigmasterol with Bclxl (4QNQ).

SUPPLEMENTARY FIGURE 6 | Standard curve for ascorbic acid (20–200 μg/ml) for the calculation of electron donating capacity (molybdate ion reduction assay).

REFERENCES

Abe, K., and Matsuki, N. (2000). Measurement of cellular 3-(4,5-dimethylthiazol-2-yl)-2,5-diphenyltetrazolium bromide (MTT) reduction activity and lactate dehydrogenase release using MTT. *Neurosci. Res.* 38, 325–329. doi: 10.1016/S0168-0102(00)00188-7

Al-Rimawi, F., Rishmawi, S., Ariqat, S. H., Khalid, M. F., Warad, I., and Salah, Z. (2016). Anticancer activity, antioxidant activity, and phenolic and flavonoids content of wild *Tragopogon porrifolius* plant extracts. *Evidence-Based Complement. Altern. Med.* 2016, 7. doi: 10.1155/2016/9612490

Bahuguna, R. P., Jangwan, J. S., Singh, R., and Bhatt, U. P. (2015). In vitro cytotoxic, in vitro and in vivo antidiabetic activity of *Roylea cinerea*. *Sci. Revs. Chem. Commun.* 5, 69–76.

Basu, A. K. (2018). DNA damage, mutagenesis and cancer. *Int. J. Mol. Sci.* 19 (4), 970. doi: 10.3390/ijms19040970

Bhatia, A., Kaur, T., Singh, B., Arora, R., and Arora, S. (2019). Reverse phase HPLC method validation for estimation of polyphenols in medicinal plants and their possible role in reticence of xanthine oxidase activity. *Sep. Sci. Plus* 2 (7), 237–244. doi: 10.1002/sscp.201900015

Blois, M. S. (1958). Antioxidant determinations by the use of a stable free radical. *Nature* 26, 1199–1200. doi: 10.1038/1811199a0

Bortner, C. D., and Cidlowski, J. A. (1999). Caspase independent/dependent regulation of K+, cell shrinkage, and mitochondrial membrane potential during lymphocyte apoptosis. *J. Biol. Chem.* 274 (31), 21953–21962. doi: 10.1074/jbc.274.31.21953

Cai, Y., Luo, Q., Sun, M., and Corke, H. (2004). Antioxidant activity and phenolic compounds of 112 traditional Chinese medicinal plants associated with anticancer. *Life Sci.* 74 (17), 2157–2184. doi: 10.1016/j.lfs.2003.09.047

Chen, X., Liu, Z., Meng, R., Shi, C., and Guo, N. (2017). Antioxidative and anticancer properties of Licochalcone A from licorice. *J. Ethnopharmacol.* 198, 331–337. doi: 10.1016/j.jep.2017.01.028

Chikara, S., Nagaprashantha, L. D., Singhal, J., Horne, D., Awasthi, S., and Singhal, S. S. (2018). Oxidative stress and dietary phytochemicals: Role in cancer chemoprevention and treatment. *Cancer Lett.* 413, 122–134. doi: 10.1016/j.canlet.2017.11.002

Deng, S., Yuan, H., Yi, J., Lu, Y., Wei, Q., Guo, C., et al. (2013). Gossypol acetic acid induces apoptosis in RAW 264.7 cells via a caspase-dependent mitochondrial signaling pathway. *J. Vet. Sci.* 14, 281–289. doi: 10.4142/jvs.2013.14.3.281

Dimas, K., Demetzos, C., Marsellos, M., Sotiriadou, R., Malamas, M., and Kokkinopoulos, D. (1998). Cytotoxic activity of labdane type diterpenes against human leukemic cell lines in vitro. *Planta Med.* 64 (03), 208–211. doi: 10.1055/s-2006-957410

Dobhal, M. P., and Joshi, B. C. (1979). Chemical investigations of *Roylea elegans* Wall Part I. *Herba Pol.* 25, 95–97.

Dua, V. K., Verma, G., Agarwal, D. D., Kaiser, M., and Brun, R. (2011). Antiprotozoal activities of traditional medicinal plants from the Garhwal region of North West Himalaya, India. J. *Ethnopharmacology* 136, 123–128. doi: 10.1016/j.jep.2011.04.024

Franco-Molina, M. A., Mendoza-Gamboa, E., Sierra-Rivera, C. A., Gómez-Flores, R. A., Zapata-Benavides, P., Castillo-Tello, P., et al. (2010). Antitumor activity of colloidal silver on MCF-7 human breast cancer cells. *J. Exp. Clin. Cancer Res.* 29 (1), 148. doi: 10.1186/1756-9966-29-148

Ghasemzadeh, A., and Ghasemzadeh, N. (2011). Flavonoids and phenolic acids: Role and biochemical activity in plants and human. *J. Med. Plants Res.* 5 (31), 6697–6703. doi: 10.5897/JMPR11.1404

Hansen, J. M., Go, Y. M., and Jones, D. P. (2006). Nuclear and mitochondrial compartmentation of oxidative stress and redox signaling. *Annu. Rev. Pharmacol. Toxicol.* 46, 215–234. doi: 10.1146/annurev.pharmtox.46.120604.141122

Jordan, M. A., Wendell, K., Gardiner, S., Derry, W. B., Copp, H., and Wilson, L. (1996). Mitotic block induced in HeLa cells by low concentrations of paclitaxel (Taxol) results in abnormal mitotic exit and apoptotic cell death. *Cancer research* 56 (4), 816–825.

Kasibhatla, S., Amarante-Mendes, G. P., Finucane, D., Brunner, T., Bossy-Wetzel, E., and Green, D. R. (2006). Acridine orange/ethidium bromide (AO/EB) staining to detect apoptosis. *Cold Spring Harbor Protoc.* 2006 (3). pdb-prot4493. doi: 10.1101/pdb.prot4493

Khan, F., Pandey, P., Upadhyay, T. K., Jafri, A., Jha, N. K., Mishra, R., et al. (2019). Anti-cancerous Effect of RutinAgainst HPV-C33A Cervical Cancer Cells via G0/G1 Cell Cycle Arrest and Apoptotic Induction. *Endocr. Metab. Immune Disord. Drug Targets.* 20 (3), 409. doi: 10.2174/1871530319666190806122257

Khare, C. P. (2007). *Indian Medicinal Plants – An Illustrative Dictionary* (Heidelberg, Germany: Springer Publishers), 559.

Kim, D. O., Jeong, S. W., and Sharma, A. (2003). Antioxidant capacity of phytochemicals from various cultivars of plums. *Food Chem.* 81, 321–326. doi: 10.1016/S0308-8146(02)00423-5

Konkimalla, V. B., and Efferth, T. (2008). Evidence-based Chinese medicine for cancer therapy. *J. Ethnopharmacol.* 116 (2), 207–210. doi: 10.1016/j.jep.2007.12.009

Lee, J. C., Kim, H. R., Kim, J., and Jang, Y. S. (2002). Antioxidant property of an ethanol extract of the stem of *Opuntia ficus-indica* var. *Saboten*. *J. Agric. Food Chem.* 50, 6490–6496. doi: 10.1021/jf020388c

Liu, J., Li, Y., Ren, W., and Hu, W. X. (2006). Apoptosis of HL-60 cells induced by extracts from *Narcissus tazetta* var. *chinensis*. *Cancer Lett.* 242 (1), 133–140. doi: 10.1016/j.canlet.2005.11.023

Lou, W., Zhao, M., Yang, B., Ren, J., Shen, G., and Rao, G. (2011). Antioxidant and anti-proliferative capacities of phenolics purified from *Phyllanthus emblica* L. fruit. *Food Chem.* 126 (1), 277–282. doi: 10.1016/j.foodchem.2010.11.018

Majumder, P. L., Maiti, R. N., Panda, S. K., and Mal, D. (1979). Structure of moronic acid. *J. Org. Chem.* 44, 2811–2812. doi: 10.1021/jo01329a053

Mates, J. M., Segura, J. A., Alonso, F. J., and Marquez, J. (2012). Oxidative stress in apoptosis and cancer: An update. *Arch. Toxicol.* 86 (11), 1649–1665. doi: 10.1007/s00204-012-0906-3

Menon, S. G., and Goswami, P. C. (2007). A redox cycle within the cell cycle: Ring in the old with the new. *Oncogene* 26 (8), 1101–1109. doi: 10.1038/sj.onc.1209895

Parkash, V., and Aggarwal, A. (2010). Traditional uses of ethnomedicinal plants of lower foot-hills of Himachal Pradesh-I. *Indian J. Tradit. Knowl.* 9, 519–521. doi: hdl.handle.net/123456789/9785

Prakash, O., Bhakuni, D., Kapil, R. S., Subba Rao, G. S. R., and Ravindranath, B. (1979). Diterpenoids of *Roylea calycina* (Roxb.) Briq. *J. Chem. Soc Perkin Trans.* 5, 1305– 1308. doi: 10.1039/p19790001305

Prieto, P., Pineda, M., and Aguilar, M. (1999). Spectrophotometric Quantitation of Antioxidant capacity through the Formation of a Phosphomolybdenum Complex: Specific Application to the Determination of Vitamin E. *Anal. Biochem.* 269, 337–341. doi: 10.1006/abio.1999.4019

Pundir, S., and Mahindroo, N. (2019). *Roylea cinerea* (D. Don) Baillon: Ethnomedicinal uses, phytochemistry and pharmacology: A review. *J. Ethnopharmacol.* 232, 193–200. doi: 10.1016/j.jep.2018.12.042

Ramasamy, S., Wahab, N. A., Abidin, N. Z., and Manickam, S. (2013). Effect of extracts from *Phyllanthus watsonii* Airy Shaw on cell apoptosis in cultured human breast cancer MCF-7 cells. *Exp. Toxicol. Pathol.* 65, 341–349. doi: 10.1016/j.etp.2011.11.005

Rashid, S. (2017). "Molecular Mechanism of Carcinogenesis," in *Cancer and Chemoprevention: An Overview* (Singapore: Springer), 27–29.

Rastogi, R. P., and Dhawan, B. N. (1990). Anticancer and antiviral activities in Indian medicinal plants: a review. *Drug Dev. Res.* 19 (1), 1–12. doi: 10.1002/ddr.430190102

Rawat, R., and Vashistha, D. P. (2013). *Roylea cinerea* (D. Don) Baillon: a traditional curative of diabetes, its cultivation prospects in Srinagar valley of uttarakhand. *Int. J. Adv. Pharm. Biol. Chem.* 2, 372–375.

Reuben, S. C., Gopalan, A., Petit, D. M., and Bishayee, A. (2012). Modulation of angiogenesis by dietary phytoconstituents in the prevention and intervention of breast cancer. *Mol. Nutr. Food Res.* 56 (1), 14–29. doi: 10.1002/mnfr.201100619

Roleira, F. M., Tavares-da-Silva, E. J., Varela, C. L., Costa, S. C., Silva, T., Garrido, J., et al. (2015). Plant derived and dietary phenolic antioxidants: Anticancer properties. *Food Chem.* 183, 235–258. doi: 10.1016/j.foodchem.2015.03.039

Serra, A. T., Seabra, I., Braga, M. E. M., Bronze, M. R., de Sousa, H. C., and Duarte, C. M. M. (2010). Processing cherries (*Prunus avium*) using supercritical fluid technology. Part 1: Recovery of extract fractions rich in bioactive compounds. *J. Supercrit. Fluids* 55 (1), 184–. doi: 10.1016/j.supflu.2010.06.005

Sharma, R., Chebolu, R., and Ravikumar, P. C. (2015). Isolation and structural elucidation of two new labdane diterpenoids from the aerial part of *Roylea cinerea*. *Phytochem. Lett.* 13, 187–193. doi: 10.1016/j.phytol.2015.06.008

Sharma, R., Mohammadi-Ostad-Kalayeh, S., Stahl, F., Zeilinger, C., Dräger, G., Kirschning, A., et al. (2017). Two new labdane diterpenoids and one new β-lactam from the aerial parts of *Roylea cinerea*. *Phytochem. Lett.* 19, 101–107. doi: 10.1016/j.phytol.2016.12.013

Singh, C. K., Siddiqui, I. A., El-Abd, S., Mukhtar, H., and Ahmad, N. (2016). Combination chemoprevention with grape antioxidants. *Mol. Nutr. Food Res.* 60 (6), 1406–1415. doi: 10.1002/mnfr.201500945

Singh, S. K., Patel, J. R., and Dangi, A. (2019). Physicochemical, qualitative and quantitative determination of secondary metabolites and antioxidant potential of *Alocasia macrorrhizos* leaf extracts. *The Pharma Innovation*, 8 (1), 399–404. doi: 10.22270/jddt.v9i1.2225

Wang, S. Y., Bowman, L., and Ding, M. (2008). Methyl jasmonate enhances antioxidant activity and flavonoid content in blackberries (*Rubus* sp.) and promotes anti-proliferation of human cancer cells. *Food Chem.* 107 (3), 1261–1269. doi: 10.1016/j.foodchem.2007.09.065

Weinberg, R. A. (1989). Oncogenes, antioncogenes, and the molecular bases of multistep carcinogenesis. *Cancer Res.* 49 (14), 3713–3721.

Wen, L., You, L., Yang, X., Yang, J., Chen, F., Jiang, Y., et al. (2015). Identification of phenolics in litchi and evaluation of anticancer cell proliferation activity and intracellular antioxidant activity. *Free Radical Biol. Med.* 84, 171–184. doi: 10.1016/j.freeradbiomed.2015.03.023

Yang, J., Guo, J., and Yuan, J. (2008). In vitro antioxidant properties of rutin. *LWT-Food Sci. Technol.* 41 (6), 1060–1066. doi: 10.1016/j.lwt.2007.06.010

Ye, L. H., Li, W. J., Jiang, X. Q., Chen, Y. L., Tao, S. X., Qian, W. L., et al. (2012). Study on the autophagy of prostate cancer PC-3 cells induced by oridonin. *Anatomical Rec.* 295, 417–422. doi: 10.1002/ar.21528

Yu, L., Haley, S., Perret, J., Harris, M., Wilson, J., and Qian, M. (2002). Free radical scavenging properties of wheat extracts. *J. Agric. Food Chem.* 50, 1619–1624. doi: 10.1021/jf010964p

Zhang, C. X., Huang, J., Xu, M., Luo, W. P., and Fang, Y. J. (2016). Dietary phytosterols intakes are inversely associated with colorectal cancer risk among Chinese population. *FASEB J.* 30 (1_supplement), 42–3.

Zheng, C. J., Hu, C. L., Ma, X. Q., Peng, C., Zhang, H., and Qin, L. P. (2012). Cytotoxic phenylpropanoid glycosides from *Fagopyrum tataricum* (L.) Gaertn. *Food Chem.* 132 (1), 433–438. doi: 10.1016/j.foodchem.2011.11.017

Ziech, D., Anestopoulos, I., Hanafi, R., Voulgaridou, G. P., Franco, R., Georgakilas, A. G., et al. (2012). Pleiotrophic effects of natural products in ROS-induced carcinogenesis: the role of plant-derived natural products in oral cancer chemoprevention. *Cancer Lett.* 327 (1-2), 16–25. doi: 10.1016/j.canlet.2012.02.025

Conflict of Interest: The authors declare that the research was conducted in the absence of any commercial or financial relationships that could be construed as a potential conflict of interest.

The handling editor declared a past co-authorship with one of the authors HS.

frontiers in Oncology

SYSTEMATIC REVIEW
published: 17 March 2020
doi: 10.3389/fonc.2019.01573

Genetic Polymorphisms and Platinum-Based Chemotherapy-Induced Toxicities in Patients With Lung Cancer: A Systematic Review and Meta-Analysis

Wenhui Liu[1,2], *Ying Wang*[1,2], *Jianquan Luo*[1,2], *Haiyan Yuan*[1,2] *and Zhiying Luo*[1,2]*

[1] *Department of Pharmacy, The Second Xiangya Hospital, Central South University, Changsha, China,* [2] *Institute of Clinical Pharmacy, Central South University, Changsha, China*

OPEN ACCESS

Edited by:
Mukerrem Betul Yerer Aycan, Erciyes University, Turkey

Reviewed by:
Ji-Ye Yin, Xiangya Hospital, Central South University, China
Massimiliano Berretta, Centro di Riferimento Oncologico di Aviano (IRCCS), Italy

****Correspondence:***
Zhiying Luo
lzhy199089@csu.edu.cn

Specialty section:
This article was submitted to Pharmacology of Anti-Cancer Drugs, a section of the journal Frontiers in Oncology

Received: *16 October 2019*
Accepted: *30 December 2019*
Published: *17 March 2020*

Citation:
Liu W, Wang Y, Luo J, Yuan H and Luo Z (2020) Genetic Polymorphisms and Platinum-Based Chemotherapy-Induced Toxicities in Patients With Lung Cancer: A Systematic Review and Meta-Analysis. Front. Oncol. 9:1573. doi: 10.3389/fonc.2019.01573

Background: Platinum-based agents, including cisplatin, carboplatin, and oxaliplatin, are indispensable for the treatment of lung cancer. The development of toxicity frequently necessitates dose reduction or discontinuation of therapy, despite the clinical response. Pharmacogenomics studies were reviewed to identify the possible genetic variants that underlie individual susceptibility to platinum-related toxicities.

Method: We conducted a systematic search in PubMed and Embase for pharmacogenomics reports that focused on commonly reported platinum-induced toxicities, such as gastrointestinal (GI), hematological, neurological, and other toxicities, in patients diagnosed with lung cancer. Meta-analyses were conducted to determine the association between genetic polymorphisms and platinum-induced toxicity by checking the odds ratio (OR) and 95% confidence interval (CI) using random or fixed-effects models as appropriate.

Results: Twenty eligible studies that met the inclusion criteria with sufficient data were extracted and presented comprehensively. A total of 16 polymorphisms from 11 genes were included in the meta-analysis. *MTHFR* rs1801131 and *MDM2* rs1690924 were significantly correlated with platinum-induced GI toxicity ($P = 0.04$ and $P = 0.02$, respectively). Patients with the *MTHFR* rs1801131AA and *MDM2* rs1690924TC/CC genotype tended to have a higher risk of GI toxicity than patients with other genotypes did (OR = 1.73, 95% CI = 0.86–2.18; and OR = 0.51, 95% CI = 0.29–0.88, respectively). Compared to carriers of the *MTHFR* rs1801133CC genotype, carriers of the CT/TT genotype had a significantly increased risk of hematological toxicity ($P = 0.01$, OR = 1.68, 95% CI = 1.12–2.52).

Conclusion: In the future, physicians should pay careful attention to *MTHFR* and *MDM2* for personalized chemotherapy treatment among patients with lung cancer.

Keywords: platinum, pharmacogenomics, toxicity, individual difference, meta-analysis

BACKGROUND

Lung cancer is the second most commonly diagnosed malignant tumor in men and women and is one of the main causes of mortality worldwide (1). There are two major forms of lung cancer, including small cell lung cancer (SCLC) and non-small cell lung cancer (NSCLC); NSCLC accounts for 85% of all cases of lung cancer (2). Because of the difficulty in early diagnosis, most patients are diagnosed with advanced stage disease when surgery is no longer a treatment option. Therefore, chemotherapy is the major treatment choice for these patients (3).

Platinum-based agents, including cisplatin, carboplatin, and oxaliplatin, in combination with other cytotoxic drugs have been recommended as the first-line chemotherapy for lung cancer (4). The antitumor effect of platinum-based agents is by interfering with DNA repair, thereby suppressing and eventually killing cancer cells (5). Unfortunately, platinum can also hamper the growth of normal cells. Although platinum-based agents are effective for cancer therapy, platinum-induced toxicity is very common in clinical settings. The use of platinum-based agents may lead to serious or permanent adverse events, such as hematotoxicity, GI, nephrotoxicity, hearing loss, and other toxicities (6). Severe toxicities can result in dose reduction, treatment delay, or even chemotherapy discontinuation, as well as carry the risk of life-threatening complications (7). Moreover, differences exist among patients considering the severity of platinum-induced toxicities. Therefore, personalized medicine aims to identify patients who have received platinum agent treatment and are more likely to benefit from anticancer agents or more likely to experience adverse events.

Genetic polymorphisms contribute to the differences in platinum-related toxicities, and there is accumulating evidence to support this speculation (8). Therefore, determining the association between polymorphisms and platinum-related toxicities will be beneficial for individualized chemotherapy. Previously, two genome-wide association studies and one whole-exome sequencing study were conducted to identify the genetic markers for platinum-induced toxicities (9–11). In addition, Yin et al. aimed to establish models to explain and predict platinum toxicity interindividual difference by simultaneously incorporating multiple genetic and clinical factors to explore the association of their interactions with platinum-induced toxicities (12, 13).

Although many studies have investigated this issue, there is still no consensus regarding the relationship between genetic polymorphisms and platinum-induced toxicities in patients with lung cancer. For example, Cristina et al. found that *ERCC1* C118T was significantly associated with platinum-induced toxicity while other studies presented contradictory results (14–16). Similar associations were found for *XRCC1* codon 399, *XPD* Lys751Gln, and other mutations (17, 18). Hence, quantitative evaluation is needed for determining the association between gene polymorphisms and platinum-induced toxicities.

The aims of this study were as follows: (1) to summarize the pharmacogenomics of platinum-based toxicities in patients with lung cancer and (2) to provide a comprehensive assessment of the association between genetic polymorphisms and platinum-based drug response in patients with lung cancer. We collected all available publications on pharmacogenomics studies that platinum-based toxicities in patients with NSCLC and SCLC and quantitatively studied them using a meta-analysis strategy.

METHODS

Search Strategy

For the literature search, two authors (Z. Y. Luo and W. H. Liu) independently performed a systematic literature search in three databases: PubMed database, Cochrane Library, and ISI Web of Knowledge. The search results were reviewed and compared by a third reviewer (Y. Zheng), and discrepancies between searchers were discussed and solved with consensus. The literature was searched from the first available article to June 18, 2019. Publications were retrieved using terms associated with platinum drugs ("platinum" or "cisplatin" or "carboplatin" or "oxaliplatin") in combination with keywords associated with genetic variation ("polymorphism" or "SNP" or "single nucleotide polymorphism" or "mutation" or "variation") and "toxicity" or "adverse effect," and "lung cancer."

Inclusion Criteria

All identified abstracts were carefully and independently reviewed by two investigators (Z. Y. Luo and W. H. Liu) for eligibility. The inclusion criteria were as follows: (i) clinical studies, regardless of the sample size; (ii) studies that assessed the associations between genetic polymorphisms and platinum-induced severe (grade 3–4) toxicities in patients with lung cancer, and toxicities were evaluated and graded according to the Common Terminology Criteria for Adverse Events; (iii) numbers for each genotype were available or could be calculated in different groups; and (iv) at least two studies that evaluated one polymorphism met the abovementioned three criteria. If the two investigators disagreed about the eligibility of an article, it was resolved by consensus with a third reviewer (J. Q. Luo).

Data Extraction

Data were manually extracted by two reviewers (Z. Y. Luo, W. H. Liu) who were blinded to each other and used the same data recording form. All data were reviewed by the third reviewer (J. Q. Luo) until they reached a consensus on all of the data extraction items. The following information was extracted from each study: name of the first author, publication year, country of the study and ethnicity of the patients, sample size, tumor type, disease stage, chemotherapeutic drugs, platinum-induced toxicities, toxicity evaluation criteria, genes and Single Nucleotide Polymorphism Database number of the investigated polymorphisms, and genotype methods.

Statistical Analysis

The patients were divided into two groups: those with grade 3–4 (severe) toxicities and those with grade 0–2 (no or mild) toxicities. The pooled odds ratio (OR) and associated 95% CI were calculated and used to evaluate the strength of association in different genotype groups. The significance of the pooled estimates of the OR was determined using the Z-test. The

Cochran's Q-test and I^2 metric were performed to determine the possibility of between-study heterogeneity. The heterogeneity of publications in each meta-analysis was considered to be significant at $P < 0.05$ for the Q statistics and $I^2 > 50\%$ for the I^2 metric. Sensitivity analysis was conducted if publication bias existed; one study was excluded at a time, and the others were analyzed to estimate whether the results were affected markedly by a single study. Subgroup analysis based on toxicity [categorized as overall, gastrointestinal (GI), and hematological toxicities] was conducted to assess the sources of heterogeneity across the studies. Potential publication bias was assessed using the Begg and Egger tests, with $P < 0.05$ considered to indicate a significant publication bias. All statistical analyses were performed with by the Cochrane Collaboration software (Review Manager 5, the Cochrane Collaboration, Oxford, United Kingdom).

RESULTS

Literature Review and Characteristics of the Included Studies

The initial research yielded 1,003 publications. A total of 608 articles were excluded owing to duplicate publication; in addition, 306 studies were excluded in the first round of review, among which 30 were irrelevant literature articles, 5 were not English articles, 64 were reviews or meta-analysis, 27 were case reports or abstracts, 19 were non-clinical-related studies, 13 focused on other tumors, 41 did not evaluate platinum-based chemotherapy, 20 did not focus on platinum-related toxicities, and 89 were not pharmacogenomic studies. After reading the full text of these articles, we found that 12 studies did not provide detailed data owing to the lack of significant association between gene polymorphisms and platinum-based toxicities.

Finally, 20 publications with sufficient data met the inclusion criteria and were extracted (**Figure 1**). The general characteristics of the studies included in the meta-analysis are presented in **Table 1**. The included publications included 16 polymorphisms in 11 genes, and the detailed information of these mutation are listed in **Table 2**. A candidate gene approach was employed for the identification of single nucleotide polymorphisms (SNPs) that conferred susceptibility to platinum-based toxicities, and this methodology directly evaluated the relationship between one variant and a particular toxicity or several toxicities.

Quantitative Synthesis of the Association Between Polymorphisms and Platinum-Related Toxicities

The main results of this meta-analysis showing the association between polymorphisms and risk of platinum-based grade 3–4 toxicities are shown in **Table 3** and **Supplemental Figures**.

ERCC1 C118T and C8092A

The most extensively studied polymorphism was *ERCC1* C118T. The association between C118T polymorphism and platinum-based grade 3–4 hematological and GI toxicity was found and replicated by six and three studies, respectively. We first performed a meta-analysis to determine the association between C118T polymorphism and grade 3–4 hematological toxicity by including 1,450 subjects. No significant relationship was detected between C118T polymorphism and grade 3–4 hematological toxicity (OR = 0.80, 95% CI: 0.56–1.15, $P = 0.23$) using a fixed-effect model. On subgroup analyses based on ethnicity, the combined OR for risk and the I^2 were consistent and did not show any apparent fluctuation (**Supplemental Table 1**).

We further analyzed the relationship between C118T polymorphism and grade 3–4 GI toxicity by including 790 patients. Pooled data from these investigations showed grade

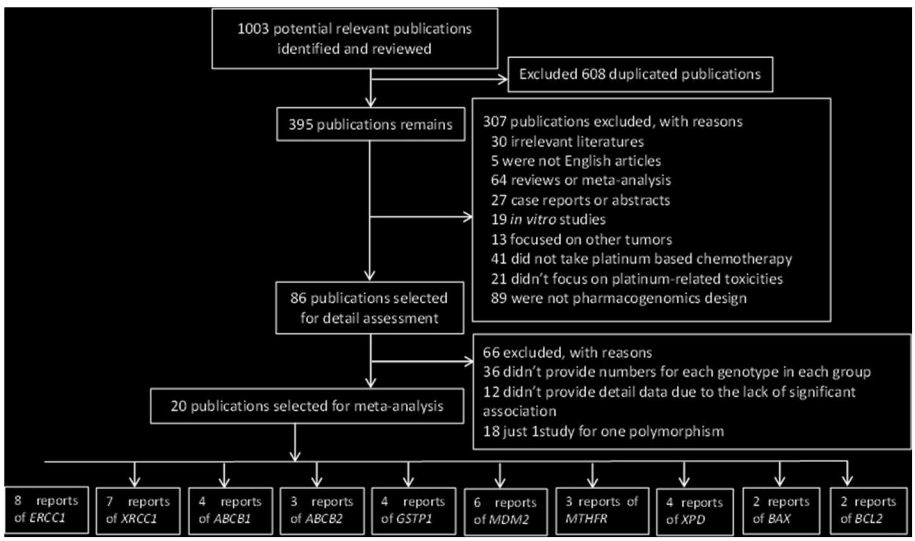

FIGURE 1 | Flow chart of literature selection.

TABLE 1 | Characteristics of studies involved in the meta-analysis.

Authors	Year	Country	*N*	Disease stage	Cancer type	Toxicity evaluation	Genotype method	Genes and SNP	References
Beatrice et al.	2019	Italy	82	II–IV	NSCLC + SCLC	CTCAE v4.03	TaqMan	*ABCB1*: rs1045642 *ABCB2*: rs717620 *GSTP1*: rs1695	(19)
Wang et al.	2018	China	490	III–IV	NSCLC	NCI-CTC 3.0	MALDI-TOF mass spectrometer	504 SNPs of 185 genes	(12)
Zheng et al.	2017	China	1218	IIIa–IV	NSCLC	NCI-CTC 3.0	MassARRAY	*ERCC1*: rs11615, rs3212986 *XRCC1*: rs25487 *MDM2*: rs2279744	(20)
Qian et al.	2016	China	403	I–IV	NSCLC	NCI-CTC 3.0	MassARRAY	*ABCB1*: rs1045642, *ABCB2*: rs717620	(21)
Cristina et al.	2016	Spain	141	I–IV	NSCLC	NCI-CTCAE 4.0	TaqMan	*ERCC1*: rs11615, rs3212986 *XRCC1*: rs25487 *ABCB1*: rs1045642 *MDM2*: rs1470383, rs1690924 *MTHFR*: rs1801131, rs1801133	(14)
Powrozek et al.	2016	Poland	55	IIIb–IV	NSCLC	NCI-CTC 4.03	Mini-sequencing	*ERCC1*: rs11615, rs3212986 *XRCC1:* rs25487	(18)
Deng et al.	2015	China	97	IIIb–IV	NSCLC	CTCAE, V2.0	Pyrosequencing	*XRCC1*: rs25487	(22)
Qian et al.	2015	China	663	IIIa–IV	NSCLC	NCI-CTC 3.0	iSelect HD BeadChip	*MDM2*: rs1470383, rs1690924	(23)
Peng et al.	2015	China	235	III–IV	NSCLC	NCI-CTC 3.0	PCR-RFLP	BAX: rs4645878 BCL2: rs2279115	(24)
Li et al.	2014	China	1004	III–IV	NSCLC	NCI-CTC 3.0	iSelect HD BeadChip	*MTHFR*: rs1801133, rs1801131	(25)
Peng et al.	2014	China	235	III–IV	NSCLC	NCI-CTC 3.0	PCR-CTTP	*XRCC1*: rs25487	(26)
Wang et al.	2014	China	119	NA	SCLC	NCI-CTCAE 3.0	MassARRAY	*MDM2*: rs2279744	(27)
Zheng et al.	2014	China	444	IIIa–IV	NSCLC	NCI-CTC 3.0	PCR-RFLP	*MDM2:* rs2279744, *MDM2*: rs937282	(28)
Gu et al.	2012	China	445	IIIa–IV	NSCLC	NCI-CTC 3.0	MALDI-TOF mass spectrometer	BAX: rs4645878 BCL2: rs2279115	(29)
Markus et al.	2011	Switzerland	137	IIIb–IV	NSCLC	NCI-CTC 3.0	sequencing	*GSTP1*: rs1695	(15)
Vienna et al.	2011	Italy	192	IIIb–IV	NSCLC	NCI-CTC 3.0	TaqMan	*XPD*: rs13181	(30)
Wang et al.	2008	China	139	IIIb–IV	Advanced lung cancer	NCI-CTC 3.0	PCR-RFLP	*XRCC1*: rs25487	(31)
Carmelo et al.	2008	Italy	65	IIIb–IV	NSCLC	NCI-CTC 3.0	Taqman	*ERCC1*: rs11615 *XPD*: rs13181, rs1799793	
Richard et al.	2006	United Kingdom	108	III–IV	NSCLC	NCI-CTC 2.0	Sequencing	*GSTP1*: rs1695	(32)
Rebecca et al.	2005	USA	214	III–IV	NSCLC	NCI-CTC 3.0	Taqman	*ERCC1*: rs11615, rs3212986	(33)

NCI-CTC, National Cancer Institute Common Toxicity Criteria; NCI-CTCAE, National Cancer Institute Common Terminology Criteria for Adverse Events; PCR-CTTP, PCR with confronting two-pair primers; PCR-RFLP, PCR-based restriction fragment length polymorphism.

3–4 GI toxicity rates of 13.49 and 14.15% in the CC + CT genotype and the TT genotype groups, respectively. No significant relationship was detected between C118T polymorphism and grade 3–4 GI toxicity (OR = 0.77, 95% CI: 0.43–1.38, $P = 0.38$) using a fixed-effect model. This association did not significantly change on subgroup analyses based on ethnicity.

A total of four and two studies examined the association between C8092A mutation and platinum-based grade 3–4 hematological toxicity and nephrotoxicity, respectively. No significant association was detected between C8092A polymorphism and grade 3–4 hematological toxicity (OR = 0.86, 95% CI: 0.65–1.15, $P = 0.31$) using a fixed-effect model. This association had no significant change on subgroup analyses

TABLE 2 | Polymorphisms and phenotypes analyzed in this study.

Genes	Polymorphisms	NCBI ID	Alleles	Platinum-related toxicities	References
ERCC1	C118T (Asn118Asn)	rs11615	C>T	Grade 3–4 hematological toxicity	(12, 14, 20, 30, 33, 34)
				Grade 3–4 GI toxicity	(12, 14, 33)
	C8092A	rs3212986	C>A	Grade 3–4 hematological toxicity	(12, 14, 18, 20)
				Grade 3–4 nephrotoxicity toxicity	(14, 18)
XRCC1	G1196A (Arg399Gln)	rs25487	G>A	Grade 3–4 GI toxicity	(12, 14, 20, 26, 31)
				Grade 3–4 hematological toxicity	(12, 14, 20, 26, 31)
P53	Arg72Pro	rs1042522	G>C	Grade 3–4 hematological toxicity	(12, 27, 28, 30)
ABCB1	G2677T/A (Ala893Ser/Thr)	rs1045642	G>T/A	Grade 3–4 overall toxicity	(12, 14, 21)
				Grade 3–4 hematological toxicity	(12, 14, 19, 21)
				Grade 3–4 GI toxicity	(12, 14, 21)
ABCB2	−24C>T	rs717620	C>T	Grade 3–4 hematological toxicity	(12, 19, 21)
GSTP1	A313G (Ile105Val)	rs1695	A>G	Grade 3–4 hematological toxicity	(12, 15, 19, 32)
XPD	A2251C (Lys751Gln)	rs13181	C>A	Grade 3–4 hematological toxicity	(12, 18, 30, 34)
	G934A (Asp312Asn)	rs1799793	G>A	Grade 3–4 hematological toxicity	(12, 18, 34)
MTHFR	A1298C	rs1801131	A>C	Grade 3–4 GI toxicity	(14, 25)
				Grade 3–4 hematological toxicity	(14, 25)
	C677T	rs1801133	C>T	Grade 3–4 GI toxicity	(12, 14, 25)
				Grade 3–4 hematological toxicity	(12, 14, 25)
MDM2	Intron variant	rs1470383	C>T	Grade 3–4 overall toxicity	(14, 23)
				Grade 3–4 hematological toxicity	(14, 23)
				Grade 3–4 GI toxicity	(14, 23)
	309T>G	rs2279744	G>T	Grade 3–4 hematological toxicity	(12, 20, 27, 28)
	Intron variant	rs1690924	C>T	Grade 3–4 overall toxicity	(14, 23)
				Grade 3–4 hematological toxicity	(14, 23)
				Grade 3–4 GI toxicity	(14, 23)
BAX	−248G>A	rs4645878	G>A	Grade 3–4 hematological toxicity	(24, 29)
				Grade 3–4 GI toxicity	(24, 29)
BCL2	938C>A	rs2279115	G>A	Grade 3–4 hematological toxicity	(24, 29)
				Grade 3–4 GI toxicity	(24, 29)

based on ethnicity. Among 196 patients who were included to determine the association between C8092A polymorphism and grade 3–4 nephrotoxicity, no significant association was observed (OR = 0.88, 95% CI: 0.62–1.25, $P = 0.58$) using a fixed-effect model.

XRCC1 G1196A

Five studies were eligible to determine the association between G1196A polymorphism and grade 3–4 GI and hematological toxicities. Pooled analysis showed that there was no significant association between G1196A polymorphism and grade 3–4 GI toxicity (OR = 1.29, 95% CI: 0.53–3.16, $P = 0.56$) using a random-effect model (**Table 3** and **Supplemental Figure 2**). A sensitivity analysis was conducted because of publication bias ($I^2 = 71\%$). After removing the study by Peng et al., the publication bias disappeared ($I^2 = 10\%$). We further examined the raw data of this study and found that the G1196A mutation was not considered in the Hardy–Weinberg equation ($P = 0.002$). No significant association was detected between G1196A polymorphism and grade 3–4 hematological toxicity (OR = 0.94, 95% CI: 0.65–1.35, $P = 0.35$) using a fixed-effect model. On subgroup analyses based on ethnicity, the combined risk of G1196A mutation on platinum-based grade 3–4 GI toxicities was consistent and did not show any apparent fluctuation (**Supplemental Table 1**).

P53 Arg72Pro

A total of four studies with 1,033 patients were included to determine the association between *P53* Arg72Pro polymorphism and grade 3–4 hematological toxicity. However, the pooled analysis showed no significant association between Arg72Pro polymorphism and grade 3–4 hematological toxicity (OR = 0.82, 95% CI: 0.59–1.15, $P = 0.25$) using a fixed-effect model. This association did not significantly change on subgroup analyses based on ethnicity (**Supplemental Table 1**).

ABCB1 G2677T/A

A total of three, four, and three studies were available to determine the association between G2677T/A polymorphism and platinum-induced grade 3–4 overall, hematological, and GI toxicities, respectively. On overall analysis, no significant association was detected between G2677T/A polymorphism

TABLE 3 | Summary of meta-analysis of the association of genetic polymorphisms with platinum induced toxicities.

Gene	SNP	Toxicity	Polled OR (95% CI)	*Z*	*P*	*N*	Model	I^2 (%)	P_{hetero}
ERCC1	C118T	Grade 3–4 GI toxicity	0.77 [0.43, 1.38]	0.88	0.38	790	F	0	0.94
		Grade 3–4 hematological toxicity	0.80 [0.56, 1.15]	1.20	0.23	1,450	F	0	0.81
	C8092A	Grade 3–4 hematological toxicity	0.86 [0.65, 1.15]	1.01	0.31	1,037	F	0	0.88
		Grade 3–4 nephrotoxicity toxicity	0.88 [0.62, 1.25]	0.73	0.47	196	F	0	0.37
XRCC1	rs25487	Grade 3–4 hematological toxicity	0.94 [0.65, 1.35]	0.35	0.72	1,366	F	15	0.32
		Grade 3–4 GI toxicity	1.29 [0.53, 3.16]	0.56	0.57	1,366	R	71	0.009
P53	rs1042522	Grade 3–4 hematological toxicity	0.82 [0.59, 1.15]	1.15	0.25	1,033	F	30	0.23
ABCB1	rs1045642	Grade 3–4 overall toxicity	1.77 [0.79, 3.95]	1.39	0.16	1,045	R	87	0.0006
		Grade 3–4 hematological toxicity	1.97 [0.87, 4.47]	1.63	0.10	1,153	R	85	0.0002
		Grade 3–4 GI toxicity	1.34 [0.38, 4.75]	0.46	0.65	957	R	83	0.003
ABCB2	rs717620	Grade 3–4 hematological toxicity	1.35 [0.43, 4.25]	0.51	0.61	923	R	90	<0.0001
GSTP1	A313G	Grade 3–4 hematological toxicity	1.44 [0.77, 2.7]	1.14	0.26	745	F	0	0.49
XPD	rs13181	Grade 3–4 hematological toxicity	1.00 [0.55, 1.85]	0.01	0.99	742	F	0	0.75
	rs1799793	Grade 3–4 hematological toxicity	2.46 [0.46, 13.04]	1.06	0.29	548	R	72	0.03
MTHFR	rs1801131	Grade 3–4 GI toxicity	1.73 [0.86, 2.18]	2.02	0.04	1,106	F	24	0.25
		Grade 3–4 hematological toxicity	0.74 [0.44, 1.24]	1.14	0.26	1,231	F	0	0.94
	rs1801133	Grade 3–4 GI toxicity	1.29 [0.86, 1.92]	1.23	0.22	1,227	F	0	0.52
		Grade 3–4 hematological toxicity	1.68 [1.12, 2.52]	2.49	0.01	1,229	F	0	0.40
MDM2	rs2279744	Grade 3–4 hematological toxicity	0.69 [0.29, 1.62]	0.85	0.39	1,189	R	80	0.002
	rs1470383	Grade 3–4 overall toxicity	0.99 [0.71, 1.37]	0.07	0.95	786	F	0	0.48
		Grade 3–4 hematological toxicity	0.91 [0.64, 1.28]	0.56	0.57	786	F	35	0.21
		Grade 3–4 GI toxicity	1.35 [0.74, 2.46]	0.98	0.33	786	F	0	0.57
	rs1690924	Grade 3–4 overall toxicity	0.83 [0.60, 1.13]	1.19	0.23	786	F	0	0.74
		Grade 3–4 hematological toxicity	0.98 [0.70, 1.38]	0.10	0.92	755	F	7	0.30
		Grade 3–4 GI toxicity	0.51 [0.29, 0.88]	2.40	0.02	782	F	0	0.74
BAX	rs4645878	Grade 3–4 hematological toxicity	1.46 [0.96, 2.20]	1.79	0.07	647	F	0	0.52
		Grade 3–4 GI toxicity	1.15 [0.63, 2.09]	0.46	0.64	635	F	43	0.19
BCL2	rs2279115	Grade 3–4 hematological toxicity	1.00 [0.72, 1.39]	0.02	0.98	643	F	0	0.91
		Grade 3–4 GI toxicity	0.81 [0.48, 1.38]	0.78	0,44	632	F	0	0.62

F, fixed-effects model; R, random model; P_{hetero}*, P-value for heterogeneity test.*

and grade 3–4 overall toxicity (OR = 1.77, 95% CI: 0.79–3.95, $P = 0.16$) using a random-effect model. In addition, publication bias disappeared ($I^2 = 0\%$) after the study by Wang et al. was removed. The possible reason is that the call rate for G2677T/A genotypes was <90% in their study, which could have led to inaccuracy in their results. On subgroup analyses based on ethnicity, different ethnic populations showed distinct effects for the G2677T/A polymorphism. There were significant protective effects of the T/A allele on the risk of platinum-based overall toxicity in the non-Chinese subgroup (**Supplemental Table 1**).

Moreover, no significant association was detected between the G2677T/A polymorphism and grade 3–4 hematological toxicity (OR = 1.97, 95% CI: 0.87–4.47, $P = 0.10$) using a random-effect model. After removing the study by Qian et al., publication bias disappeared ($I^2 = 17\%$). Furthermore, the association between the G2677T/A polymorphism and grade 3–4 GI toxicity was analyzed. No significant association was detected between the G2677T/A polymorphism and grade 3–4 GI toxicity (OR = 1.34, 95% CI: 0.38–4.75, $P = 0.46$) using a random-effect model. In addition, the publication bias vanished ($I^2 = 0\%$) when the study by Qian et al. was removed. The study by Qian et al. was a high-quality well-designed study, with the appropriate sample size. The association between the G2677T/A polymorphism and grade 3–4 hematological and GI toxicities was still non-significant after the study by Qian et al. was removed.

ABCB2 −24C>T

Only three studies were qualified for analyzing the association between the −24C>T polymorphism and platinum-induced grade 3–4 hematological toxicity. No significant association was observed between the −24C>T polymorphism and grade 3–4 hematological toxicity (OR = 1.35, 95% CI: 0.43–4.25, $P = 0.51$) using a random-effect model. In addition, the publication bias vanished ($I^2 = 0\%$) when the study by Wang et al. was removed. The call rate for the −24C>T genotype was 83% in this study, which could have led to inaccuracy in the result. On subgroup analyses based on ethnicity, the association between the −24C>T polymorphism and grade 3–4 hematological toxicity was still non-significant (**Supplemental Table 1**).

GSTP1 A313G

Data from 745 patients included in 4 studies were used for analyzing the association between the A313G polymorphism and platinum-induced grade 3–4 hematological toxicity. There was no significant relationship between the A313G polymorphism and grade 3–4 hematological toxicity (OR = 1.44, 95% CI: 0.77–2.70, $P = 0.26$) using a fixed-effect model. On subgroup analyses based on ethnicity, the association between the A313G polymorphism and grade 3–4 hematological toxicity was still non-significant (**Supplemental Table 1**).

XPD A2251C and G934A

A total of four studies determined the association between the A2251C polymorphism and grade 3–4 hematological toxicity. No significant correlation was detected between the A2251C polymorphism and grade 3–4 hematological toxicity (OR = 1.00, 95% CI: 0.55–1.85, $P = 0.99$) using a fixed-effect model. Three studies examined the association between the G934A polymorphism and grade 3–4 hematological toxicity. No significant association was detected between the G934A polymorphism and grade 3–4 hematological toxicity (OR = 2.46, 95% CI: 0.46–13.04, $P = 0.29$) using a random-effect model. The publication bias disappeared ($I^2 = 0\%$) when the study by Tibaldi et al. or that by Powrozek et al. was removed. The main reason for this phenomenon was the small sample size of these two studies.

On subgroup analyses based on ethnicity, a non-significant association was found between these two polymorphisms and grade 3–4 hematological toxicity (**Supplemental Table 1**).

MTHFR A1298C and C677T

In total, three included studies evaluated the association between the A1298C polymorphism and grade 3–4 GI and hematological toxicities. Carriers of the AA genotype had more severe GI toxicity than carriers of the AC + CC genotype did (OR = 1.73, 95% CI: 0.86–2.18, $P = 0.04$) on a fixed-effect model. However, no significant association was found between the A1298C polymorphism and grade 3–4 hematological toxicities (OR = 0.74, 95% CI: 0.44–1.24, $P = 0.26$) using a fixed-effect model.

Two studies evaluated the association between the C677T polymorphism and grade 3–4 GI and hematological toxicities. No significant association was detected between the C677T polymorphism and grade 3–4 GI toxicity (OR = 1.29, 95% CI: 0.86–1.92, $P = 0.22$) using a fixed-effect model. The pooled data showed that patients with the 677CC genotype had an increased risk of severe hematological toxicity than the carriers of the CT + TT genotype did (OR = 1.86, 95% CI: 1.12–2.52, $P = 0.01$) using a fixed-effect model. The association between these two polymorphisms and grade 3–4 hematological toxicity was unchanged on subgroup analyses based on ethnicity (**Supplemental Table 1**).

MDM2 rs1470383, rs2279744, and rs1690924

Four studies with 1,189 Chinese patients evaluated the correlation between the rs2279744 polymorphism and grade 3–4 hematologic toxicity. There was no significant correlation between the rs2279744 polymorphism and grade 3–4 hematological toxicity (OR = 0.69, 95% CI: 0.29–1.62, $P = 0.39$) using a random-effect model. Similarly, we investigated the influence of a single study on the overall risk by excluding one study at a time. However, the combined overall risk and I^2 were consistent and did not show any apparent fluctuation.

Data from 786 subjects in 2 studies were used for analyzing the association between the rs1470383 polymorphism and platinum-based toxicities, including grade 3–4 overall, hematological, and GI toxicities. The pooled results showed no significant correlations between the rs1470383 polymorphism and grade 3–4 overall, hematological, and GI toxicities.

Two studies were used for analyzing the association between the rs1690924 polymorphism and platinum-based toxicities, including grade 3–4 overall, hematological, and GI toxicities. The pooled results showed no significant correlations between the rs1470383 polymorphism and grade 3–4 overall and hematological toxicities. The pooled results from all patients indicated that the carriers of the TT + TC genotype had a markedly increased risk of grade 3–4 GI toxicity than carriers of the CC genotype did (OR = 0.51, 95% CI: 0.29–2.43, $P = 0.02$) using a fixed-effect model.

BAX rs4645878

Two studies were included to analyze the association between the rs4645878 polymorphism and grade 3–4 hematological and GI toxicities. The pooled analysis showed no significant difference between the rs4645878 mutation and grade 3–4 hematological and GI toxicities using a fixed-effect model.

BCL2 rs2279115

The two studies that were included to the determine association between the rs4645878 polymorphism and grade 3–4 hematological and GI toxicities were included to evaluate the association between the rs2279115 polymorphism and grade 3–4 hematological and GI toxicities. The pooled analysis showed no significant differences between the rs4645878 mutation and grade 3–4 hematological and GI toxicities using a fixed-effect model.

DISCUSSION

Researchers had intense interest in the influence of genetic factors on the platinum-based adverse events considering interindividual differences. In the present meta-analysis, we included 20 studies with 6,287 patients with lung cancer who were treated with platinum-based regiments, and we systematically evaluated the impact of genetic polymorphisms on platinum-based grade 3–4 toxicities. A total of 16 polymorphisms in 11 genes were analyzed, and our results provided evidence that *MTHFR* A1298C and C677T and *MDM2* rs1470383 polymorphisms were significantly associated with platinum-based grade 3–4 toxicities.

To date, platinum-based chemotherapy is widely used as first-line therapy for the treatment of lung cancer and is highly cost-effective in Chinese patients (35). As the cytotoxic effects of

platinum are not specific, the mechanism of toxicity appears to involve multiple systems during chemotherapy. In the current study, we found that A1298C and C677T mutations of *MTHFR* were significantly associated with platinum-based grade 3–4 GI and hematological toxicities, respectively. *MTHFR* encodes the methylenetetrahydrofolate reductase enzyme that is involved in the folate metabolism pathway. The folate metabolism pathway plays an essential role in platinum cytotoxicity, and *MTHFR* is essential for transmethylation reactions including DNA methylation and DNA synthesis, thereby contributing to cancer prognosis (36). Both A1298C and C677T polymorphisms were associated with reduced enzyme activity and correlated with DNA hypomethylation, both of which alter the sensitivity of tumor cell to platinum compounds (37).

The gene encoding murine double minute 2 (*MDM2*) is a proto-oncogene and a key negative regulator of p53. *MDM2* plays a role in P53-independent antitumor activity through directing binding, ubiquitination, and degradation of the *p53* gene (38). A previous meta-analysis found that the *MDM2* gene polymorphism (rs2279744) was associated with the risk of lung cancer and the clinical outcomes (39). A previous study verified that unnatural change in the expression of *MDM2*, mediated by polymorphisms, contributed to subsequent attenuation of the p53 pathway, thereby accelerating the spread of NSCLC (40). In the current study, the *MDM2* rs1690924 mutation was significantly associated with grade 3–4 GI toxicity, and the carriers of the TT + TC genotype had a markedly increased risk of grade 3–4 GI toxicity than the carriers of the CC genotype did. To date, only one study found an association between this polymorphism and overall survival (41). However, the function of *MDM2* rs1690924 polymorphism is unknown.

Findings on genetic polymorphisms that affect platinum-induced toxicities were inconclusive in most studies, and the sample size of most studies was generally small. Polymorphisms in genes encoding the nucleotide excision repair (NER) pathway are among the most clinically relevant genetic determinants with susceptibility to platinum-based toxicities (42). The NER pathway is responsible for repairing DNA intrastrand cross-links induced by platinum-based chemotherapy, and the most commonly reported candidate gene associated with platinum-based toxicities include *ERCC1*, *XRCC1*, and *XPD* (43). In fact, genes involved in the NER pathway were most commonly evaluated in this meta-analysis. However, results from our meta-analysis showed no significant association between the gene polymorphisms of the NER pathway and platinum-induced severe toxicities.

Although previous studies validated that polymorphisms in genes act as potential risk factors for platinum-induced toxicities considering individual differences, the results of our research indicated that some polymorphisms correlated with platinum-induced toxicities had limited contribution to the interindividual differences in platinum-induced toxicities. The reasons for negative or conflicting results may be complicated. (i) The incidence of toxicities between cisplatin, carboplatin, and oxaliplatin varied (44). (ii) Although all patients in these studies were receiving treatment with platinum-based drugs, the use of non-platinum drugs, such as antimicrotubule agents, antifolate agents, or pyrimidine antagonists, as part of the chemotherapy regimens can affect toxicities profiles (45). (iii) The evaluation of toxicities was based on a standard handbook, while bias may have occurred when certain toxicities such as GI toxicity mainly depend on the subjective assessment by physicians. (iv) Platinum-induced toxicities were aggravated by the cumulative dosage; therefore, different chemotherapy cycles may also affect the results. (v) Platinum-induced toxicities may be affected by other factors, such as the demographic characteristics, molecular features of tumors, comorbidity, ethnicity, and intestinal bacteria.

Till date, the candidate gene approach is the most widely used strategy to identify platinum-induced toxicities and their associated polymorphisms. Novel variants will not be identified using this method, although the likelihood of a positive or negative association with a particular adverse event may be considerable in robust studies. Nevertheless, although previous GWAS and whole-exon sequencing had found novel genetic factors associated with platinum-induced toxicities, all these identified interactions need further verification to determine the mechanism.

The current meta-analysis has several limitations. First, studies without detailed data were excluded because of the lack of information regarding a significant association between gene polymorphisms and platinum-induced toxicities, and we were unable to contact these authors to provide us with the detailed data. This may have caused publication bias. Second, some of the included studies had small sample sizes, which may result in a decreased power to detect significant differences in the distribution of genotypes between grade 3–4 toxicities and grade 0–2 toxicities. Third, the occurrence of platinum-induced toxicities is affected by various factors, and hence, the pooled OR in this meta-analysis was based on the crude OR from the original studies. Because we could not obtain the raw data from individual studies, the pooled OR in this study was not adjusted for potential confounding factors such as sex, age, smoking status, comedications, gene–gene interactions, and gene–environment interactions, among other factors.

The results of our study indicated that single grade 3–4 toxicities that were associated with genetic polymorphisms might partly be the cause for inter-individual differences. Hence, further pharmacogenomics research is needed to determine the novel mutations and their associations. The combined effect of the genetic and clinical factors via gene–gene and gene–environment interactions should be considered in future studies, which may help to predict the risk of lung cancer. Nevertheless, more number of prospective, high-quality, multicenter clinical trials are urgently needed to explore the impact of gene polymorphisms on platinum-based toxicities in patients with lung cancer.

CONCLUSION

Our study found that *MTHFR* A1298C and C677T polymorphisms and *MDM2* rs1470383 polymorphisms were

significantly correlated with platinum-induced severe toxicities in patients with lung cancer. These polymorphisms should be considered for personalized chemotherapy treatment for lung cancer in the future.

DATA AVAILABILITY STATEMENT

The raw data supporting the conclusions of this article will be made available by the authors, without undue reservation, to any qualified researcher.

AUTHOR CONTRIBUTIONS

ZL and WL conceived and designed the study. ZL and YW performed research. ZL and JL conducted data analysis. ZL, HY, and WL accomplishment the manuscript, reference collection, data management, statistical analyses, paper writing, and study design.

ACKNOWLEDGMENTS

We would like to thank the researchers and study participants for their contributions.

SUPPLEMENTARY MATERIAL

The Supplementary Material for this article can be found online at: https://www.frontiersin.org/articles/10.3389/fonc.2019.01573/full#supplementary-material

REFERENCES

1. Siegel RL, Miller KD. Cancer statistics, 2019. *J Clin*. (2019) 69:7–34. doi: 10.3322/caac.21551
2. Herbst RS, Heymach JV, Lippman SM. Lung cancer. *N Engl J Med*. (2008) 359:1367–80. doi: 10.1056/NEJMra0802714
3. Lebwohl D, Canetta R. Clinical development of platinum complexes in cancer therapy: an historical perspective and an update. *Eur J Cancer*. (1998) 34:1522–34. doi: 10.1016/s0959-8049(98)00224-x
4. Novello S, Barlesi F, Califano R, Cufer T, Ekman S, Levra MG, et al. Metastatic non-small-cell lung cancer: ESMO Clinical Practice Guidelines for diagnosis, treatment and follow-up. *Ann Oncol*. (2016) 27:v1–27. doi: 10.1093/annonc/mdw326
5. Shi Y, Sun Y. Medical management of lung cancer: experience in China. *Thorac Cancer*. (2015) 6:10–6. doi: 10.1111/1759-7714.12168
6. Pilkington G, Boland A, Brown T, Oyee J, Bagust A, Dickson R. A systematic review of the clinical effectiveness of first-line chemotherapy for adult patients with locally advanced or metastatic non-small cell lung cancer. *Thorax*. (2015) 70:359–67. doi: 10.1136/thoraxjnl-2014-205914
7. Jiang N, Chen XC, Zhao Y. Analysis of the risk factors for myelosuppression after concurrent chemoradiotherapy for patients with advanced non-small cell lung cancer. *Support Care Cancer*. (2013) 21:785–91. doi: 10.1007/s00520-012-1580-y
8. Xiong Y, Huang BY, Yin JY. Pharmacogenomics of platinum-based chemotherapy in non-small cell lung cancer: focusing on DNA repair systems. *Med Oncol*. (2017) 34:48. doi: 10.1007/s12032-017-0905-6
9. Cao S, Wang S, Ma H, Tang S, Sun C, Dai J, et al. Genome-wide association study of myelosuppression in non-small-cell lung cancer patients with platinum-based chemotherapy. *Pharmacogenomics J*. (2016) 16:41–6. doi: 10.1038/tpj.2015.22
10. Green H, Hasmats J, Kupershmidt I, Edsgard D, de Petris L, Lewensohn R, et al. Using whole-exome sequencing to identify genetic markers for carboplatin and gemcitabine-induced toxicities. *Clin Cancer Res*. (2016) 22:366–73. doi: 10.1158/1078-0432.CCR-15-0964
11. Cao S, Wang C, Ma H, Yin R, Zhu M, Shen W, et al. Genome-wide association study on platinum-induced hepatotoxicity in non-small cell lung cancer patients. *Sci Rep*. (2015) 5:11556. doi: 10.1038/srep11556
12. Wang LY, Cui JJ, Liu JY, Guo AX, Zhao ZY, Liu YZ, et al. Gene-gene and gene-environment interaction data for platinum-based chemotherapy in non-small cell lung cancer. *Sci Data*. (2018) 5:180284. doi: 10.1038/sdata.2018.284
13. Cui JJ, Wang LY, Zhu T, Gong WJ, Zhou HH, Liu ZQ, et al. Gene-gene and gene-environment interactions influence platinum-based chemotherapy response and toxicity in non-small cell lung cancer patients. *Sci Rep*. (2017) 7:5082. doi: 10.1038/s41598-017-05246-8
14. Perez-Ramirez C, Canadas-Garre M, Alnatsha A, Villar E, Delgado JR, Faus-Dader MJ, et al. Pharmacogenetic predictors of toxicity to platinum based chemotherapy in non-small cell lung cancer patients. *Pharmacol Res*. (2016) 111:877–84. doi: 10.1016/j.phrs.2016.08.002
15. Joerger M, Burgers SA, Baas P, Smit EF, Haitjema TJ, Bard MP, et al. Germline polymorphisms in patients with advanced nonsmall cell lung cancer receiving first-line platinum-gemcitabine chemotherapy: a prospective clinical study. *Cancer*. (2012) 118:2466–75. doi: 10.1002/cncr.26562
16. Gandara DR, Kawaguchi T, Crowley J, Moon J, Furuse K, Kawahara M, et al. Japanese-US common-arm analysis of paclitaxel plus carboplatin in advanced non-small-cell lung cancer: a model for assessing population-related pharmacogenomics. *J Clin Oncol*. (2009) 27:3540–6. doi: 10.1200/jco.2008.20.8793
17. Li Y, Huang XE, Jin GF, Shen HB, Xu L. Lack of any relationship between chemotherapy toxicity in non-small cell lung cancer cases and polymorphisms in XRCC1 codon 399 or XPD codon 751. *Asian Pac J Cancer Prev*. (2011) 12:739–42.
18. Powrozek T, Mlak R, Krawczyk P, Homa I, Ciesielka M, Koziol P, et al. The relationship between polymorphisms of genes regulating DNA repair or cell division and the toxicity of platinum and vinorelbine chemotherapy in advanced NSCLC patients. *Clin Transl Oncol*. (2016) 18:125–31. doi: 10.1007/s12094-015-1343-6
19. De Troia B, Dalu D, Filipazzi V, Isabella L, Tosca N, Ferrario S, et al. ABCB1 c.3435C>T polymorphism is associated with platinum toxicity: a preliminary study. *Cancer Chemother Pharmacol*. (2019) 83:803–8. doi: 10.1007/s00280-019-03794-6
20. Zheng Y, Deng Z, Yin J, Wang S, Lu D, Wen X, et al. The association of genetic variations in DNA repair pathways with severe toxicities in NSCLC patients undergoing platinum-based chemotherapy. *Int J Cancer*. (2017) 141:2336–47. doi: 10.1002/ijc.30921
21. Qian CY, Zheng Y, Wang Y, Chen J, Liu JY, Zhou HH, et al. Associations of genetic polymorphisms of the transporters organic cation transporter 2 (OCT2), multidrug and toxin extrusion 1 (MATE1), and ATP-binding cassette subfamily C member 2 (ABCC2) with platinum-based chemotherapy response and toxicity in non-small cell lung cancer patients. *Chin J Cancer*. (2016) 35:85. doi: 10.1186/s40880-016-0145-8
22. Deng JH, Deng J, Shi DH, Ouyang XN, Niu PG. Clinical outcome of cisplatin-based chemotherapy is associated with the polymorphisms of GSTP1 and XRCC1 in advanced non-small cell lung cancer patients. *Clin Transl Oncol*. (2015) 17:720–6. doi: 10.1007/s12094-015-1299-6
23. Qian J, Liu H, Gu S, Wu Q, Zhao X, Wu W, et al. Genetic variants of the MDM2 gene are predictive of treatment-related toxicities and overall survival in patients with advanced NSCLC. *Clin Lung Cancer*. (2015) 16:e37–53. doi: 10.1016/j.cllc.2015.02.001
24. Peng Y, Wang L, Qing Y, Li C, Ren T, Li Q, et al. Polymorphisms of BCL2 and BAX genes associate with outcomes in advanced non-small cell lung cancer

patients treated with platinum-based chemotherapy. *Sci Rep*. (2015) 5:17766. doi: 10.1038/srep17766
25. Li X, Shao M, Wang S, Zhao X, Chen H, Qian J, et al. Heterozygote advantage of methylenetetrahydrofolate reductase polymorphisms on clinical outcomes in advanced non-small cell lung cancer (NSCLC) patients treated with platinum-based chemotherapy. *Tumour Biol*. (2014) 35:11159–70. doi: 10.1007/s13277-014-2427-6
26. Peng Y, Li Z, Zhang S, Xiong Y, Cun Y, Qian C, et al. Association of DNA base excision repair genes (OGG1, APE1 and XRCC1) polymorphisms with outcome to platinum-based chemotherapy in advanced nonsmall-cell lung cancer patients. *Int J Cancer*. (2014) 135:2687–96. doi: 10.1002/ijc.28892
27. Wang X, Wang YZ, Ma KW, Chen X, Li W. MDM2 rs2279744 and TP53 rs1042522 polymorphisms associated with etoposide- and cisplatin-induced grade III/IV neutropenia in Chinese extensive-stage small-cell lung cancer patients. *Oncol Res Treat*. (2014) 37:176–80. doi: 10.1159/000360785
28. Zheng D, Chen Y, Gao C, Wei Y, Cao G, Lu N, et al. Polymorphisms of p53 and MDM2 genes are associated with severe toxicities in patients with non-small cell lung cancer. *Cancer Biol Ther*. (2014) 15:1542–51. doi: 10.4161/15384047.2014.956599
29. Gu S, Wu Q, Zhao X, Wu W, Gao Z, Tan X, et al. Association of CASP3 polymorphism with hematologic toxicity in patients with advanced non-small-cell lung carcinoma treated with platinum-based chemotherapy. *Cancer Sci*. (2012) 103:1451–9. doi: 10.1111/j.1349-7006.2012.02323.x
30. Ludovini V, Floriani I, Pistola L, Minotti V, Meacci M, Chiari R, et al. Association of cytidine deaminase and xeroderma pigmentosum group D polymorphisms with response, toxicity, and survival in cisplatin/gemcitabine-treated advanced non-small cell lung cancer patients. *J Thorac Oncol*. (2011) 6:2018–26. doi: 10.1097/JTO.0b013e3182307e1f
31. Wang Z, Xu B, Lin D, Tan W, Leaw S, Hong X, et al. XRCC1 polymorphisms and severe toxicity in lung cancer patients treated with cisplatin-based chemotherapy in Chinese population. *Lung Cancer*. (2008) 62:99–104. doi: 10.1016/j.lungcan.2008.02.019
32. Booton R, Ward T, Heighway J, Ashcroft L, Morris J, Thatcher N. Glutathione-S-transferase P1 isoenzyme polymorphisms, platinum-based chemotherapy, and non-small cell lung cancer. *J Thorac Oncol*. (2006) 1:679–83. doi: 10.1097/01243894-200609000-00013
33. Suk R, Gurubhagavatula S, Park S, Zhou W, Su L, Lynch TJ, et al. Polymorphisms in ERCC1 and grade 3 or 4 toxicity in non-small cell lung cancer patients. *Clin Cancer Res*. (2005) 11:1534–8. doi: 10.1158/1078-0432.CCR-04-1953
34. Tibaldi C, Giovannetti E, Vasile E, Mey V, Laan AC, Nannizzi S, et al. Correlation of CDA, ERCC1, and XPD polymorphisms with response and survival in gemcitabine/cisplatin-treated advanced non-small cell lung cancer patients. *Clin Cancer Res*. (2008) 14:1797–803. doi: 10.1158/1078-0432.CCR-07-1364
35. Peng Y, Ma F, Tan C, Wan X, Yi L, Peng L, et al. Model-based economic evaluation of ceritinib and platinum-based chemotherapy as first-line treatments for advanced non-small cell lung cancer in China. *Adv Ther*. (2019) 36:3047–58. doi: 10.1007/s12325-019-01103-4
36. Zhang X, Zhang D, Huang L, Li G, Chen L, Ma J, et al. Discovery of novel biomarkers of therapeutic responses in Han Chinese pemetrexed-based treated advanced NSCLC patients. *Front Pharmacol*. (2019) 10:944. doi: 10.3389/fphar.2019.00944
37. Weisberg IS, Jacques PF, Selhub J, Bostom AG, Chen Z, Curtis Ellison R, et al. The 1298A–>C polymorphism in methylenetetrahydrofolate reductase (MTHFR): *in vitro* expression and association with homocysteine. *Atherosclerosis*. (2001) 156:409–15. doi: 10.1016/s0021-9150(00)00671-7
38. Hashemi M, Omrani M, Eskandari-Nasab E, Hasani SS, Mashhadi MA, Taheri M. A 40-bp insertion/deletion polymorphism of Murine Double Minute2 (MDM2) increased the risk of breast cancer in Zahedan, Southeast Iran. *Iran Biomed J*. (2014) 18:245–9. doi: 10.6091/ibj.13332.2014
39. Luan L, Wang H, Zhao B, Wang F, Shi J, Xu X. Association of MDM2 gene SNP 309 polymorphism and human non-small cell lung cancer susceptibility: a meta-analysis. *Pathol Res Pract*. (2019) 215:152538. doi: 10.1016/j.prp.2019.152538
40. Zhuo W, Zhang L, Zhu B, Ling J, Chen Z. Association of MDM2 SNP309 variation with lung cancer risk: evidence from 7196 cases and 8456 controls. *PLoS ONE*. (2012) 7:e41546. doi: 10.1371/journal.pone.0041546
41. Perez-Ramirez C, Canadas-Garre M. Pharmacogenetics of platinum-based chemotherapy: impact of DNA repair and folate metabolism gene polymorphisms on prognosis of non-small cell lung cancer patients. *Pharmacogenomics J*. (2019) 19:164–77. doi: 10.1038/s41397-018-0014-8
42. Perez-Ramirez C, Canadas-Garre M, Molina MA, Robles AI, Faus-Dader MJ, Calleja-Hernandez MA. Contribution of genetic factors to platinum-based chemotherapy sensitivity and prognosis of non-small cell lung cancer. *Mutat Res*. (2017) 771:32–58. doi: 10.1016/j.mrrev.2016.11.003
43. Zhang R, Zhou F, Cheng L, Yu A, Zhu M, Wang M, et al. Genetic variants in nucleotide excision repair pathway predict survival of esophageal squamous cell cancer patients receiving platinum-based chemotherapy. *Mol Carcinog*. (2018) 57:1553–65. doi: 10.1002/mc.22877
44. Yu J, Xiao J, Yang Y, Cao B. Oxaliplatin-based doublets versus cisplatin or carboplatin-based doublets in the first-line treatment of advanced nonsmall cell lung cancer. *Medicine*. (2015) 94:e1072. doi: 10.1097/md.0000000000001072
45. Amarasena IU, Chatterjee S, Walters JA, Wood-Baker R, Fong KM. Platinum versus non-platinum chemotherapy regimens for small cell lung cancer. *Cochrane Database Syst Rev*. (2015) Cd006849. doi: 10.1002/14651858.CD006849.pub3

Conflict of Interest: The authors declare that the research was conducted in the absence of any commercial or financial relationships that could be construed as a potential conflict of interest.

The reviewer J-YY declared a shared affiliation, with no collaboration, with the authors to the handling editor at the time of review.

frontiers in Oncology

ORIGINAL RESEARCH
published: 27 March 2020
doi: 10.3389/fonc.2020.00400

Expert Consensus on Effective Management of Chemotherapy-Induced Nausea and Vomiting: An Indian Perspective

Ashok K. Vaid[1], Sudeep Gupta[2], Dinesh C. Doval[3], Shyam Agarwal[4], Shona Nag[5], Poonam Patil[6], Chanchal Goswami[7], Vikas Ostwal[8], Sagar Bhagat[9], Saiprasad Patil[10] and Hanmant Barkate[11]*

[1] Medical Oncology and Hematology, Medanta – The Medicity, Gurugram, India, [2] ACTREC-TATA Memorial Centre, Navi Mumbai, India, [3] Medical Oncology, Rajiv Gandhi Cancer Institute and Research Centre, New Delhi, India, [4] Medical Oncology, Sir Ganga Ram Hospital, New Delhi, India, [5] Medical Oncology, Sahyadri Hospital, Pune, India, [6] Medical Oncologist, Manipal Hospital, Bangalore, India, [7] Oncology Services, MEDICA Super Speciality Hospital, Kolkata, India, [8] Medical Oncology, TATA Memorial Hospital, Mumbai, India, [9] Medical Services, HO IF, Glenmark Pharmaceuticals Ltd., Mumbai, India, [10] Medical Services, IF, Glenmark Pharmaceuticals Ltd., Mumbai, India, [11] Medical Services, IF & MEA, Glenmark Pharmaceuticals Ltd., Mumbai, India

OPEN ACCESS

Edited by:
Katrin Sak,
NGO Praeventio, Estonia

Reviewed by:
Harlokesh Narayan Yadav,
All India Institute of Medical Sciences, India
Alexandra Doina Carides,
Temple University, United States

***Correspondence:**
Sagar Bhagat
bq.pub1@yahoo.com

Specialty section:
This article was submitted to Pharmacology of Anti-Cancer Drugs, a section of the journal Frontiers in Oncology

Received: 30 September 2019
Accepted: 05 March 2020
Published: 27 March 2020

Citation:
Vaid AK, Gupta S, Doval DC, Agarwal S, Nag S, Patil P, Goswami C, Ostwal V, Bhagat S, Patil S and Barkate H (2020) Expert Consensus on Effective Management of Chemotherapy-Induced Nausea and Vomiting: An Indian Perspective. Front. Oncol. 10:400. doi: 10.3389/fonc.2020.00400

Chemotherapy-induced nausea and vomiting (CINV) is one of the most common and feared side effects in cancer patients undergoing chemotherapy. Scientific evidence proves its detrimental impact on a patient's quality of life (QoL), treatment compliance, and overall healthcare cost. Despite the CINV-management landscape witnessing a radical shift with the introduction of novel, receptor-targeting antiemetic agents, this side effect remains a chink in the armor of a treating oncologist. Though global guidelines acknowledge patient-specific risk factors and chemotherapeutic agent emetogenic potential in CINV control, a "one-fit-for-all" approach cannot be followed across all geographies. Hence, in a pioneering attempt, India-based oncologists conveyed easily implementable, region-specific, consensus-based statements on CINV prevention and management. These statements resulted from integrating the analysis of scientific evidence and guidelines on CINV by the experts, with their clinical experience. The statements will strengthen decision-making abilities of Indian oncologists/clinicians and help in achieving consistency in CINV prevention and management in the country. Furthermore, this document shall lay the foundation for developing robust Indian guidelines for CINV prevention and control.

Keywords: CINV, risk scoring, antiemetics, consensus, quality of life

INTRODUCTION

Chemotherapeutic approach for cancer is associated with the management of various adverse effects, which poses a great challenge to healthcare providers, thus having a detrimental impact on a patient's overall QoL (1, 2). Scientific evidence over time reveals nausea and vomiting to be the two most frequent and feared, yet underestimated, side effects in patients receiving chemotherapy (3–7). Physiologically, uncontrolled/poorly controlled and prolonged CINV leads to malnutrition, dehydration, and electrolyte imbalance. These adverse effects further lead to complications such as esophageal tears and declining behavior (toward the treatment) (8). The physiological distress

caused by CINV further transcends by negatively affecting a patient's ability to carry out normal daily activities/chores (9).

Severe and poorly controlled CINV was ranked near death by patients undergoing chemotherapy (6). Chemotherapy-induced nausea and vomiting not only has the propensity to increase morbidity, and healthcare cost, but also interferes with the chemotherapy adherence and patient's QoL (9–17). The current antiemetic agents exert their action by targeting various receptors [5-hydroxytryptamine (5-HT3), neurokinin 1 (NK1), dopamine, etc.] involved in the emesis mechanism (18).

Even though current global guidelines acknowledge the emetogenic potential of chemotherapeutic agents and patient-specific risk factors, management of delayed emesis is still a battle un-won. The Indian oncologists largely depend upon the National Comprehensive Cancer Network (NCCN) recommendations, the American Society of Clinical Oncology (ASCO) clinical updates and European society for medical oncology/multinational Association of Supportive Care in Cancer (ESMO/MASCC) recommendations. However, it is pertinent to state that these global guidelines are tailored according to the functioning of the healthcare setups in developed nations and do not account for factors unique to the healthcare systems of developing countries (19). Healthcare dynamics in a developing economy as ours are different from those of the developed nations. Healthcare accessibility, coupled with issues such as variable management practices and lack of sensitization for guidelines, has made the development of region-specific CINV-management guidelines the need of the hour (19). Findings from previously conducted multination Pan Australasian ChemoTherapy InduCed Emesis burden of illness (PrACTICE) study reported vast variation in the complete response (CR) rate (∼50–87%) among patients from different participating countries (20).

India reported a better overall CR rate when compared to Australia, China, and Singapore. On the other hand, Australia reported higher proportions of patients with no emesis compared to other Asian countries. Additionally, Asian countries, including India, reported high use and prescribing behavior of CINV rescue medication (20). Considering the response variations of various antiemetic agents, region-specific management guidelines are the need of the hour. Structuring region-specific recommendations for CINV will acknowledge the patient-related risk factors, affordability, sociocultural influence, and prevalent clinical oncology practice aspects in the country.

Hence, in a pioneering attempt, this document aims at guiding Indian oncologists on effective management of CINV in clinical practice.

METHODOLOGY

Consensus Development Process

The consensus-based clinical statements (**Table 1**) presented in the document were developed by the cumulative efforts of 45 oncologists, of whom eight oncologists constituted the core expert group. The initial inputs were gathered from the core group committee face-to–face interaction in August 2018. The clinical statements were validated, and then responses were gathered from the core expert group. Modified Delphi methodology was applied to achieve consensus on the initial votes from the core group. Following the initial votes, inputs from 35 India-based oncologists were taken through a Google survey link, using a 5-point Likert scale, to measure the cumulative agreement on 45 clinical statements. These inputs were received in September 2018. The anonymity of the participating oncologists was duly maintained. The 5-point Likert scale reads as follows:

Strongly disagree: Score of 1; Disagree: Score of 2; Neutral: Score of 3, Agree: Score of 4; Strongly agree: Score of 5.

The consensus-based statements were categorized as follows:

- Consensus: A mean score of ≥ 4 was considered as a consensus agreement.
- Near Consensus: A mean score of 3 to <4 was considered a near consensus agreement. Institutional and regional clinical practice may be considered for such statements.
- No consensus: Statements that did not meet the criteria of consensus or near consensus statements.

Descriptive statistics was calculated for each statement to include the mean and median of the responses. The levels of evidence and strength of recommendation were based on the two-level grading system by Guyatt et al. (21) (**Figure 1**) .

RESULTS

The participating experts critically analyzed existing literature, including randomized clinical trials, systematic reviews, and meta-analyses through a systematic search of MEDLINE (via PubMed), and Cochrane-indexed databases, and guidelines (e.g., NCCN) on CINV management published between 1983 and 2018. A summary of clinical statements with mean score has been provided in **Table 1**. Consensus was achieved for a total of 12 clinical statements, while 31 statements achieved a near consensus agreement from the experts.

DISCUSSION

Chemotherapy-Induced Nausea and Vomiting: A Chink in the Armor of an Oncologist

Chemotherapy-induced emesis exhibits pronounce effects and consequences.

Effect and Consequences of Chemotherapy-Induced Nausea and Vomiting

An observational study revealed both acute and delayed CINV to negatively impact a patient's QoL, with delayed variant showing a higher impact on QoL compared to acute CINV (14). In a prospective study, functional status of the patients, as assessed by Functional Living Index-Emesis (FLIE) score [ranging from 0 (not at all affected) to 100 (affected to a great extent)] was considered. A significant increase in the FLIE score for nausea before (day 1) and after chemotherapy (day 5) was observed (6.5 vs. 22.5; $p < 0.001$) (14).

TABLE 1 | Summary of clinical consensus statements.

S. No	Clinical statements	Mean score	Level of evidence and grade of recommendation
1	The risk for CINV depends not only on the type of chemotherapy administered but also on the patient's profile.	4.2	1A
2	Risk of chemotherapy induced nausea vomiting is higher during the first two cycles of chemotherapy.	3.8	2A
3	Nausea and vomiting in the previous cycle are a significant predictor of subsequent and clinically significant nausea and/or vomiting.	4.2	1A
4	Anxiety increases the risk of nausea and vomiting in patients scheduled for chemotherapy.	4.4	1A
5	History of motion sickness is important predictors of CINV.	3.8	2A
6	History of morning sickness in pregnancy increases patients' risk of CINV.	3.5	2A
7	Concomitant radiotherapy increases the risk of CINV in patients undergoing chemotherapy.	4.0	1C
8	Patients with poor performance status especially due to the disease process (ECOG status > 1) are more likely to experience nausea and vomiting.	3.9	2C
9	Females are at a higher risk of nausea vomiting (both acute and delayed) than males.	4.1	1A
10	Younger patients, <60 years of age, the risk of nausea vomiting is high.	3.4	2A
11	Pain and Cancer-related fatigue increases patients' risk of nausea and vomiting.	3.8	2C
12	Lack of sleep, the night previous to chemotherapy, increases the risk of nausea vomiting.	4.0	1C
13	Low or no alcohol intake is an independent risk factor for nausea vomiting. (both acute and delayed).	3.5	2A
14	Non-smokers are at a higher risk for nausea vomiting. (both acute and delayed).	2.9	2C
15	Risk of nausea- vomiting increases in patients on alternative (homeopathic/ayurvedic) medications.	3.0	2C
16	The risk of CINV increases if the patient is bombarded with the thought of CINV by family members.	4.0	1C
17	Classification of intravenous chemotherapeutic agents by NCCN guideline 2018 into HEC /MEC/LEC/Minimal is comprehensive.	4.1	1A
18	Cisplatin irrespective of the dose and regimen should be considered as HEC.	3.7	2A
19	AC combination should be considered as HEC.	4.0	1A
20	Carboplatin combination should be considered as HEC.	3.5	2B
21	Oxaliplatin combination should be considered as HEC.	3.0	2C
22	NK1RA needs to be used as a dexa sparing regime, especially while administering oxaliplatin in dextrose in patients with uncontrolled or poorly controlled diabetes.	3.4	2C
23	Netupitant being CYP3A4 inhibitor, expected to increase the exposure (AUC) of oral dexamethasone; hence, reduction in oral dexamethasone dose can be adapted during co-administration (from 20 to 12 mg).	3.9	2A
24	ECG monitoring is essential in patients on 5HT3 RA, considering the increased risk of QT prolongation associated with 5HT3 RA.	3.5	2A
25	Fear of QTc prolongation with antiemetics regimen is spurious.	3.6	2C
26	Patients who receive HEC—for controlling acute CINV (day 1), should be treated with triple combination therapy containing 5HT3 RA, dexamethasone and NK1 RA.	4.3	1A
27	Patients who receive HEC—for controlling acute CINV (day 1), should be treated with four drug combination therapy containing 5HT3 RA, dexamethasone, NK1 RA and olanzapine.	3.5	2A
28	Patients who receive HEC—for controlling delayed CINV (days 2–5), should be treated with dual therapy containing NK1 RA and dexamethasone.	3.7	2A
29	Patients who receive HEC—for controlling delayed CINV (days 2–5), should be treated with dual therapy containing olanzapine and dexamethasone.	3.3	2A
30	Patients who receive HEC—palonosetron is the preferred 5-HT3 antagonist.	3.8	2A
31	Patients who receive HEC—increased drowsiness is a worrisome side effect with olanzapine.	3.6	2C
32	Patients who receive MEC—for controlling acute CINV (day 1), should be treated with dual therapy containing 5HT3 RA and dexamethasone.	4.0	1A
33	Patients who receive MEC—for controlling delayed CINV, triple therapy with NK1RA improves outcome.	4.1	1A
34	Patients who receive MEC—for controlling delayed CINV (days 2–5), should be treated with dexamethasone only.	3.0	2A
35	Patients who receive MEC—for controlling delayed CINV (days 2–5), should be treated with NK1RA + dexamethasone.	3.3	2B
36	Patients who receive MEC—for controlling delayed CINV (days 2–5), patients should be treated with olanzapine + dexamethasone.	3.3	2C

(Continued)

TABLE 1 | Continued

S. No	Clinical statements	Mean score	Level of evidence and grade of recommendation
37	Patients who receive LEC and minimally emetogenic regimen—for controlling acute and delayed CINV, patients should be treated with dexamethasone only on day 1.	3.4	2A
38	Patients who receive minimally emetogenic regimen—needs no treatment to prevent CINV.	3.2	2A
39	Patients who receive multiday chemotherapy—long acting NK1RA to be given only on day 1.	3.8	2A
40	Patients who receive multiday chemotherapy—long acting NK1 RA should be given on days 1,3, and 5.	2.8	2C
41	Patients who receive multiday chemotherapy—5-HT3 receptor antagonist should be given daily.	3.5	2A
42	Patients who receive multiday chemotherapy–palonosetron, should be given on days 1, 3, and 5.	3.1	2A
43	Benzodiazepines are the only agents that have been shown to reduce the incidence of anticipatory nausea and vomiting.	3.7	2A
44	Olanzapine is the drug of choice in patients with breakthrough CINV.	3.4	2A
45	Sedation associated with olanzapine can be useful in the overall management of CINV.	3.4	2B

AC, Adriamycin-cyclophosphamide; AUC, Area under the curve; CINV, Chemotherapy-induced nausea and vomiting; ECOG, Eastern Cooperative Oncology Group; HEC, Highly emetogenic chemotherapy; MEC, Moderately emetogenic chemotherapy; LEC, Low emetogenic chemotherapy; NCCN, National Comprehensive Cancer Network; NK1 RA, Neurokinin-1 receptor antagonist; 5-HT3 RA, 5-hydroxytryptamine receptor antagonists.

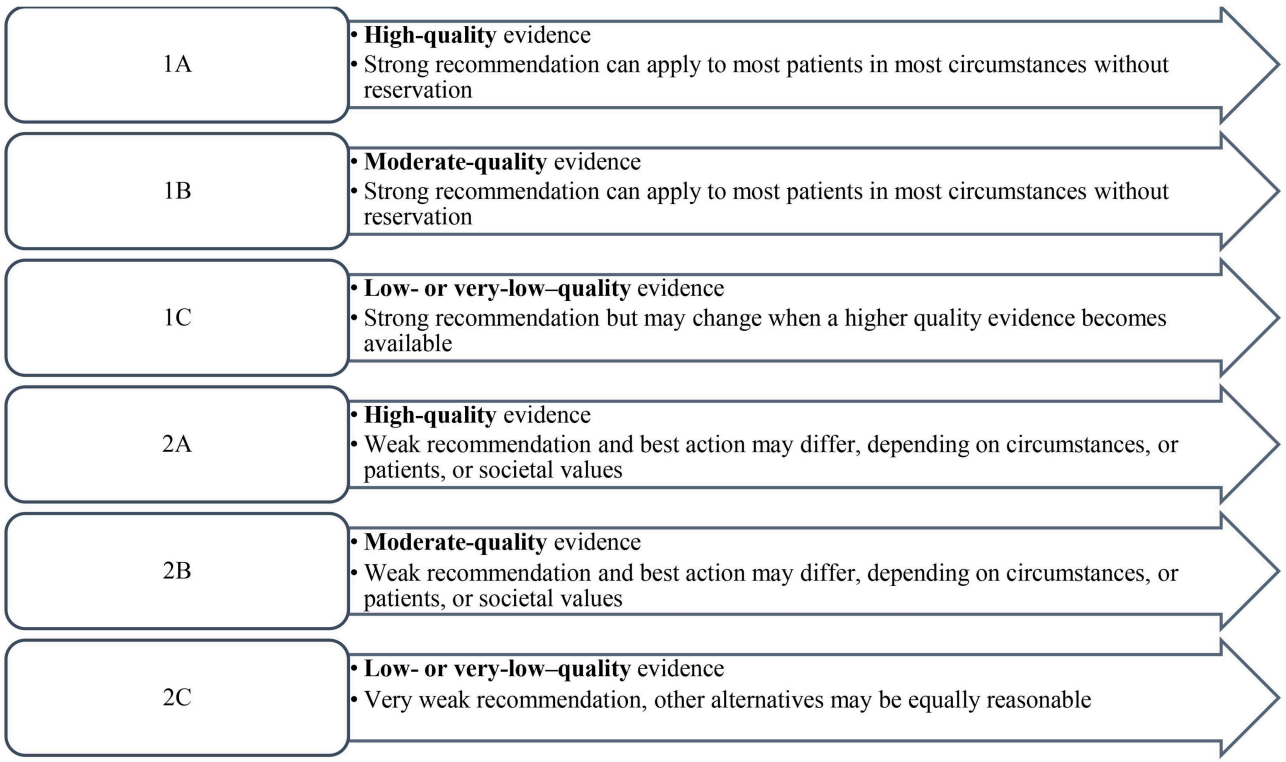

FIGURE 1 | Level of evidence and strength of recommendation.

The FLIE scores revealed a significant decline in the functional state of the patient by CINV, particularly in the first 24 h (15). In a retrospective analysis of three studies, results for emesis index from one of the trials showed a significant ($p < 0.0001$), negative effect of CINV on adherence to protocol therapy. Nonadherence to protocol therapy, in turn, affected the survival of the patient [16]. Furthermore, uncontrolled CINV leads to increased resource utilization, thereby increasing the total healthcare cost (11).

Risk Factors for Chemotherapy-Induced Nausea and Vomiting

The risk factors for CINV can be categorized into: patient-related and chemotherapeutic-agent–related factors.

Chemotherapy-Related Risk Factors

The chemotherapeutic agents used alone or in combination trigger different CINV patterns with varying intensity. The NCCN guideline states that for chemotherapies with minimal or low emetic risk, clinicians should avoid overusing antiemetic agents. This will further prevent the patients from adverse effects and reduce the healthcare expenditure (22). Experts recognized that treating oncologists should consider both patient-related and chemotherapy-related risk factors for CINV risk assessment. A good consensus was formed on classifying cisplatin as a highly emetogenic chemotherapy (HEC), irrespective of the dose and regimen and acknowledging Adriamycin-cyclophosphamide (AC) combination as HEC, instead of high-risk moderately emetogenic chemotherapy (MEC), as categorized by the NCCN guideline.

Patient-Related Risk Factors

Apart from the chemotherapeutic regimen administered, evidence suggests certain patient-related risk factors to form an integral part of the overall emetic risks for a patient receiving chemotherapy (23–27). Study conducted among chemotherapy-naive patients of phase II and III trials revealed increased nausea in both acute and delayed phases, as the number of risk factors increases. Treatment failure (any emetic episodes or administration of any rescue medication) was significantly higher in patients with three risk factors compared with patients with no risk factors (acute phase: 46.2 vs. 8.9%, $p < 0.001$; delayed phase: 39.3 vs. 54.2%, $p < 0.001$) (27). Furthermore, female gender, nonhabitual alcohol intake and age of <55 years are significant patient-related risk factors for CINV, as they are associated with treatment failure in the acute CINV phase (27). In another observational study conducted in patients undergoing HEC or MEC chemotherapy, female gender was identified as a major prognostic risk factor for CINV [odds ratio (OR): 3.087, 95% confidence interval (CI): 2.219–4.295; $p < 0.0001$]. Older age from both genders was associated with a decrease in acute and delayed CINV ($p < 0.0001$). Furthermore, alcohol intake was found to be associated with decreased risk of delayed CINV ($p = 0.003$), particularly in men (28). High alcohol intake is thought to affect the chemoreceptor trigger zone, thereby having a less pronounced effect by the chemotherapeutic agents (29).

Results from a double-blind, randomized trial showed female gender and age <60 years as significant risk factors (30). A longitudinal observational study echoed similar results of female gender along with other patient-related risk factors to be significant risk factors for CINV. However, the study did not identify young age as a significant risk factor for CINV (31). Strong consensus was formed by the experts on female gender having significantly higher risk of both acute and delayed CINV compared to males. However, a near consensus agreement was built on the increased risk of CINV at young age and decreased CINV risk with alcohol use.

Apart from age and gender, evidence from a univariate analysis in a study revealed history of morning sickness (OR: 2.111, 95% CI: 1.634–2.728; $p < 0.0001$) and motion sickness (OR: 2.796, 95% CI: 2.069–3.778; $p < 0.0001$) in women to be high-risk patient-related factors for acute CINV. Morning sickness was also significantly related to high risk of delayed CINV ($p < 0.0001$) (28). In a prospective study, motion sickness and history of morning sickness experienced in pregnancy were the key prognostic risk factors for CINV (32). In a *post-hoc* analysis, history of morning sickness associated with pregnancy, or morning sickness, contributed as significant patient-related factors in increasing CINV risk (33).

In line with the literature, reasonable consensus came from the experts on the predictors of CINV, such as previous history of motion sickness and morning sickness associated with pregnancy. Psychological factors cannot be ruled out while assessing the risk factors for CINV. Patients' past experiences with CINV can govern and influence response expectancy of nausea for their upcoming chemotherapy (34).

Evidence from a registry trial showed high level anxiety pre-chemotherapy to be a strong predictor of anticipatory CINV in the first cycle of the chemotherapeutic regimen. Patients who experienced CINV in the previous cycle had 3.7 and 3.3 times more chances to develop anticipatory CINV in Cycles 2 and 3, respectively, compared to those who had no prior CINV experience (35). Furthermore, the likelihood of CINV was increased by 6.5 times in Cycle 2, and 14 times in Cycle 3 through the uncontrolled CINV in the previous cycle (35).

A good consensus was obtained on increased risk of CINV with increased anxiety and history of CINV in previous chemotherapeutic cycles. Furthermore, experts acknowledged that CINV risk is high in the first two cycles of chemotherapy, and pain and cancer-related fatigue increase the patients' risk of CINV. Hence, optimum care should be exercised in the first two chemotherapeutic cycles.

Apart from patients' anxiety, role of family as an influencer to CINV episode cannot be ruled out. Finding from a prospective study revealed family support to have a direct impact on the severity of anticipatory CINV. The result from the study suggested that communicating with families might be beneficial in reducing CINV symptoms (34).

A good consensus was achieved for the role of family in CINV risk occurrence, validating the need for patient's family education and counseling. Poor sleep quality and insomnia emerged as other strong predictive risk factors for CINV. Results from an observational study revealed CINV to be significantly associated with poor sleep quality (OR: 2.48, 95% CI: 1.13–5.46; $p = 0.024$) (36). A prospective multicenter, multivariate analysis identified another important independent risk factor for delayed CINV—Eastern Cooperative Oncology Group (ECOG) performance status ≥ 1 in acute phase (OR: 2.23, 95% CI: 1.04–4.78; $p = 0.04$) (37).

Experts duly acknowledged the increased risk of CINV if the patients received concomitant radiotherapy along with chemotherapy and lack of adequate sleep, a night before the

scheduled chemotherapy. A fair consensus was built among the experts, in support for the patients with poor performance status (ECOG) to be an independent risk factor for CINV.

In Asian countries, including India, there is significant usage of alternative medicine (traditional medicine systems) in cancer patients with or without allopathy. However, there is limited evidence concerning their safety and efficacy; a few herbs can interact with the chemotherapeutic agent, leading to several adverse reactions (38). Experts had a near consensus agreement on increased CINV risk in patients on alternative (homeopathic/ayurvedic) medications. Hence, clinicians should also educate and accordingly exercise caution to patients on their use. In absence of robust scientific evidence, no consensus was achieved on the correlation of acute and delayed CINV with history of smoking.

Management of Chemotherapy-Induced Nausea and Vomiting

Antiemetic regimens are selected based on the drug with the highest emetic risk as well as patient-specific risk factors. The guideline further acknowledges that the risk of nausea/vomiting in patients receiving HEC or MEC lasts for at least 3 days, and 2 days for HEC and MEC settings, after the last dose of chemotherapy. Hence, patients need to be protected throughout the full duration of risk (22). Experts had a good agreement on the recent classification of various intravenous chemotherapeutic agents, according to their emetogenic potential, by the NCCN guideline. A fair consensus surfaced for avoiding prophylaxis of CINV in patients on the minimally emetogenic regimen.

Various Antiemetic Agents

5-Hydroxytryptamine (5-HT3) receptor antagonists

As serotonin plays an integral role in the pathophysiology of CINV, 5-HT3 RAs (ondansetron, granisetron, dolasetron, and palonosetron) are invaluable antiemetic agents in the management landscape of CINV (39). The first-generation 5-HT3 RAs are more effective in controlling acute emesis compared to delayed CINV. Based on the scientific evidence, palonosetron has emerged to be a more efficacious and safer 5-HT3 RA agent compared to other agents of the class (39–43). Palonosetron was found to be highly selective, with a strong binding affinity and a long plasma elimination half-life. It has shown its efficacy in preventing CINV in both HEC and MEC settings along with other drugs (40, 41, 44, 45).

A prospective observational study in South Indian patients receiving cancer chemotherapy revealed that as compared to ondansetron, palonosetron is clinically more efficient in controlling CINV. Statistically significant difference in antiemetic response to these two types of prophylaxis was observed, palonosetron being more efficient particularly in delayed phase and overall CINV ($p = 0.006$ for delayed phase, and $p = 0.008$ for overall response). Complete response was observed in 82.1 and 65.1% patients in palonosetron and ondansetron groups, respectively (46). In another prospective, randomized, crossover study involving patients aged between 2 and 18 years, no significant difference was observed in the CR rates across both the treatment groups. Therefore, the findings indicated that ondansetron is noninferior to palonosetron, and can be used as alternative antiemetic drugs (47).

However, it is pertinent to specify the cardiac adverse effects of these agents. QT prolongation is a class adverse effect of these agents. In the light of evidence, special attention is warranted for cancer patients with cardiac disease or elderly cancer patients on polypharmacy (48–50). The NCCN guidelines recommend intravenous palonosetron as the preferred 5-HT3 antagonist (22).

For MEC regimen, the NCCN guideline recommends intravenous palonosetron or subcutaneous granisetron extended-release injection as a preferred 5-HT3 RA, along with dexamethasone. The guideline further recommends a triple-drug regimen, containing NK1 RA or olanzapine, or a four-antiemetic drug regimen, including NK 1RA or olanzapine for HEC setting (22). Additionally, the guidelines duly acknowledge the cardiac effects of the 5-HT3 RAs and suggest routine electrocardiogram (ECG) monitoring during treatment with regimens that include 5-HT3 RAs for patients who may have concomitant risk factors for QT prolongation (22). A fair near consensus agreement was formed for palonosetron as the preferred 5-HT3 RA for HEC setting and ECG monitoring to be essential in patients receiving 5-HT3 RAs. However, experts also opined that the fear of QTc prolongation with antiemetics regimen is spurious.

Dexamethasone

Evidence collected over the years shows dexamethasone increasing the efficacy of 5-HT3 RAs in MEC and HEC settings. Efficacy of 5-HT3 RA in terms of complete CINV protection, when combined with dexamethasone for acute CINV, ranged from 68 to 92%; for delayed CINV: 47–73% (42, 43, 51, 52). Though the agent is generally effective, in monotherapy or combination therapy, and is typically administered for multiple days after the start of chemotherapy to prevent delayed CINV, it is associated with insomnia, agitation, rashes, gastrointestinal symptoms, and weight gain (52, 53).

The NCCN guideline acknowledges the side effects of dexamethasone, i.e., insomnia, and hence it recommends specific dosing of dexamethasone for both HEC and MEC regimens. For the triple combination (NK1 RA/palonosetron/dexamethasone) regimen of HEC and MEC settings, the dose of dexamethasone was decreased to 12 mg per oral/intravenous (PO/IV) for day 1. For all the HEC regimens, the guideline recommended dexamethasone 8 mg PO/IV daily on days 2–4 (22). A near consensus emerged for prescribing dexamethasone only on day 1 for acute and delayed CINV in patients on low emetogenic chemotherapy (LEC) and minimal emetogenic regimen. Consistent with the evidence and recommendation for reduction of dexamethasone dose, the experts had a fair consensus on reduction in dose of oral dexamethasone (20–12 mg) during co-administration with an NK1 RA (netupitant).

NK1 receptor antagonists

Another important and relatively new class of antiemetics are NK1 RAs (aprepitant, fosaprepitant, netupitant, fosnetupitant, and rolapitant). More and more evidence on efficacy and tolerability of NK1RAs are surfacing from Indian region, highlighting safe and efficacious nature of fosaprepitant,

and aprepitant formulations in the Indian population in HEC and MEC settings (54–56). A phase III, randomized, double-blind, placebo-controlled trial was performed in Indian pediatric oncology patients aged 1–12 years on MEC or HEC (ondansetron plus dexamethasone, and fosaprepitant). As compared to the patients in the placebo arm, significantly lower number of patients in the fosaprepitant arm required rescue anti-emetics (20 vs. 4%, $p = 0.0017$) (57). Another single center retrospective cohort study from South India revealed that use of single-dose fosaprepitant in combination with palonosetron, and dexamethasone, effectively prevented CINV (CR: 100%) in both HEC and MEC therapeutic regimens (58).

Furthermore, scientific literature has provided good evidence on the effectiveness and safety of netupitant–palonosetron combination in both HEC and MEC settings (59–62). The NCCN guideline recommends NK1 RA to be added to a 5-HT3/dexamethasone regimen for patients receiving MEC anticancer therapy who have additional risk factors, or previous treatment failure with the two-drug regimen. Patients receiving anticancer therapy, with a higher risk of emesis, are at greater risk of emesis and might require the addition of an NK1 RA (22). Furthermore, for the HEC regimen, any NK1 RA could be used in the four-drug regimen on day 1 (olanzapine/NK1 RA/5-HT3/dexamethasone) (22).

Olanzapine

Olanzapine is an atypical antipsychotic, which has antagonizing activity against dopamine (D1–D4 brain receptors), 5-HT2a, 5-HT2c, 5-HT3, histamine (H1 receptors), and muscarinic receptors (63). In a randomized, controlled, Indian trial conducted among 100 chemotherapy-naïve patients on any platinum-based chemotherapy received either, palonosetron and dexamethasone combination or olanzapine (10 mg/day). Results revealed patients in add-on olanzapine group to have significantly better control of delayed compared to dual therapy group (CR: 96 vs. 42%; $p < 0.0001$). Additionally, failure of anti-CINV measure was significantly less in add-on olanzapine group compared to dual (4 vs. 26%) (64). In another randomized, prospective trial; olanzapine as a triple therapy component (with palonosetron and dexamethasone) was found to be as effective as safe as aprepitant for controlling CINV in HEC setting (65). Apart from being effective in breakthrough CINV, olanzapine may serve as a cost-effective alternative to aprepitant in HEC setting and also in patients on HEC regimen who fail on NK1 RA therapy (66, 67). In a prospective, randomized, controlled study conducted in a center in North India, olanzapine group (olanzapine, palonosetron, and dexamethasone) was found to be associated with significantly lowered vomiting and severity of nausea than the control group (palonosetron and dexamethasone). In addition, better control of delayed emesis was observed in the olanzapine-treated patients (CR: 42 vs. 96% in the control and olanzapine-treated groups, respectively, $p < 0.0001$), and overall quality of life was better in this group of patients (64).

In line with the evidence, the NCCN guideline recommended olanzapine-containing three-drug or four-antiemetic drug regimens for both HEC and MEC settings. Furthermore, it was stated that olanzapine could be substituted for dexamethasone in patients who are unable to tolerate dexamethasone (22). However, the only dose-limiting side effects associated with the agent are sedation and drowsiness, which can significantly impact the daily activities of a patient (65). A fair near consensus agreement was achieved for olanzapine as the drug of choice in patients with breakthrough CINV. However, experts felt that sedation associated with olanzapine could be useful in the overall management of CINV, as the already distressed cancer patients can get a good amount of sleep. Hence, based on a patient's condition and nature of job, the antiemetic agent should be individualized.

HEC and MEC Regimens (Acute and Delayed Phases)

Many challenges plague CINV management in patients receiving HEC and MEC regimens. An observational study in patients receiving MEC/HEC for the first time revealed >75% of clinicians and nurses underestimated the incidence of delayed CINV. The representation of the prediction of incidence vs. a patient's experience of CINV variants is presented in **Figure 2** (40).

In a retrospective analysis of three clinical trials, various chemotherapy-related toxicities by patients and clinicians were compared. The result from the analysis revealed underreporting of the toxicities (including nausea and vomiting) by the physicians (68).

In a prospective multicenter study, in patients administered HEC/MEC, a significant difference in the control of nausea and CINV was observed in a patient receiving guideline-consistent measures for CINV prevention when compared to patients receiving inconsistent prophylaxis for CINV (CR: 59.9 vs. 50.7%; $p = 0.008$) (9).

In a survey conducted among healthcare providers, significant discrepancies were observed between the recommendations and clinical use of the antiemetic agent in HEC settings with underutilization of NK-1 RAs on day 1 and high use of 5-HT3 RAs on day 2 beyond the chemotherapeutic regimen. There was underutilization of dexamethasone in the MEC setting. The marked uses of phenothiazines (47%) and benzodiazepines (30%) on day 2 and beyond of chemotherapy were found to be inconsistent with the guideline recommendations (69).

Furthermore, the wide range of expected emesis in the MEC regimen (30–90%) makes it challenging to narrow down a specific antiemetic regimen for the whole category (62). In a systematic review conducted by Jordan et al. addition of NK1 RA in a MEC setting exerted a clinically significant benefit in carboplatin-based chemotherapy. The OR obtained for NK1 RA antiemetic regimen for acute and delayed CINV was 1.60 (95% CI: 1.06–2.40; $p = 0.02$) and 2.25 (95% CI: 1.70–2.98; $p < 0.00001$), respectively (62). In Indian scenario, triple therapy with NK1RAs (aprepitant, palonosetron, and dexamethasone) was found to be efficacious and safe with an overall CR rate of 92 and 90.9%, for HEC and MEC regimen, respectively (55). Furthermore, triple therapy with

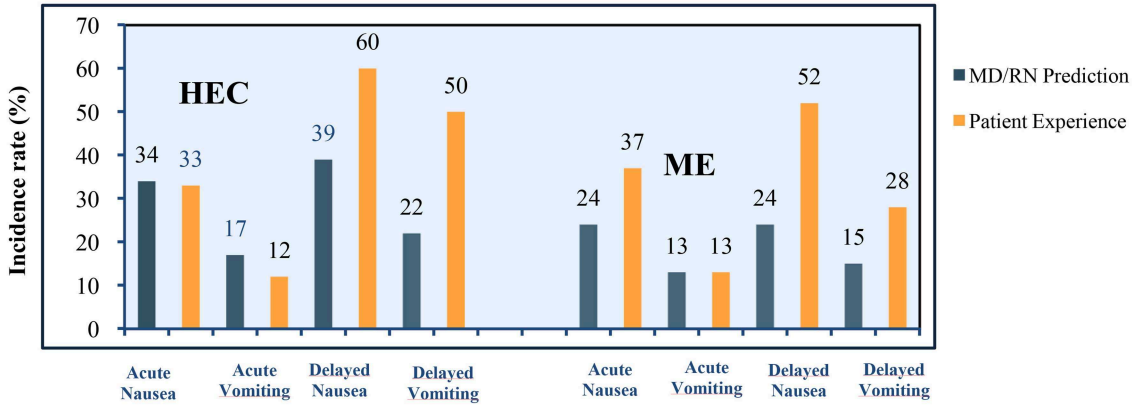

Adapted from *Grunberg SM, et al. Cancer. 2004;100:2261-2268.*

FIGURE 2 | Incidence rates of nausea and vomiting (actual vs. prediction).

NK1RA was also found to be significantly effective compared to dual therapy (5 HT3 RA+ dexamethasone) in preventing acute and delayed CINV among patients with head and neck cancer (54).

Experts recommended a triple combination therapy (NK1 RA + 5-HT3 RA + dexamethasone) for CINV management in patients receiving AC combination. The experts strongly supported the use of triple combination therapy on day 1 for controlling acute CINV in patients receiving HEC regimen. Compared to olanzapine and dexamethasone combination, the experts had a fair consensus agreement for the use of dual therapy containing NK1 RA and dexamethasone for controlling delayed CINV (days 2–5) in patients receiving HEC.

Experts further acknowledged that triple antiemetic therapy with NK1 RA has the potential to improve outcome in patients on MEC regimen, who have additional risk factors such as female gender, anxiety, motion sickness, etc. Furthermore, for controlling acute CINV in patients receiving a MEC regimen, the consensus was formed on the use of dual therapy (5-HT3 RA + dexamethasone). For patients on MEC, a fair consensus on the use of NK1 RA + dexamethasone or olanzapine + dexamethasone compared to dexamethasone alone was obtained to control delayed CINV (days 2–5).

Multiday Chemotherapy

Multiday chemotherapy poses a great management challenge; as the mechanism and pattern of CINV might differ from the single-day chemotherapeutic regimen. Therefore, efficacy of antiemetic agent as observed in single-day chemotherapy may not be extrapolated to the multiday scenario. There is a shortage of data exploring the efficacy and safety of various agents in the specific setting. Patients receiving such regimens are at risk of both acute and delayed CINV (22, 70). As the chemotherapy is extended over several days, it becomes further difficult to specify individual antiemetic agent/regimen for each day of the therapy. However, 5-HT3 RA, dexamethasone, and NK1 RA have greatly improved the management landscape for acute and delayed CINV in multiday chemotherapy (71–73).

There was a good consensus on the use of NK1 RAs to be given only on day 1 for patients who receive multiday chemotherapy. A fair consensus was achieved for 5-HT3 RA daily and palonosetron on days 1, 3, and 5 for patients on multiday chemotherapy. However, no consensus was formed among the experts for the use of long-acting NK1 RA on days 1, 3, and 5 of the multiday chemotherapy. The use of NK1 RA shall further require robust scientific evidence.

CONCLUSION AND FUTURE DIRECTIVES

The current evidence indicates that there is still room for improvement concerning CINV management. This document is a sincere effort to address the common unmet needs in CINV-management landscape in the country. The definitive consensus-based clinical statements churned out from the multifaceted approach of the participating experts will guide Indian oncologists to tackle CINV holistically. These statements will also ensure a consistent CINV prevention and management approach in the region.

To further strengthen our discussion, we propose (1) establishing robust resource-stratified guidelines for CINV management, specific to the Indian region, and (2) nation-wide programs to sensitize Indian oncologists toward effective implementation of the drafted guidelines. The CINV guidelines will, in turn, empower the treating oncologists to make informed and individualized decisions on CINV across various healthcare settings. Furthermore, following a consistent preventive and management strategy for the side effect will help in promoting the judicious use of antiemetic agents and, ultimately, help improve the overall QoL in patients undergoing chemotherapy.

DATA AVAILABILITY STATEMENT

All datasets for this study are included in the article/supplementary material.

AUTHOR CONTRIBUTIONS

All authors listed have made a substantial, direct and intellectual contribution to the work, and approved it for publication.

FUNDING

This work was supported by Glenmark Pharmaceuticals Ltd.

ACKNOWLEDGMENTS

We would like to thank BioQuest solutions for editorial assistance.

REFERENCES

1. Janelsins MC, Tejani MA, Kamen C, Peoples AR, Mustian KM, Morrow GR. Current pharmacotherapy for chemotherapy-induced nausea and vomiting in cancer patients. *Expert Opin Pharmacother.* (2013) 14:757–66. doi: 10.1517/14656566.2013.776541
2. Passik SD, Kirsh KL, Rosenfeld B, McDonald MV, Theobald DE. The changeable nature of patients' fears regarding chemotherapy: implications for palliative care. *J Pain Symptom Manage.* (2001) 21:113–20. doi: 10.1016/S0885-3924(00)00249-9
3. Lindley C, Mccune JS, Thomason TE, Lauder D, Sauls A, Adkins S, et al. Perception of chemotherapy side effects cancer versus noncancer patients. *Cancer Pract.* (1999) 7:59–65. doi: 10.1046/j.1523-5394.1999.07205.x
4. Grunberg SM, Deuson RR, Mavros P, Geling O, Hansen M, Cruciani G, et al. Incidence of chemotherapy-induced nausea and emesis after modern antiemetics perception versus reality. *Cancer.* (2004) 100:2261–68. doi: 10.1002/cncr.20230
5. Coates A, Abraham S, Kaye SB, Sowerbutts T, Frewin C, Fox RM, et al. On the receiving end–patient perception of the side-effects of cancer chemotherapy. *Eur J Cancer Clin Oncol.* (1983) 19:203–08. doi: 10.1016/0277-5379(83)90418-2
6. Sun CC, Bodurka DC, Weaver CB, Rasu R, Wolf JK, Bevers MW, et al. Rankings and symptom assessments of side effects from chemotherapy: insights from experienced patients with ovarian cancer. *Support Care Cancer.* (2005) 13:219–27. doi: 10.1007/s00520-004-0710-6
7. Griffin AM, Butow PN, Coates AS, Childs AM, Ellis PM, Dunn SM, et al. On the receiving end. V: Patient perceptions of the side effects of cancer chemotherapy in 1993. *Ann Oncol.* (1996) 7:189–95. doi: 10.1093/oxfordjournals.annonc.a010548
8. Curran MP, Robinson DM. Aprepitant: a review of its use in the prevention of nausea and vomiting. *Drugs.* (2009) 69:1853–78. doi: 10.2165/11203680-000000000-00000
9. Aapro M, Molassiotis A, Dicato M, Peláez I, Rodríguez-Lescure Á, Pastorelli D, et al. The effect of guideline-consistent antiemetic therapy on chemotherapy-induced nausea and vomiting (CINV): The Pan European Emesis Registry (PEER). *Ann Oncol.* (2012) 23:1986–92. doi: 10.1093/annonc/mds021
10. Burke TA, Wisniewski T, Ernst FR. Resource utilization and costs associated with chemotherapy-induced nausea and vomiting (CINV) following highly or moderately emetogenic chemotherapy administered in the US outpatient hospital setting. *Support Care Cancer.* (2011) 19:131–40. doi: 10.1007/s00520-009-0797-x
11. Turini M, Piovesana V, Ruffo P, Ripellino C, Cataldo N. An assessment of chemotherapy-induced nausea and vomiting direct costs in three EU countries. *Drugs Context.* (2015) 4:212285. doi: 10.7573/dic.212285
12. Chan A Low XH, Yap KY. Assessment of the relationship between adherence with antiemetic. *J Manag Care Pharm.* (2012) 18:385–94. doi: 10.18553/jmcp.2012.18.5.385
13. Perwitasari DA, Atthobari J, Mustofa M, Dwiprahasto I, Hakimi M, Gelderblom H, et al. Impact of chemotherapy-induced nausea and vomiting on quality of life in indonesian patients with gynecologic cancer. *Int J Gynecol Cancer.* (2012) 22:139–45. doi: 10.1097/IGC.0b013e318234f9ee
14. Abdul B Hassan, Binti Z. Negative impact of chemotherapy on breast cancer patients QOL - Utility of antiemetic treatment guidelines and the role of race. *Asian Pac J Cancer Prev.* (2010) 11:1523–27. Available online at: http://journal.waocp.org/article_25408_fe55030cc3e36e59764f8d7f7b9bf649.pdf
15. Brien BJO, Rusthoven J, Rocchi A, Latreille J, Fine S, Vandenberg T, et al. Impact of chemotherapy-associated nausea and vomiting on patients' functional status and on costs: Survey of five Canadian centres. *CMAJ.* (1993) 149:296–02.
16. Neymark N, Crott R. Impact of emesis on clinical and economic outcomes of cancer therapy with highly emetogenic chemotherapy regimens: a retrospective analysis of three clinical trials. *Support Care Cancer.* (2005) 13:812–18. doi: 10.1007/s00520-005-0803-x
17. Sommariva S, Pongiglione B, Tarricone R. Impact of chemotherapy-induced nausea and vomiting on health-related quality of life and resource utilization: a systematic review. *Crit Rev Oncol Hematol.* (2016) 99:13–36. doi: 10.1016/j.critrevonc.2015.12.001
18. Frame DG. Best practice management of CINV in oncology patients: I. Physiology and treatment of CINV. Multiple neurotransmitters and receptors and the need for combination therapeutic approaches. *J Support Oncol.* (2010) 8(2 Suppl. 1):5–9.
19. Patil V, Noronha V, Joshi A, Parikh P, Bhattacharjee A, Chakraborty S, et al. Survey of implementation of antiemetic prescription standards in Indian oncology practices and its adherence to the American Society of Clinical Oncology Antiemetic Clinical Guideline. *J Glob Oncol.* (2017) 3:346–59. doi: 10.1200/JGO.2016.006023
20. Lee MA, Cho EK, Oh SY, Ahn JB, Lee JY, Thomas B, et al. Clinical practices and outcomes on chemotherapy-induced nausea and vomiting management in South Korea: comparison with Asia-Pacific Data of the Pan Australasian Chemotherapy Induced Emesis Burden of Illness Study. *Cancer Res Treat.* (2016) 48:1420–28. doi: 10.4143/crt.2015.309
21. Guyatt G, Gutterman D, Baumann MH, Addrizzo-Harris D, Hylek EM, Phillips B, et al. Grading strength of recommendations and quality of evidence in clinical guidelines: report from an American college of chest physicians task force. *Chest.* (2006) 129:174–81. doi: 10.1378/chest.129.1.174
22. *NCCN Guidelines Antiemesis.* (2018). Available online at: https://www.nccn.org/professionals/physician_gls/pdf/antiemesis.pdf (accessed January 31, 2019).
23. Morrow GR, Roscoe JA, Kirshner JJ, Hynes HE, Rosenbluth RJ. Anticipatory nausea and vomiting in the era of 5-HT 3 antiemetics. *Support Care Cancer.* (1998) 6:244–47. doi: 10.1007/s005200050161
24. Roila F, Boschetti E, Tonato M, Basurto C, Bracarda S, Picciafuoco M, et al. Predictive factors of delayed emesis in cisplatin-treated patients and antiemetic activity and tolerability of metoclopramide or dexamethasone. A randomized, single-blind study. *Am J Clin Oncol.* (1991) 14:238–42. doi: 10.1097/00000421-199106000-00010
25. Gregory RE, Ettinger DS. 5-HT 3 receptor antagonists for the prevention of chemotherapy-induced nausea and vomiting: a comparison of their pharmacology and clinical efficacy. *Drugs.* (1998) 55:173–89. doi: 10.2165/00003495-199855020-00002
26. Pollera CF, Giannarelli D. Prognostic factors influencing cisplatin-induced emesis. Definition and validation of a predictive logistic model. *Cancer.* (1989) 64:1117–22. doi: 10.1002/1097-0142(19890901)64:5<1117::AID-CNCR2820640525>3.0.CO;2-R
27. Sekine I, Segawa Y, Kubota K, Saeki T. Risk factors of chemotherapy-induced nausea and vomiting: index for personalized antiemetic prophylaxis. *Cancer Sci.* (2013) 104:711–17. doi: 10.1111/cas.12146

28. Tamura K, Aiba K, Saeki T, Nakanishi Y, Kamura T, Baba H, et al. Testing the effectiveness of antiemetic guidelines : results of a prospective registry by the CINV Study Group of Japan. *Int J Clin Oncol.* (2015) 20:855–65. doi: 10.1007/s10147-015-0786-7
29. Sullivan JR, Leyden MJ, Bell R. Decreased cisplatin-induced nausea and vomiting with chronic alcohol ingestion. *N Engl J Med.* (1983) 309:796. doi: 10.1056/NEJM198309293091316
30. Tsuji D, Suzuki K, Kawasaki Y, Goto K, Matsui R, Seki N et al. Risk factors associated with chemotherapy-induced nausea and vomiting in the triplet antiemetic regimen including palonosetron or granisetron for cisplatin-based chemotherapy : analysis of a randomized, double-blind controlled trial. *Support Care Cancer.* (2019) 27:1139–47. doi: 10.1007/s00520-018-4403-y
31. Pirri C, Katris P, Trotter J, Bayliss E, Bennett R, Drummond P. Risk factors at pretreatment predicting treatment-induced nausea and vomiting in Australian cancer patients : a prospective, longitudinal, observational study. *Support Care Cancer.* (2011) 19:1549–63. doi: 10.1007/s00520-010-0982-y
32. Molassiotis, Yam BM, Yung H, Chan FY, Mok TS. Pretreatment factors predicting the development of post chemotherapy nausea and vomiting in Chinese breast cancer patients. *Support Care Cancer.* (2002) 10:139–45. doi: 10.1007/s00520-001-0321-4
33. Warr DG, Street JC, Carides AD. Evaluation of risk factors predictive of nausea and vomiting with current standard-of-care antiemetic treatment:analysis of phase 3 trial of aprepitant in patients receiving adriamycin - cyclophosphamide-based chemotherapy. *Support Care Cancer.* (2011) 19:807–13. doi: 10.1007/s00520-010-0899-5
34. Kim Y, Morrow GR. The effects of family support, anxiety, and post-treatment nausea on the development of anticipatory nausea : a latent growth model. *J Pain Symptom Manage.* (2007) 34:265–76. doi: 10.1016/j.jpainsymman.2006.11.014
35. Molassiotis A, Lee PH, Burke TA, Dicato M, Gascon P, Roila F, et al. Anticipatory nausea, risk factors, and its impact on chemotherapy-induced nausea and vomiting : results from the Pan European Emesis Registry Study. *J Pain Symptom Manage.* (2016) 51:987–93. doi: 10.1016/j.jpainsymman.2015.12.317
36. Jung D, Lee K, Kim W, Lee JY, Kim TY, Im SA, et al. Longitudinal association of poor sleep quality with chemotherapy-induced nausea and vomiting in patients with breast cancer. *Psychosom Med.* (2016) 78:959–65. doi: 10.1097/PSY.0000000000000372
37. Matsuo K, Miyoshi T, Yokota C, Hanada K. Risk factors for delayed chemotherapy-induced nausea and vomiting with low-emetic-risk chemotherapy : a prospective, observational, multicenter study. *Cancer Manag Res.* (2018) 10:4249–55. doi: 10.2147/CMAR.S176574
38. Cassileth BR, Deng G. Complementary and alternative therapies for cancer. *Oncologist.* (2004) 9:80–9. doi: 10.1634/theoncologist.9-1-80
39. Popovic M, Warr DG, Deangelis C, Tsao M, Chan KK, Poon M, et al. Efficacy and safety of palonosetron for the prophylaxis of chemotherapy-induced nausea and vomiting (CINV): a systematic review and meta-analysis of randomized controlled trials. *Support Care Cancer.* (2014) 22:1685–97. doi: 10.1007/s00520-014-2175-6
40. Aapro MS, Grunberg SM, Manikhas GM, Olivares G, Suarez T, Tjulandin SA, et al. A phase III, double-blind, randomized trial of palonosetron compared with ondansetron in preventing chemotherapy-induced nausea and vomiting following highly emetogenic chemotherapy. *Ann Oncol.* (2006) 17:1441–49. doi: 10.1093/annonc/mdl137
41. Eisenberg P, Figueroa-vadillo J, Zamora R, Charu V, Hajdenberg J, Cartmell A, et al. Improved prevention of moderately emetogenic chemotherapy-induced nausea and vomiting with palonosetron, a pharmacologically novel 5-HT 3 results of a phase III, single-dose trial versus dolasetron. *Cancer.* (2003) 98:2473–82. doi: 10.1002/cncr.11817
42. Grunberg SM, Koeller JM. Palonosetron-a unique 5-HT 3 -receptor antagonist for the prevention of chemotherapy-induced emesis. *Expert Opin Pharmacother.* (2003) 4:2297–303. doi: 10.1517/14656566.4.12.2297
43. Kaushal J, Gupta MC, Kaushal V, Bhutani G, Dhankar R, Atri R, et al. Clinical evaluation of two antiemetic combinations palonosetron dexamethasone versus ondansetron dexamethasone in chemotherapy of head and neck cancer. *Singapore Med J.* (2010) 51:871−75.
44. Saito M, Aogi K, Sekine I, Yoshizawa H, Yanagita Y, Sakai H, et al. Palonosetron plus dexamethasone versus granisetron plus dexamethasone for prevention of nausea and vomiting during chemotherapy : a double-blind, double-dummy, randomised, comparative phase III trial. *Lancet Oncol.* (2009) 10:115–24. doi: 10.1016/S1470-2045(08)70313-9
45. Jordan K, Gralla R, Rizzi G, Kashef K. Efficacy benefit of an NK 1 receptor antagonist (NK 1 RA) in patients receiving carboplatin : supportive evidence with NEPA (a fixed combination of the NK 1 RA, netupitant, and palonosetron) and aprepitant regimens. *Support Care Cancer.* (2016) 24:4617–25. doi: 10.1007/s00520-016-3304-1
46. Parathoduvil AA, Sisupalan A, Rema PL. Comparison of antiemetic effectiveness of palonosetron versus ondansetron in patients on cancer chemotherapy: a prospective observational Study in South Indians. *J Clin Diagn Res.* (2017) 11:FC10–4. doi: 10.7860/JCDR/2017/25129.9818
47. Patil V, Prasada H, Prasad K, et al. Comparison of antiemetic efficacy and safety of palonosetron vs ondansetron in the prevention of chemotherapy-induced nausea and vomiting in children. *J Community Support Oncol.* (2015) 13:209–13. doi: 10.12788/jcso.0139
48. Tricco AC, Soobiah C, Blondal E, Veroniki AA, Khan PA, Vafaei A, et al. Comparative safety of serotonin (5-HT 3) receptor antagonists in patients undergoing surgery : a systematic review and network meta-analysis. *BMC Med.* (2015) 13:142. doi: 10.1186/s12916-015-0379-3
49. Brygger L, Herrstedt J. Academy of Geriatric Cancer Research (AgeCare). 5-Hydroxytryptamine3 receptor antagonists and cardiac side effects. *Expert Opin Drug Saf.* (2014) 13:1407–22. doi: 10.1517/14740338.2014.954546
50. United States Food and Drug Administration. *FDA Drug Safety Communication: New information regarding QT prolongation with ondansetron (Zofran).* (2012). Available online at: http://www.fda.gov/Drugs/DrugSafety/ucm310190.htm (accessed January 31, 2019).
51. Villalon A, Chan V. Multicenter, randomized trial of ramosetron plus dexamethasone versus ramosetron alone in controlling cisplatin-induced emesis. *Support Care Cancer.* (2004) 12:58–63. doi: 10.1007/s00520-003-0528-7
52. Grunberg SM. Antiemetic activity of corticosteroids in patients receiving cancer chemotherapy: dosing, efficacy, and tolerability analysis. *Ann Oncol.* (2007) 18:233–40. doi: 10.1093/annonc/mdl347
53. Chow R, Warr DG, Navari RM, Tsao M, Milakovic M, Popovic M, et al. Efficacy and safety of 1-day versus 3-day dexamethasone for the prophylaxis of chemotherapy-induced nausea and vomiting: a systematic review and meta-analysis of randomized controlled trials. *JHMHP.* (2018) 2:1–13. doi: 10.21037/jhmhp.2018.04.05
54. Kaushal P, Atri R, Soni A, Kaushal V. Comparative evaluation of triplet antiemetic schedule versus doublet antiemetic schedule in chemotherapy-induced emesis in head and neck cancer patients. *Ecancermedicalscience.* (2015) 9:567. doi: 10.3332/ecancer.2015.567
55. Hingmire S, Raut N. Open-label observational study to assess the efficacy and safety of aprepitant for chemotherapy-induced nausea and vomiting prophylaxis in Indian patients receiving chemotherapy with highly emetogenic chemotherapy/moderately emetogenic chemotherapy regimens. *South Asian J Cancer.* (2015) 4:7–10. doi: 10.4103/2278-330X.149923
56. Maru A, Gangadharan VP, Desai CJ, Mohapatra RK, Carides AD. A Phase 3, randomized, double blind study of single dose fosaprepitant for prevention of cisplatin induced nausea and vomiting : results of an Indian population sub analysis. *Indian J Cancer.* (2013) 50:285–91. doi: 10.4103/0019-509X.123580
57. Radhakrishnan V, Joshi A, Ramamoorthy J, Rajaraman S, Ganesan P, Ganesan TS, et al. Intravenous fosaprepitant for the prevention of chemotherapy-induced vomiting in children: a double-blind, placebo-controlled, phase III randomized trial. *Pediatr Blood Cancer.* (2019) 66:e27551. doi: 10.1002/pbc.27551
58. Ramesh AC, Bhagat SB. A retrospective case cohort analysis on the clinical utility of fosaprepitant for CINV prophylaxis in day care center of South India. *J Curr Oncol.* (2019) 2:15–8. doi: 10.4103/JCO.JCO_2_19
59. Navari R Schwartzberg L. Evolving role of neurokinin 1-receptor antagonists for chemotherapy-induced nausea and vomiting. *Onco Targets Ther.* (2018) 11:6459–78. doi: 10.2147/OTT.S158570

60. Yuan D-M, Li Q, Zhang Q, Xiao XW, Yao YW, Zhang Y, et al. Efficacy and safety of neurokinin-1 receptor antagonists for prevention of chemotherapy-induced nausea and vomiting: systematic review and meta-analysis of randomized controlled trials. *Asian Pac J Cancer Prev.* (2016) 17:1661–75. doi: 10.7314/APJCP.2016.17.4.1661
61. Roila F, Ruggeri B, Ballatori E, Del Favero A, Tonato M. Aprepitant versus dexamethasone for prevention chemotherapy-induced delayed emesis in patients with breast cancer: a randomized double-blind Study. *J Clin Oncol.* (2014) 32:101–06. doi: 10.1200/JCO.2013.51.4547
62. Jordan K, Blättermann L, Hinke A, Müller-Tidow C, Jahn F. Is the addition of a neurokinin-1 receptor antagonist beneficial in moderately emetogenic chemotherapy? - a systematic review and meta-analysis. *Support Care Cancer.* (2018) 26:21–32. doi: 10.1007/s00520-017-3857-7
63. Zhang Z, Zhang Y, Chen G, Hong S, Yang Y, Fang W, et al. Olanzapine-based triple regimens versus neurokinin-1 receptor antagonist-based triple regimens in preventing chemotherapy- induced nausea and vomiting associated with highly emetogenic chemotherapy : a network meta-analysis. *Oncologist.* (2018) 23:603–16. doi: 10.1634/theoncologist.2017-0378
64. Mukhopadhyay S, Kwatra G, Alice KP, Badyal D. Role of olanzapine in chemotherapy-induced nausea and vomiting on platinum-based chemotherapy patients : a randomized controlled study. *Support Care Cancer.* (2017) 25:145–54. doi: 10.1007/s00520-016-3386-9
65. Babu G, Saldanha SC, Chinnagiriyappa LK, Jacob LA, Mallekavu SB, Dasappa L, et al. The efficacy, safety, and cost benefit of olanzapine versus aprepitant in highly emetogenic chemotherapy: a Pilot Study from South India. *Chemother Res Pract.* (2016) 2016:3439707. doi: 10.1155/2016/3439707
66. Mehra N, Ganesan P, Ganesan TS, Veeriah S, Boopathy A, Radhakrishnan V, et al. Effectiveness of olanzapine in patients who fail therapy with aprepitant while receiving highly emetogenic chemotherapy. *Med Oncol.* (2017) 35:12. doi: 10.1007/s12032-017-1074-3
67. Shivaprakash G, Udupa KS, Sarayu V, Thomas J, Gupta V, Pallavi LC, et al. Olanzapine versus aprepitant for the prophylaxis of chemotherapy-induced nausea and vomiting in breast cancer patients receiving doxorubicin-cyclophosphamide regimen: A prospective, nonrandomized, open-label study. *Indian J Pharmacol.* (2017) 49:451–57. doi: 10.4103/ijp.IJP_846_16
68. Maio MD, Gallo C, Leighl NB, Piccirillo MC1, Daniele G1, Nuzzo F, et al. Symptomatic toxicities experienced during anticancer treatment : agreement between patient and physician reporting in three randomized trials. *J Clin Oncol.* (2015) 33:910–15. doi: 10.1200/JCO.2014.57.9334
69. Clark-Snow R, Affronti ML, Rittenberg CN. Chemotherapy-induced nausea and vomiting (CINV) and adherence to antiemetic guidelines: results of a survey of oncology nurses. *Support Care Cancer.* (2017) 26:557–64. doi: 10.1007/s00520-017-3866-6
70. Ranganath P, Einhorn L, Albany C. Management of chemotherapy induced nausea and vomiting in patients on multiday cisplatin based combination chemotherapy. *Biomed Res Int.* (2015) 2015:943618. doi: 10.1155/2015/943618
71. Olver IN, Grimison P, Chatfield M, Stockler MR, Toner GC, Gebski V, et al. Results of a 7-day aprepitant schedule for the prevention of nausea and vomiting in 5-day cisplatin-based germ cell tumor chemotherapy. *Support Care Cancer.* (2013) 21:1561–68. doi: 10.1007/s00520-012-1696-0
72. Einhorn LH Grunberg SM. Antiemetic therapy for multiple-day chemotherapy and high-dose chemotherapy with stem cell transplant : review and consensus statement. *Support Care Cancer.* (2011) 19 (Suppl. 1):S1–4. doi: 10.1007/s00520-010-0920-z
73. Einhorn LH, Brames MJ, Dreicer R, Nichols CR, Cullen MT Jr, Bubalo J. Palonosetron plus dexamethasone for prevention of chemotherapy-induced nausea and vomiting in patients receiving multiple-day cisplatin chemotherapy for germ cell cancer. *Support Care Cancer.* (2007) 15:1293–300. doi: 10.1007/s00520-007-0255-6

Conflict of Interest: SB, SP, and HB are employees of Glenmark Pharmaceuticals Ltd. who contributed toward literature search and manuscript writing. The design or procedure of the consensus and the content of the paper are in no way influenced by the grant provider. The authors have no other relevant affiliations or financial involvement with any organization or entity with a financial interest in or financial conflict with the subject matter or materials discussed in the manuscript apart from those disclosed.

frontiers in Pharmacology

ORIGINAL RESEARCH
published: 03 April 2020
doi: 10.3389/fphar.2020.00410

Controlled Synthesis and Characterization of Micrometric Single Crystalline Magnetite With Superparamagnetic Behavior and Cytocompatibility/Cytotoxicity Assessments

Claudia Geanina Farcas[1,2†], Ioana Macasoi[2†], Iulia Pinzaru[2], Marius Chirita[3*], Marius Constantin Chirita Mihaila[3,4,5], Cristina Dehelean[2], Stefana Avram[2], Felicia Loghin[1], Liviu Mocanu[3], Virgil Rotaru[6], Adrian Ieta[7], Aurel Ercuta[8] and Dorina Coricovac[2]*

[1] Department of Toxicology, Faculty of Pharmacy, "Iuliu Hatieganu" University of Medicine and Pharmacy, Cluj-Napoca, Romania, [2] Faculty of Pharmacy, "Victor Babes" University of Medicine and Pharmacy, Timisoara, Romania, [3] Department of Condensed Matter, National Institute for Research and Development in Electrochemistry and Condensed Matter, Timisoara, Romania, [4] Max F. Prutz Laboratories, Department of Structural and Computational Biology, University of Vienna, Vienna, Austria, [5] Quantum Optics, Quantum Nanophysics and Quantum Information, Faculty of Physics, University of Vienna, Vienna, Austria, [6] Faculty of Medicine, "Victor Babes" University of Medicine and Pharmacy, Timisoara, Romania, [7] Electrical and Computer Science Department SUNY Oswego, Oswego, NY, United States, [8] Faculty of Physics, West University of Timisoara, Timisoara, Romania

A new class of magnetite (Fe_3O_4) particles, coined as "Single Crystalline Micrometric Iron Oxide Particles" (SCMIOPs), were obtained by hydrothermal synthesis. Both the single Fe_3O_4 phase content and the particle sizes range, from 1 μm to 30 μm, can be controlled by synthesis. The notable finding states that these particles exhibit vanishing remanent magnetization (σr=0.28 emu/g) and coercive force (Hc=1.5 Oe), which indicate a superparamagnetic-like behavior (unexpected at micrometric particles size), and remarkably high saturation magnetization (σs=95.5 emu/g), what ensures strong magnetic response, and the lack of agglomeration after the magnetic field removal. These qualities make such particles candidates for biomedical applications, to be used instead of magnetic nanoparticles which inevitably involve some drawbacks like aglommeration and insufficient magnetic response. In this sense, cytocompatibility/cytotoxicity tests were performed on human cells, and the results have clearly indicated that SCMIOPs are cytocompatible for healthy cell lines HaCaT (human keratinocytes) and HEMa (primary epidermal melanocytes) and cytotoxic for neoplastic cell lines A375 (human melanoma) and B164A5 (murine melanoma) in a dose-dependent manner.

Keywords: single-crystalline, superparamagnetic, micrometric, healthy/tumor cells, viability

OPEN ACCESS

Edited by:
Mukerrem Betul Yerer Aycan, Erciyes University, Turkey

Reviewed by:
Amarjit Luniwal, North American Science Associates Inc., United States
Hakan Kockar, Balıkesir University, Turkey

***Correspondence:**
Iulia Pinzaru
iuliapinzaru@umft.ro
Marius Chirita
chirifiz@gmail.com

†These authors have contributed equally to this work

Specialty section:
This article was submitted to Pharmacology of Anti-Cancer Drugs, a section of the journal Frontiers in Pharmacology

Received: *23 July 2019*
Accepted: *18 March 2020*
Published: *03 April 2020*

Citation:
Farcas CG, Macasoi I, Pinzaru I, Chirita M, Chirita Mihaila MC, Dehelean C, Avram S, Loghin F, Mocanu L, Rotaru V, Ieta A, Ercuta A and Coricovac D (2020) Controlled Synthesis and Characterization of Micrometric Single Crystalline Magnetite With Superparamagnetic Behavior and Cytocompatibility/Cytotoxicity Assessments. Front. Pharmacol. 11:410. doi: 10.3389/fphar.2020.00410

INTRODUCTION

Iron oxides manufactured as nanoparticles or microparticles are considered materials with multi-purpose biomedical potential that proved great results in different biomedical applications, as: drug-delivery carriers, cancer therapy (targeted therapy by applying an external magnetic field), hyperthermia, diagnostic agents (nuclear magnetic resonance – NMR, magnetic resonance imaging - MRI), tools for *in vitro* techniques (diagnostic separation, magnetorelaxometry), etc (Catalano, 2017). Application of iron oxides (of nanometric or micrometric size) in biomedical fields has considerably developed in the recent years, as well as human exposure, and it became mandatory for the novel synthetized magnetic particles to be quantitatively analyzed from physico-chemically and toxicological perspectives.

The large variety of existing iron oxide particles (IOPs) on the market can be classified into ultra-small (USIOPs; 20 nm–50 nm diameters), small (SIOPs; 60 nm to cca. 250 nm), and micrometric (MIOPs; 0.9 μm and larger) synthesized by clustering superparamagnetic nanoparticles (Runge, 1996; Carroll et al., 2010). There is solid experimental evidence that nanoparticles smaller than 10 nm exhibit both toxicity risks, and the occurrence of physiological barriers for an enhanced permeability and retention (EPR) effect; these particles strongly interact with the immune system, and penetrate into capillaries (Hughes, 2015; Lauterwasser, 2015). The multiple challenges regarding nanoparticles biocompatibility, toxicological and immunological issues (Arias et al., 2018) determined the researchers to channel their interest in obtaining microparticles that possess similar features as nanoparticles (like superparamagnetism), but with an enhanced biocompatibility and low/absence of toxicity. Two options are mentioned in the literature: embedding thousands of individual SPIONs into micro-clusters or increasing every single particle dimension (Xie and Zhang, 2011). Mankia et al. (2011) verified the toxicological profile of MIOPs by performing animal studies and the results showed that neither tissue infarction, thrombosis, or vessel plugging *in vivo*, nor other noxious effects were noticed (Mankia et al., 2011). Moreover, it was demonstrated that liver and spleen cleared far more rapidly MIOPs from the blood circulation than USIOPs. Due to their size and incompressible nature, MIOPs are less susceptible to non-specific vascular egress or uptake by endothelial cells. By applying different methods of synthesis were obtained iron oxide microparticles with enhanced biological properties: agglomerations of magnetite nanoparticles with a superparamagnetic core (11.8 μm) and amoxicillin cover for the treatment of the spiral form of gram-negative bacteria *Helicobacter pylori* (Silva et al., 2009); MIOPs in the range of 1 μm—as contrast agents in mouse brain inflammatory pathology which enabled *in vivo* detection of the disease; larger MIOPs for cellular MRI imaging (Wu et al., 2006), characterization of vascular inflammatory disease (McAteer et al., 2008; Ye et al., 2008), molecular imaging of thrombosis (Von Zur Muhlen et al., 2009), molecular imaging of tissue ischemia (Akhtar et al., 2010) and as contrast agents for the detection of endovascular molecular targets by MRI (McAteer et al., 2011); magnetic oxide particle suspension in distilled water (10.82 μm average size) as MRI contrast agents (Mathieu and Martel, 2006). Nevertheless, it was reported that for molecular magnetic resonance imaging (mMRI), microparticles of iron oxide (MIOPs) create potent hypo intense contrast effects, especially due to their physical size (Mankia et al., 2011).

Despite the many advantages presented above, the major drawback in using micro-clusters resulted from multiple individual SPIONs is the small value for magnetic saturation (Ms) which means a weak magnetic response and all the disadvantages that arise due to a low response in MRI or the difficulty of handling them *via* an external magnetic field. In this context, our research group has focused on developing a controlled hydrothermal synthesis technique for producing "Single Crystalline Micrometric Iron Oxide Particles" SCMIOPs (from 1 μm to 30 μm), qualified for biomedical applications and able to overcome the above-mentioned limitations in using nanoparticles and micro-clusters. This report also presents an area of novelty regarding the cytocompatibility/cytotoxicity of SCMIOPs on both normal—keratinocytes and melanocytes and tumoral—human and murine melanoma cells by using specific *in vitro* methods such as viability assay and fluorescence staining.

MATERIALS AND METHODS

Materials

Chemicals and Reagents

Analytical pure ferric ammonium sulphate $FeNH_4(SO_4)_2 \bullet 12H_2O$ (FAS), tetrasodium ethylenediaminetetraacetate (Na_4EDTA), and urea $(NH_2)_2CO$ were supplied by Fluka (Sigma-Aldrich) and used for Fe_3O_4 synthesis.

In Vitro Experiments

Dulbecco's Modified Eagle's Medium (DMEM) high glucose, fetal calf serum (FCS), saline phosphate-buffered (PBS), penicillin/streptomycin mixture, trypsin-EDTA solution, Trypan blue, Dermal Cell Basal Medium and Adult Melanocyte Growth Kit were purchased from Sigma Aldrich (Germany), Thermo Fisher Scientific (USA), and ATCC (American Type Culture Collection). The provider of MTT Cell Proliferation Assay Kit was Roche Applied Science (Mannheim, Germany).

Methods

Synthesis and Characterization of SCMIOPs

Presently, SCIMIOPs were synthesized using a two-step method. Step one consists in the obtaining of Fe-EDTA complex using an aqueous solution of 1.05×10^{-1}M FAS, 1.05×10^{-1}M Na_4EDTA, and 9.71×10^{-1} M urea. The Fe(III)EDTA complex formation is marked by the color change from purple to dark red. Step two consists in hydrothermal decomposition of Fe-EDTA. The solution was transferred into a 70 ml volume Teflon-lined stainless-steel autoclave and heated up to 230°C by a rate of 1.7°C/min. Three degrees of filling were selected for autoclaves: 50%, 60%, and 70%. For each filling level the high-pressure

treatment time was progressively increased from 4 h to 40 h with a 2-hour growth rate. Abrupt cooling with cold water ensured the freezing of phase transitions inside the autoclaves. All the pH measurements indicated a value between 9.4 and 9.5 for the final solutions. The obtained microparticles were washed with bi-distilled water and dried two hours at 60°C.

The morphological examination of Fe_3O_4 crystals was carried out by scanning electron microscopy (SEM) using the Quanta 3D 200i, FEI Co. The chemical components were then identified by energy-dispersive X-ray spectroscopy (EDX) analysis. Structure analysis was performed at room temperature, using the X'Pert PRO MPD diffractometer (PANalytical) using Cu-Kα radiation (0.15418 nm, Ni filter) in θ:θ configuration. An AC hysteresigraph (Ercuta, 2020) was used to test the magnetic properties of the particles.

Cell Culture

The *in vitro* cytocompatibility/cytotoxicity tests were developed on two types of healthy cell lines and on two tumor cell lines: immortalized human keratinocytes (HaCaT - 300493; CLS Cell Lines Service GmbH), primary epidermal melanocytes (HEMa - ATCC® PCS-200-013™), human melanoma (A375 - ATCC® CRL-1619™), and murine melanoma (B164A5 – 94042254; ECACC). HaCaT, A375, and B164A5 cells were cultured in specific culture medium - Dulbecco's modified Eagle Medium high glucose supplemented with 10% fetal calf serum and 1% penicillin/streptomycin solution. HEMa cells culture required Dermal Cell Basal Medium supplemented with Adult Melanocyte growth kit, 1% penicillin/streptomycin mixture, and 1% FCS. Throughout the experiments, the cells were maintained in a humidified incubator in standard conditions (5% CO_2 at 37°C) and were passaged every other day. The cells were counted using Countess™ II Automated Cell Counter in the presence of Trypan blue.

Cell Viability Assessment

The cytotoxicity evaluation of Fe_3O_4 micrometric particles was performed according to the ISO standard 10993-5:2009 on Biological Evaluation of Medical Devices (https://www.iso.org/obp/ui/#iso:std:iso:10993:-5:ed-3:v1:en). The cells ($1x10^4$ cells/200 µl culture medium) were seeded in 96-well culture plates with flat-bottom and allowed to attach until the confluence was appropriate (generally, for 24 h). The old medium was replaced by 100 µl fresh medium that contained different concentrations of Fe_3O_4 microparticles (25, 50, 100, 150, 250, 500, and 1000 µg/ml) and incubated for 24 h. The viability was assessed using MTT (3-(4,5-Dimethylthiazol-2-yl)-2,5-diphenyltetrazolium bromide) assay. In brief, a volume of 10 µl MTT reagent was added to each well and the plate was incubated for three hours at 37°C, followed by addition of 100 µl of solubilization buffer/well and incubation for 30 min at room temperature and dark. Further, the samples were spectrophotometrically analyzed at 570 nm, using a microplate reader (xMark™Microplate, Biorad). The results are presented as the mean % of viable cells compared to the control ± SD (n=3 for each concentration). The unstimulated cells were considered as control. The changes in cells morphology were monitored by Olympus IX73 inverted microscope under bright light illumination.

Prussian Blue Staining

This technique was performed in order to detect the localization of the SCMIOPs in cells monolayer. A number of $2x10^5$ cells/well were plated in 12-well culture plates to achieve a confluent culture cell monolayer. When the confluence was above 80%, the cells were stimulated with different concentrations of SCMIOPs (25, 50, 100, and 150 µg/ml) for 24 h. Thereafter, cells were washed two times with PBS, fixed with 4% paraformaldehyde at 4°C for 30 min, followed by staining at room temperature for 20 min with an equal volume of a freshly prepared mixture of 5% HCl in PBS and 5% potassium ferrocyanide. Cells were further counterstained with 1% neutral red solution for 5 min and destained with PBS (Jadhav et al., 2013). Cells were observed and pictured under bright field (BF) microscopy, at 40x magnification.

DAPI (4',6-Diamidino-2- Phenylindole) Staining

In order to visualize the nuclear alterations specific for apoptosis induction, all the cell lines were stained with DAPI and analyzed under an inverted fluorescence microscope (Olympus IX73, Tokyo, Japan). A number of $1x10^6$ cells/well were seeded onto 6-well plates and were allowed to attach to the bottom of the well, overnight. The following day the old medium was removed, and the cells were treated for 24 h with a fresh medium containing different concentrations of SCMIOPs (25, 50, 100, and 150 µg/ml). Upon completion of the incubation period, the cells were washed twice with ice-cold PBS, fixed with 4% paraformaldehyde in PBS and permeabilized with 2% Triton-X/PBS for 30 min. The protocol was continued by a blocking step (30% FCS in 0.01% Triton-X), a washing step with PBS, and staining process with DAPI (300 nM) in a dark chamber. The cells were analyzed under a fluorescence microscope, at 40x magnification.

Statistical Analysis

Graph Pad Prism 6 and cellSens Dimensions v.1.8. software were used for the presentation and interpretation of the results. The results were expressed as the mean ± standard deviation (SD). One-way ANOVA analyze was applied to determine the statistical differences followed by Tukey post-test (* $p < 0.05$; ** $p < 0.01$; *** $p < 0.001$).

RESULTS

Characterization of SCMIOPs

All samples resulted during synthesis process were characterized. The samples obtained at 30 h of high-pressure treatment time in autoclave with a filling level of 50% were chosen for presentation, due to the lack of $FeCO_3$ traces on the surface of Fe_3O_4 microcrystals. The SEM images of the 30 h magnetite microcrystals obtained from hydrothermal reaction are presented in **Figures 1A, B**. The microcrystals have a compact structure (no porosity observed), size between 1 µm and 30 µm,

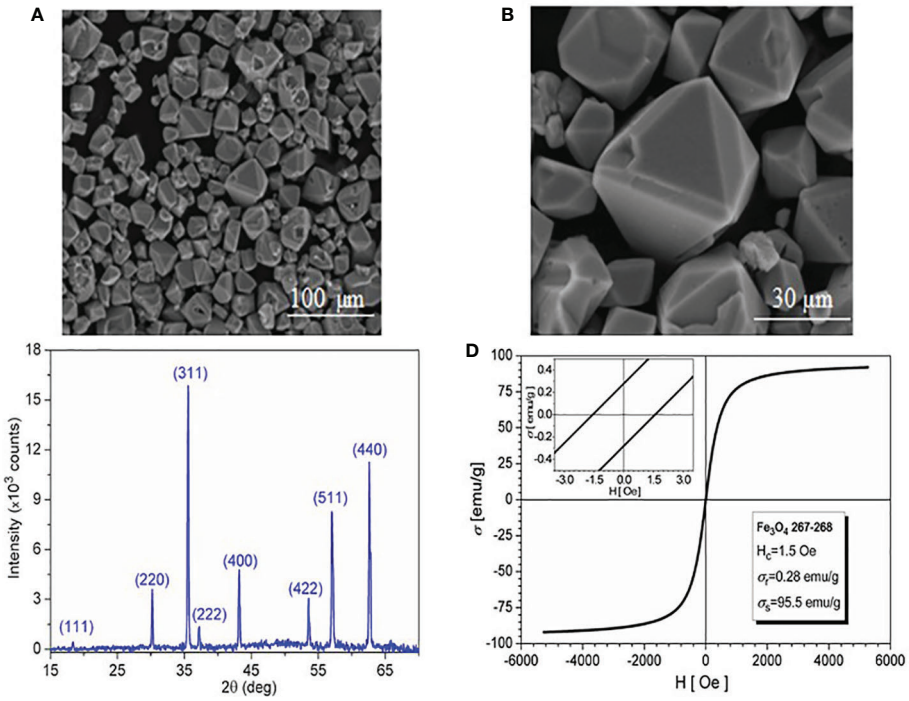

FIGURE 1 | (A) SEM image of magnetite; **(B)** SEM image detail; **(C)** XRD spectrum; and **(D)** Hysteresis loop at room temperature.

and morphologies that represent a combination of octahedral and dodecahedral faces. The XRD spectrum presented in **Figure 1C** allows the identification of the Fe_3O_4 after 30 h of high pressure-temperature treatment; the diffraction peaks were indexed using the ICSD (Inorganic Crystal Structure Database) reference code: 01-088-0315 for Fe_3O_4. The high purity of the 30 h final product is confirmed by the EDAX spectrum (chart not presented here), with no traces of Na, S, C, and N (which could result from EDTA and FAS decomposition).

The magnetic behavior at 300°K (the hysteresis loop) of the 30 h magnetite microcrystals is shown in **Figure 1D**. Fitting the hysteresis loop branches to Langevin-type functions, the saturation magnetization of the sample was estimated within ±3 emu/g accuracy to 95.5 emu/g. The vanishing values of both coercivity (Hc=1.5 Oe) and remanence (σr=0.28 emu/g) indicate superparamagnetic behavior.

In Vitro Impact of SCMIOPs

Since the magnetite microparticles designed and synthesized in the present study are intended for biomedical applications, it is mandatory to verify their effects by performing *in vitro* assays to confirm or infirm their toxicological profile. The impact of SCMIOPs was tested for cytocompatibility on two healthy cell lines: HaCaT (immortalized human keratinocytes) and HEMa (primary epidermal melanocytes). In the case of HaCaT cells (**Figure 2 - left panel**), the lower concentrations of SCMIOPs (25, 50, and 100 µg/ml) induced an increased cell viability, whereas higher concentrations (250, 500, and 1000 µg/ml) were associated with a decrease in the cell viability percentage in a concentration-dependent manner. The displayed viability rates were 92.18%, 82.52%, and 70.62%, respectively. At the 150 µg/ml, the viability has a value very close to the control sample.

HEMa cells proved to be more sensitive to SCMIOPs treatment (**Figure 2 - right panel**) as compared to HaCaT cells; a decrease in the cell viability percentage starting with the lowest concentration tested (25 µg/ml) was observed. However, a significant reduction was recorded at 150 µg/ml (about 82%) when compared to control cells. Nevertheless, stimulation at higher SCMIOPs concentrations (250, 500, and 1000 µg/ml) led to a constant viability rate above 80%, similar to the one induced at 150 µg/ml, effect that is in contrast to the one observed in HaCaT cells which expressed a dose-dependent cell viability decrease.

The results obtained when the human - A375 and murine - B164A5 melanoma cells were stimulated with Fe_3O_4 microparticles (**Figure 3**) appear to be of particular interest. The magnetite microparticles induced a significant decrease of melanoma cells viability. The effect is more significant in the case of murine melanoma cells - B164A5 (**Figure 3 - left panel**). A significant drop of cell viability starts at 100 µg/ml (about 92%) and decreases in a concentration-dependent manner to 49.87% (at 1000 µg/ml). The effect on human - A375 melanoma cell line (**Figure 3 - right panel**) did not display a linear dependence with

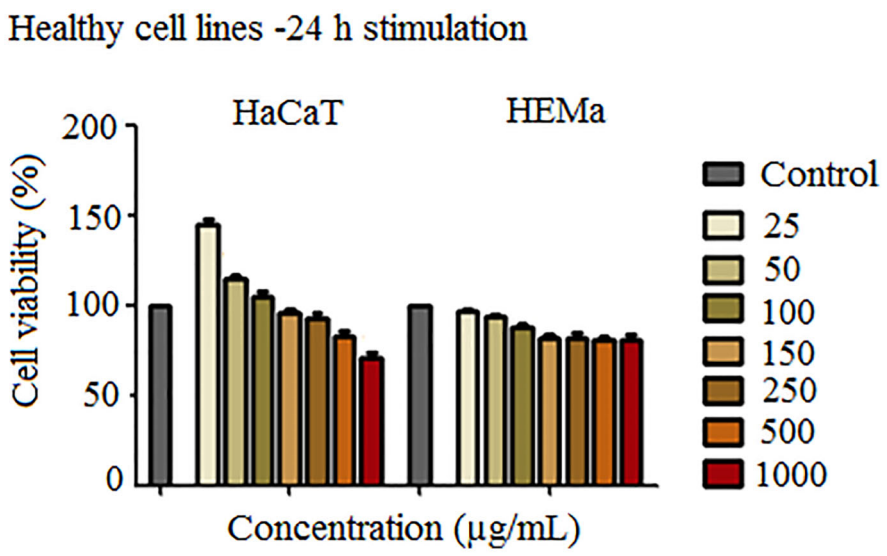

FIGURE 2 | Cell viability assessment of SCMIOPs (25, 50, 100, 150, 250, 500, and 1000 µg/ml) on HaCaT and HEMa cells at 24 h post-stimulation by the means of MTT assay. The results are expressed as cell viability percentage (%) normalized to control cells (no stimulation). The data represent the mean values ± SD of three independent experiments performed in triplicate. One-way ANOVA analysis was applied to determine the statistical differences followed by Tukey post-test (**$p < 0.01$; ***$p < 0.001$).

Fe_3O_4 concentration. However, A375 cells seemed sensitive to Fe_3O_4 treatment, even at the lowest concentration tested (25 µg/ml), showing a cell viability about 92%.

However, the viability rate decreased to 73% after treatment with 150 µg/ml SCMIOPs. Above this concentration an increase of cell viability was observed after stimulation at 250 and 500 µg/ml (89.26% and 80.21% viable cells, respectively). Nevertheless, the highest concentration (1000 µg/ml) induced the most significant decrease in A375 cell viability (about 71%).

Cell Morphology and Apoptotic Markers

The morphological aspect of the cells was monitored by bright field (BF) microscopy at 0, 3, 6, and 24 h post stimulation. The most significant morphological changes were recorded at 24 h

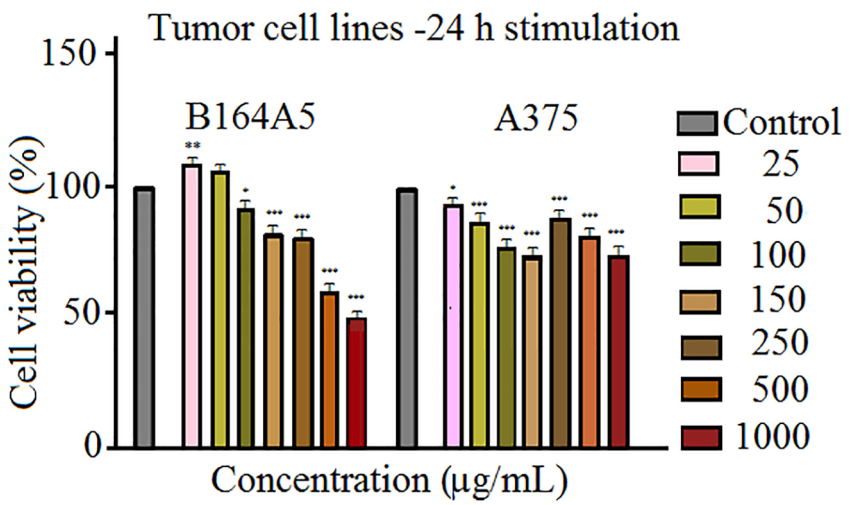

FIGURE 3 | Cell viability assessment of SCMIOPs (25, 50, 100, 150, 250, 500, and 1,000 µg/ml) on B164A5 and A375 cells at 24 h post-stimulation by the means of MTT assay. The results are expressed as cell viability percentage (%) normalized to control cells (no stimulation). The data represent the mean values ± SD of three independent experiments performed in triplicate. One-way ANOVA analysis was applied to determine the statistical differences followed by Tukey post-test (*$p < 0.05$; **$p < 0.01$; ***$p < 0.001$).

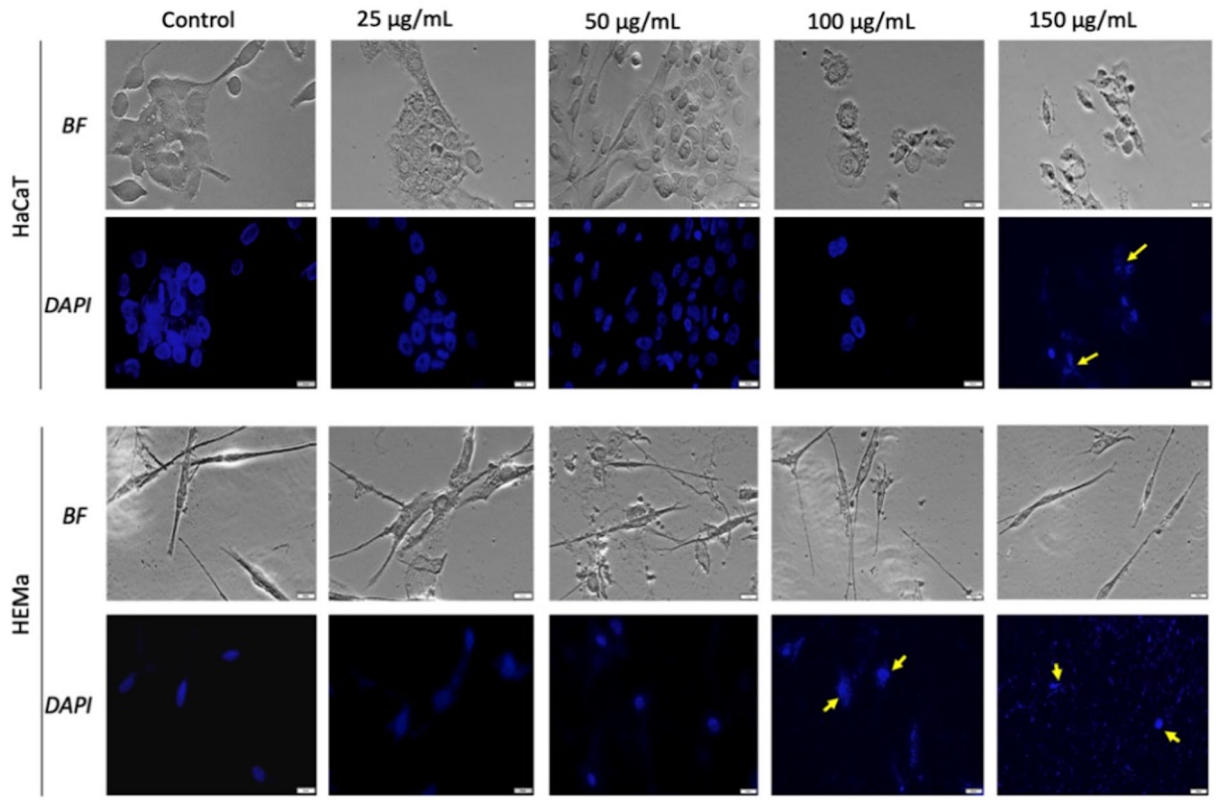

FIGURE 4 | Healthy - HaCaT and HEMa cells treated with SCMIOPs at different concentrations (25, 50, 100, and 150 µg/ml) for 24 h. Bright field (BF) microscopy was employed to analyze morphological changes; DAPI staining (blue) was performed to evaluate cell nuclei modifications. Scale bars represent 20 µm.

post-stimulation. Accordingly, assessment of possible nuclei alterations *via* DAPI staining was performed at the same time (24 h post-stimulation).

As shown in **Figures 4** and **5**, the control cells display well defined elongated shape for HaCaT, HEMa, and B164A5 cell lines and a round shape for human melanoma A375 cells; also, the cells have a large nucleus with uniform chromatin density. Modification of cell morphology with apoptotic characteristics (cell shrinkage, DNA fragmentation and chromatin condensation) was observed in all cell lines, after SCMIOPs stimulation with 150 µg/ml. Nevertheless, HEMa and B164A5 cells were also affected by a lower concentration (100 µg/ml). Apoptotic aspects are marked with yellow arrows (**Figures 4** and **5**).

SCMIOPs Detection Within the Cell Monolayer

Prussian blue assay is a specific technique used to determine the *in vitro* cellular iron uptake, highlighting the presence of SCMIOPs by staining them blue. However, a large number of Fe_3O_4 microparticles did not penetrate the cell membrane (see yellow arrows in **Figures 6** and **7**). This happens mainly when HaCaT and A375 cells are present in the culture medium, whereas in the case of HEMa and B164A5 cells, the microparticles seem to be adherent to cells membranes.

SCMIOPs Stability in Cell Growth Medium

Agglomerations of Fe_3O_4 microparticles were macroscopically observed during the *in vitro* experiments. Therefore, the stability of SCMIOPs' was examined in complete cell medium (Dulbecco's modified Eagle Medium supplemented with 10% fetal calf serum). The wells containing the cell medium with SCMIOPs at 25, 50, 100, and 150 µg/ml were pictured initially and at 24 h post incubation (figures not shown here). The plate was maintained in the same conditions as the ones used for *in vitro* experiments. It was observed that the Fe_3O_4 microparticles agglomerated after 24 h. The fact may be caused by the high salt concentration in the medium which can induce attractive electrostatic forces between microparticles leading to aggregates formation (Park et al., 2014).

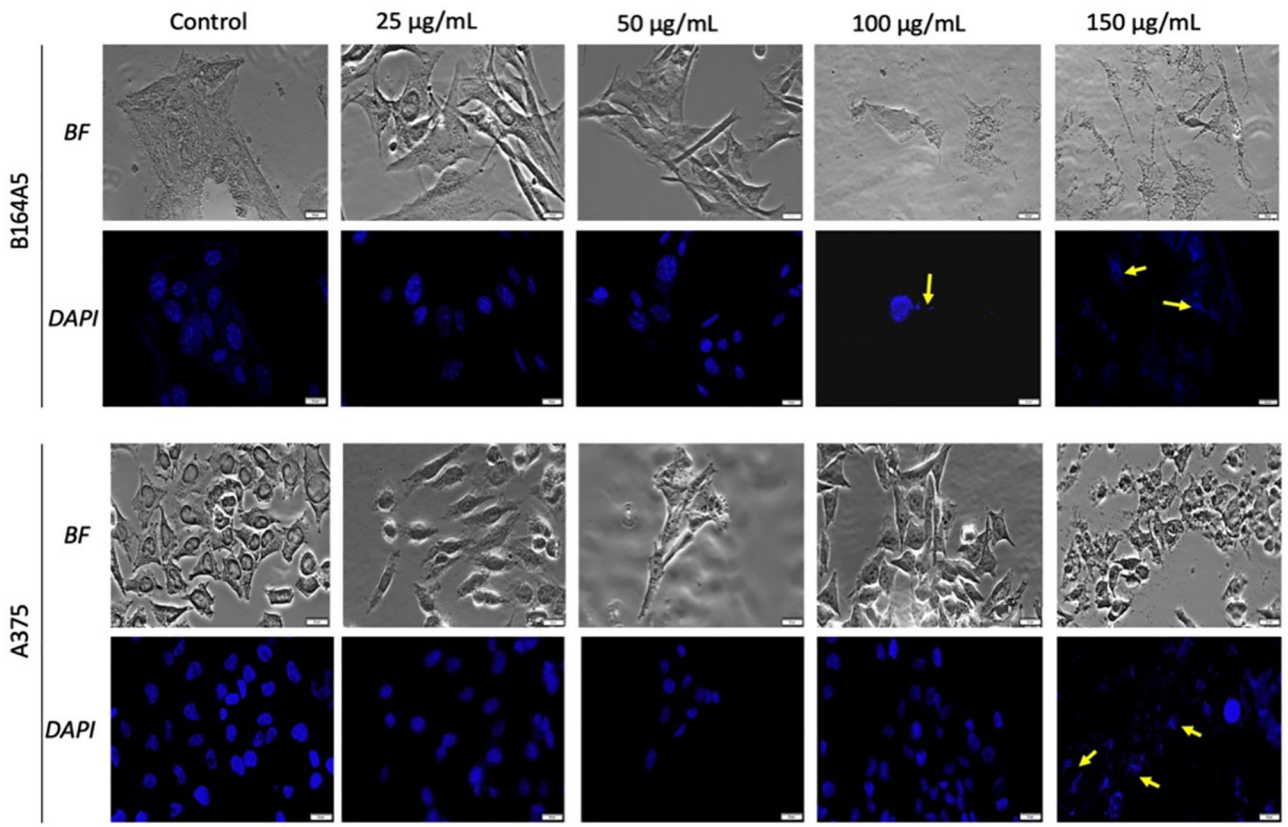

FIGURE 5 | Melanoma - B164A5 and A375 cells treated with SCMIOPs at different concentrations (25, 50, 100, and 150 µg/ml) for 24 h. Bright field (BF) microscopy was employed to analyze morphological changes; DAPI staining (blue) was performed to evaluate cell nuclei modifications. Scale bars represent 20 µm.

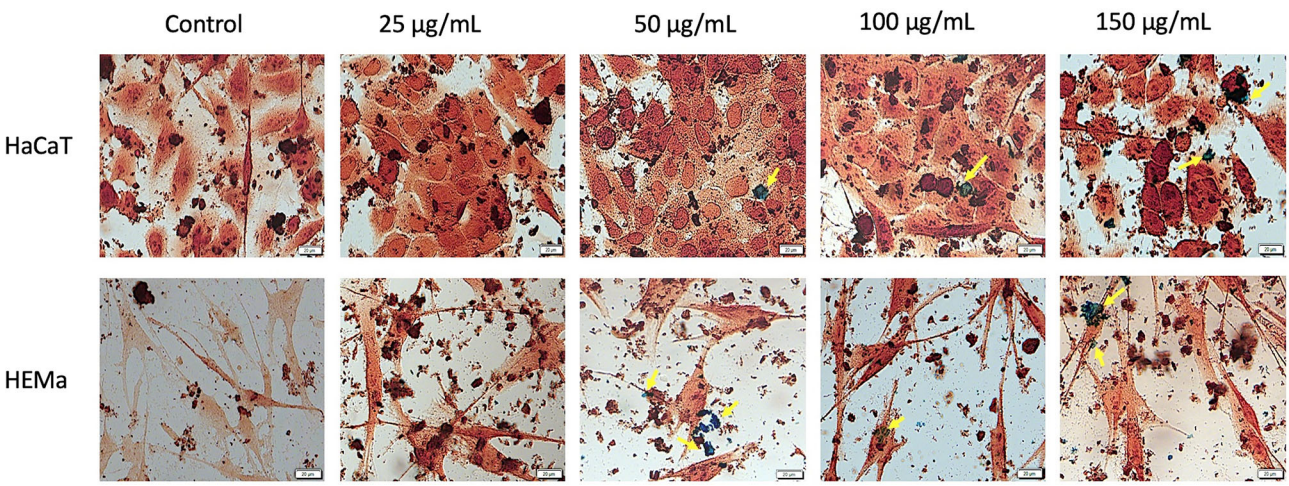

FIGURE 6 | Healthy - HaCaT and HEMa cells incubated with different concentrations (25, 50, 100, and 150 µg/ml) of SCMIOPs for 24 h and stained with Prussian blue reagent. Pictures were taken using Bright field (BF) microscopy. Scale bars represent 20 µm.

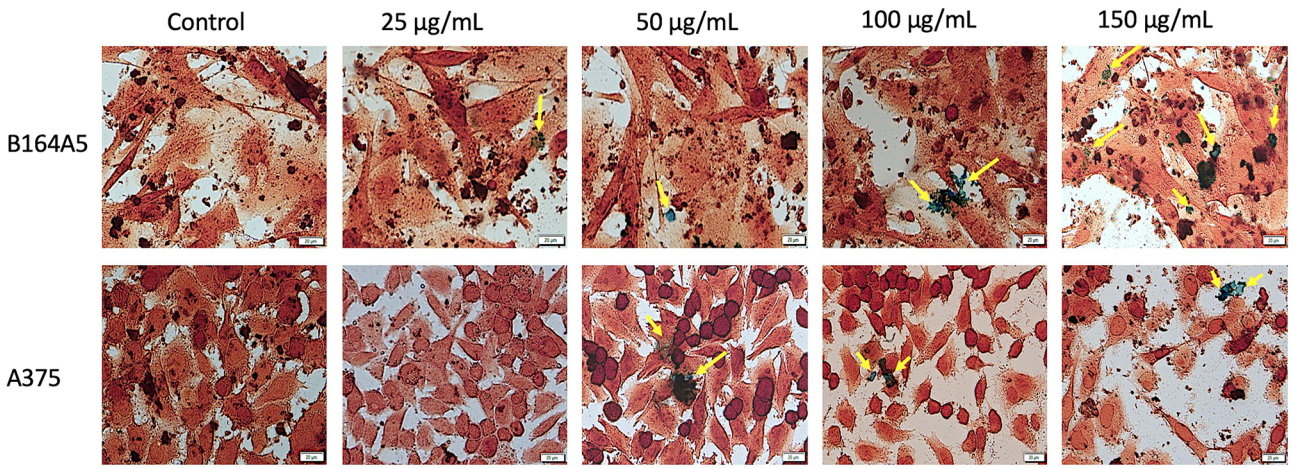

FIGURE 7 | Tumor - B164A5 and A375 cells incubated with different concentrations (25, 50, 100, and 150 µg/ml) of SCMIOPs for 24 h and stained with Prussian blue reagent. Pictures were taken using Bright field (BF) microscopy. Scale bars represent 20 µm.

DISCUSSIONS

Magnetite is known as the only metallic compound produced by the human body (a few hundred micrograms) and other living organisms as biochemical precipitate that possesses electrical conductivity leading to strong interactions with external magnetic field. These interactions determine different cellular effects, and thus far it is not clearly defined the impact of magnetite particles on human health (Kirschvink et al., 1992; Giere, 2016). Each type of magnetic particle has both advantages and disadvantages, especially depending on their properties which play a key role in biomedical field. The main factors which significantly influence these properties are related to the methods of synthesis and the [Fe2+]/[Fe3+] ratio. The hydrothermal process can be employed to control the size and the corresponding structural and magnetic properties which leads to an increased saturation magnetization as nanoparticles increase in size and also, to the formation of high crystalline iron oxide nanoparticles with increasing reaction time and temperature (Ozel and Kockar, 2015; Ozel et al., 2015). On the other hand, an optimization of magnetic saturation is related likewise for nanoparticles produced by co-precipitation in air atmosphere by using orthogonal design technique while particle sizes and magnetization increased with the increase of [Fe2+]/[Fe3+] ratio (Karaagac and Kockar, 2012; Karaagac and Kockar, 2016). Since iron microparticles present a better safety profile as compared to nanoparticles, different methods of synthesis were proposed to obtain magnetite microparticles with superparamagnetic properties (Ma and Chen, 2016), still each technique presents its limitations, and to the best of our knowledge, it was not described yet the method that fulfills all the requirements for biocompatible Fe_3O_4 microparticles. IOPs have an iron oxide core, which is covered by polyethylene glycol, dextran, or other biocompatible materials. For this reason, their size is generally referred to as the hydrodynamic diameter. Below 10 nm, the magnetization exhibits thermally activated fluctuations inside the particle core from an easy axis of magnetization to another (e.g., the <111> directions in the case of magnetite), which leads to superparamagnetic relaxation (Néel, 1949). Thus, the particles do not remain agglomerated after field removal, an important requirement in biomedical applications, not commonly found in particles larger than 10–20 nm.

In the present study it was proposed as method for Fe_3O_4 microparticles synthesis the hydrothermal decomposition of Fe-Na_4EDTA complex in the presence of urea and were obtained magnetite particles with compact (not porous) single-crystalline structure, and size beyond nanometric range. The very low values of both magnetic remanence (σr=0.28 emu/g) and coercitivity (Hc=1.5 Oe), similar to nanoparticles, ensures superparamagnetic behavior. In addition, as the magnetic saturation is very close to the bulk value (σs=92 emu/g), these particles are highly magnetizable. Bean and Livingston (1959) showed that large particles (larger than 15 nm) are not superparamagnetic (Bean and Livingston, 1959), but they can easily combine as a solution to form a superparamagnetic aggregate, the magnetic saturation of the nanoparticles is diminished (commonly to 30 emu/g to 50 emu/g) due to the greater fraction of metal ions located on the crystal surface (Cornell and Schwertmann, 2003; Yuan et al., 2012). Also, spontaneous oxidation in air yields γ-Fe_2O_3 with additional loss (up to 20%) of magnetic saturation (Kucheryavy et al., 2013). To increase the transverse relaxivity, Berret et al. (2006) fabricated maghemite aggregates in the range of 70–150 nm by using block copolymers template (Berret et al., 2006). Shapiro et al. (2004) showed that MIOPs carry iron at an order of magnitude greater than USPIOs and can cause a local magnetic field in homogeneity extending approximately 50 times beyond the physical diameter of the particle. Accordingly, such particles could be suitable for biomedical applications (Shapiro et al., 2004).

Regarding our synthesis, the major concern was to eliminate the secondary synthesis product, iron carbonate ($FeCO_3$), that appears in the form of individual rhombohedral single-crystals alongside the magnetite. Therefore, the particle mixture was washed in a solution of hydrochloric acid (HCl) to ensure its removal. The solution concentration, the washing time and temperature were chosen not to affect the integrity of the magnetite particles. Multiple tests had shown that keeping products for three hours in a solution of HCl, pH=0.5 at 70°C leads to complete dissolution of $FeCO_3$ without altering the surface of the Fe_3O_4 crystallites. Attempts to wash the mixture with other chemical solvents did not led to the desired results. It was noticed that the filling level of autoclaves significantly influences the synthesis processes well as the $FeCO_3$ content (**Figure 8**). For a filling at 70%, the single-phase Fe_3O_4 with an average size of 40 μm was obtained after about 40 h of high-pressure treatment time. Otherwise, only mixture of α-Fe_2O_3, Fe_3O_4, and $FeCO_3$ was obtained. For a filling at 60%, the same mixture of α-Fe_2O_3, Fe_3O_4, and $FeCO_3$ was obtained except at 32, 34, 36, 38, and 40 h of high-pressure treatment time. Single-phase magnetite was obtained around 30 μm, at such instances. When the filling level was reduced to 50% or less, only a single phase of magnetite was obtained with no trace of $FeCO_3$ for any 4 to 40 h treatment times. Full control of the particle size growing progressively from 1 μm to 30 μm is so achieved and no HCl-based washing is needed.

In order to verify the uncoated SCMIOPs' potential applications to biomedical field *in vitro* cytocompatibility/cytotoxicity tests were performed on tumor and non-tumor cell lines. Iron oxide particles (particularly of nanoscale size) can promote cellular damage in human and mammalian cells characterized by DNA damage, disruption of cytoskeleton, apoptosis and oxidative stress by inducing generation of ROS (reactive oxygen species) *via* Fenton reaction (Dissanayake et al., 2015). The results indicate that the 24 h direct contact of SCMIOPs with HaCaT cells led to a decrease of cell viability in a dose-dependent manner. The lowest viability rate (70.62%) was recorded at the highest concentration (1000 μg/ml), whereas in the case of HEMa (human primary melanocytes) cells stimulation at 250, 500, and 1000 μg/ml rendered linear viability variation above 80% viable cells (**Figure 2**). According to the ISO standard 10993-5:2009 on Biological Evaluation of Medical Devices, a compound is considered cytotoxic if reduces cell viability by more than 30% (https://www.iso.org/obp/ui/#iso:std:iso:10993:-5:ed-3:v1:en). In this context, it can be stated that the tested 1-30 μm size uncoated SCMIOPs are cytocompatible. The different behavior of HaCaT and HEMa cells to SCMIOPs' can be attributed to: cell type (immortalized – HaCaT *vs*. primary cells – HEMa), and growth rate (HaCaT becomes 80–90% confluent within 48 h, whereas HEMa cells require more than 72 h). Moreover, it could be assumed that melanin produced by melanocytes is responsible for the constant viability rate (around 80%) of HEMa cells even at the highest concentration of SCMIOPs, since it is known that in normal conditions, melanin acts as an iron scavenger/chelator by forming complexes with iron and suppresses the iron ions potential toxicity (Ben-ShaChar and Youdim, 1992). In the case of tumor cells (particularly for murine melanoma cells - B164A5), SCMIOPs exerted a dose-dependent cytotoxic effect, with a viability rate of 49.87% calculated at the highest concentration tested – 1000 μg/ml (**Figure 3**). The response of human melanoma cells - A375 (amelanotic cells) to SCMIOPs' impact was somehow different as compared to B164A5 cells. The viability rate at 1000 μg/ml was of 71.26%, a value that can be

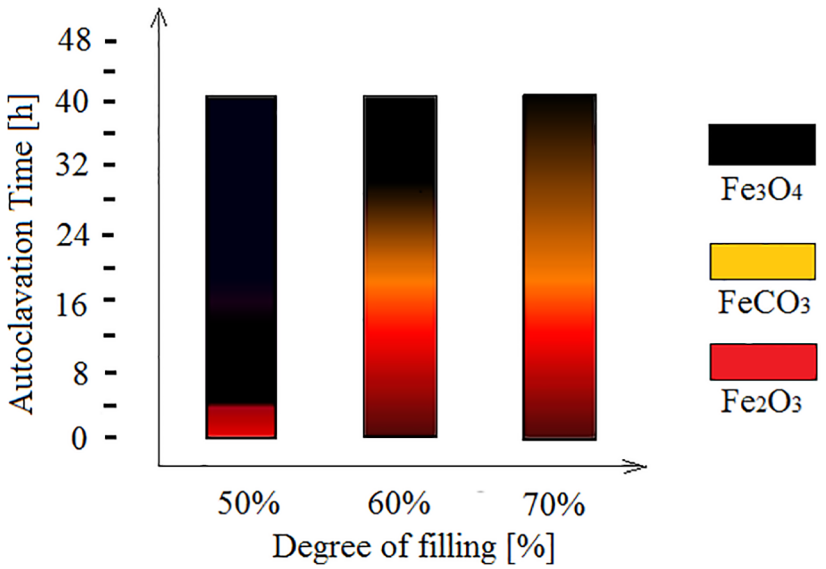

FIGURE 8 | Final products depending on degree of autoclaves filling.

considered non-toxic according to the ISO standard 10993-5:2009 on Biological Evaluation of Medical Devices (https://www.iso.org/obp/ui/#iso:std:iso:10993:-5:ed-3:v1:en).

These disparities between the response of human and murine cells to stimulation may be explained by the following: (i) different origin (A375 – human *vs*. B164A5 - murine), (ii) cells phenotype (A375 – epithelial *vs*. B164A5 - mesenchymal), and (iii) metastatic potential (A375 – low *vs*. B164A5 - high). In addition, it could be hypothesized that melanin plays a key role in SCMIOPs induced cytotoxicity (B164A5 cells are melanin-producing cells, whereas A375 cells are amelanotic). However, the validity of this hypothesis must be further investigated. The hypothesis originates from the fact that melanin can act as a double-edge sword in brain tissue. It can act as a protector by scavenging iron ions (in normal conditions) and as a promoter of Fe^{3+}induced toxicity (synergistic effect by increasing the production of ROS), which can lead to neurodegenerative damage (Zucca et al., 2017). Further studies are required to verify if the iron-melanin interactions induce similar effects in melanoma cells as the ones described for brain cells.

One of the mechanisms described for iron oxides cytotoxicity was induction of apoptosis with cytoskeleton reorganization and nuclear fragmentation (Dissanayake et al., 2015; Moaca et al., 2018). DAPI staining assay was performed in order to identify the type of cytotoxicity exerted by SCMIOPs. The presence of nuclear fragmentation observed in all cell types (mainly in tumor cells - **Figures 4** and **5**) after stimulation with SCMIOPs at 150 μg/ml confirms that the uncoated particles induced apoptosis in a dose-dependent manner. Therefore, the results confirm cell viability data. Cell morphology changes were also observed after stimulation with concentrations larger than 100 μg/ml (bright field images - **Figures 4** and **5**). A very relevant feature of iron oxide particles in terms of biocompatibility and effectiveness, is represented by their capacity to be internalized by cells (Catalano, 2017). However, the cellular uptake of iron oxide particles depends on various factors such as: cell type, surface charge, cell size and coating agents (Zhou et al., 2017). In this respect, the intracellular accumulation of uncoated SCMIOPs was assessed by Prussian blue staining method. As shown in **Figures 6** and **7**, the internalization of the uncoated SCMIOPs was rather absent in the case of HaCaT and A375 cells, whereas in the case of HEMa and B164A5 cell lines, the cell membrane adhesion is more likely as opposed to particle cell internalization. The cell iron penetration mechanism described in the literature is clathrin-mediated endocytosis *via* transferrin carrier. According to several experimental studies, 50 nm is the optimum nanoparticle size needed to reach the highest cellular uptake. However, this value is also cell-type dependent (Hoshyar et al., 2016; Behzadi et al., 2017). Other studies showed that 500 nm particles can be internalized by cells *via* clathrin-mediated endocytosis (Chaves et al., 2017). Hinds et al. (2003) showed that MIOPs can be effectively endocytosed by various cells and can thus contribute to the improvement of MRI (magnetic resonance imaging) signal (Hinds et al., 2003). By coating this particles with a polymer and further label them with a fluorescent agent, they can be used both for the improvement of MRI imaging and for tracking cells by fluorescence microscopy. In a recent study, Chaves et al. (2017) showed that maghemite nanoparticles were more intensively internalized by breast cancer cells as compared to normal cells (Chaves et al., 2017). In addition, the invasive breast metastatic cells - MDA-MB-231 presented a higher uptake of the nanoparticles as MCF7 cells (non-metastatic cells). These results are similar with our data. A possible explanation for the lack of intracellular SCMIOPs accumulation could be the reduced 24 h incubation time. Jarockyte et al. (2016) noticed that for the cellular uptake of superparamagnetic magnetite nanoparticles a 24–48 h incubation time was required, during the first hours the nanoparticles were attached to cell membranes (Jarockyte et al., 2016), a phenomenon that was observed in HEMa and B164A5 cells. The coating agent on the particle surface may facilitate particle access within the cells. Hence, the lack of the agent in the uncoated particles may be responsible to some degree to the absence of SCMIOPs intracellular accumulation noted in our study. Similar results were also described in a recent study published by our research group which revealed that naked Fe_3O_4 nanoparticles did not affect the viability of HaCaT, B164A5 and A375 cells, up to a concentration of 50 μg/ml, whereas the presence of oleic acid (OA) coating on the surface of Fe_3O_4 nanoparticles led to damage of melanoma cell lines (B164A5 and A375 cells) at a concentration of 10 μg/ml, whereas the viability of HaCaT cells was affected only at the highest concentration - 50 μg/ml (Moaca et al., 2019). Comparable data were reported by Marcus et al. (2016) who evaluated the effect of different MNPs coatings on neuronal cells (Marcus et al., 2016).

CONCLUSIONS

Developing a synthesis pathway for obtaining 1–30 μm magnetite micro octahedrons with superparamagnetic behavior (Hc=1.5 Oe, σr=0.28 emu/g) at room temperature by hydrothermal decomposition of Fe-Na_4EDTA complex in the presence of urea led to a saturation magnetization like in bulk (σs=92 emu/g), that guarantees a strong magnetic response. Such behavior is very unusual in the case of monocrystalline particles with micrometric dimensions which should have a typical ferrimagnetic rather than superparamagnetic behavior.

Present *in vitro* findings reveal that the uncoated magnetite microparticles are cytocompatible/cytotoxic in a cell-dependent manner on non-tumor/tumor cells accordingly, in agreement to ISO standard 10993-5:2009. In the case of HaCaT cells (non-tumor cells with a high proliferation rate) no microparticle accumulation within the cells was observed, however a dose-dependent decrease of cells viability resulted. For HEMa cells (low proliferation rate melanin-producing non-tumor cells) microparticles adhered to the cell membrane and the effect on cell viability becomes linear at concentrations higher than 150 μg/ml (above 80%). In case of B164A5 cells (melanin-producing murine metastatic melanoma cells), microparticles adhered to cells membranes and induced cytotoxicity *via* apoptosis in a dose-dependent manner. Regarding A375 cells (amelanotic non-metastatic human melanoma cells), no intracellular

accumulation of the microparticles was detected and the cytotoxic effect was less pronounced when compared to B164A5 cells. The results indicate that SCMIOPs are cytocompatible for non-tumor cells with a low proliferation rate and cytotoxic for tumor metastatic cells, hypothesizing that melanin is the key player in the mechanism of action involved. Here was demonstrated that a new class of micrometric magnetite particles overcome the limitations in using magnetic nanoparticles and micro-clusters. These new reported SCMIOPs possess a difference between magnetic saturation and magnetic remanence of 95.5 emu/g. Carefully selecting their size, it could be possible that applications like cellular MRI, monitoring cell migration for cell therapy, MRI contrast agents, detection, immobilization, and modification of biologically active compounds, cell labeling, magnetic separation of cells and others, to benefit from using SCMIOPs.

DATA AVAILABILITY STATEMENT

The datasets generated for this study are available on request to the corresponding authors.

AUTHOR CONTRIBUTIONS

CF, IM, IP, and DC – conception of the study, performed the *in vitro* tests, analysis and interpretation of the data acquired, drafting the work, and prepared the manuscript for submission. MCC, MC, LM, and AI – performed the synthesis, analysis and interpretation of the data acquired related to iron microparticles, and drafting the work. SA – performed *in vitro* tests, analysis of the results, and drafting the work. IP, CD, FL, VR, and AE – elaboration of the final version of the manuscript, correction of the language, analysis of the data, and revised critically the work. All authors contributed to manuscript revision, read, and approved the submitted version.

FUNDING

This work was supported by a grant of Ministery of Research and Innovation, CNCS-UEFISCDI, project number PN-III-P1-1.1-PD-2016-1982, within PNCDI III - lines 1109-1111 and by a grant offered by "Iuliu Hatieganu" University of Medicine and Pharmacy, Cluj-Napoca PCD contract no. 3066/17/01.02.2018, awarded by Claudia Geanina Farcaş.

ACKNOWLEDGMENTS

The *in vitro* experiments were conducted within the Center of Pharmaco-toxicological evaluations from the Faculty of Pharmacy, "Victor Babes" University of Medicine and Pharmacy, Timisoara.

REFERENCES

Akhtar, A., Schneider, J., and Chapman, S. (2010). In vivo quantification of VCAM-1 expression in renal ischaemia reperfusion injury using non-invasive magnetic resonance molecular imaging. *PloS One* 5 (9), e12800. doi: 10.1371/journal.pone.0012800

Arias, L. S., Pessan, J. P., Vieira, A. P. M., Lima, T. M. T., Delbem, A. C. B., and Monteiro, D. R. (2018). Iron Oxide Nanoparticles for Biomedical Applications: A Perspective on Synthesis, Drugs, Antimicrobial Activity, and Toxicity. *Antibiot. (Basel)* 7 (2), 46. doi: 10.3390/antibiotics7020046

Bean, C., and Livingston, J. (1959). Superparamagnetism. *J. Appl. Phys.* 30, S120–S129. doi: 10.1063/1.2185850

Behzadi, S., Serpooshan, V., Tao, W., Hamaly, M. A., Alkawareek, M. Y., Dreaden, E. C., et al. (2017). Cellular uptake of nanoparticles: journey inside the cell. *Chem. Soc. Rev.* 46 (14), 4218–4244. doi: 10.1039/c6cs00636a

Ben-Shachar, D., and Youdim, M. B. H. (1992). "Brain Iron and Nigrostriatal Dopamine Neurons in Parkinson's Disease," in *Iron and Human Diseases*. Ed. R. B. Lauffer (Boca Raton: CRC Press), 349–364.

Berret, J., Schonbeck, N., and Gazeau, F. (2006). Controlled clustering of superparamagnetic nanoparticles using block copolymers: design of new contrast agents for magnetic resonance imaging. *J. Am. Chem. Soc.* 128 (5), 1755–1761. doi: 10.1021/ja0562999

Carroll, M., Woodward, R., and House, M. J. (2010). Experimental validation of proton transverse relaxivity models for superparamagnetic nanoparticle MRI contrast agents. *Nanotechnology* 21 (3), 035103. doi: 10.1088/0957-4484/21/3/035103

Catalano, E. (2017). In vitro Biological Validation and Cytocompatibility Evaluation of Hydrogel Iron-oxide Nanoparticles. *AIP Conf. Proc.* 1873, 02001. doi: 10.1063/1.4997140

Chaves, N. L., Estrela-Lopis, I., Böttner, J., Lopes, C. A., Guido, B. C., and De Sousa, A. R. (2017). Báo SN. Exploring cellular uptake of iron oxide nanoparticles associated with rhodium citrate in breast cancer cells. *Int. J. Nanomed.* 12, 5511–5523. doi: 10.2147/IJN.S141582

Cornell, R. M., and Schwertmann, U. (2003). *The Iron Oxides. Structure, Properties, Reactions, Occurences and Uses* (Weinheim; [Cambridge]: Wiley-VCH, 2003.).

Dissanayake, N. M., Current, K. M., and Obare, S. O. (2015). Mutagenic Effects of Iron Oxide Nanoparticles on Biological Cells. *Int. J. Mol. Sci.* 16 (10), 23482–23516. doi: 10.3390/ijms161023482

Ercuta, A. (2020). Sensitive AC Hysteresigraph of Extended Driving Field Capability. *IEEE T. Istrum. Meas.* 69 (4), 1643–1651. doi: 10.1109/TIM.2019.2917237

Giere, R. (2016). Magnetite in the human body: Biogenic vs. anthropogenic. *Proc. Natl. Acad. Sci. U. S. A* 113 (43), 11986–11987. doi: 10.1073/pnas.1613349113

Hinds, K., Hill, J., Shapiro, E., Laukkanen, M., Silva, A., Combs, C., et al. (2003). Highly efficient endosomal labeling of progenitor and stem cells with large magnetic particles allows magnetic resonance imaging of single cells. *Blood* 102, 867–872. doi: 10.1182/blood-2002-12-3669

Hoshyar, N., Gray, S., Han, H., and Bao, G. (2016). The effect of nanoparticle size on in vivo pharmacokinetics and cellular interaction. *Nanomed. (Lond)* 6, 673–692. doi: 10.2217/nnm.16.5

Hughes, E. (2015). Big problems with little particles? *Chem. World*.

ISO 10993-5:2009(en) Biological evaluation of medical devices — Part 5: Tests for in vitro cytotoxicity. https://www.iso.org/obp/ui/#iso:std:iso:10993:-5:ed-3:v1:en:en. [Accessed January 15, 2019].

Jadhav, N. V., Prasad, A. I., Kumar, A., Mishra, R., Dhara, S., Babu, K. R., et al. (2013). Synthesis of oleic acid functionalized Fe_3O_4 magnetic nanoparticles and studying their interaction with tumor cells for potential hyperthermia application. *Colloids Surf. B. Biointerfaces* 108, 158–168. doi: 10.1016/j.colsurfb.2013.02.035

Jarockyte, G., Daugelaite, E., Stasys, M., Statkute, U., Poderys, V., Tseng, T. C., et al. (2016). Accumulation and Toxicity of Superparamagnetic Iron Oxide Nanoparticles in Cells and Experimental Animals. *Int. J. Mol. Sci.* 17 (8), pii: E1193,2016. doi: 10.3390/ijms17081193

Karaagac, O., and Kockar, H. (2012). Iron Oxide Nanoparticles Co-Precipitated in Air Environment: Effect of [Fe $^{+2}$]/[Fe $^{+3}$] Ratio. *IEEE Trans. Magn.* 48 (4), 1532–1536. doi: 10.1109/TMAG.2011.2173313

Karaagac, O., and Kockar, H. (2016). A simple way to obtain high saturation magnetization for superparamagnetic iron oxide nanoparticles synthesized in

air atmosphere: Optimization by experimental design. *J. Magn. Magn. Mater* 409, 116–123. doi: 10.1016/j.jmmm.2016.02.076

Kirschvink, J. L., Kobayashi-Kirschvink, A., Diaz-Ricci, J. C., and Kirschvink, S. J. (1992). Magnetite in human tissues: a mechanism for the biological effects of weak ELF magnetic fields. *Bioelectromagnetics* Suppl 1, 101–113. doi: 10.1002/bem.2250130710

Kucheryavy, P., He, J., Vijay, T. J., Maharjan, P., Spinu, L., Goloverda, G. Z., et al. (2013). Superparamagnetic Iron Oxide Nanoparticles with Variable Size and an Iron Oxidation State as Prospective Imaging Agents. *Langmuir* 29 (2), 710–716. doi: 10.1021/la3037007

Lauterwasser, C. (2015). Small sizes that matter: Opportunities and risks of Nanotechnologies, Report in co-operation with the OECD International Futures, Allianz Center for Technology.

Ma, J., and Chen, Z. (2016). Discovery of superparamagnetism in sub-millimeter-sized magnetite porous single crystals. *Phys. Lett. A* 380, 3313–3318. doi: 10.1016/j.physleta.2016.07.065

Mankia, K. S., McAteer, M. A., and Choudhury, R. P. (2011). Microparticle-Based Molecular MRI of Atherosclerosis, Thrombosis, and Tissue Ischemia. *Curr. Cardiovasc. Imaging Rep.* 4, 17–23. doi: 10.1007/s12410-010-9059-z

Marcus, M., Karni, M., Baranes, K., Levy, I., Alon, N., Margel, S., et al. (2016). Iron oxide nanoparticles for neuronal cell applications: uptake study and magnetic manipulations. *J. Nanobiotechnol.* 14, 37. doi: 10.1186/s12951-016-0190-0

Mathieu, J. B., and Martel, S. (2006). Magnetic steering of iron oxide microparticles using propulsion gradient coils in MRI, in: *Proceedings of the 28th IEEE EMBS Annual International Conference*, New York City, USA. p. 472–475. doi: 10.1109/IEMBS.2006.259818

McAteer, M., Schneider, J., and Ali, Z. E. A. (2008). Magnetic resonance imaging of endothelial adhesion molecules in mouse atherosclerosis using dual-targeted microparticles of iron oxide. *Atheroscler. Thromb. Vasc. Biol.* 28 (1), 77–83. doi: 10.1161/ATVBAHA.107.145466

McAteer, M. A., Von ZurMuhlen, C., Anthony, D. C., Sibson, N. R., and Choudhury, R. P. (2011). Magnetic Resonance Imaging of Brain Inflammation Using Microparticles of Iron Oxide. *Methods Mol. Biol.* 680, 103–115. doi: 10.1007/978-1-60761-901-7_7

Moaca, E. A., Coricovac, D. E., Soica, C. M., Pinzaru, I. A., Pacurariu, C. S., and Dehelean, C. A. (2018). "Preclinical Aspects on Magnetic Iron Oxide Nanoparticles and Their Interventions as Anticancer Agents: Enucleation, Apoptosis and Other Mechanism," in *Iron Ores and Iron Oxide Materials,* Ed. V Shatokha. (London, UK: IntechOpen), 229–254. doi: 10.5772/intechopen.74176

Moaca, E. A., Farcas, C., Coricovac, D., Avram, S., Mihali, C. V., Draghici, G. A., et al. (2019). Oleic Acid Double Coated Fe_3O_4 Nanoparticles as Anti- Melanoma Compounds with a Complex Mechanism of Activity—In Vitro and In Ovo Assessment. *J. BioMed. Nanotechnol.* 15 (5), 893–909. doi: 10.1166/jbn.2019.2726

Néel, L. (1949). Théorie du trainage magnétique desferromagnétiques en grains fins avec applications aux terres cuites. *Ann. Geogr.* 5, 99–136.

Ozel, F., and Kockar, H. (2015). Growth and characterizations of magnetic nanoparticles under hydrothermal conditions: Reaction time and temperature. *J. Magn. Magn. Mater* 373, 213–216. doi: 10.1016/j.jmmm.2014.02.072

Ozel, F., Kokkar, H., and Karaagac, O. (2015). Growth of Iron Oxide Nanoparticles by Hydrothermal Process: Effect of Reaction Parameters on the Nanoparticle Size. *J. Supercond. Nov. Magn.* 28, 823–829. doi: 10.1007/s10948-014-2707-9

Park, Y. C., Smith, J. B., Pham, T., Whitaker, R. D., Sucato, C. A., Hamilton, J. A., et al. (2014). Effect of PEG molecular weight on stability, T2 contrast, cytotoxicity, and cellular uptake of superparamagnetic iron oxide nanoparticles (SPIONs). *Colloids Surf. B. Biointerfaces* 119, 106–114. doi: 10.1016/j.colsurfb.2014.04.027

Runge, V.M. (1996). "Contrast-Enhanced Clinical Magnetic Resonance Imaging, *Medicine and Health Sciences*. 7.

Shapiro, E., Stanko, S., Sharer, K., Jonathan, M., Dunbar, C., and Koretsky, A. (2004). MRI detection of single particles for cellular imaging. *Proc. Natl. Acad. Sci. U. S. A* 101 (30), 10901–10906. doi: 10.1073/pnas.0403918101

Silva, E. L., Carvalho, J. F., Pontes, T. R. F., Oliveira, E. E., Francelino, B. L., Medeiros, A. C., et al. (2009). Development of a magnetic system for the treatment of Helicobacter pylori infections. *J. Magn. Mag. Mater* 321 (10), 1566–1570. doi: 10.1016/j.jmmm.2009.02.087

Von Zur Muhlen, C., Peter, K., Ali, Z., Schneider, J. E., McAteer, M. A., Neubauer, S., et al. (2009). Visualisation of activated platelets by targeted magnetic resonance imaging utilizing conformation-specific antibodies against glycoprotein IIb/IIIa. *J. Vasc. Res.* 46, 6–14. doi: 10.1159/000135660

Wu, Y. L., Ye, Q., Foley, L. M., Hitchens, T. K., Sato, K., Williams, J. B., et al. (2006). In situ labelling of immune cells with iron oxide particles: an approach to detect organ rejection by cellular MRI. *Proc. Natl. Acad. Sci. U.S.A.* 103 (6), 1852–1857. doi: 10.1073/pnas.0507198103

Xie, X., and Zhang, C. (2011). Controllable Assembly of Hydrophobic Superparamagnetic Iron Oxide Nanoparticle withm PEG-PLA Copolymer and Its Effect on MR Transverse Relaxation Rate. *J. Nanomater.* 2011 (152524), 7. doi: 10.1155/2011/152524

Ye, Q., Wu, Y. L., Foley, L. M., Hitchens, T. K., Eytan, D. F., Shirwan, H., et al. (2008). Longitudinal tracking of recipient macrophages in a rat chronic cardiac allograft rejection model with non-invasive magnetic resonance imaging using micrometer-sized paramagnetic iron oxide particles. *Circulation* 118 (2), 149–156. doi: 10.1161/CIRCULATIONAHA.107.746354

Yuan, Y., Rende, D., Altan, C. L., Bucak, S., Ozisik, R., and Borca-Tasciuc, D. A. (2012). Effect of Surface Modificationon Magnetization of Iron Oxide Nanoparticle Colloids. *Langmuir* 28, 13051–13059. doi: 10.1021/la3022479

Zhou, S., Yin, T., Zou, Q., Zhang, K., Gao, G., Shapter, J. G., et al. (2017). Labeling adipose derived stem cell sheet by ultrasmall superparamagnetic Fe3O4 nanoparticles and magnetic resonance tracking in vivo. *Sci. Rep.* 7, 42793. doi: 10.1038/srep42793

Zucca, F. A., Segura-Aguilar, J., Ferrari, E. P., Muñoz Paris, I., Sulzer, D., Sarna, T., et al. (2017). Interactions of iron, dopamine and neuromelanin pathways in brain aging and Parkinson's disease. *Prog. Neurobiol.* 155, 96–119. doi: 10.1016/j.pneurobio.2015.09.012,2015

Conflict of Interest: The authors declare that the research was conducted in the absence of any commercial or financial relationships that could be construed as a potential conflict of interest.

frontiers in Pharmacology

MINI REVIEW
published: 03 April 2020
doi: 10.3389/fphar.2020.00323

Cancer Chemoprevention Using Nanotechnology-Based Approaches

*Preshita Desai[1], Naga Jyothi Thumma[1], Pushkaraj Rajendra Wagh[1], Shuyu Zhan[1,2], David Ann[3], Jeffrey Wang[1] and Sunil Prabhu[1]**

[1] Department of Pharmaceutical Sciences, College of Pharmacy, Western University of Health Sciences, Pomona, CA, United States, [2] Department of Pharmaceutics, College of Medicine, Jiaxing University, Jiaxing, China, [3] Department of Diabetes and Metabolic Diseases Research, Beckman Research Institute, City of Hope, Duarte, CA, United States

Cancer research in pursuit of better diagnostic and treatment modalities has seen great advances in recent years. However, the incidence rate of cancer is still very high. Almost 40% of women and men are diagnosed with cancer during their lifetime. Such high incidence has not only resulted in high mortality but also severely compromised patient lifestyles, and added a great socioeconomic burden. In view of this, chemoprevention has gained wide attention as a method to reduce cancer incidence and its relapse after treatment. Among various stems of chemoprevention research, nanotechnology-based chemoprevention approaches have established their potential to offer better efficacy and safety. This review summarizes recent advances in nanotechnology-based chemoprevention strategies for various cancers with emphasis on lung and bronchial cancer, colorectal, pancreatic, and breast cancer and highlights the unmet needs in this developing field towards successful clinical translation.

Keywords: chemoprevention, nanotechnology, targeted delivery, efficacy, relapse

OPEN ACCESS

Edited by:
Katrin Sak,
NGO Praeventio, Estonia

Reviewed by:
Marcello Locatelli,
Università degli Studi G. d'Annunzio Chieti e Pescara, Italy
Mariangela Garofalo,
University of Padova, Italy

***Correspondence:**
Sunil Prabhu
sprabhu@westernu.edu

Specialty section:
This article was submitted to Pharmacology of Anti-Cancer Drugs, a section of the journal Frontiers in Pharmacology

Received: *19 December 2019*
Accepted: *05 March 2020*
Published: *03 April 2020*

Citation:
Desai P, Thumma NJ, Wagh PR, Zhan S, Ann D, Wang J and Prabhu S (2020) Cancer Chemoprevention Using Nanotechnology-Based Approaches. Front. Pharmacol. 11:323. doi: 10.3389/fphar.2020.00323

INTRODUCTION

Cancer poses a severe socioeconomic impact all over the world. As per the American Cancer Society, over 1,762,450 new cancer cases and about 606,880 cancer related deaths are estimated in the United States alone in 2019 (average of 4,830 new cases and 1,660 deaths per day) (American Cancer Society, 2019a). Late/limited diagnostic opportunities, faster progression, limited treatment options with severe toxicities, and frequent relapse are the key reasons for high cancer fatality and is an alarming concern despite extensive research conducted in this field and available clinical treatments thus far. Therefore, alternatives like cancer chemoprevention, which focus on reducing cancer incidence and/or relapse, are gaining wide attention in recent years. Cancer chemoprevention can be looked upon as a strategy designed to minimize and delay the incidence, progression, or relapse of cancer. The objective is to interfere with the process of carcinogenesis so as to arrest or substantially retard the growth of precancerous lesions to reduce cancer incidence (Patterson et al., 2013).

Over the decades, literature reports few hundreds of molecules to elicit such chemopreventive potential and among them the widely reported drug classes are nonsteroidal anti-inflammatory drugs or NSAIDS (e.g., aspirin, ibuprofen, etc.); antioxidants [curcumin, ferulic acid, resveratrol, ellagic acid, epigallocatechin-3-gallate (EGCG), etc.]; extracts from natural origin (tea, wheat bran, etc.); minerals and ions (calcium, zinc, etc.). However, very few have been clinically approved under

the broader umbrella of chemoprevention strategies with a listed use to treat or mitigate risk of precancerous lesions (Patterson et al., 2013). Evidently, the clinical success of these actives is restricted due to drug delivery challenges. Hence, use of smart nano drug delivery systems ensuring *in vivo* absorption and transportation of such actives at chemoprevention sites using passive and active targeting approaches is gradually coming on the forefront (Siddiqui et al., 2012; Desai et al., 2019a; Desai et al., 2019b). Though nanochemoprevention research is in its infancy, its potential is evident from increasing research in the field and reported scientific literature. This review summarizes recent advances in this niche field and highlights the unmet needs towards successful clinical translation.

Role of Nanotechnology in Chemoprevention

Nanotechnology-based products broadly refer to nanoformulation comprising of particles ≤100 nm and from literature perspective those <1000 nm (Jeevanandam et al., 2018). Such nanoscale size elicits superior properties to these drug carrier system from absorption, targeting, and safety aspect which are summarized in **Figure 1** (modified from Desai et al., 2019a). Briefly, the overall drug efficacy and safety depend upon its intrinsic potency and variable factors like drug pharmacokinetics, toxicity, targeted delivery, and stability. Nanotechnology-based drug carriers successfully enhance these variable properties and thereby increase drug efficacy. Further, implementation of nanotechnology-based formulation in cancer prevention and therapy becomes very important in view of chemotherapy-associated side effects as they can provide an opportunity for possible dose reduction and drug targeting which can additionally enhance drug safety by minimizing off-target toxicities. Nanoformulations can be broadly classified based on their excipient composition and are depicted in **Figure 2** (modified from Desai et al., 2019a), which can be polymeric, lipid, carbon based, inorganic, or combinations thereof (Muqbil et al., 2011; Siddiqui et al., 2012; Miller et al., 2016).

Nanotechnology-Based Chemoprevention Approaches

Lung and Bronchial Cancer

Lung and bronchial cancer is the leading cause of cancer-related deaths in the United States (American Cancer Society, 2019a). The key carcinogenesis factor is long-term tobacco use while other factors include exposure to radon gas, asbestos, air pollution, and second-hand smoke (Office on and Health, 2006; Gemine et al., 2019). The long-term prevention strategy is smoking withdrawal but the cancer risk of prior or current smoking population remains high. The average age of cohort diagnosed with lung cancer is 50–75 years with majority of patients being 65 years or older. The existing treatment modalities (surgery, chemotherapy, or radiation therapy) have succeeded in elongating life expectancy but in most cases, the disease is incurable leading to high fatality (American Cancer Society, 2019b; Farr et al., 2019; Mieras et al., 2019). Chemoprevention has been explored for management of lung cancer using natural or synthetic compounds to inhibit progression or suppress, reverse tumor growth. To overcome hydrophobicity and low bioavailability of such actives, nanotechnology-based approaches have been investigated. One such hydrophobic active is luteolin from green vegetables. Majumdar et al. developed nanoluteolin comprising luteolin nanocapsules with water-soluble polymer. They reported enhanced chemoprevention efficacy with nanoluteolin in an *in vitro* setting using cell lines of lung cancer (H292) and squamous carcinoma head and neck cancer (Tu212) and similar significant efficacy was observed in a tumor xenograft model (Emory Health

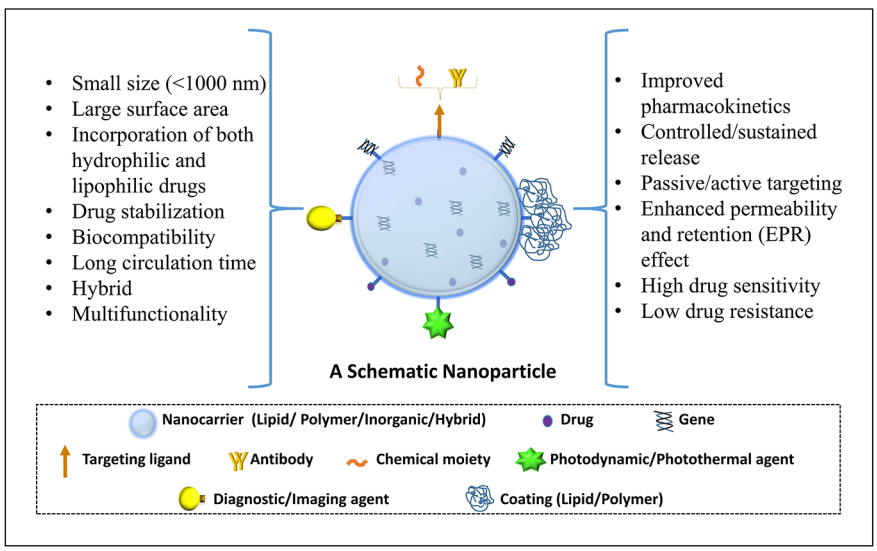

FIGURE 1 | Schematic representation of a functional nanocarrier and its superior properties.

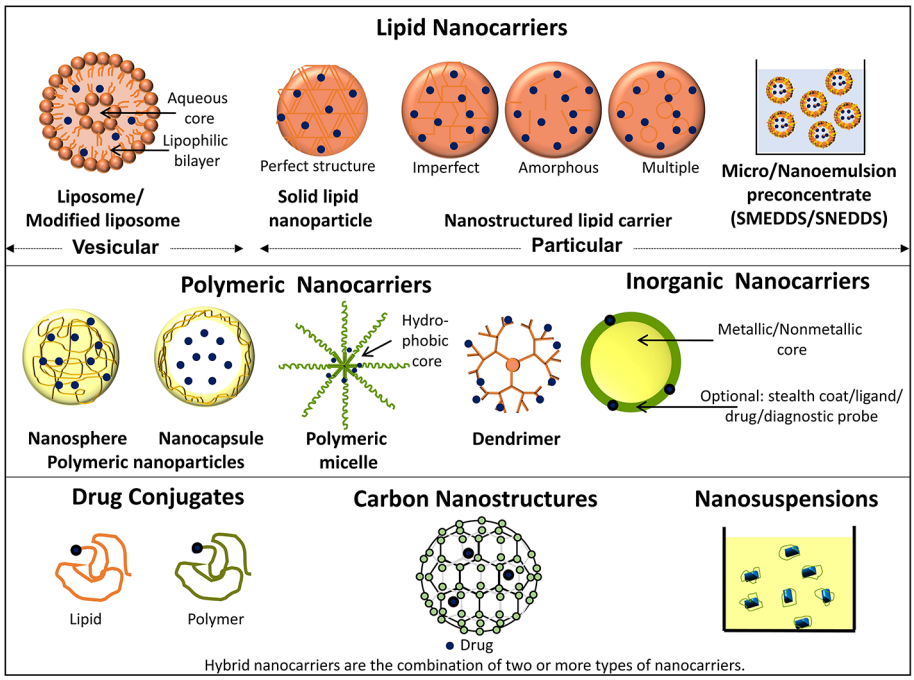

FIGURE 2 | Schematic representation depicting types of nanocarriers.

Sciences, 2014; Majumdar et al., 2014). In another study, to enhance the solubility of chemopreventive antioxidant resveratrol, hydroxypropyl-β-cyclodextrin complex was developed for intranasal delivery. A 25-day *in vivo* study in A/J mice lung carcinogenesis model demonstrated 27% reduction in tumor multiplicity with 45% lower tumor volume confirming the efficacy of the developed formulation. Such a formulation approach is anticipated to enhance the drug bioavailability and hence has great potential in future clinical studies (Monteillier et al., 2018). In another study, lipid nanoparticles (NPs) of three chemopreventive drugs N-acetyl-L-cysteine, phenethyl isothiocyanate, and resveratrol were developed and their chemopreventive potential was assessed in bronchial epithelial cells. The study revealed significant enhancement in reducing the DNA fragmentation due to cigarette smoke with resveratrol lipid NPs confirming its potential to increase efficacy of lipophilic drug. However, the results were not significant with hydrophilic drug N-acetyl-L-cysteine indicating that appropriate selection of drug and NPs combination is very essential in development of successful chemoprevention strategy (Pulliero et al., 2015). Similarly, to enhance the *in vivo* performance of well-reported natural chemopreventive agent naringenin, polycaprolactone NPs of naringenin were developed with hyaluronic acid as an active targeting agent. The developed NPs were proven to show enhanced inhibitory potential against lung cancer cell line A549 but was found to be safe against J774 macrophage cell line confirming both enhanced efficacy and safety. The *in vivo* studies using urethane-induced lung cancer in rat model established significant tumor inhibitory activity confirming the *in vivo* drug targeting (Parashar et al., 2018). Further, a natural antioxidant, curcumin has shown a strong lung cancer stem cells suppression potency but its poor bioavailability makes it ineffective *in vivo*. Therefore, enhancing the bioavailability of drug is a potential approach and various NPs like lipid, polymer, liposomes have been reported to do so. Other promising agents such as vitamin A (retinoids or carotenoids), isothiocyanates, green tea extract, and bitter melon extract have also shown promise in head and neck cancer and their efficacy could be improvised to clinical significance using nanotechnology-based approaches.

Colorectal Cancer

Colorectal cancer is the second common cause of cancer related deaths in the United States (Americancancersociety, 2019a). Most of the colon cancers develop from the noncancerous adenomatous polyps, but when left untreated these polyps can become cancerous (Testa et al., 2018). Though surgical resection is the primary line of treatment, uncertainty in the detection methods and poor compliance leads to development of metastatic cancer and relapse (Vernon, 1997). Hence, prevention of polyp formation and development can be considered as a first line prevention approach.

For colon cancer chemoprevention, NSAIDs are most widely used (U.S. Preventive Services Task Force, 2007; Alizadeh et al., 2012; Drew et al., 2016; Pan et al., 2018). The epidemiological studies show that among all the NSAIDs, aspirin is the most promising agent in reducing adenomatous cancer recurrence due to the availability of remarkably consistent data with no cardiovascular risk and minimal gastrointestinal toxicity (Umezawa et al., 2019). Further, aspirin has also received a Grade B recommendation by the (U.S. Preventive Services Task Force, 2016) for its use as a chronic prophylaxis agent for colorectal cancer

(Dehmer et al., 2015). Although it has been proved that aspirin alone or in combination have colon chemopreventive activity, nanoencapsulation of aspirin can further potentiate the efficacy with decreased dose. Chaudhary et al. studied chemopreventive effect of a mixture of aspirin, folic acid, and calcium on azoxymethane treated 7-week-old male Sprague-Dawley rats. The polymeric nanocapsules of drug combination prepared using polylactic-co-glycolic acid (PLGA) 50:50 polymer showed 1.7-fold more effective in chemoprevention than their unmodified counterpart regimen (Prabhu et al., 2007; Chaudhary et al., 2011). Celecoxib is another NSAID which is being widely explored in clinical setting for its chemoprevention potential but offers cardiotoxicity and pharmacokinetic variability (Solomon et al., 2005). Studies show that polymeric NPs of celecoxib prepared using ethyl cellulose with sodium caseinate/bile salt, lipid hybrid NPs, and microemulsions improved its bioavailability allowing reduction in dose, related cardiotoxicity, and crystallization (Margulis-Goshen et al., 2011; Tan et al., 2011; Morgen et al., 2012). Naturally derived phytochemicals are widely studied as potential chemopreventive agents for their pleiotropic effects and non-toxicity (Thomasset et al., 2007; Zubair et al., 2017; Wong et al., 2019). Curcumin has shown efficient chemoprotective activity in intestinal and colon cancer, but has minimal water solubility, poor absorption, and low bioavailability. To overcome this issue, curcumin-whey protein nanocapsules were developed that not only showed >70% release in 48 h but also exhibited enhanced cell internalization and bioavailability. (Jayaprakasha et al., 2016). In another study, it was revealed that curcumin encapsulated in polymeric nanocarrier improved the solubility of curcumin and showed significantly reduced number of tumors, less structural abnormalities and beta-catenin (a key intracellular messenger in gastrointestinal tract malignancies) in curcumin NPs-treated group when compared to the curcumin (Alizadeh et al., 2012).

Pancreatic Cancer

Pancreatic cancer is the third leading cause of all cancer-related deaths in the United States (American Cancer Society, 2019a). Late diagnosis, faster progression, low 5-year survival rate (merely 9%), and high risk of relapse make pancreatic cancer treatment and management challenging despite available first-line drug treatment involving use of gemcitabine combinations and Folfirinox® (a drug cocktail of fluorouracil, leucovorin, irinotecan, and oxaliplatin) (Rahman et al., 2017; Malatesta et al., 2018; American Cancer Society, 2019a; Desai et al., 2019a; Desai et al., 2019b). Hence, chemoprevention has gained wide attention as an alternative strategy to control the occurrence and relapse.

Lipid nanocarriers have been widely investigated for this purpose, Prabhu et al. developed solid lipid NPs comprising aspirin, curcumin, and free sulforaphane as a nanocombination chemoprevention platform. The developed formulation showed significant enhancement in inhibition in Panc-1 and Mia PaCa-2 cell line models and synergism due to use of multiple drugs eliciting chemoprevention activity *via* variable mechanisms. Further, an *in vivo* chemoprevention study using *LSL-Kras* $^{G12D/+}$; *Pdx-1* $^{Cre/+}$ transgenic mice indicated significant reduction in tumor incidence with the combination nanoformulation compared to control (Sutaria et al., 2012; Thakkar et al., 2013). In another study, self micro-emulsifying drug delivery system (SMEDDS) of classical antihistaminic drug loratadine and sulforaphane was reported with enhanced oral bioavailability and chemoprevention potential in Panc-1 and Mia PaCa-2 PC cell lines (Desai et al., 2019b). Based on similar rational liposomes, dendrimers, micelles of potent chemopreventive phytochemical like curcumin, ellagic acid, etc. have been reported to show enhanced inhibition in pancreatic cancer cell lines and their application can be extended for pancreatic cancer chemoprevention (Song et al., 2011; Kesharwani et al., 2015; Wei et al., 2017).

Gene therapy has also been investigated for prevention purpose and various siRNAs, viral vectors have been studied (Lebedeva et al., 2008; Sarkar et al., 2014; Lei et al., 2017). In an interesting study by Fisher et al., replication incompetent adenoviruses capable of delivering a melanoma differentiation associated gene-7/Interleukin-24 (mda-7/IL-24) in presence of perillyl alcohol was developed. The formed nanoviral vector exhibited synergistic inhibition of pancreatic cancer cells with antitumor "bystander" response leading to suppression of primary as well as distant tumor growth. Hence, this strategy can be considered as a future clinical solution for chemoprevention and treatment and can also play a critical role in arresting pancreatic cancer relapse (Lebedeva et al., 2008; Sarkar et al., 2014).

Breast Cancer

Breast cancer has highest incidence and is listed to be the fourth leading cause of cancer-associated deaths in the United States (American Cancer Society, 2019a). Though chemotherapy using drugs like selective estrogen receptor modulators (tamoxifen, raloxifene, etc.), aromatase inhibitors (exemestane, anastrozole, letrozole, etc.) have shown treatment efficacy, very high incidence of breast cancer warrants development of promising preventive strategies (Ales-Martinez et al., 2015; Decensi et al., 2015; Locatelli et al., 2018). In recent years, natural products and some antineoplastic agents such as tamoxifen or raloxifene have displayed potential in chemoprevention of breast cancer (Mitra and Dash, 2018; Uramova et al., 2018). However, to enhance drug stability, achieve sustained drug release and to circumvent side effects, delivery of these agents using nanoformulations has been warranted. According to the reports, various nanoformulations such as liposome, nanofibers, nanocapsules, and NPs have been developed and investigated for prevention of breast cancer cells proliferation, breast cancer recurrence and metastasis after chemotherapy (Li et al., 2011; Roy et al., 2015; Shirode et al., 2015; Ding et al., 2016). A polymeric NPs formulation of curcumin (NanoCurc) was designed and studied to significantly attenuate incidence of mammary tumors in a rodent chemical carcinogenesis model, confirming its breast cancer chemoprevention potential in at-risk populations (Chun et al., 2012). In another study, the composite polycaprolactone/silk fibroin nanofibrous scaffolds loaded with titanocene were developed and reported to have potential for preventing the proliferation of breast cancer cells (Laiva et al., 2015). Interestingly, dietary soy isoflavones

(genistein, etc.) have shown potential in reducing cancer incidence and their nanoformulations like PEGylated silica NPs, Chitosan NPs have shown significant enhancement in breast and cervical cancer inhibition (Sarkar and Li, 2003; Cai et al., 2017; Pool et al., 2018). Also, poly (ethylene glycol)-modified chitosan NPs were synthesized to encapsulate and deliver small interfering RNA (siRNA). The siRNA loaded NPs showed 4T1 cell inhibition both *in vitro* and *in vivo* ensuring its efficacy in reduction of tumor growth and metastasis (Sun et al., 2016). Wan et al. developed the lapatinib-loaded human serum albumin NPs that exhibited a core-shell structure with stealth properties preventing brain metastasis from triple-negative breast cancer (Wan et al., 2016). Interestingly, overcoming drug resistance and increasing cancer cell sensitivity towards drugs have also been investigated under this umbrella using a glycolipid-like nanocarrier encapsulating anti-tumor drug doxorubicin, which restricted drug resistance upon long-term use (Meng et al., 2019).

Hybrid NPs have also been explored for chemoprevention. Tran et al. developed the hyaluronic acid coated solid lipid NPs for co-delivery of ibuprofen and paclitaxel that resulted in synergistic inhibition on the proliferation of cancer cells (Tran et al., 2017). Zhang et al. designed a multifunctional hybrid nanomedicine integrating multiple FDA-approved modalities like radiotherapy, chemotherapy, photothermal therapy, and immunotherapy, which demonstrated elimination of the primary breast tumor and efficiently prevented tumor recurrence and metastasis to lung (Zhang et al., 2019b). Further, small peptide T4 (NLLMAAS) has been reported to inhibit tyrosine kinase, immunoglobulin, and epidermal growth factor homology-2 (Tie2), required for blood vessels reconstruction during tumor recurrence. To achieve this inhibition effectively and in targeted manner, selective NPs comprising dual-responsive amphiphilic peptide (mPEG1000-K (DEAP)-AANNLLMAAS) were developed. The NPs were capable of releasing the peptide T4 under acidic tumor environment and could achieve targeted inhibition resulting in breast tumor relapse inhibition (Zhang et al., 2019a). In another study, nanographene oxide-methylene blue formulations in combination with photodynamic and photothermal treatment were reported to prevent breast tumor regrowth and metastasis to the liver, lung, and spleen (Dos Santos et al., 2018).

Miscellaneous Cancers

Chemoprevention has also been studied in other less common forms of cancers including but not limited to head, neck, skin, prostate, liver. Head and neck squamous cell carcinoma is a fast progressive form of cancer and oral cancer is highly prevalent subtype therein (Crooker et al., 2018). Recently, indigenous extracellular vesicles like exosomes, microvesicles, apoptic bodies derived from mammalian or tumor cells are gaining wide attention as chemopreventive and treatment tools. They have been recognized as valuable carriers for drugs like paclitaxel, RNAs, peptides, etc. and have shown potential in inhibiting of various types of cancers (Wang et al., 2017; Han et al., 2019; Rahbarghazi et al., 2019; Wu et al., 2019)

For the site-specific local treatment and chemoprevention of oral squamous cell carcinoma, several polymeric drug delivery systems have been developed using nanotechnology which has shown enhanced activity (Desai, 2018; Ketabat et al., 2019). Some studies include drugs nanoformulations such as naringenin NPs, ellagic acid chitosan NPs, which showed significant enhancement in both bioavailability and efficacy (Arulmozhi et al., 2013; Sulfikkarali et al., 2013; Desai, 2018). In addition, cisplatin when encapsulated in polymeric micelles was reported to eliminate cisplatin induced nephrotoxicity (Endo et al., 2013; Desai, 2018). Further, PEGylated nanoliposomes of paclitaxel, resveratrol, and 5-fluorouracil were reported to show controlled drug release in inhibition of head and neck carcinoma and liposomal formulation of irinotecan (Onivyde®) has already been in market for pancreatic cancer management (Nie et al., 2011; Desai, 2018). Another natural chemopreventive agent, salvianolic acid B was encapsulated in phospholipid complex loaded NPs and the studies showed significant increase in intracellular uptake and improved cell inhibition when compared to drug for head and neck carcinoma (Li et al., 2016).

In the past few years, green tea and its major polyphenol, catechin have been demonstrated to superior chemoprevention activity on multiple cancer types mainly because of their antioxidant/pro-oxidant properties (Naponelli et al., 2017). To improve the drug's bioavailability, stability, and tumor selectivity, nanotechnology-based drug delivery systems have been widely studied (Tyagi et al., 2017). To study the chemoprevention efficacy of combination, gold-conjugated green tea NPs were designed that demonstrated selective toxicity towards Ehrlich's Ascites Carcinoma and breast cancer cells MCF-7 and interestingly had hepatoprotective behavior against the tumor-induced cellular damage (Mukherjee et al., 2015). For prostate cancer prevention and therapy, targeted EGCG polymeric NPs were developed using a biocompatible polymer polylactic-co-glycolic acid–polyethylene glycol-A (PLGA-PEG-A) which have a specific binding and high inhibitory action against prostate cancer cells *via* specific membrane antigen resulting in enhanced bioavailability, limited toxicity, and in turn enhanced efficacy (Sanna et al., 2017).

Hesperetin, a bio-flavonoid, plays a potential role in liver cancer management. To overcome it poor solubility, bioavailability, biocompatibility issues, hesperetin, loaded gold NPs were designed. These NPs demonstrated significantly higher *in vivo* prevention activity against lipid per-oxidation, hepatic cell damage in diethylnitrosamine-induced liver cancer model compared to the drug alone (Gokuladhas et al., 2016).

In the area of skin cancer prevention, nanotechnology-based drug formulation such as nanoemulsion of 5-fluorouracil, bromelain polymeric NPs using PLGA, solid lipid NPs of doxorubicin, 5-flurouracil have been reported (Bhatnagar et al., 2015; Shakeel et al., 2015; Ravikumar and Tatke, 2019). Use of NPs to enhance the skin deposition of chemopreventive agents is an ideal way to enhance the chemopreventive efficacy. Such examples include shell-enriched solid lipid NPs of 5-fluorouracil, curcumin-ceramide niososmes, etc. (Heenatigala Palliyage et al., 2019; Ravikumar and Tatke, 2019). NPs have also been

developed and studied to elicit enhanced protection against UV radiation. Several studies including development of ultra-flexible NPs of an antioxidant diindolylmethane derivative, silver NPs, etc. (Boakye et al., 2016; Bagde et al., 2018).

Regulatory, Clinical Insights, and Future Directions

Application of nanotechnology in cancer chemoprevention has certainly proven its potential to deliver the drugs in more effective, safer, and targeted manner. The research in this area is further advancing towards development of nanovaccines for cancer prevention. Also, early detection techniques using nanoplatforms capable of identifying pre-malignant markers are gaining attention as a preventive measure and nanodevices comprising nanochips, nanodots, quantum dots, nanoshells, and nanotubes have been reported (Bentolila et al., 2009; Boisselier and Astruc, 2009; Larocque et al., 2009; Singh et al., 2018; Facciola et al., 2019; Kheirollahpour et al., 2019; Shen et al., 2019). Despite of such advances in research, their bench-to-bedside translation for cancer prevention has a long way to go owing to regulatory and clinical considerations. In this context, mainly NSAIDS, retinoids, cyclooxygenase inhibitors, etc. have shown clinical potential through randomized clinical studies. However, more concentrated efforts and well-planned studies with measurable clinical outcomes are warranted. Further, proving the safety of nanoformulations is an urgently needed aspect. In view of regulatory approval of nanotechnology-based products for cancer treatment and other conditions, we should expect the clinical translation of nanotechnology-based products for cancer chemoprevention in near future.

AUTHOR CONTRIBUTIONS

PD, JW, and SP conceived and proposed the idea. PD compiled the manuscript with support from NT, PW, SZ. DA, JW and SP reviewed and revised the manuscript.

REFERENCES

Ales-Martinez, J. E., Ruiz, A., Chacon, J. I., Lluch Hernandez, A., Ramos, M., Cordoba, O., et al. (2015). Preventive treatments for breast cancer: recent developments. *Clin. Transl. Oncol.* 17, 257–263. doi: 10.1007/s12094-014-1250-2

Alizadeh, A. M., Khaniki, M., Azizian, S., Mohaghgheghi, M. A., Sadeghizadeh, M., and Najafi, F. (2012). Chemoprevention of azoxymethane-initiated colon cancer in rat by using a novel polymeric nanocarrier–curcumin. *Eur. J. Pharmacol.* 689, 226–232. doi: 10.1016/j.ejphar.2012.06.016

American Cancer Society (2019a). *Cancer statistics center*, American Cancer Society. [Online]. Available: https://cancerstatisticscenter.cancer.org/#!/ [Accessed 2019/12/12].

American Cancer Society (2019b). *Key Statistics for Lung Cancer*, American Cancer Society. [Online]. Available: https://www.cancer.org/cancer/lung-cancer/about/key-statistics.html [Accessed 2019/12/12].

Arulmozhi, V., Pandian, K., and Mirunalini, S. (2013). Ellagic acid encapsulated chitosan nanoparticles for drug delivery system in human oral cancer cell line (KB). *Colloids Surf. B B.* 110, 313–320. doi: 10.1016/j.colsurfb.2013.03.039

Bagde, A., Mondal, A., and Singh, M. (2018). Drug delivery strategies for chemoprevention of UVB-induced skin cancer: A review. *Photodermatol. Photoimmunol. Photomed.* 34, 60–68. doi: 10.1111/phpp.12368

Bentolila, L. A., Ebenstein, Y., and Weiss, S. (2009). Quantum dots for in vivo small-animal imaging. *J. Nucl. Med.* 50, 493–496. doi: 10.2967/jnumed.108.053561

Bhatnagar, P., Pant, A. B., Shukla, Y., Chaudhari, B., Kumar, P., and Gupta, K. C. (2015). Bromelain nanoparticles protect against 7,12-dimethylbenz[a] anthracene induced skin carcinogenesis in mouse model. *Eur. J. Pharm. Biopharm.* 91, 35–46. doi: 10.1016/j.ejpb.2015.01.015

Boakye, C. H. A., Patel, K., Doddapaneni, R., Bagde, A., Behl, G., Chowdhury, N., et al. (2016). Ultra-flexible nanocarriers for enhanced topical delivery of a highly lipophilic antioxidative molecule for skin cancer chemoprevention. *Colloids Surf. B: B.* 143, 156–167. doi: 10.1016/j.colsurfb.2016.03.036

Boisselier, E., and Astruc, D. (2009). Gold nanoparticles in nanomedicine: preparations, imaging, diagnostics, therapies and toxicity. *Chem. Soc. Rev.* 38, 1759–1782. doi: 10.1039/b806051g

Cai, L., Yu, R., Hao, X., and Ding, X. (2017). Folate Receptor-targeted Bioflavonoid Genistein-loaded Chitosan Nanoparticles for Enhanced Anticancer Effect in Cervical Cancers. *Nanoscale Res. Lett.* 12, 509–509. doi: 10.1186/s11671-017-2253-z

Chaudhary, A., Sutaria, D., Huang, Y., Wang, J., and Prabhu, S. (2011). Chemoprevention of colon cancer in a rat carcinogenesis model using a novel nanotechnology-based combined treatment system. *Cancer Prev. Res. (Phila)* 4, 1655–1664. doi: 10.1158/1940-6207.CAPR-11-0129

Chun, Y. S., Bisht, S., Chenna, V., Pramanik, D., Yoshida, T., Hong, S. M., et al. (2012). Intraductal administration of a polymeric nanoparticle formulation of curcumin (NanoCurc) significantly attenuates incidence of mammary tumors in a rodent chemical carcinogenesis model: Implications for breast cancer chemoprevention in at-risk populations. *Carcinogenesis* 33, 2242–2249. doi: 10.1093/carcin/bgs248

Crooker, K., Aliani, R., Ananth, M., Arnold, L., Anant, S., and Thomas, S. M. (2018). A Review of Promising Natural Chemopreventive Agents for Head and Neck Cancer. *Cancer Prev. Res. (Phila)* 11, 441–450. doi: 10.1158/1940-6207.CAPR-17-0419

Decensi, A., Thorat, M. A., Bonanni, B., Smith, S. G., and Cuzick, J. (2015). Barriers to preventive therapy for breast and other major cancers and strategies to improve uptake. *Ecancermedicalscience* 9, 595. doi: 10.3332/ecancer.2015.595

Dehmer, S. P., Maciosek, M. V., and Flottemesch, T. J. (2015). "U.S. Preventive Services Task Force Evidence Syntheses, formerly Systematic Evidence Reviews," in *Aspirin Use to Prevent Cardiovascular Disease and Colorectal Cancer: A Decision Analysis: Technical Report.* (Rockville (MD): Agency for Healthcare Research and Quality (US)).

Desai, P., Ann, D., Wang, J., and Prabhu, S. (2019a). Pancreatic Cancer: Recent Advances in Nanoformulation-Based Therapies. *Crit. Rev. Ther. Drug Carrier Syst.* 36, 59–91. doi: 10.1615/CritRevTherDrugCarrierSyst.2018025459

Desai, P., Thakkar, A., Ann, D., Wang, J., and Prabhu, S. (2019b). Loratadine self-microemulsifying drug delivery systems (SMEDDS) in combination with sulforaphane for the synergistic chemoprevention of pancreatic cancer. *Drug Delivery Transl. Res.* 9, 641–651. doi: 10.1007/s13346-019-00619-0

Desai, K. G. H. (2018). Polymeric drug delivery systems for intraoral site-specific chemoprevention of oral cancer. *J. BioMed. Mater. Res. B Appl. Biomater.* 106, 1383–1413. doi: 10.1002/jbm.b.33943

Ding, Q., Li, Z., Yang, Y., Guo, G., Luo, F., Chen, Z., et al. (2016). Preparation and therapeutic application of docetaxel-loaded poly(d,l-lactide) nanofibers in preventing breast cancer recurrence. *Drug Deliv.* 23, 2677–2685. doi: 10.3109/10717544.2015.1048490

Dos Santos, M. S. C., Gouvea, A. L., De Moura, L. D., Paterno, L. G., De Souza, P. E. N., Bastos, A. P., et al. (2018). Nanographene oxide-methylene blue as phototherapies platform for breast tumor ablation and metastasis prevention in a syngeneic orthotopic murine model. *J. Nanobiotechnol.* 16, 9. doi: 10.1186/s12951-018-0333-6

Drew, D. A., Cao, Y., and Chan, A. T. (2016). Aspirin and colorectal cancer: the promise of precision chemoprevention. *Nat. Rev. Cancer* 16, 173–186. doi: 10.1038/nrc.2016.4

Endo, K., Ueno, T., Kondo, S., Wakisaka, N., Murono, S., Ito, M., et al. (2013). Tumor-targeted chemotherapy with the nanopolymer-based drug NC-6004 for oral squamous cell carcinoma. *Cancer Sci.* 104, 369–374. doi: 10.1111/cas.12079

Facciola, A., Visalli, G., Lagana, P., La Fauci, V., Squeri, R., Pellicano, G. F., et al. (2019). The new era of vaccines: the "nanovaccinology". *Eur. Rev. Med. Pharmacol. Sci.* 23, 7163–7182. doi: 10.26355/eurrev_201908_18763

Farr, K. P., West, K., Yeghiaian-Alvandi, R., Farlow, D., Stensmyr, R., Chicco, A., et al. (2019). Functional perfusion image guided radiation treatment planning for locally advanced lung cancer. *Phys. Imaging Radiat. Oncol.* 11, 76–81. doi: 10.1016/j.phro.2019.08.007

Emory Health Sciences (2014). *Nano-capsules show potential for more potent chemoprevention*, [Online]. Available: https://www.sciencedaily.com/releases/2014/01/140108081219.htm [Accessed 2019/12/12]. ScienceDaily.

Gemine, R. E., Ghosal, R., Collier, G., Parry, D., Campbell, I., Davies, G., et al. (2019). Longitudinal study to assess impact of smoking at diagnosis and quitting on 1-year survival for people with non-small cell lung cancer. *Lung Cancer* 129, 1–7. doi: 10.1016/j.lungcan.2018.12.028

Gokuladhas, K., Jayakumar, S., Rajan, B., Elamaran, R., Pramila, C. S., Gopikrishnan, M., et al. (2016). Exploring the Potential Role of Chemopreventive Agent, Hesperetin Conjugated Pegylated Gold Nanoparticles in Diethylnitrosamine-Induced Hepatocellular Carcinoma in Male Wistar Albino Rats. *Indian J. Clin. Biochem.* 31, 171–184. doi: 10.1007/s12291-015-0520-2

Han, L., Lam, E. W. F., and Sun, Y. (2019). Extracellular vesicles in the tumor microenvironment: old stories, but new tales. *Mol. Cancer* 18, 59. doi: 10.1186/s12943-019-0980-8

Heenatigala Palliyage, G., Singh, S., Ashby, C. R.Jr., Tiwari, A. K., and Chauhan, H. (2019). Pharmaceutical Topical Delivery of Poorly Soluble Polyphenols: Potential Role in Prevention and Treatment of Melanoma. *AAPS PharmSciTech* 20, 250. doi: 10.1208/s12249-019-1457-1

Jayaprakasha, G. K., Chidambara Murthy, K. N., and Patil, B. S. (2016). Enhanced colon cancer chemoprevention of curcumin by nanoencapsulation with whey protein. *Eur. J. Pharmacol.* 789, 291–300. doi: 10.1016/j.ejphar.2016.07.017

Jeevanandam, J., Barhoum, A., Chan, Y. S., Dufresne, A., and Danquah, M. K. (2018). Review on nanoparticles and nanostructured materials: history, sources, toxicity and regulations. *Beilstein J. Nanotechnol.* 9, 1050–1074. doi: 10.3762/bjnano.9.98

Kesharwani, P., Xie, L., Banerjee, S., Mao, G., Padhye, S., Sarkar, F. H., et al. (2015). Hyaluronic acid-conjugated polyamidoamine dendrimers for targeted delivery of 3,4-difluorobenzylidene curcumin to CD44 overexpressing pancreatic cancer cells. *Colloids Surf. B B.* 136, 413–423. doi: 10.1016/j.colsurfb.2015.09.043

Ketabat, F., Pundir, M., Mohabatpour, F., Lobanova, L., Koutsopoulos, S., Hadjiiski, L., et al. (2019). Controlled Drug Delivery Systems for Oral Cancer Treatment-Current Status and Future Perspectives. *Pharmaceutics* 11, pii: E302. doi: 10.3390/pharmaceutics11070302

Kheirollahpour, M., Mehrabi, M., Dounighi, N. M., Mohammadi, M., and Masoudi, A. (2019). Nanoparticles and Vaccine Development. *Pharm. Nanotechnol.* 8, (1) 6–21. doi: 10.2174/2211738507666191024162042

Laiva, A. L., Venugopal, J. R., Karuppuswamy, P., Navaneethan, B., Gora, A., and Ramakrishna, S. (2015). Controlled release of titanocene into the hybrid nanofibrous scaffolds to prevent the proliferation of breast cancer cells. *Int. J. Pharm.* 483, 115–123. doi: 10.1016/j.ijpharm.2015.02.025

Larocque, J., Bharali, D. J., and Mousa, S. A. (2009). Cancer detection and treatment: the role of nanomedicines. *Mol. Biotechnol.* 42, 358–366. doi: 10.1007/s12033-009-9161-0

Lebedeva, I. V., Su, Z. Z., Vozhilla, N., Chatman, L., Sarkar, D., Dent, P., et al. (2008). Chemoprevention by perillyl alcohol coupled with viral gene therapy reduces pancreatic cancer pathogenesis. *Mol. Cancer Ther.* 7, 2042–2050. doi: 10.1158/1535-7163.MCT-08-0245

Lei, Y., Tang, L., Xie, Y., Xianyu, Y., Zhang, L., Wang, P., et al. (2017). Gold nanoclusters-assisted delivery of NGF siRNA for effective treatment of pancreatic cancer. *Nat. Commun.* 8, 15130. doi: 10.1038/ncomms15130

Li, R. J., Ying, X., Zhang, Y., Ju, R. J., Wang, X. X., Yao, H. J., et al. (2011). All-trans retinoic acid stealth liposomes prevent the relapse of breast cancer arising from the cancer stem cells. *J. Control Release* 149, 281–291. doi: 10.1016/j.jconrel.2010.10.019

Li, H., Shi, L., Wei, J., Zhang, C., Zhou, Z., Wu, L., et al. (2016). Cellular uptake and anticancer activity of salvianolic acid B phospholipid complex loaded nanoparticles in head and neck cancer and precancer cells. *Colloids Surf. B B.* 147, 65–72. doi: 10.1016/j.colsurfb.2016.07.053

Locatelli, M., Tinari, N., Grassadonia, A., Tartaglia, A., Macerola, D., Piccolantonio, S., et al. (2018). FPSE-HPLC-DAD method for the quantification of anticancer drugs in human whole blood, plasma, and urine. *J. Chromatogr. B* 1095, 204–213. doi: 10.1016/j.jchromb.2018.07.042

Majumdar, D., Jung, K. H., Zhang, H., Nannapaneni, S., Wang, X., Amin, A. R., et al. (2014). Luteolin nanoparticle in chemoprevention: in vitro and in vivo anticancer activity. *Cancer Prev. Res. (Phila)* 7, 65–73. doi: 10.1158/1940-6207.CAPR-13-0230

Malatesta, L., Cosco, D., Paolino, D., Cilurzo, F., Costa, N., Di Tullio, A., et al. (2018). Simultaneous quantification of Gemcitabine and Irinotecan hydrochloride in rat plasma by using high performance liquid chromatography-diode array detector. *J. Pharm. Biomed. Anal.* 159, 192–199. doi: 10.1016/j.jpba.2018.06.060

Margulis-Goshen, K., Weitman, M., Major, D. T., and Magdassi, S. (2011). Inhibition of crystallization and growth of celecoxib nanoparticles formed from volatile microemulsions. *J. Pharm. Sci.* 100, 4390–4400. doi: 10.1002/jps.22623

Meng, T., Qiu, G., Hong, Y., Yuan, M., Lu, B., Wu, J., et al. (2019). Effect of chitosan based glycolipid-like nanocarrier in prevention of developing acquired drug resistance in tri-cycle treatment of breast cancer. *Int. J. Pharm.* 555, 303–313. doi: 10.1016/j.ijpharm.2018.11.056

Mieras, A., Pasman, H. R. W., Onwuteaka-Philipsen, B. D., Dingemans, A. M. C., Kok, E. V., Cornelissen, R., et al. (2019). Is In-Hospital Mortality Higher in Patients With Metastatic Lung Cancer Who Received Treatment in the Last Month of Life? A Retrospective Cohort Study. *J. Pain Symptom Manage.* 58, 805–811. doi: 10.1016/j.jpainsymman.2019.06.026

Miller, M. S., Allen, P., Brentnall, T. A., Goggins, M., Hruban, R. H., Petersen, G. M., et al. (2016). Pancreatic Cancer Chemoprevention Translational Workshop: Meeting Report. *Pancreas* 45, 1080–1091. doi: 10.1097/MPA.0000000000000705

Mitra, S., and Dash, R. (2018). Natural Products for the Management and Prevention of Breast Cancer. *Evid Based Complement Altern. Med.* 2018, 8324696. doi: 10.1155/2018/8324696

Monteillier, A., Voisin, A., Furrer, P., Allémann, E., and Cuendet, M. (2018). Intranasal administration of resveratrol successfully prevents lung cancer in A/J mice. *Sci. Rep.* 8, 14257. doi: 10.1038/s41598-018-32423-0

Morgen, M., Bloom, C., Beyerinck, R., Bello, A., Song, W., Wilkinson, K., et al. (2012). Polymeric nanoparticles for increased oral bioavailability and rapid absorption using celecoxib as a model of a low-solubility, high-permeability drug. *Pharm. Res.* 29, 427–440. doi: 10.1007/s11095-011-0558-7

Mukherjee, S., Ghosh, S., Das, D. K., Chakraborty, P., Choudhury, S., Gupta, P., et al. (2015). Gold-conjugated green tea nanoparticles for enhanced anti-tumor activities and hepatoprotection–synthesis, characterization and in vitro evaluation. *J. Nutr. Biochem.* 26, 1283–1297. doi: 10.1016/j.jnutbio.2015.06.003

Muqbil, I., Masood, A., Sarkar, F. H., Mohammad, R. M., and Azmi, A. S. (2011). Progress in nanotechnology based approaches to enhance the potential of chemopreventive agents. *Cancers* 3, 428–445. doi: 10.3390/cancers3010428

Naponelli, V., Ramazzina, I., Lenzi, C., Bettuzzi, S., and Rizzi, F. (2017). Green Tea Catechins for Prostate Cancer Prevention: Present Achievements and Future Challenges. *Antioxid. (Basel)* 6, pii: E26. doi: 10.3390/antiox6020026

Nie, S., Hsiao, W. L., Pan, W., and Yang, Z. (2011). Thermoreversible Pluronic F127-based hydrogel containing liposomes for the controlled delivery of paclitaxel: in vitro drug release, cell cytotoxicity, and uptake studies. *Int. J. Nanomed.* 6, 151–166. doi: 10.2147/IJN.S15057

Office On, S., and Health (2006). "Publications and Reports of the Surgeon General," in *The Health Consequences of Involuntary Exposure to Tobacco Smoke: A Report of the Surgeon General.* (Atlanta (GA): Centers for Disease Control and Prevention (US)).

Pan, P., Huang, Y. W., Oshima, K., Yearsley, M., Zhang, J., Yu, J., et al. (2018). Could Aspirin and Diets High in Fiber Act Synergistically to Reduce the Risk of Colon Cancer in Humans? *Int. J. Mol. Sci.* 19, pii: E166. doi: 10.3390/ijms19010166

Parashar, P., Rathor, M., Dwivedi, M., and Saraf, S. A. (2018). Hyaluronic Acid Decorated Naringenin Nanoparticles: Appraisal of Chemopreventive and Curative Potential for Lung Cancer. *Pharmaceutics* 10, 33. doi: 10.3390/pharmaceutics10010033

Patterson, S. L., Colbert Maresso, K., and Hawk, E. (2013). Cancer Chemoprevention: Successes and Failures. *Clin. Chem.* 59, 94. doi: 10.1373/clinchem.2012.185389

Pool, H., Campos-Vega, R., Herrera-Hernández, M. G., García-Solis, P., García-Gasca, T., Sánchez, I. C., et al. (2018). Development of genistein-PEGylated silica hybrid nanomaterials with enhanced antioxidant and antiproliferative properties on HT29 human colon cancer cells. *Am. J. Trans. Res.* 10, 2306–2323.

Prabhu, S., Kanthamneni, N., and Wang, J. (2007). Synergistic chemoprevention of colorectal cancer using colon-targeted polymer nanoparticles. *Cancer Res.* 67, 1–1.

Pulliero, A., Wu, Y., Fenoglio, D., Parodi, A., Romani, M., Soares, C. P., et al. (2015). Nanoparticles increase the efficacy of cancer chemopreventive agents in cells exposed to cigarette smoke condensate. *Carcinogenesis* 36, 368–377. doi: 10.1093/carcin/bgv008

Rahbarghazi, R., Jabbari, N., Sani, N. A., Asghari, R., Salimi, L., Kalashani, S. A., et al. (2019). Tumor-derived extracellular vesicles: reliable tools for Cancer diagnosis and clinical applications. *Cell Commun. Signaling* 17, 73–73. doi: 10.1186/s12964-019-0390-y

Rahman, F. A. U., Ali, S., and Saif, M. W. (2017). Update on the role of nanoliposomal irinotecan in the treatment of metastatic pancreatic cancer. *Ther. Adv. Gastroenterol.* 10, 563–572. doi: 10.1177/1756283X17705328

Ravikumar, P., and Tatke, P. (2019). Advances in encapsulated dermal formulations in chemoprevention of melanoma: An overview. *J. Cosmet. Dermatol.* 18, 1606–1612. doi: 10.1111/jocd.13105

Roy, J., Oliveira, L. T., Oger, C., Galano, J. M., Bultel-Ponce, V., Richard, S., et al. (2015). Polymeric nanocapsules prevent oxidation of core-loaded molecules: evidence based on the effects of docosahexaenoic acid and neuroprostane on breast cancer cells proliferation. *J. Exp. Clin. Cancer Res.* 34, 155. doi: 10.1186/s13046-015-0273-z

Sanna, V., Singh, C. K., Jashari, R., Adhami, V. M., Chamcheu, J. C., Rady, I., et al. (2017). Targeted nanoparticles encapsulating (-)-epigallocatechin-3-gallate for prostate cancer prevention and therapy. *Sci. Rep.* 7, 41573. doi: 10.1038/srep41573

Sarkar, F. H., and Li, Y. (2003). Soy isoflavones and cancer prevention. *Cancer Invest.* 21, 744–757. doi: 10.1081/CNV-120023773

Sarkar, S., Azab, B., Quinn, B. A., Shen, X., Dent, P., Klibanov, A. L., et al. (2014). Chemoprevention gene therapy (CGT) of pancreatic cancer using perillyl alcohol and a novel chimeric serotype cancer terminator virus. *Curr. Mol. Med.* 14, 125–140. doi: 10.2174/1566524013666131118110827

Shakeel, F., Haq, N., Al-Dhfyan, A., Alanazi, F. K., and Alsarra, I. A. (2015). Chemoprevention of skin cancer using low HLB surfactant nanoemulsion of 5-fluorouracil: a preliminary study. *Drug Deliv.* 22, 573–580. doi: 10.3109/10717544.2013.868557

Shen, Z., Fan, W., Yang, Z., Liu, Y., Bregadze, V. I., Mandal, S. K., et al. (2019). Exceedingly Small Gadolinium Oxide Nanoparticles with Remarkable Relaxivities for Magnetic Resonance Imaging of Tumors. *Small* 15, e1903422. doi: 10.1002/smll.201903422

Shirode, A. B., Bharali, D. J., Nallanthighal, S., Coon, J. K., Mousa, S. A., and Reliene, R. (2015). Nanoencapsulation of pomegranate bioactive compounds for breast cancer chemoprevention. *Int. J. Nanomed.* 10, 475–484. doi: 10.2147/IJN.S65145

Siddiqui, I. A., Adhami, V. M., Chamcheu, J. C., and Mukhtar, H. (2012). Impact of nanotechnology in cancer: emphasis on nanochemoprevention. *Int. J. nanomed.* 7, 591–605. doi: 10.2147/IJN.S26026

Singh, P., Pandit, S., Mokkapati, V., Garg, A., Ravikumar, V., and Mijakovic, I. (2018). Gold Nanoparticles in Diagnostics and Therapeutics for Human Cancer. *Int. J. Mol. Sci.* 19, pii: E1979. doi: 10.3390/ijms19071979

Solomon, S. D., Mcmurray, J. J., Pfeffer, M. A., Wittes, J., Fowler, R., Finn, P., et al. (2005). Cardiovascular risk associated with celecoxib in a clinical trial for colorectal adenoma prevention. *N Engl. J. Med.* 352, 1071–1080. doi: 10.1056/NEJMoa050405

Song, Z., Feng, R., Sun, M., Guo, C., Gao, Y., Li, L., et al. (2011). Curcumin-loaded PLGA-PEG-PLGA triblock copolymeric micelles: Preparation, pharmacokinetics and distribution in vivo. *J. Colloid Interface Sci.* 354, 116–123. doi: 10.1016/j.jcis.2010.10.024

Sulfikkarali, N., Krishnakumar, N., Manoharan, S., and Nirmal, R. M. (2013). Chemopreventive efficacy of naringenin-loaded nanoparticles in 7,12-dimethylbenz(a)anthracene induced experimental oral carcinogenesis. *Pathol. Oncol. Res.* 19, 287–296. doi: 10.1007/s12253-012-9581-1

Sun, P., Huang, W., Jin, M., Wang, Q., Fan, B., Kang, L., et al. (2016). Chitosan-based nanoparticles for survivin targeted siRNA delivery in breast tumor therapy and preventing its metastasis. *Int. J. Nanomed.* 11, 4931–4945. doi: 10.2147/IJN.S105427

Sutaria, D., Grandhi, B. K., Thakkar, A., Wang, J., and Prabhu, S. (2012). Chemoprevention of pancreatic cancer using solid-lipid nanoparticulate delivery of a novel aspirin, curcumin and sulforaphane drug combination regimen. *Int. J. Oncol.* 41, 2260–2268. doi: 10.3892/ijo.2012.1636

Tan, A., Davey, A. K., and Prestidge, C. A. (2011). Silica-Lipid Hybrid (SLH) Versus Non-lipid Formulations for Optimising the Dose-Dependent Oral Absorption of Celecoxib. *Pharm. Res.* 28, 2273–2287. doi: 10.1007/s11095-011-0458-x

Testa, U., Pelosi, E., and Castelli, G. (2018). Colorectal cancer: genetic abnormalities, tumor progression, tumor heterogeneity, clonal evolution and tumor-initiating cells. *Med. Sci. (Basel Switzerland)* 6, 31. doi: 10.3390/medsci6020031

Thakkar, A., Sutaria, D., Grandhi, B. K., Wang, J., and Prabhu, S. (2013). The molecular mechanism of action of aspirin, curcumin and sulforaphane combinations in the chemoprevention of pancreatic cancer. *Oncol. Rep.* 29, 1671–1677. doi: 10.3892/or.2013.2276

Thomasset, S. C., Berry, D. P., Garcea, G., Marczylo, T., Steward, W. P., and Gescher, A. J. (2007). Dietary polyphenolic phytochemicals–promising cancer chemopreventive agents in humans? A review of their clinical properties. *Int. J. Cancer* 120, 451–458. doi: 10.1002/ijc.22419

Tran, B. N., Nguyen, H. T., Kim, J. O., Yong, C. S., and Nguyen, C. N. (2017). Combination of a chemopreventive agent and paclitaxel in CD44-targeted hybrid nanoparticles for breast cancer treatment. *Arch. Pharm. Res.* 40, 1420–1432. doi: 10.1007/s12272-017-0968-0

Tyagi, N., De, R., Begun, J., and Popat, A. (2017). Cancer therapeutics with epigallocatechin-3-gallate encapsulated in biopolymeric nanoparticles. *Int. J. Pharm.* 518, 220–227. doi: 10.1016/j.ijpharm.2016.12.030

U.S. Preventive Services Task Force (2007). Routine aspirin or nonsteroidal anti-inflammatory drugs for the primary prevention of colorectal cancer: U.S. Preventive Services Task Force recommendation statement. *Ann. Intern Med.* 146, 361–364.

U.S. Preventive Services Task Force (2016). Aspirin Use to Prevent Cardiovascular Disease and Colorectal Cancer: Preventive Medication,. [Online] Available: https://www.uspreventiveservicestaskforce.org/Page/Document/Recommendation Statement Final/aspirin-to-prevent-cardiovascular-disease-and-cancer [Accessed 2019/12/12]

Umezawa, S., Higurashi, T., Komiya, Y., Arimoto, J., Horita, N., Kaneko, T., et al. (2019). Chemoprevention of colorectal cancer: Past, present, and future. *Cancer Sci.* 110, 3018–3026. doi: 10.1111/cas.14149

Uramova, S., Kubatka, P., Dankova, Z., Kapinova, A., Zolakova, B., Samec, M., et al. (2018). Plant natural modulators in breast cancer prevention: status quo and future perspectives reinforced by predictive, preventive, and personalized medical approach. *EPMA J.* 9, 403–419. doi: 10.1007/s13167-018-0154-6

Vernon, S. W. (1997). Participation in Colorectal Cancer Screening: A Review. *JNCI: J. Natl. Cancer Inst.* 89, 1406–1422.

Wan, X., Zheng, X., Pang, X., Pang, Z., Zhao, J., Zhang, Z., et al. (2016). Lapatinib-loaded human serum albumin nanoparticles for the prevention and treatment of triple-negative breast cancer metastasis to the brain. *Oncotarget* 7, 34038–34051. doi: 10.18632/oncotarget.8697

Wang, J., Sun, X., Zhao, J., Yang, Y., Cai, X., Xu, J., et al. (2017). Exosomes: A Novel Strategy for Treatment and Prevention of Diseases. *Front. Pharmacol.* 8, 300–300. doi: 10.3389/fphar.2017.00300

Wei, Y., Wang, Y., Xia, D., Guo, S., Wang, F., Zhang, X., et al. (2017). Thermosensitive Liposomal Codelivery of HSA-Paclitaxel and HSA-Ellagic Acid Complexes for Enhanced Drug Perfusion and Efficacy Against Pancreatic Cancer. *ACS Appl. Mater. Interfaces* 9, 25138–25151. doi: 10.1021/acsami.7b07132

Wong, K. E., Ngai, S. C., Chan, K.-G., Lee, L.-H., Goh, B.-H., and Chuah, L.-H. (2019). Curcumin Nanoformulations for Colorectal Cancer: A Review. *Front. Pharmacol.* 10, 152. doi: 10.3389/fphar.2019.00152

Wu, M., Wang, G., Hu, W., Yao, Y., and Yu, X.-F. (2019). Emerging roles and therapeutic value of exosomes in cancer metastasis. *Mol. Cancer* 18, 53. doi: 10.1186/s12943-019-0964-8

Zhang, L., Qi, Y., Min, H., Ni, C., Wang, F., Wang, B., et al. (2019a). Cooperatively Responsive Peptide Nanotherapeutic that Regulates Angiopoietin Receptor Tie2 Activity in Tumor Microenvironment To Prevent Breast Tumor Relapse after Chemotherapy. *ACS Nano* 13, 5091–5102. doi: 10.1021/acsnano.8b08142

Zhang, L. X., Sun, X. M., Xu, Z. P., and Liu, R. T. (2019b). Development of Multifunctional Clay-Based Nanomedicine for Elimination of Primary Invasive Breast Cancer and Prevention of Its Lung Metastasis and Distant Inoculation. *ACS Appl. Mater. Interfaces* 11, 35566–35576. doi: 10.1021/acsami.9b11746

Zubair, H., Azim, S., Ahmad, A., Khan, M. A., Patel, G. K., Singh, S., et al. (2017). Cancer Chemoprevention by Phytochemicals: Nature's Healing Touch. *Mol. (Basel Switzerland)* 22, 395. doi: 10.3390/molecules22030395

Conflict of Interest: The authors declare that the research was conducted in the absence of any commercial or financial relationships that could be construed as a potential conflict of interest.

frontiers in Pharmacology

ORIGINAL RESEARCH
published: 22 April 2020
doi: 10.3389/fphar.2020.00484

Hydroxypropyl-β-Cyclodextrin Complexes of Styryllactones Enhance the Anti-Tumor Effect in SW1116 Cell Line

*Ru Ma[1], Jie-tao Chen[1], Xiao-yue Ji[2], Xiao-li Xu[3] and Qing Mu[1]**

[1] School of Pharmacy, Fudan University, Shanghai, China, [2] School of Chemistry and Chemical Engineering, Queen's University Belfast, Belfast, United Kingdom, [3] Cancer Hospital, Fudan University, Shanghai, China

OPEN ACCESS

Edited by:
Mukerrem Betul Yerer Aycan, Erciyes University, Turkey

Reviewed by:
Aaditya Kashyap Bhatt, Amneal Pharmaceuticals, United States
Amarjit Luniwal, North American Science Associates Inc., United States

***Correspondence:**
Qing Mu
muqing@fudan.edu.cn

Specialty section:
This article was submitted to Pharmacology of Anti-Cancer Drugs, a section of the journal Frontiers in Pharmacology

Received: 19 December 2019
Accepted: 27 March 2020
Published: 22 April 2020

Citation:
Ma R, Chen J-t, Ji X-y, Xu X-l and Mu Q (2020) Hydroxypropyl-β-Cyclodextrin Complexes of Styryllactones Enhance the Anti-Tumor Effect in SW1116 Cell Line. Front. Pharmacol. 11:484. doi: 10.3389/fphar.2020.00484

Styryllactones, a class of compounds obtained from the genus *Goniothalamus* (Annonaceae), have demonstrated *in vitro* antitumor activity. However, the aqueous solubility of these compounds is poor. In this study, we identified the absolute configurations of the previously isolated compounds, which were first isolated in our laboratory, by single-crystal X-ray diffraction analysis using Cu Kα radiation. Subsequently, the antitumor activities of the compounds were evaluated by 3-(4,5-dimethylthiazol-2-yl)-2,5-diphenyl-tetrazolium bromide staining in four tumor cell lines. The induced apoptosis activity of leiocarpin E-7′-Monoacetate was studied by an annexin V fluorescein isothiocyanate/propidium iodide double-staining experiment, and the caspase activity was tested in the SW1116 cell line. The results demonstrated that the antitumor activities of cheliensisin A and goniodiol-7-monoacetate were limited by their poor water solubility. To address this issue, hydroxypropyl-β-cyclodextrin (HP-β-CD) complexes of the compounds were synthesized by the saturated aqueous method. The complexes were then analyzed using a differential scanning calorimeter. The IC_{50} of cheliensisin A was reduced by 45% and 58% against SW1116 and SMMC-7721 cell lines, respectively. Similarly, the IC_{50} of goniodiol-7-monoacetate was reduced by 55% and 34% against the two tumor cell lines, respectively. To further evaluate whether the styryllactones and complexes possessed selectivity against cancer cell lines and normal cell lines, toxicity against human normal cell line (HEK293T) was evaluated. The results demonstrated that the HP-β-CD complexes displayed more cytotoxicity than the respective pristine compounds against the HEK293T cell line. However, there existed a therapeutic window when the complexes were applied against cancer cell lines. In summary, the synthesis of several styryllactone compounds complexed with HP-β-CD was reported for the first time. These complexes could significantly enhance the cytotoxic effects of styryllactone compounds.

Keywords: styryllactone, absolute configuration, HP-β-CD, apoptosis, DSC

INTRODUCTION

Colon cancer is the third most common type of cancer worldwide in both men and women, and is associated with a high recurrence rate and increasing mortality rate (Lao and Grady, 2011; Purushotham et al., 2012; Altobelli et al., 2014; Siegel et al., 2014; Sunkara and Hebert, 2015). The existing treatment regimens for colon cancer include chemotherapy, radiotherapy, and surgical ablation. Among these, chemotherapy is the most common strategy (Wang et al., 2014b; Pohl and Schmiegel, 2016). However, the two major challenges for the effective treatment of colon cancer are adverse effects due to cancer chemotherapy and drug resistance (Kozovska et al., 2014; Lim et al., 2019). Hence, it is imperative to search for new chemotherapeutic agents that have better safety and efficacy profiles. In this context, the application of natural compounds is a promising approach (Sridhar et al., 2014; Levrier et al., 2015; Wang et al., 2016).

Styryllactones represent a series of natural products, isolated exclusively from the genus *Goniothalamus* belonging to the Annonaceae family, which are mostly indigenous in southeast Asia. Styryllactones are classified based on different structural skeletons as follows (Bermejo et al., 1997; Bermejo et al., 1998; Cao et al., 1998; Bermejo et al., 1999; Hu et al., 1999; Mu et al., 1999a; Peris et al., 2000; Lan et al., 2005; Liou et al., 2014): styrene–pyrone (**Figure 1A**), styrene–furanone (**Figure 1B**), furan–pyrone (**Figure 1C**), furan–furanone (**Figure 1D**), pyran–pyrone (**Figure 1E**), and heptyl esters (**Figure 1F**).

Studies have shown that some styryllactones possess potent cytotoxicity against human colon tumor cell lines. Ali et al. reported that goniothalamin exhibited the highest cytotoxic activity against HGC-27 cells among the different cell lines tested (HGC-27, MCF-7, PANC-1, HeLa) (Ali et al., 1997). Vendramini-Costa et al. demonstrated the importance of goniothalamin as a proapoptotic, and therapeutic agent for the treatment inflammatory bowel disease and emphasized its potential as a chemopreventive agent for colon cancer (Vendramini-Costa et al., 2016). Cheliensisin A, a novel styryllactone isolated from *Goniothalamus cheliensis* Hu, could trigger p53-mediated apoptosis, accompanied by dramatic inhibition of the anchorage-independent growth of HCT116 cells, thus highlighting its potential cancer therapeutic effect (Zhang et al., 2014).

In recent years, mechanisms related to the antitumor activity of styryllactone compounds have been reported. For example, goniothalamin induced the release of inflammatory cytokines by upregulating the B-cell lymphoma-2 (Bcl-2)-associated X protein (Bax)/Bcl-2, phosphorylate c-Jun N-terminal kinase (p-JNK1)/JNK1, and p-p38/p38 ratios, which led to cleavage of poly (ADP-ribose) polymerase (PARP) and, finally resulted in apoptosis of the HT-29 cells (Vendramini-Costa et al., 2016). The cells were unable to grow without the BIRC 5 (Full name: the baculoviral inhibitor of apoptosis repeat-containing 5) protein. While goniothalamin has demonstrated inhibitory action against transcription of the *BIRC5* gene at the RNA level, thus subjecting NCI-H460 cells to DNA damage (Semprebon et al., 2014).

In our previous work, styryllactone compounds were extracted from *Goniothalamus griffithii* (Annonaceae) and *Goniothalamus leiocarpus* (Annonaceae) (Mu et al., 1996; Li et al., 1997; Li et al., 1998; Mu et al., 1998; Mu et al., 1999a; Mu et al., 1999b; Mu et al., 2002; Mu et al., 2003; Mu et al., 2004). Their relative configurations were initially established on the basis of spectroscopic data (Li et al., 1997; Li et al., 1998; Mu et al., 1999a; Mu et al., 1999b; Mu et al., 2002; Mu et al., 2004).

In this study, the absolute configurations of several styryllactone compounds, first isolated in our laboratory, were determined by single-crystal X-ray diffraction analysis using Cu Kα radiation. In addition, we evaluated the effect of complexation of sytryllactones with HP-β-CD on their antitumor activity. The styryllactones displayed enhanced antitumor activity when complexd with HP-β-CD.

MATERIALS AND METHODS

Materials

Dulbecco's modified Eagle's medium (DMEM), Roswell Park Memorial Institute 1640 (RPMI-1640) medium, minimum

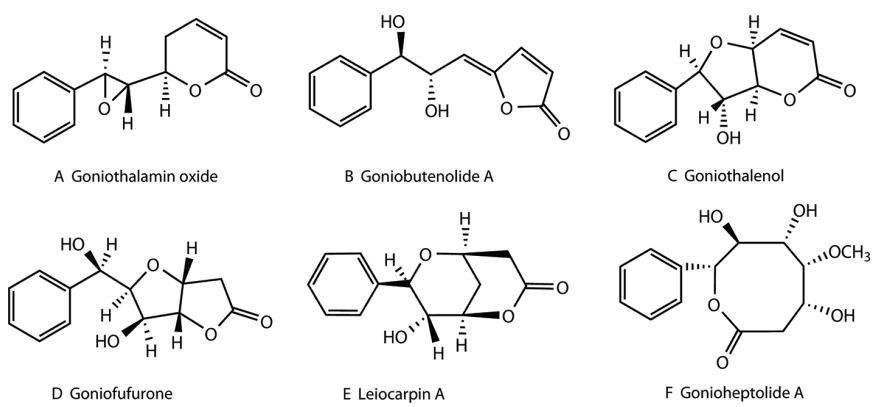

FIGURE 1 | Structures of different styryllactones. Styryllactones are classified based on different structural skeletons as follows: styrene -pyrone **(A)**, styrene -furanone **(B)**, furan -pyrone **(C)**, furan -furanone **(D)**, pyran -pyrone **(E)**, and heptyl esters **(F)**.

Eagle's medium (MEM), fetal bovine serum (FBS), and 0.25% trypsin–ethylenediaminetetraacetic acid (EDTA) were obtained from Life Technologies INC. (Grand Island, NY, USA). Trypan blue, penicillin, streptomycin, dimethyl sulfoxide (DMSO), VP-16 (Etoposide) and taxol were supplied by Sigma Chemical Co. (St. Louis, MO, USA). 3-(4,5-dimethylthiazol-2-yl)-2,5-diphenyl-tetrazolium bromide (MTT) was purchased from Molecular Probes Inc. (Eugene, OR, USA). Hydroxypopyl-β-cyclodextrin (HP-β-CD) was obtained from Nihon Shoukuhin Kako Co. Ltd. (Shibuya-ku, Tokyo, Japan). Phosphate buffer saline (PBS), annexin V fluorescein isothiocyanate (FITC)/propidium iodide (PI) Apoptosis Detection Kit, and caspase activity kit were purchased from Keygentec (Nanjing, Jiangsu, China). The water used in the experiments was obtained from the Milli-Q Water Purification System (MilliporeCorp., Billerica, MA, USA).

Single-Crystal X-Ray Analysis

Data for diffraction intensity was obtained using a Bruker APEX-IICCD X-ray diffractometer (Bruker AXSGmbH, Karlsruhe, Germany) and graphite-monochromated Cu Kα radiation (λ= 1.54178 Å). Cell refinement and data reduction were performed with Bruker SAINT (Bruker AXS, GmbH, Karlsruhe, Germany). The absorption correction was determined semi-empirically from equivalent compounds. The structures were determined *via* direct methods using SHELXS-97 (Institute of Inorganic Chemistry of Georg-August-Universität Göttingen, Gottingen, Germany). Non–hydrogen atoms were anisotropically refined with SHELXL-97 (Non–hydrogen atoms of leiocarpin B were anisotropically refined with SHELXL-2014). Hydrogen atoms were located by geometry and positioned on the related atoms during refinements, with a temperature factor.

Cell Culture and Assay

The human colon cancer SW1116 cell line, the human hepatocellular carcinoma SMMC-7721 cell line, the human gastric cancer SGC-7901 cell line, and the human hepatocellular carcinoma HepG2 cell line were kindly provided by Xiao-li Xu from the Cancer Center, Fudan University. The human embryonic kidney 293T (HEK293T) cell line was kindly donated by Professor You-hua Xie from Fudan University. These human cancer cell lines were cultured in DMEM medium or RPMI-1640 medium, whereas the HEK293T cell line was cultured in MEM medium. All of the cell lines were supplemented with 10% FBS, penicillin (100 U/ml), and streptomycin (100 mg/ml) under a humidified atmosphere of 5% CO_2 at 37°C using a CO_2 incubator (SANYO, Osaka, Japan). Cell count was assessed using the trypan blue dye exclusion method.

The antiproliferative effects of the treatments were evaluated using the MTT assay. Cells were seeded at a density of 5×10^3 cells/well in 96-well plates (Corning, NY, USA). After attachment, the culture media were replaced with various concentrations of chemicals for 24 h. Then, the media in 96-well plates were incubated with MTT reagent (5 mg/ml) for 4 h at 37°C. Subsequently, the culture medium was discarded and 100 μl of DMSO was added to each well, to solubilize the formazan crystal formed. The absorbance of formazan crystal solution was determined at 570 nm on a Multiskan FC from Thermo Fisher Scientific Inc. (Waltham, MA, USA).

Annexin V-FITC/PI Double Staining by Flow Cytometry

The growing cells were incubated in 24-well microplates (Corning, NY, USA) for 24 h. The cells were then treated with various concentrations of leiocarpin E-7′-monoacetate or taxol in humidified air with 5% CO_2 at 37°C. After 36 h of incubation, the culture medium was discarded, and the cells were collected. For the apoptosis analysis, cells were suspended with 1×binding buffer (1×10^6 cells/ml) and then labeled with annexin V-FITC/PI, as per the manufacturer's instructions (Keygentec, Nanjing, Jiangsu, China). The analysis of the samples was performed by flow cytometry (Becton-Dickinson Bioscience, San Jose, CA, USA), and the acquired data was analyzed by the CellQuest software (Becton-Dickinson Bioscience, San Jose, CA, USA).

Caspase Activity

To evaluate the activity of caspases, cell lysates were prepared after their respective designated treatments. The incubation of the growing cells was carried out in 24-well microplates (Corning, NY, USA) for 24 h. The cells were then treated with different concentrations of leiocarpin E-7′-monoacetate under humidified air with 5% CO_2 at 37°C. After 8 h of incubation, the culture medium was discarded, the cells collected and washed twice with PBS. The mixture was then centrifuged at 2,000 rpm for 5 min. The PBS supernatant was discarded and the cells (concentration, 5×10^6 cells) were collected. To these cells, ice-cold lysis buffer (150~200 μl) was added. The mixture was placed on ice for 30 min, and then centrifuged (10,000 rpm, 1 min) at 4° C. The supernatant, containing lysed protein, was carefully aspirated and transferred to a new tube. The protein concentration was then measured in 2 μl of the supernatant using the Bradford method. The caspase assays were then performed in 96-well microtiter plates (Keygentec, Nanjing, Jiangsu, China) by incubating 10 μl of protein cell lysate per sample in 80 μl of reaction buffer (1% NP-40, 20 mM Tris-HCl (pH 7.5), 137 mM NaCl, and 10% glycerol) containing 10 μl of caspase substrate (2 mM). Lysates were incubated at 37°C for 4 h. Measuremet was done at 405 nm on a Multiskan FC from Thermo Fisher Scientific Inc. (Waltham, MA, USA). The detailed analysis procedure is described in the manufacturer's protocol (Keygentec, Nanjing, Jiangsu, China).

Preparation of HP-β-CD Complex

A fixed quantity of the compound was weighed and evenly dispersed in an aqueous solution of HP-β-CD (molecular ratio of 1:2). The dispersion was equilibrated for 24 h at room temperature, under constant stirring. The supernatant was then lyophilized using a Christ Alpha1-2 Ld10 Freeze Dryer (Martin Christ Gefriertrocknungsanlagen GmbH, Osterode, Germany) to obtain the inclusion complex in a dry powder form. The content of styryllactones in the complex was determined using an ultraviolet (UV) spectrophotometer (Shimadzu, Kyoto, Japan). When the complexes were used in

the antitumor test, we first prepared a solution of the compound, and then performed full wavelength scanning. Subsequently, we selected the maximum absorption wavelength of the compound as the detection wavelength. A 20-mg quantity of the complex was accurately weighed and placed in a 10-ml volumetric flask. It was then dissolved in 0.1 mol/L hydrochloric acid-acetonitrile-water (1:1:2), and the volume was recorded. The absorbance was measured at the detection wavelength. We calculated the total amount of compound (W1) in the complex, according to the standard equation obtained with a compound solution prepared with 0.1 mol/L hydrochloric acid-acetonitrile-water (1:1:2). Another 20 mg of the same complex was accurately weighed, and dissolved in 0.1 mol/L hydrochloric acid-acetonitrile (1:1) and placed in an ultrasound machine for 10 min. Subsequently, it was filtered and the filtrate was used to measure the absorbance at the detection wavelength. We calculated the free compound content (W2), according to the standard equation obtained with a compound solution prepared with 0.1 mol/L hydrochloric acid-acetonitrile (1:1). The difference between W1 and W2 represented the quantity of the compound that formed HP-β-CD complex in a 20-mg inclusion compound sample.

Differential Scanning Calorimetry

The thermal characteristics of the raw material, HP-β-CD, the physical mixtures, and the complexes were determined using a differential scanning calorimeter (DSC; NETZSCH DSC system), equipped with a computerized data station (TA-50WS/PC, Selb, Bavaria, Germany). Samples were accurately weighed in a crimped aluminum pan and heated under an inert atmosphere of nitrogen. An empty pan sealed in the same manner, was used as a reference. The scanning rate was 10°C/min, and the scanning temperature ranged between 30°C and 400°C.

Statistical Analysis

All data were expressed as means ± standard error of the mean (SEM) and were analyzed using two-tailed Student's *t*-tests. Statistical analyses were performed using SPSS 16.0 (SPSS Inc., Chicago, IL, USA). A value of $p < 0.05$ was considered statistically significant.

RESULTS

Determination of the Absolute Configurations of Styryllactones

Single-crystal X-ray diffraction analysis, using Cu Kα radiation, was used to identify the absolute configurations of styryllactone compounds (**Figure 2**). Based on single-crystal X-ray diffraction, the structure of cheliensisin A was established as (2*R*,3*S*)-6-oxo-2-((2*S*,3*R*)-3-phenyloxiran-2-yl)-3,6-dihydro-2*H*-pyran-3-yl acetate, and the absolute configuration of cheliensisin A was defined as 5*S*, 6*S*, 7*S*, 8*R*. The structure of leiocarpin B was established as (*S*)-5-hydroxy-7-((1*R*,2*R*)-2-hydroxy-2-((*R*)-6-oxo-3,6-dihydro-2*H*-pyran-2-yl)-1-phenylethoxy)-2-phenylchroman-4-one, and the absolute configuration of leiocarpin B was defined as 2′*S*, 6*R*, 7*S*, 8*R*. The structure of leiocarpin E was established as (*R*)-6-((*R*)-hydroxy((1*S*,3*S*,4*S*)-3-((*R*)-6-oxo-3,6-dihydro-2*H*-pyran-2-yl)-4-phenylisochroman-1-yl)methyl)-5,6-dihydro-2*H*-pyran-2-one, and the absolute configuration of leiocarpa E was defined as 6*R*, 6′*R*, 7*S*, 7′S, 8*S*, 8′*S*. Both goniodiol and goniodiol-7-monoacetate were identified as 6*R*, 7*R*, 8*R*. The structure of goniodiol was established as (*R*)-6-((1*R*,2*R*)-1,2-dihydroxy-2-phenylethyl)-5,6-dihydro-2*H*-pyran-2-one. The absolute configuration of leiocarpin E-7′-monoacetate, which is the acetate of leiocarpin E, was consistent with that of leiocarpin E.

The crystal data of cheliensisin A ($C_{15}H_{14}O_5$) were as follows (detailed parameter shown in **Supplementary Table 1**): molecular weight (MW) = 274.26; orthorhombic, space group $P2_12_12_1$; a = 7.0297 (10) Å, b = 11.0918 (10) Å, c = 17.5287 (3) Å; α= 90°, β= 90°, γ= 90°; V = 1366.75 (3) Å^3, T = 123 (2) K; Z = 4; D_{calc} = 1.333 g·cm^{-3}; index range: $-8 \le h \le 8$, $-13 \le k \le 13$, $-18 \le l \le 20$; absorption coefficient = 0.842 mm^{-1}; completeness: 99.9%; *F*(0 0 0) = 576; GOF (goodness of fit) = 1.068. A colorless prismatic crystal with approximate dimensions of 0.21 mm × 0.15 mm × 0.14 mm was chosen and mounted on a Bruker APEX-II CCD diffractometer. The θ range for data collection was 4.72°–67.48°. A total of 8,080 reflections were collected, of which 2,435 were unique (*R*(int) = 0.0300) and 2,418 were considered observed ($I > 2\sigma(I)$). The maximum and minimum transmissions were 0.7456 and 0.3475. The refinement method was full-matrix least squares on F2. Data/restraints/parameters were 2435/0/183. The final *R* values were R_1 = 0.0272 and wR_2 = 0.0670 for 2,418 observed reflections, and R_1 = 0.0274 and wR_2 = 0.0673 for all observations. A full list of crystallographic data was deposited at the Cambridge Crystallographic Data Center, CCDC 1007949.

The crystal data of leiocarpin B ($C_{28}H_{24}O_7$) were as follows (detailed parameter shown in **Supplementary Table 2**): MW= 472.47; monoclinic, space group *C*2; a = 21.0501 (4) Å, b = 7.9013 (10) Å, c = 16.4209 (3) Å; α = 90°, β = 121.2160 (10)°, γ = 90°; V = 2335.75 (7) Å^3, T = 140 (2) K; Z = 4; D_{calc} = 1.344 g·cm^{-3}; index range: $-25 \le h \le 25$, $-9 \le k \le 9$, $-19 \le l \le 19$; absorption coefficient = 0.798 mm^{-1}; completeness: 98.2%; *F*(0 0 0) = 992; GOF (goodness of fit) = 1.079. A colorless block crystal, with approximate dimensions of 0.35 mm × 0.26 mm × 0.20 mm, was chosen and mounted on a Bruker APEX-II CCD diffractometer. The θ range for data collection was 3.15°–69.15°. A total of 6,301 reflections were collected, of which 3,373 were unique (*R*(int) = 0.0432) and 3,343 were considered observed ($I > 2\sigma(I)$). The maximum and minimum transmissions were 0.7532 and 0.4386. The refinement method was full-matrix least squares on F2. Data/restraints/parameters were 3373/1/319. The final *R* values were R_1 = 0.0419 and wR_2 = 0.1082 for 3,343 observed reflections, and R_1 = 0.0421 and wR_2 = 0.1089 for all observations. A full list of crystallographic data was deposited at the Cambridge Crystallographic Data Center, CCDC 1008036.

The crystal data of leiocarpin E ($C_{26}H_{24}O_6$) were as follows (detailed parameter shown in **Supplementary Table 3**): MW= 432.45; orthorhombic, space group $P2_12_12_1$; a = 9.7380 (10) Å, b = 11.1611 (2) Å, c = 20.3823 (3) Å; α = 90°, β = 90°, γ = 90°; V = 2215.29 (6) Å^3, T = 123 (2) K; Z = 4; D_{calc} = 1.297 g·cm^{-3}; index

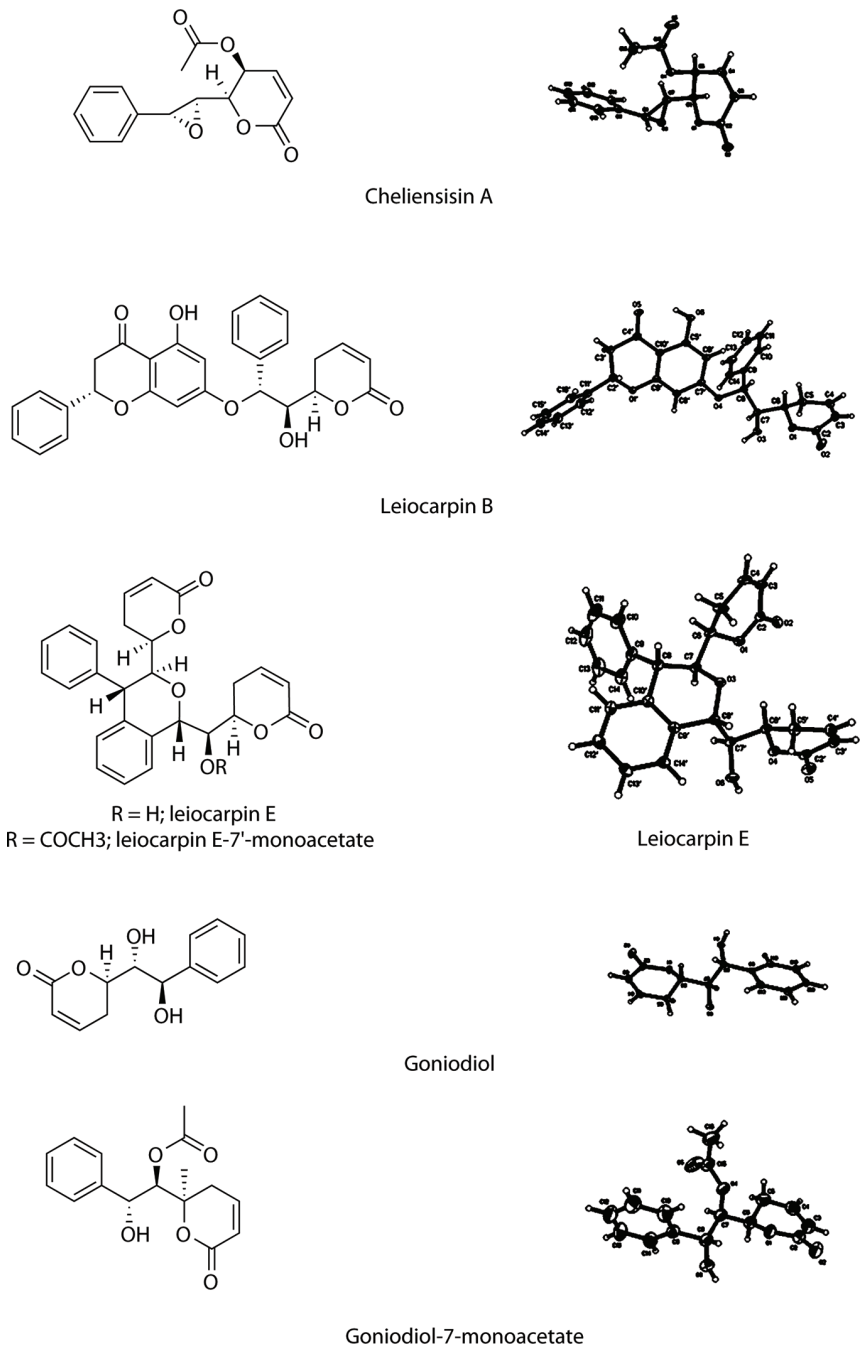

FIGURE 2 | Structure and X-ray crystallography of the styryllactones.

range: $-11 \leq h \leq 11$, $-13 \leq k \leq 13$, $-24 \leq l \leq 24$; absorption coefficient = 0.754 mm^{-1}; completeness: 99.5%; $F(0\ 0\ 0) = 912$; GOF (goodness of fit) = 1.058. A colorless prismatic crystal, with approximate dimensions of 0.19 mm × 0.15 mm × 0.12 mm, was chosen and mounted on a Bruker APEX-II CCD diffractometer. The θ range for data collection was 4.34°–65.50°. A total of 12,242 reflections were collected, of which 3,746 were unique (R (int) = 0.0432) and 3,700 were considered observed ($I > 2\sigma(I)$). The maximum and minimum transmissions were 0.9129 and 0.8706. The refinement method was full-matrix least squares on F2. Data/restraints/parameters were 3746/0/291. The final R values were $R_1 = 0.0426$ and $wR_2 = 0.1191$ for 3,700 observed

reflections, and R_1 = 0.0430 and wR_2 = 0.1195 for all observations. A full list of crystallographic data was deposited at the Cambridge Crystallographic Data Center, CCDC 1007951.

The crystal data of goniodiol ($C_{13}H_{14}O_4$) were as follows (detailed parameter shown in **Supplementary Table 4**): MW = 234.24; orthorhombic, space group $P2_12_12_1$; a = 9.2443 (2) Å, b = 9.7650 (2) Å, c = 13.0267 (3) Å; α = 90°, β = 90°, γ = 90°; V = 1175.93 (4) Å^3; T = 140 (2) K; Z = 4; D_{calc} = 1.323 g·cm^{-3}; index ranges: $-10 \leq h \leq 10$, $-10 \leq k \leq 11$, $-14 \leq l \leq 15$; absorption coefficient = 0.814 mm^{-1}; completeness: 98.1%; F(0 0 0) = 496; GOF (goodness of fit) = 1.141. A colorless block crystal, with approximate dimensions of 0.35 mm × 0.26 mm × 0.22 mm, was chosen and mounted on a Bruker APEX-II CCD diffractometer. The θ range for data collection was 5.66°–69.43°. A total of 5,322 reflections were collected, of which 2,070 were unique (R(int) = 0.0369) and 2,058 were considered observed ($I > 2\sigma(I)$). The maximum and minimum transmissions were 0.7532 and 0.5891. The refinement method was full-matrix least squares on F2. Data/restraints/parameters were 2070/0/157. The final R values were R_1 = 0.0404 and wR_2 = 0.1007 for 2,058 observed reflections, and R_1 = 0.0405 and wR_2 = 0.1008 for all observations. A full list of crystallographic data was deposited at the Cambridge Crystallographic Data Center, CCDC 1008511.

The crystal data of goniodiol-7-monoacetate ($C_{15}H_{16}O_5$) were as follows (detailed parameter shown in **Supplementary Table 5**): MW= 276.28; triclinic, space group $P1$; a = 5.4547 (5) Å, b = 8.8394 (7) Å, c = 15.3120 (13) Å; α = 94.379 (6)°, β = 91.949 (5)°, γ= 105.106 (6)°; V = 709.58 (11) Å^3; T = 296 (2) K; Z = 2; D_{calc} = 1.293 g·cm^{-3}; index ranges: $-6 \leq h \leq 6$, $-10 \leq k \leq 10$, $-18 \leq l \leq 15$; absorption coefficient = 0.811 mm^{-1}; completeness: 94.0%; F(0 0 0) = 292; GOF (goodness of fit) = 1.042. A colorless block crystal, with approximate dimensions of 0.2 mm × 0.12 mm × 0.05 mm, was chosen and mounted on a Bruker APEX-II CCD diffractometer. The θ range for data collection was 2.90°–69.66°. In total, 5,692 reflections were collected, of which 3,307 were unique (R(int) = 0.0419) and 3,046 were considered observed ($I > 2\sigma(I)$). The maximum and minimum transmissions were 0.7532 and 0.4727. The refinement method was full-matrix least squares on F2. Data/restraints/parameters were 3307/3/365. The final R values were R_1 = 0.0468 and wR_2 = 0.1251 for 3,046 observed reflections, and R_1 = 0.0505 and wR_2 = 0.1309 for all observations. A full list of crystallographic data was deposited at the Cambridge Crystallographic Data Center, CCDC 1442700.

Styryllactones Inhibit the Proliferation of Tumor Cell Lines

The *in vitro* cytotoxic activity of styryllactones was evaluated in four human tumor cell lines by the MTT assay (**Figure 3**). VP-16 was chosen as the positive control, because it is one of the most widely used cancer chemotherapy agents to treat many kinds of cancers, and it could induce apoptosis of cancer cells by acting as a toposiomerase II inhibitor (Berger et al., 1996; Chiu et al., 2005). The results showed that cheliensisin A, goniodiol and goniodiol-7-monoacetate had no cytotoxic effect on the SGC-7901, SMMC-7721 and HepG2 cell lines since the IC_{50} of these compounds were greater than 100 μM. In contrast, leiocarpin B, leiocarpin E, and leiocarpin E-7′-monoacetate showed excellent cytotoxicity against the SW1116 cell line, when their concentrations were 30 μM, the cell viability of SW1116 cells was significantly less ($p < 0.01$) than the normal group (cell viability in 0 μM). The highest cytotoxic effect against SW1116

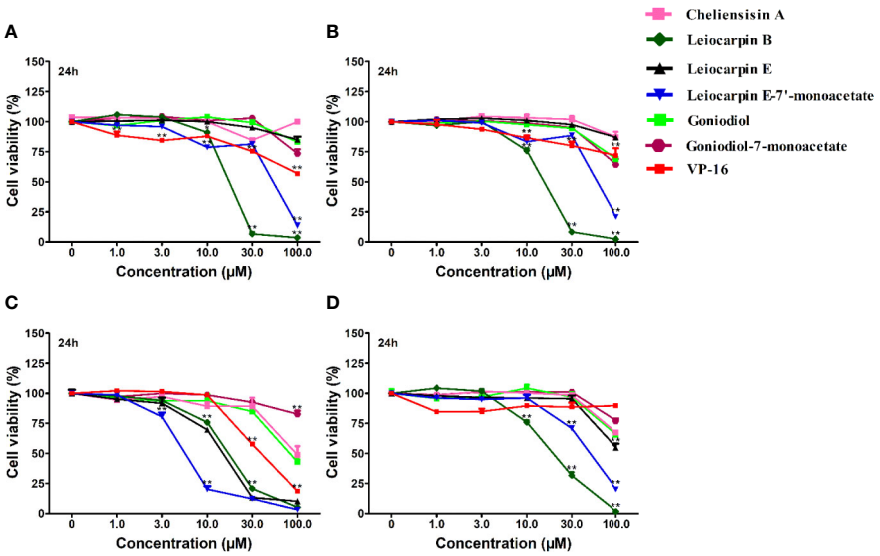

FIGURE 3 | Styryllactones inhibited proliferation of tumor cell lines. The cells (5×10^4 cells/ml) were cultured in the absence or presence of various compounds (1.0, 3.0, 10.0, 30.0, 100.0 μM) for 24 h. VP-16 (1.0, 3.0, 10.0, 30.0, 100.0 μM) were used as a positive control. **(A)** SGC-7901 cell line; **(B)** SMMC-7721 cell line; **(C)** SW1116 cell line; **(D)** HepG2 cell line. Data are means ± standard error of the mean (SEM) (n=3). Results are representative of three separate experiments. *P<0.05, **P<0.01 compared with the group (cell viability in 0 μM).

cells was demonstrated by leiocarpin E-7′-monoacetate, while cheliensisin A and goniodiol-7-monoacetate showed relatively lower inhibitory effect (**Table 1**). Thus, it was concluded that the human colon cancer SW1116 cell line was much more sensitive to the cytotoxic effect of styryllactones.

Cytotoxic Effect of Styryllactones Against the Human Normal Cell Line HEK293T

The human embryonic kidney 293T (HEK293T) cell line is used as a normal human cell line in various biological experiments (Chen et al., 2016; Vemuri et al., 2019). In this study, we investigated the *in vitro* cytotoxic effect of styryllactones (concentration ranging from 0 and 100 μM) against HEK293T cells (**Figure 4**). The results showed that the IC_{50} values of all the compounds against HEK293T cells were above 100 μM (**Table 1**). This indicated that styryllactones did not show cytotoxicity against normal human cell line.

Leiocarpin E-7′-Monoacetate Induces the Early Apoptosis of SW1116 Cells

In the *in vitro* cytotoxicity experiments, SW1116 cells were found to be sensitive to leiocarpin E-7′-monoacetate. To further evaluate the apoptotic activity of leiocarpin E-7′-monoacetate, the cells were treated with various concentrations of leiocarpin E-7′-monoacetate and then analyzed by flow cytometry. Taxol was chosen as the positive control, because it could stabilize microtubules, and subsequently cause cell apoptosis by arresting the cell cycle at G2/M (Ruden and Puri, 2013; Luo et al., 2015). The results showed that the early apoptosis rates were 2.6%, 21.8%, and 55.2% when the concentration of leiocarpin E-7′-monoacetate was 3, 10, and 30 μM, respectively (**Figure 5**). In summary, the results indicated that leiocarpin E-7'-monoacetate was able to induce the apoptosis of SW1116 cells in a concentration-dependent manner.

Leiocarpin E-7′-Monoacetate-Induced Apoptosis is Caspase-Dependent

To further examine the cytotoxicity induced by leiocarpin E-7′-monoacetate, the activity of the apoptosis-associated protease was studied, using an enzyme activity assay kit. The results showed that different kinds of caspase proteases were activated as the concentration of leiocarpin E-7′-monoacetate was increased (**Figure 6**). When the concentration was 3 μM, the ration of

TABLE 1 | Styryllactones inhibited proliferation of cell lines.

	IC_{50} (μM)				
	SGC-7901	**SMMC-7721**	**SW1116**	**HepG2**	**HEK293T**
Cheliensisin A	>100	>100	93.18 ± 0.78	>100	>100
Leiocarpin B	18.21 ± 0.88	15.45 ± 1.11	17.50 ± 0.69	19.34 ± 1.42	>100
Leiocarpin E	>100	>100	15.11 ± 1.87	>100	>100
Leiocarpin E-7′-monoacetate	45.03 ± 4.27	61.71 ± 10.14	6.73 ± 0.89	50.11 ± 3.25	>100
Goniodiol	>100	>100	80.05 ± 4.16	>100	>100
Goniodiol-7-monoacetate	>100	>100	>100	>100	>100
VP-16	*>100*	*>100*	*41.87 ± 0.98*	*>100*	*>100*

Data are means ± SEM (n=3). Results are representative of three separate experiments.

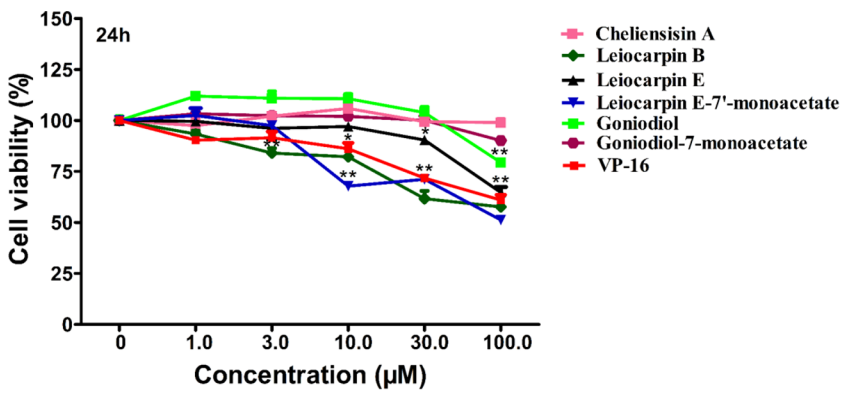

FIGURE 4 | Cytotoxic effect of styryllactones against the human normal cell line human embryonic kidney 293T (HEK293T). The cells (5×10^4 cells/ml) were cultured in the absence or presence of styryllactone compounds (1.0, 3.0, 10.0, 30.0, 100.0 μM) for 24 h. VP-16 (1.0, 3.0, 10.0, 30.0, 100.0 μM) were used as a positive control. Data are means ± standard error of the mean (SEM) (*n*=3). Results are representative of three separate experiments. $^*P < 0.05$, $^{**}P < 0.01$ compared with the group (cell viability in 0 μM).

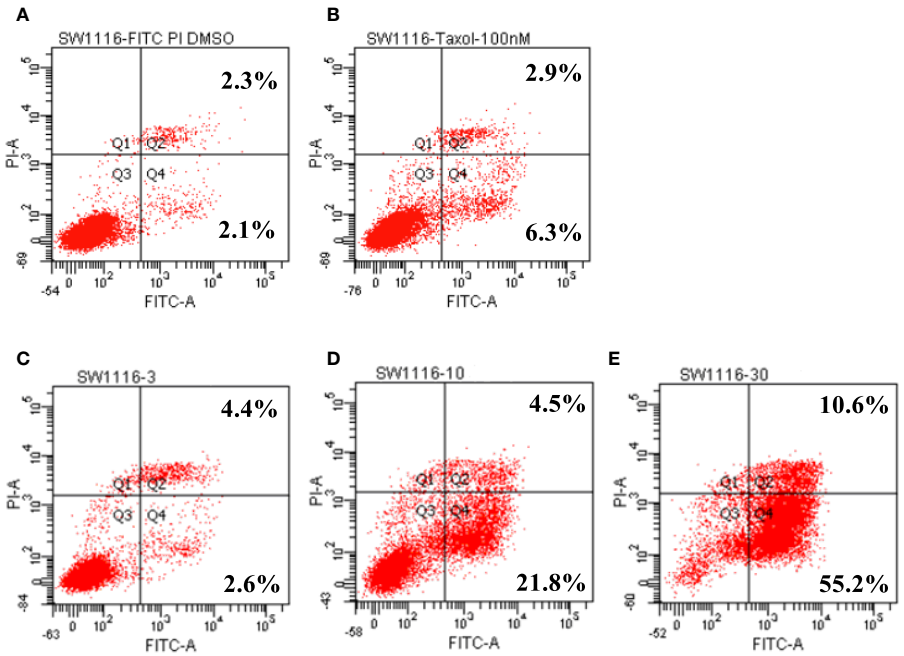

FIGURE 5 | Leiocarpin E-7′-monoacetate induced early apoptosis. The annexin V fluorescein isothiocyanate (FITC)/propidium iodide (PI) staining assay was analyzed by flow cytometry. SW 1116 cells were cultured with chemicals for 36 h: **(A)** vehicle; **(B)** Taxol (100 nM); **(C)** leiocarpin E-7′-monoacetate (3 μM); **(D)** leiocarpin E-7′-monoacetate (10 μM); **(E)** leiocarpin E-7′-monoacetate (30 μM).

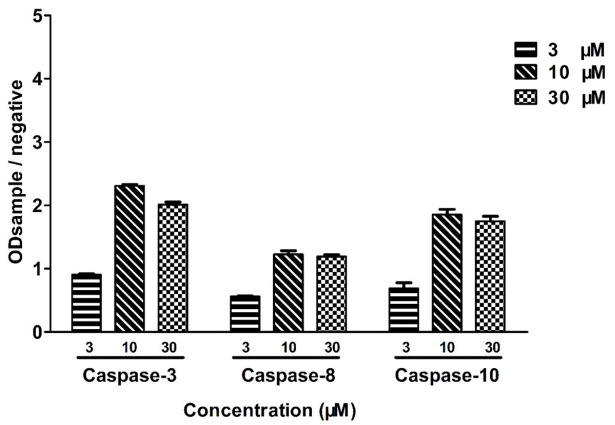

FIGURE 6 | Leiocarpin E-7′-monoacetate induced-apoptosis was caspase-dependent. SW1116 cells were treated with leiocarpin E-7′-monoacetate (3, 10, and 30 μM) for 8 h. Data are presented as means ± SEM (*n*=3).

OD_{sample} to $OD_{negative}$ was not greater than 1, as it indicated that the caspase enzymes were not activated. However, when the concentration was increased to 10 and 30 μM, the ration was greater than 1, as it demonstrated that the activation of caspase enzymes increased significantly.

Identification of Complexes by Differential Scanning Calorimetry

In the cytotoxicity experiments, cheliensisin A and gonidiol-7-monoacetate showed no effects on tumor growth. This could be attributed to the poor water solubility of these compounds. To improve the solubility, the styryllactones HP-β-CD complexes were synthesized *via* the saturated aqueous solution method. A DSC analysis was then carried out for HP-β-CD, styryllactone, a styryllactone/HP-β-CD physical mixture, and the styryllactone/HP-β-CD complex (**Figure 7**).

The raw cheliensisin A (**Figure 7A**) had a sharp endothermic peak and a sharp exothermic peak near 150°C and 300°C, respectively. HP-β-CD had a broad endotherm near 350°C, which was also present in the mixture. However, in the spectrum of the complex, the characteristic peak of cheliensisin A disappeared. This indicated that the compound penetrated into the cyclodextrin cavity and replaced the water molecules.

The raw goniodiol-7-monostearate monomer (**Figure 7B**) had a sharp endothermic peak at 150°C, which were also present in the mixture. The DSC curves of the complex showed that the characteristic peaks of the goniodiol-7-monostearate monomer disappeared, which confirmed the formation of the styryllactone complex with HP-β-CD.

Increased Cytotoxicity Activity of the Complex

To examine whether complexation of styryllactone with HP-β-CD resulted in an enhancement of antitumor activity against

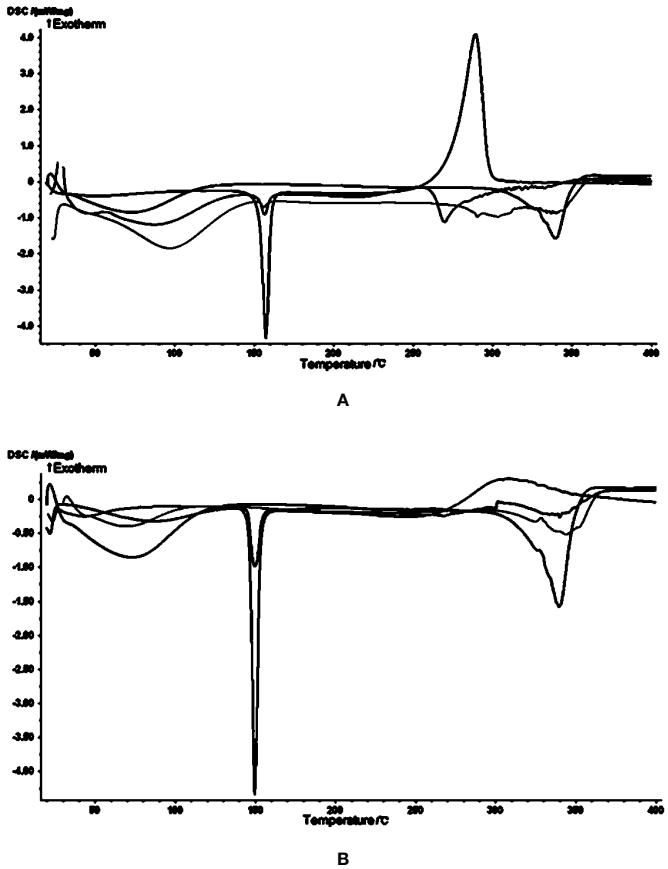

FIGURE 7 | Images from the differential scanning calorimetry (DSC) analysis. Green line: hydroxypropyl-β-cyclodextrin (HP-β-CD); blue line: styryllactone only; brown line: physical mixture; pink line: complexes of HP-β-CD with **(A)** cheliensisin A and **(B)** gonidiol-7-monoacetate.

different human cell lines, cytotoxicity experiments were evaluated in SMMC-7721 and SW1116 cell lines, using the MTT assay (**Figure 8**).

The results showed that the styryllactone/HP-β-CD complexes were significantly more cytotoxic than their respective pristine form ($P < 0.01$), while HP-β-CD did not show any inhibition of the growth of the two cell lines (**Table 2**). The IC_{50} of cheliensisin A and goniodiol-7-monoacetate were reduced by 45% and 55%, respectively against the SW1116 cell line. Similarly, the IC_{50} values of the two compounds were reduced by 58% and 34%, respectively against the SMMC-7721 cell line.

Cytotoxicity Activity Against HEK293T Cells is Increased by the Complex

Based on the results, it was observed that the complexes demonstrated enhanced cytotoxic effect against tumer cell lines, when compared with the styryllactone compounds. To study whether there is obviously enhanced cytotoxicity of complex in normal cell lines, the human normal cell line HEK293T was treated with styryllactone HP-β-CD complexes.

Figure 9 suggested that the complexes showed significantly higher cytotoxic activity than the compounds against HEK293T cell line ($P < 0.01$). For example, the IC_{50} of cheliensisin A complex and goniodiol-7-monoacetate complex were 98.46 ± 3.00 and 35.02 ± 0.63 μM, respectively (**Table 2**). When the cells were treated with the pristine forms of cheliensisin A and goniodiol-7-monoacetate, the IC_{50} values obtained were beyond 200 μM. In addition, HP-β-CD did not show any inhibitory activity against the HEK293T cell line (**Figure 9**).

DISCUSSION

Styryllactones are a series of secondary metabolites isolated from the genus *Goniothalamus*, which generally contains 1 benzene ring and 1 unsaturated lactone ring (Bermejo et al., 1997; Bermejo et al., 1998; Cao et al., 1998; Bermejo et al., 1999; Hu et al., 1999; Mu et al., 1999a; Peris et al., 2000; Lan et al., 2005; Liou et al., 2014). In our previous work, styryllactone compounds were isolated from *Goniothalamus griffithii* (Annonaceae) and

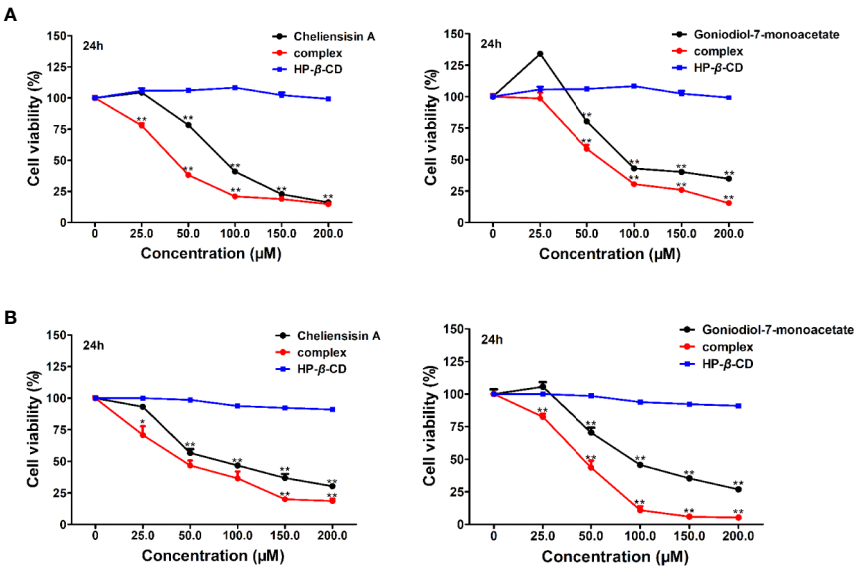

FIGURE 8 | Cytotoxic activity was enhanced by hydroxypropyl-β-cyclodextrin (HP-β-CD) complexes of styryllactones. SMMC-7721 cells **(A)** and SW1116 cells **(B)** (5×10^4 cells/ml) were cultured respectively in the absence or presence of various compounds and complexes (25.0, 50.0, 100.0, 150.0, 200.0 μM) for 24 h: cheliensisin A, cheliensisin A/HP-β-CD complex and HP-β-CD; gonidiol-7-monoacetate, goniodiol-7-monoacetate/HP-β-CD complex and HP-β-CD. Data are means ± SEM (*n*=3). Results are representative of three separate experiments. *P<0.05, **P<0.01 compared with the group (cell viability in 0 μM).

TABLE 2 | Cytotoxic activity of styryllactones increased after complexation with Hydroxypopyl-β-cyclodextrin (HP-β-CD).

	IC_{50} (μM)					
	SW1116		SMMC-7721		HEK293T	
	Compound	Complex	Compound	Complex	Compound	Complex
Cheliensisin A	93.18 ± 0.78	51.44 ± 4.78**	110.90 ± 2.41	46.91 ± 1.60**	>200	98.46 ± 3.00**
Goniodiol-7-monoacetate	102.14 ± 4.15	46.48 ± 3.25**	115.54 ± 3.97	75.76 ± 4.19**	>200	35.02 ± 0.63**

*Data are means ± SEM (n=3). Results are representative of three separate experiments. **P < 0.01 compared with the compound group.*

Goniothalamus leiocarpus (Annonaceae) (Mu et al., 1996; Li et al., 1997; Li et al., 1998; Mu et al., 1998; Mu et al., 1999a; Mu et al., 1999b; Mu et al., 2002; Mu et al., 2003; Mu et al., 2004), and the absolute configuration of leiocarpin B was determined by Mosher ester method (Mu et al., 2002). In this paper, the absolute configuration of five styryllactone compounds were determined by single-crystal X-ray diffraction analysis, using Cu Kα radiation.

Studies have shown that a number of styryllactones demonstrated cytotoxicity against various human cancer cell lines. For example, 7-acetylaltholactone had cytotoxicity against KB (oral epidermoid carcinoma cell line), HepG2 (liver cancer), and MCF7 (breast carcinoma) cell lines with IC_{50} values of 13.1, 23.7, and 60.2 μM, respectively (Trieu et al., 2014). Goniothalamin could inhibit the growth of RT4 cell line (urinary bladder) (Yen et al., 2014), HL-60 cell line (leukemia) (Ali et al., 1997), HGC-27 cell line (colon gastric) (Ali et al., 1997), HT-29 cell line (colon gastric) (Vendramini-Costa et al., 2016). Among the researches, cytotoxicity and apoptosis were induced (Ali et al., 1997; Yen et al., 2014; Vendramini-Costa et al., 2016), and caspase-3, -8 and -9 activation also occurred, suggesting caspase-dependent apoptotic pathway by other styryllactone compounds (Vendramini-Costa et al., 2016). However, the cytotoxicity and mechanism of the styryllactone compounds, first isolated in our laboratory, have not been studied in SMMC-7721, HepG2, SW1116 and SGC-7901 cell lines. Besides, SMMC-7721 cells (Kim, 2009), HepG2 cells (Li et al., 2019), SW1116 cells (Gu et al., 2018) and SGC-7901 (Wang et al., 2018) were all reported to be studied in apoptosis-induced research *via* activaing caspase proteas, indicating that they were able to be used in our mechanism research. As a result, to evaluate whether the styryllactones isolated could resulte in cytotoxicity and apoptosis *via* caspase-3, -8 and -9

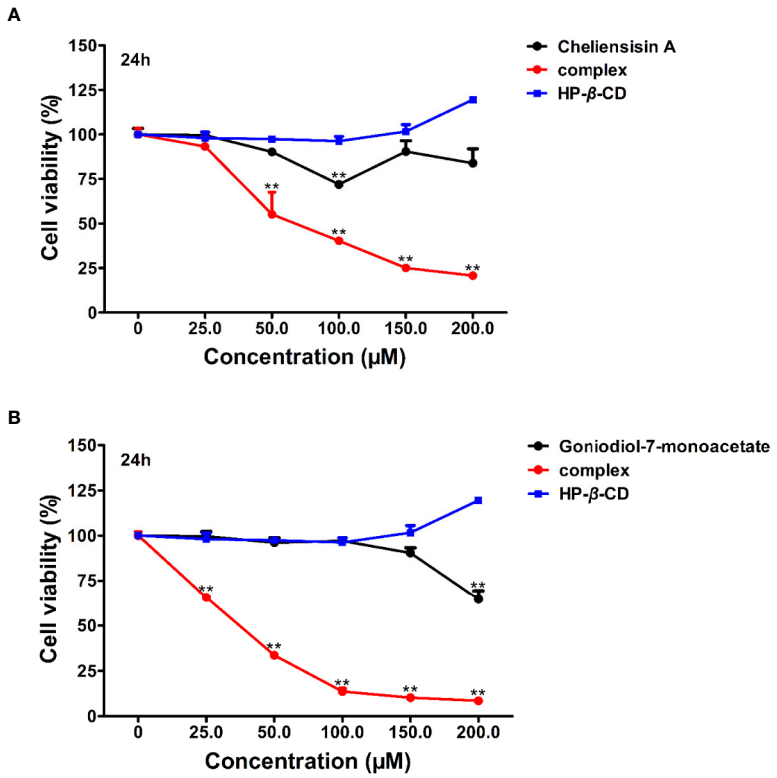

FIGURE 9 | Cytotoxic activity of hydroxypropyl-β-cyclodextrin (HP-β-CD) complexes of styryllactones was increased against human embryonic kidney 293T (HEK293T) cells. The cells (5×10^4 cells/ml) were cultured respectively in the absence or presence of various compounds and complexes (25.0, 50.0, 100.0, 150.0, 200.0 μM) for 24 h: **(A)** cheliensisin A, cheliensisin A/HP-β-CD complex and HP-β-CD; **(B)** gonidiol-7-monoacetate, goniodiol-7-monoacetate/HP-β-CD complex and HP-β-CD. Data are means ± SEM (*n*=3). Results are representative of three separate experiments. $^{**}P<0.01$ compared with the group (cell viability in 0 μM).

activation, these four human cell lines were choosen in our research.

It was found that leiocarpin B, leiocarpin E, and leiocarpin E-7'-monoacetate had significant cytotoxic activities against human colon cancer SW1116 cell line. Further, the results of Annexin V-FITC/PI double staining showed that leiocarpin E-7'-monoacetate induced apoptosis of SW1116 cells in a concentration-dependent manner (**Figure 5**).

In mammalian cells, there are two major apoptotic pathways: the first one involves a signal from the mitochondria, while the second relies on signal transduction through death receptors. Studies have shown that caspase-8 is activated through a death receptor-mediated pathway and cleavage of caspase-9 plays a key role in mitochondria apoptotic pathway. Caspase-3 is the key executive molecule of the apoptotic signal (Dodson et al., 2013; Vendramini-Costa et al., 2016). We observed the occurrence of apoptosis at the cellular level. Subsequently, we investigated whether the activity of caspase enzymes was affected owing to the intervention of leocarpin E-7'-monoacetate at the enzyme level. It was observed that caspase-3, -8 and -9 showed activation at different concentrations of leocarpin E-7'-monoacetate (**Figure 6**). When the concentration of leocarpin E-7'-monoacetate was 3 μM, in the caspase activity test the ration of OD_{sample} to $OD_{negative}$ was not greater than 1, while the apoptosis rate is low. When the concentration was increase to 10 and 30 μM, the apoptosis rate also increased.

However, cheliensisin A, goniodiol, and goniodiol-7-monoacetate showed poor *in vitro* activity. The application of styryllactones as antitumor agent has been strongly impeded owing to their poor water solubility (Zhao et al., 2008; Deng et al., 2011). In a study by Zhao et al, the solubility of cheliensisin A was improved by formulating it as a lyophilized submicron emulsion intravenous injection (Zhao et al., 2008). However, the process is complicated and expensive. In this study, we prepared inclusion complexes of styryllactones using HP-β-CD and evaluated the cytotoxic activity of the complex.

HP-β-CD is commonly used to enhance the water solubility of poorly soluble compounds. It contains a hydrophilic exterior surface and a nonpolar interior cavity. This structure allows HP-β-CD to act as a carrier that can encapsulate a poorly water-soluble compound in the internal area, thereby increasing the solubility of the compound (Kaur et al., 2014; Wang et al.,

2014a). In the pharmaceutical industry, HP-β-CD is used to increase drug stability, improve bioavailability, and reduce side effects owing to its low surface activity, low hemolytic activity, and lack of muscle irritation. Thus, it is widely used as an injection solubilizer and pharmaceutical excipient (Kryjewski et al., 2015).

Differential Scanning Calorimetry (DSC) is a suitable thermal analysis technique used in the pharmaceutical industry for determining the purity, polymorphic forms, and melting point of a sample (Demetzos, 2008). In addition, DSC can provide detailed information about both the physical and energetic properties of a substance (Green et al., 2020). The results showed that apart from the characteristic peaks of styryllactones and HP-β-CD, no other endothermic or exothermic peak was observed (**Figure 7**). In addition, cyclodextrin is a cyclic oligosaccharide composed of covalently-linked glucopyranose rings, which can assist in increasing the solubility of hydrophobic drugs by forming water-soluble inclusions (Brewster and Loftsson, 2007). HP-β-CD is a chemically modified derivate of cyclodextrin that has a higher solubility in water and can be safely used as a complexing and solubilizing excipient in various drug administration routes (Peeters et al., 2002). For example, Al- Qubaisi et al. developed an inclusion complex of thymoquinone and HP-β-CD in order to improve solubility and bioactivity of thymoquinone. In their work, they proved that the entire thymoquinone molecule was entrapped in the HP-β-CD cavity and that the molecule was not degraded by the complexation (Al-Qubaisi et al., 2019). As a result, we demonstrated that the cyclodextrin complexation did not degrade the molecular structure.

It was observed that the antitumor effect of styryllactones complexed with HP-β-CD was significantly enhanced. From the experiments, the IC_{50} of the cheliensisin A complex was 51.44 ± 4.78 μM and 46.91 ± 1.60 μM against SW1116 cells and SMMC-7721 cells, respectively. The IC_{50} of goniodiol-7-monoacetate complex was 46.48 ± 3.25 μM and 75.76 ± 4.19 μM, whereas the IC_{50} of the cheliensisin A monomer was 93.18 ± 0.78 μM and 110.90 ± 2.41 μM against SW1116 cells and SMMC-7721 cells, respectively. The IC_{50} of the goniodiol-7-monoacetate monomer was 102.14 ± 4.15 μM and 115.54 ± 3.97 μM, respectively (**Table 2**). HP-β-CD had no inhibitory effect on the growth of the two cell lines (**Figure 8**). The cytotoxicity of styryllactones and their complex was also evaluated in the human normal cell line HEK293T. It was observed that the HP-β-CD complexes showed greater cytotoxic activity than the styryllactone compounds against HEK293T cell line. This suggested that the complexes could also inhibit the growth of normal cell line. The IC_{50} of cheliensisin A complex and goniodiol-7-monoacetate complex were 98.46 ± 3.00 and 35.02 ± 0.63 μM, respectively (**Table 2**). Thus, there was a dose safety window when cheliensisin A complexes were treated against SW1116 cell line or SMMC-7721 cell line. In addition, there was a dose safety window when goniodiol-7-monoacetate complexes were treated against SW1116 cell line. However, the dose safety window was narrower when goniodiol-7-monoacetate complexes were treated against SMMC-7721 cell line. In this study, we focused on investigation of the method to enhance the cytotoxicity activity of styryllactones. HP-β-CD is known to increase the solubility of poorly water-soluble compounds (Kaur et al., 2014; Wang et al., 2014a). Thus, it was assumed that the enhanced antitumor effects of the complexes were partly because of the improved water solubility. The results from this study show that styryllactones have the potential to be developed as antitumor compounds. Next, we plan to obtain enough compounds, either by extraction from plants or chemical synthesis and then explore better compound structures based on these styryllactones. Their HP-β-CD complex will be developed and cytotoxicity will be studied. Subsequently, we intend to investigate the anticancer effect in the animal model using the styryllactones inclusion complex, and conduct efficient test methods including radiolabeling test and permeability test, to illustrate the exact mechanism underlying the improved potency of complexes toward tumor cell lines.

This paper described the identification of the absolute configurations of several styryllactones by single-crystal X-ray diffraction analysis using Cu Kα radiation. We synthesized styryllactones complexes with HP-β-CD for the first time. The *in vitro* antitumor experiments showed that the inhibitory activity of these complexes was greater than the respective pristine form of the compounds. These results suggest that the water solubility of styryllactones can be improved by complexation of styryllactones with HP-β-CD, which in turn, can enhance the antitumor activity of these compounds.

DATA AVAILABILITY STATEMENT

All datasets generated for this study are included in the article/ **Supplementary Material**.

AUTHOR CONTRIBUTIONS

RM and QM contributed to the conception and design of the study. RM performed the experiments and wrote the first draft of the manuscript. J-TC assisted in the performance of experiments. X-LX donated the cells in the research. QM and X-YJ revised the manuscript. QM gave final approval of the version to be submitted. All authors read and approved the final manuscript.

SUPPLEMENTARY MATERIAL

The Supplementary Material for this article can be found online at: https://www.frontiersin.org/articles/10.3389/fphar.2020.00484/full#supplementary-material

REFERENCES

Ali, A. M., Mackeen, M. M., Hamid, M., Aun, Q. B., Zauyah, Y., Azimahtol, H. L., et al. (1997). Cytotoxicity and electron microscopy of cell death induced by goniothalamin. *Planta Med.* 63, 81–83. doi: 10.1055/s-2006-957611

Al-Qubaisi, M. S., Rasedee, A., Flaifel, M. H., Eid, E. E. M., Hussein-Al-Ali, S., Alhassan, F. H., et al. (2019). Characterization of thymoquinone/hydroxypropyl-beta-cyclodextrin inclusion complex: Application to anti-allergy properties. *Eur. J. Pharm. Sci.* 133, 167–182. doi: 10.1016/j.ejps.2019.03.015

Altobelli, E., Lattanzi, A., Paduano, R., Varassi, G., and Di Orio, F. (2014). Colorectal cancer prevention in Europe: burden of disease and status of screening programs. *Prev. Med.* 62, 132–141. doi: 10.1016/j.ypmed.2014.02.010

Berger, J. M., Gamblin, S. J., Harrison, S. C., and Wang, J. C. (1996). Structure and mechanism of DNA topoisomerase II. *Nature* 379, 225–232. doi: 10.1038/379225a0

Bermejo, A., Blazquez, M. A., Serrano, A., And, Z. P., and Cortes, D. (1997). Preparation of 7-alkoxylated furanopyrones: Semisynthesis of (-)-etharvensin a new Styryllactone from Goniothalamus arvensis. *J. Natural products* 60, 1338–1340. doi: 10.1021/np970346w

Bermejo, A., Blazquez, M. A., Rao, K. S., and Cortes, D. (1998). Styryllactone from Goniothalamus arvensis. *Phytochemistry* 47, 1375–1380. doi: 10.1016/S0031-9422(97)00770-X

Bermejo, A., Blazquez, M. A., Rao, K. S., and Cortes, D. (1999). Styryllactone from the stem bark of Goniothalamus arvensis. *Phytochemical Anal.* 10, 127–131. doi: 10.1002/(SICI)1099-1565(199905/06)10:3<127::AID-PCA451>3.0.CO;2-5

Brewster, M. E., and Loftsson, T. (2007). Cyclodextrins as pharmaceutical solubilizers. *Adv. Drug Delivery Rev.* 59, 645–666. doi: 10.1016/j.addr.2007.05.012

Cao, S. G., Wu, X. H., Sim, K. Y., Tan, B. K. H., Pereira, J. T., and Goh, S. H. (1998). Styryllactone derivatives and alkaloids from Goniothalamus borneensis (Annonaceae). *Tetrahedron* 54, 2143–2148. doi: 10.1016/S0040-4020(97)10422-7

Chen, C., Wang, C. C., Wang, Z., Geng, W. Y., Xu, H., Song, X. M., et al. (2016). Cytotoxic activity of a synthetic deoxypodophyllotoxin derivative with an opened D-ring. *J. Asian Nat. Prod Res.* 18, 486–494. doi: 10.1080/10286020.2015.1131679

Chiu, C. C., Lin, C. H., and Fang, K. (2005). Etoposide (VP-16) sensitizes p53-deficient human non-small cell lung cancer cells to caspase-7-mediated apoptosis. *Apoptosis* 10, 643–650. doi: 10.1007/s10495-005-1898-8

Demetzos, C. (2008). Differential Scanning Calorimetry (DSC): a tool to study the thermal behavior of lipid bilayers and liposomal stability. *J. Liposome Res.* 18, 159–173. doi: 10.1080/08982100802310261

Deng, X., Su, J., Zhao, Y., Peng, L. Y., Li, Y., Yao, Z. J., et al. (2011). Development of novel conformation-constrained cytotoxic derivatives of cheliensisin A by embedment of small heterocycles. *Eur. J. Med. Chem.* 46, 4238–4244. doi: 10.1016/j.ejmech.2011.06.028

Dodson, M., Darley-Usmar, V., and Zhang, J. (2013). Cellular metabolic and autophagic pathways: traffic control by redox signaling. *Free Radic. Biol. Med.* 63, 207–221. doi: 10.1016/j.freeradbiomed.2013.05.014

Green, S. P., Wheelhouse, K. M., Payne, A. D., Hallet, J. P., Miller, P.W., and Bull, J. A. (2020). Thermal Stability and Explosive Hazard Assessment of Diazo Compounds and Diazo Transfer Reagents. *Org. Process Res. Dev* 24, 67–84. doi: 10.1021/acs.oprd.9b00422

Gu, Y. Y., Chen, M. H., May, B. H., Liao, X. Z., Liu, J. H., Tao, L. T., et al. (2018). Matrine induces apoptosis in multiple colorectal cancer cell lines in vitro and inhibits tumour growth with minimum side effects in vivo via Bcl-2 and caspase-3. *Phytomedicine* 51, 214–225. doi: 10.1016/j.phymed.2018.10.004

Hu, Z. B., Liao, S. X., Mao, S. L., Zhu, H. P., Xu, S., and Liang, H. Q. (1999). Studies on the chemical constituents of Goniothalamus griffithii Hook. f. et Thoms. *Acta pharmacologica Sin.* 34, 132–134. doi: 10.16438/j .0513-4870.1999.02.012

Kaur, M., Bhatia, R. K., Pissurlenkar, R. R., Coutinho, E. C., Jain, U. K., Katare, O. P., et al. (2014). Telmisartan complex augments solubility, dissolution and drug delivery in prostate cancer cells. *Carbohydr Polym* 101, 614–622. doi: 10.1016/j.carbpol.2013.09.077

Kim, S. H. (2009). The influence of finding meaning and worldview of accepting death on anger among bereaved older spouses. *Aging Ment. Health* 13, 38–45. doi: 10.1080/13607860802154457

Kozovska, Z., Gabrisova, V., and Kucerova, L. (2014). Colon cancer: cancer stem cells markers, drug resistance and treatment. *BioMed. Pharmacother.* 68, 911–916. doi: 10.1016/j.biopha.2014.10.019

Kryjewski, M., Goslinski, T., and Mielcarek, J. (2015). Functionality stored in the structures of cyclodextrin-porphyrinoid systems. *Coordination Chem. Rev.* 300, 101–120. doi: 10.1016/j.ccr.2015.04.009

Lan, Y. H., Chang, F. R., Liaw, C. C., Wu, C. C., Chiang, M. Y., and Wu, Y. C. (2005). Digoniodiol, deoxygoniopypyrone A, and goniofupyrone A: three new styryllactones from Goniothalamus amuyon. *Planta Med.* 71, 153–159. doi: 10.1055/s-2005-837783

Lao, V. V., and Grady, W. M. (2011). Epigenetics and colorectal cancer. *Nat. Rev. Gastroenterol. Hepatol* 8, 686–700. doi: 10.1038/nrgastro.2011.173

Levrier, C., Sadowski, M. C., Nelson, C. C., and Davis, R. A. (2015). Cytotoxic C20 Diterpenoid Alkaloids from the Australian Endemic Rainforest Plant Anopterus macleayanus. *J. Nat. Prod* 78, 2908–2916. doi: 10.1021/acs.jnatprod.5b00509

Li, C. M., Liu, Z. L., Mu, Q., Sun, H. D., Zheng, H. L., and Tao, G. D. (1997). Studies on chemical constituents from leaves of Goniothalamus Griffithii. *Actabot. yunnanica* 19, 321–323.

Li, C. M., Mu, Q., Sun, H. D., Xu, B., Tang, W. D., Zheng, H. L., et al. (1998). A new anti-cancer constituent of Goniothalamuscheliensis. *Actabot. yunnanica* 20, 102–104.

Li, X., An, J., Li, H., Qiu, X., Wei, Y., and Shang, Y. (2019). The methyl-triclosan induced caspase-dependent mitochondrial apoptosis in HepG2 cells mediated through oxidative stress. *Ecotoxicol Environ. Saf.* 182, 109391. doi: 10.1016/j.ecoenv.2019.109391

Lim, H., Kim, S. Y., Lee, E., Lee, S., Oh, S., Jung, J., et al. (2019). Sex-Dependent Adverse Drug Reactions to 5-Fluorouracil in Colorectal Cancer. *Biol. Pharm. Bull.* 42, 594–600. doi: 10.1248/bpb.b18-00707

Liou, J. R., Wu, T. Y., Thang, T. D., Hwang, T. L., Wu, C. C., Cheng, Y. B., et al. (2014). Bioactive 6S-styryllactone constituents of Polyalthia parviflora. *J. Nat. Prod* 77, 2626–2632. doi: 10.1021/np5004577

Luo, Y., Wang, X., Wang, H., Xu, Y., Wen, Q., Fan, S., et al. (2015). High Bak Expression Is Associated with a Favorable Prognosis in Breast Cancer and Sensitizes Breast Cancer Cells to Paclitaxel. *PloS One* 10, e0138955. doi: 10.1145/2818302

Mu, Q., Li, C. M., Zhang, H. J., and Sun, H. D. (1996). A styryllactone from Goniothalamus leiocapus. *Chin. Chem. Lett.* 7, 617–618.

Mu, Q., Li, C. M., Sun, H. D., Zheng, H. L., and Tao, G. D. (1998). The Chemical constituents of Goniothalamus leiocarpus. *Actabot. yunnanica* 20, 123–125.

Mu, Q., Li, C. M., He, Y. N., Sun, H. D., Zheng, H. L., Lu, Y., et al. (1999a). A new styryl-lactone compound from Goniothalamus leiocarpus. *Chin. Chem. Lett.* 10, 135–138.

Mu, Q., Tang, W. D., Li, C. M., Lu, Y., Sun, H. D., Zheng, H. L., et al. (1999b). Four new Styryllactone from Goniothalamus leiocarpus. *Heterocycles* 51, 2969–2976. doi: 10.3987/COM-99-8679

Mu, Q., Tang, W. D., Li, C. M., Xu, Y. P., Sun, H. D., Lou, L. G., et al. (2002). The absolute configuration of Leiocarpin, B. *Heterocycles* 57, 337–340. doi: 10.3987/COM-01-9399

Mu, Q., Tang, W. D., Liu, R. Y., Li, C. M., Lou, L. G., Sun, H. D., et al. (2003). Constituents from the stems of Goniothalamus griffithii. *Planta Med.* 69, 826–830. doi: 10.1055/s-2003-43219

Mu, Q., He, Y. N., Tang, W. D., Li, C. M., Lou, L. G., Sun, H. D., et al. (2004). A styrylpyrone dimer from Bark of Goniothalamus leiocarpus. *Chin. Chem. Lett.* 15, 191–193.

Peeters, J., Neeskens, P., Tollenaere, J. P., Van Remoortere, P., and Brewster, M. E. (2002). Characterization of the interaction of 2-hydroxypropyl-beta-cyclodextrin with itraconazole at pH 2, 4, and 7. *J. Pharm. Sci.* 91, 1414–1422. doi: 10.1002/jps.10126

Peris, E., Estornell, E., Cabedo, N., Cortes, D., and Bermejo, A. (2000). 3-acetylaltholactone and related styryl-lactones, mitochondrial respiratory chain inhibitors. *Phytochemistry* 54, 311–315. doi: 10.1016/S0031-9422(00)00104-7

Pohl, M., and Schmiegel, W. (2016). Therapeutic Strategies in Diseases of the Digestive Tract - 2015 and Beyond Targeted Therapies in Colon Cancer Today and Tomorrow. *Dig Dis.* 34, 574–579. doi: 10.1159/000445267

Purushotham, A. D., Lewison, G., and Sullivan, R. (2012). The state of research and development in global cancer surgery. *Ann. Surg.* 255, 427–432. doi: 10.1097/SLA.0b013e318246591f

Ruden, M., and Puri, N. (2013). Novel anticancer therapeutics targeting telomerase. *Cancer Treat Rev.* 39, 444–456. doi: 10.1016/j.ctrv.2012.06.007

Semprebon, S. C., De Fatima, A., Lepri, S. R., Sartori, D., Ribeiro, L. R., and Mantovani, M. S. (2014). (S)-Goniothalamin induces DNA damage, apoptosis, and decrease in BIRC5 messenger RNA levels in NCI-H460 cells. *Hum. Exp. Toxicol.* 33, 3–13. doi: 10.1177/0960327113491506

Siegel, R., Desantis, C., and Jemal, A. (2014). Colorectal cancer statistics 2014. *CA Cancer J. Clin.* 64, 104–117. doi: 10.3322/caac.21220

Sridhar, R., Ravanan, S., Venugopal, J. R., Sundarrajan, S., Pliszka, D., Sivasubramanian, S., et al. (2014). Curcumin- and natural extract-loaded nanofibres for potential treatment of lung and breast cancer: in vitro efficacy evaluation. *J. Biomater Sci. Polym Ed* 25, 985–998. doi: 10.1080/09205063.2014.917039

Sunkara, V., and Hebert, J. R. (2015). The colorectal cancer mortality-to-incidence ratio as an indicator of global cancer screening and care. *Cancer* 121, 1563–1569. doi: 10.1002/cncr.29228

Trieu, Q. H., Mai, H. D., Pham, V. C., Litaudon, M., Gueritte, F., Retailleau, P., et al. (2014). Styryllactones and acetogenins from the fruits of Goniothalamus macrocalyx. *Nat. Prod Commun.* 9, 495–498. doi: 10.1177/1934578X1400900417

Vemuri, S. K., Banala, R. R., Mukherjee, S., Uppula, P., Gpv, S., A. V., G., et al. (2019). Novel biosynthesized gold nanoparticles as anti-cancer agents against breast cancer: Synthesis, biological evaluation, molecular modelling studies. *Mater Sci. Eng C Mater Biol. Appl.* 99, 417–429. doi: 10.1016/j.msec.2019.01.123

Vendramini-Costa, D. B., Alcaide, A., Pelizzaro-Rocha, K. J., Talero, E., Avila-Roman, J., Garcia-Maurino, S., et al. (2016). Goniothalamin prevents the development of chemically induced and spontaneous colitis in rodents and induces apoptosis in the HT-29 human colon tumor cell line. *Toxicol. Appl. Pharmacol.* 300, 1–12. doi: 10.1016/j.taap.2016.03.009

Wang, F., Yang, B., Zhao, Y., Liao, X., Gao, C., Jiang, R., et al. (2014a). Host-guest inclusion system of scutellarein with 2-hydroxypropyl-beta-cyclodextrin: preparation, characterization, and anticancer activity. *J. Biomater Sci. Polym Ed* 25, 594–607. doi: 10.1080/09205063.2014.884875

Wang, Z. X., Cao, J. X., Liu, Z. P., Cui, Y. X., Li, C. Y., Li, D., et al. (2014b). Combination of chemotherapy and immunotherapy for colon cancer in China: a meta-analysis. *World J. Gastroenterol.* 20, 1095–1106. doi: 10.3748/wjg.v20.i4.1095

Wang, Y., Wang, J., Wang, H., and Ye, W. (2016). Novel taxane derivatives from Taxus wallichiana with high anticancer potency on tumor cells. *Chem. Biol. Drug Des.* 88, 556–561. doi: 10.1111/cbdd.12782

Wang, A., Wang, M., Pang, Q., Jia, L., Zhao, J., Chen, M., et al. (2018). Lily extracts inhibit the proliferation of gastric carcinoma SGC-7901 cells by affecting cell cycle progression and apoptosis via the upregulation of caspase-3 and Fas proteins, and the downregulation of FasL protein. *Oncol. Lett.* 16, 1397–1404. doi: 10.3892/ol.2018.8806

Yen, H. K., Fauzi, A. R., Din, L. B., Mckelvey-Martin, V. J., Meng, C. K., Inayat-Hussain, S. H., et al. (2014). Involvement of Seladin-1 in goniothalamin-induced apoptosis in urinary bladder cancer cells. *BMC Complement Altern. Med.* 14, 295. doi: 10.1186/1472-6882-14-295

Zhang, J., Gao, G., Chen, L., Li, J., Deng, X., Zhao, Q. S., et al. (2014). Hydrogen peroxide/ATR-Chk2 activation mediates p53 protein stabilization and anti-cancer activity of cheliensisin A in human cancer cells. *Oncotarget* 5, 841–852. doi: 10.18632/oncotarget.1780

Zhao, D., Gong, T., Fu, Y., Nie, Y., He, L. L., Liu, J., et al. (2008). Lyophilized Cheliensisin A submicron emulsion for intravenous injection: characterization, in vitro and in vivo antitumor effect. *Int. J. Pharm.* 357, 139–147. doi: 10.1016/j.ijpharm.2008.01.055

Conflict of Interest: The authors declare that the research was conducted in the absence of any commercial or financial relationships that could be construed as a potential conflict of interest.

frontiers in Pharmacology

MINI REVIEW
published: 01 May 2020
doi: 10.3389/fphar.2020.00567

Sulforaphane Potentiates Anticancer Effects of Doxorubicin and Cisplatin and Mitigates Their Toxic Effects

*Cinzia Calcabrini, Francesca Maffei, Eleonora Turrini and Carmela Fimognari**

Department for Life Quality Studies, Alma Mater Studiorum-Università di Bologna, Rimini, Italy

The success of cancer therapy is often compromised by the narrow therapeutic index of many anticancer drugs and the occurrence of drug resistance. The association of anticancer therapies with natural compounds is an emerging strategy to improve the pharmaco-toxicological profile of cancer chemotherapy. Sulforaphane, a phytochemical found in cruciferous vegetables, targets multiple pathways involved in cancer development, as recorded in different cancers such as breast, brain, blood, colon, lung, prostate, and so forth. As examples to make the potentialities of the association chemotherapy raise, here we highlight and critically analyze the information available for two associations, each composed by a paradigmatic anticancer drug (cisplatin or doxorubicin) and sulforaphane.

Keywords: sulforaphane, doxorubicin, cisplatin, anticancer effects, Nrf2, chemosensitization, chemoresistance, toxicity

OPEN ACCESS

Edited by:
Katrin Sak,
NGO Praeventio, Estonia

Reviewed by:
Frederick E. Williams,
University of Toledo, United States
Marco Falasca,
Curtin University, Australia

***Correspondence:**
Carmela Fimognari
carmela.fimognari@unibo.it

Specialty section:
This article was submitted to Pharmacology of Anti-Cancer Drugs, a section of the journal Frontiers in Pharmacology

Received: *22 December 2019*
Accepted: *14 April 2020*
Published: *01 May 2020*

Citation:
Calcabrini C, Maffei F, Turrini E and Fimognari C (2020) Sulforaphane Potentiates Anticancer Effects of Doxorubicin and Cisplatin and Mitigates Their Toxic Effects. Front. Pharmacol. 11:567. doi: 10.3389/fphar.2020.00567

INTRODUCTION

A promising strategy to improve the efficacy of anticancer therapy is the association of chemotherapeutic drugs with natural compounds (Farzaei et al., 2016; Negrette-Guzman, 2019). Indeed, in tumor tissues, phytochemicasl may interact with multiple molecular targets and potentiate the efficacy of traditional anticancer drugs. Moreover, they might exert a protective role against side effects caused by chemotherapeutic agents on off-target tissues.

Sulforaphane (SFN) is a natural isothiocyanate extensively studied for its pleiotropic activity on different cancer models. SFN has been found to exhibit cytotoxic and cytostatic activities through several mechanisms. The production of reactive oxygen species (ROS) is one of the most important. SFN-induced ROS generation promotes the activation of both intrinsic and extrinsic apoptotic pathways. SFN can also cause cell-cycle arrest in tumor cells, partly dependent on the modulation of epigenetic mechanisms including histone acetylation and DNA methylation (Brioness-Herrera et al., 2018). Its activity has been reported even in the most advanced stages of cancer development, where it inhibits pathways involved in metastasis and angiogenesis (Sestili and Fimognari, 2015; Negrette-Guzman, 2019). A very recent study reported that the anticancer activity of SFN involves microRNAs (miRNAs) regulation. miRNAs are post-transcriptional regulators of genes implicated in critical cellular pathways, including apoptosis, cell cycle, and cell differentiation (Rafiei et al., 2020).

A peculiar characteristic of SFN is its ability to exert dichotomous effects. Indeed, SFN is also an indirect ROS scavenger: it up-regulates phase II biotransformation enzymes by enhancing Nuclear factor E2-related factor 2 (Nrf2) activity. SFN disrupts the link between Nrf2 and its suppressor

Kelch-like ECH-associated protein 1 (Keap1) and promotes the cytoplasmic and nuclear accumulation of Nrf2 (Briones-Herrera et al., 2018). In the nucleus, Nrf2 acts as a transcription activator for DNA sequences known as antioxidant response elements (ARE). SFN *via* Nrf2 increases the expression of some ARE-target genes including NADPH-quinone oxidoreductase 1 (NQO1), heme-oxygenase (HO-1), and glutamate-cysteine ligase catalytic subunit (GCLC).

In this mini-review, we highlight and critically analyze the available evidence on the anticancer and cytoprotective effects of SFN in association with two paradigmatic anticancer drugs, i.e., doxorubicin (Doxo) and cisplatin (CIS).

SFN AND DOXO ASSOCIATION

SFN Enhances the Anticancer Efficacy of Doxo

The anthracycline Doxo induces DNA damage through different mechanisms such as topoisomerase II inhibition, generation of ROS, and DNA adduct formation. Doxo undergoes bioreductive activation by redox-cycling reactions, forming a reactive semiquinone. The semiquinone radical intercalates in DNA duplex and generates ROS. ROS increase DNA damage resulting in cytotoxic and cytostatic events (Agudelo et al., 2014). Of note, the generation of ROS is a double-edged sword. It is the key mechanism through which Doxo induces tumor cell death but, at the same time, it may contribute to Doxo toxicity (Angsutararux et al., 2015; Karasawa and Steyger, 2015) and prompt signals leading cancer cells to escape apoptosis (Alimbetov et al., 2018).

In combination with Doxo, SFN increased its proapoptotic activity in different cell lines (Fimognari et al., 2012; Bose et al., 2018; Mielczarek et al., 2019) (**Figure 1**). Furthermore, SFN reverted Doxo-resistant phenotype in p53-mutated cells, inducing apoptosis irrespective of p53 status (Fimognari et al., 2006; Fimognari et al., 2007). SFN potentiated also the RNA-damaging activity of Doxo, increasing its proapoptotic potential (Fimognari et al., 2012). Besides, SFN improved the sensitivity to Doxo by inducing autophagy *via* epigenetic mechanisms. In particular, SFN suppressed histone deacetylase HDAC6 that in turn activates PTEN (phosphatase and tensin homolog), a tumor suppressor gene and key regulator of autophagy (Yang F, et al., 2018). However, in certain cancer cell lines, SFN showed a hormetic biphasic response. At low doses, it reduced Doxo-induced oxidative stress, but at higher doses it exhibited synergistic effects and promoted DNA damage (Zanichelli et al., 2012) (**Figure 1**).

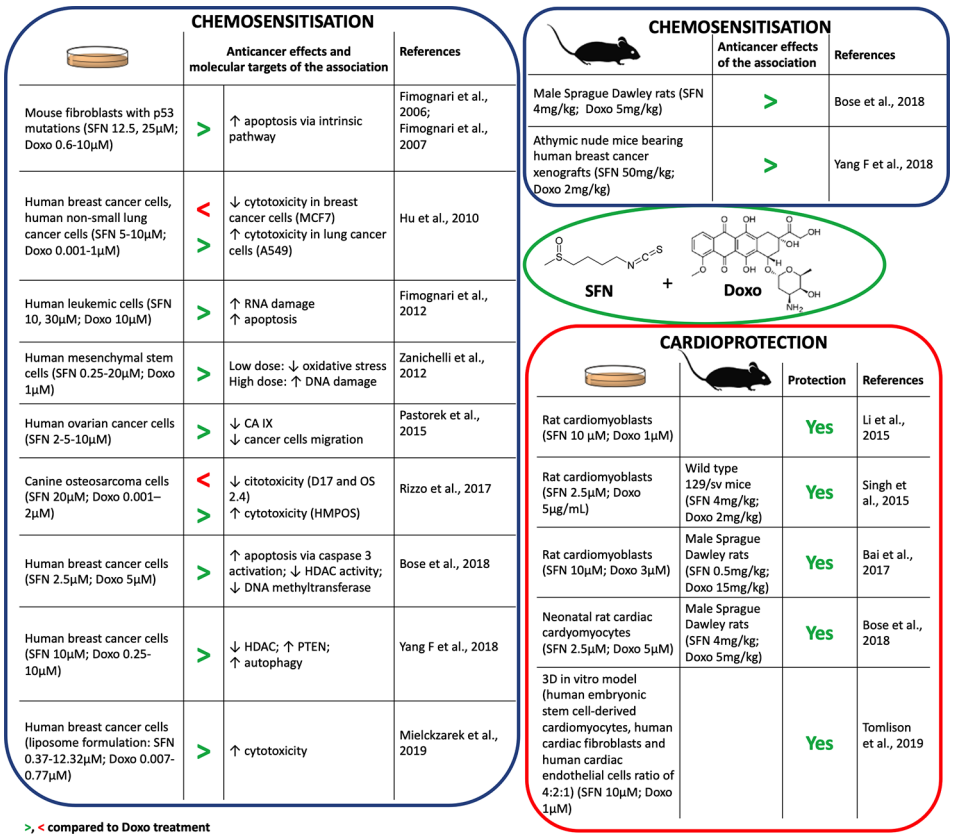

CHEMOSENSITISATION

		Anticancer effects and molecular targets of the association	References
Mouse fibroblasts with p53 mutations (SFN 12.5, 25μM; Doxo 0.6-10μM)	>	↑ apoptosis via intrinsic pathway	Fimognari et al., 2006; Fimognari et al., 2007
Human breast cancer cells, human non-small lung cancer cells (SFN 5-10μM; Doxo 0.001-1μM)	< >	↓ cytotoxicity in breast cancer cells (MCF7) ↑ cytotoxicity in lung cancer cells (A549)	Hu et al., 2010
Human leukemic cells (SFN 10, 30μM; Doxo 10μM)	>	↑ RNA damage ↑ apoptosis	Fimognari et al., 2012
Human mesenchymal stem cells (SFN 0.25-20μM; Doxo 1μM)	>	Low dose: ↓ oxidative stress High dose: ↑ DNA damage	Zanichelli et al., 2012
Human ovarian cancer cells (SFN 2-5-10μM)	>	↓ CA IX ↓ cancer cells migration	Pastorek et al., 2015
Canine osteosarcoma cells (SFN 20μM; Doxo 0.001–2μM)	< >	↓ citotoxicity (D17 and OS 2.4) ↑ cytotoxicity (HMPOS)	Rizzo et al., 2017
Human breast cancer cells (SFN 2.5μM; Doxo 5μM)	>	↑ apoptosis via caspase 3 activation; ↓ HDAC activity; ↓ DNA methyltransferase	Bose et al., 2018
Human breast cancer cells (SFN 10μM; Doxo 0.25-10μM)	>	↓ HDAC; ↑ PTEN; ↑ autophagy	Yang F et al., 2018
Human breast cancer cells (liposome formulation: SFN 0.37-12.32μM; Doxo 0.007-0.77μM)	>	↑ cytotoxicity	Mielckzarek et al., 2019

>, < compared to Doxo treatment

CHEMOSENSITISATION

	Anticancer effects of the association	References
Male Sprague Dawley rats (SFN 4mg/kg; Doxo 5mg/kg)	>	Bose et al., 2018
Athymic nude mice bearing human breast cancer xenografts (SFN 50mg/kg; Doxo 2mg/kg)	>	Yang F et al., 2018

CARDIOPROTECTION

		Protection	References
Rat cardiomyoblasts (SFN 10 μM; Doxo 1μM)		Yes	Li et al., 2015
Rat cardiomyoblasts (SFN 2.5μM; Doxo 5μg/mL)	Wild type 129/sv mice (SFN 4mg/kg; Doxo 2mg/kg)	Yes	Singh et al., 2015
Rat cardiomyoblasts (SFN 10μM; Doxo 3μM)	Male Sprague Dawley rats (SFN 0.5mg/kg; Doxo 15mg/kg)	Yes	Bai et al., 2017
Neonatal rat cardiac cardyomyocytes (SFN 2.5μM; Doxo 5μM)	Male Sprague Dawley rats (SFN 4mg/kg; Doxo 5mg/kg)	Yes	Bose et al., 2018
3D in vitro model (human embryonic stem cell-derived cardiomyocytes, human cardiac fibroblasts and human cardiac endothelial cells ratio of 4:2:1) (SFN 10μM; Doxo 1μM)		Yes	Tomlison et al., 2019

FIGURE 1 | Chemosensitization and cardioprotection of sulforaphane (SFN) in association with doxorubicin (Doxo).

Some anticancer drugs can lose their efficacy in a hypoxic cancer microenvironment (Muz et al., 2015). The master genes orchestrating molecular response to hypoxia are HIF1α (hypoxia-inducible factor 1α) and its downstream targets, such as carbonic anhydrase protein IX (CA IX). CA IX protein protects from pH imbalance provoked by hypoxia and facilitates invasion and migration of tumor cells (Tafreshi et al., 2014). SFN down-regulated the expression of HIF1α and CA IX proteins in ovarian cancer cells cultivated in hypoxia and reduced their migration (Pastorek et al., 2015) (**Figure 1**). Since HIF1α was found to be upregulated in tumor cells after Doxo treatment (Cao et al., 2013), the down-regulation of HIF1α by SFN could represent a relevant mechanism to enhance Doxo efficacy in cancer cells.

However, conflicting data on the effects of SFN when used in association with Doxo impose caution. Rizzo and coworkers showed that SFN can decrease Doxo's antitumor potential depending on the specific redox status of the cell line (Rizzo et al., 2017). SFN sensitized cells characterized by high basal Nrf2 expression to Doxo, whereas it reduced Doxo's anticancer effects in cells with very low Nrf2 basal levels (Hu et al., 2010) (**Figure 1**). Thus, the effects of SFN+Doxo may depend on the Nrf2 basal level of tumor cell type. Of note, most of the data on SFN+Doxo effects was obtained by *in vitro* studies. Evidence has started to accrue *in vivo* (**Figure 1**) and confirmed the synergistic effect of the association. The association of SFN could thus allow the use of lower doses of Doxo and a reduction of its adverse effects. Accordingly, Bose and coworkers demonstrated that the effective dosage of Doxo could be lowered by 50% in combination with SFN (Bose et al., 2018). Altogether, data on SFN-Doxo association are promising, but not conclusive.

SFN Mitigates Doxo-Induced Cardiotoxicity

The most common adverse effect in patients receiving Doxo-based chemotherapy is cardiotoxicity. The mechanism of Doxo cardiotoxicity is multifactorial. It includes ROS-mediated myocardium injury, impaired mitochondrial function, cardiomyocyte apoptosis, and dysregulation of Ca^{2+} homeostasis. All together these events lead to an increased rate of heart failure (Bai et al., 2017; Tomlinson et al., 2019).

Several *in vitro* studies showed the cardioprotective effects of SFN after pre- or co-treatment with Doxo (**Figure 1**). SFN contrasted Doxo-induced oxidative stress and cardiomyocytes' death. In particular, SFN prevented apoptosis inhibiting: i) the activation of Bax protein, ii) the release of cytochrome c, iii) the activation of caspase-3, iv) the loss of mitochondrial transmembrane potential, and v) the generation of mitochondrial ROS (Li et al., 2015; Singh et al., 2015). SFN cardioprotection was mediated by Nrf2 activation and the subsequent induction of phase II enzymes, such as HO-1 (Li et al., 2015). Interestingly, Tomlison and colleagues confirmed the pivotal role of Nrf2 in a 3D model exhibiting key features of cardiac tissue (**Figure 1**). Using this model, inducers of Nrf2, including SFN, exploited cardioprotective activity similar to dexrazoxane, used in patients receiving high cumulative dose of anthracyclines (McGowan et al., 2017). Similarly, SFN counteracted oxidative damage and heart failure induced by Doxo *in vivo* (**Figure 1**). In particular, SFN activated cardiac Nrf2 and upregulated its downstream targets, including genes involved in glutathione (GSH) synthesis, HO-1, and NQO1 (Singh et al., 2015; Bai et al., 2017; Bose et al., 2018). The reduction of Doxo-induced myocardial injury markers, such as creatine kinase-MB, aspartate aminotransferase, lactate dehydrogenase, and troponin I, further support the cardioprotective activity of SFN (Singh et al., 2015; Bai et al., 2017).

Doxo strongly compromised mitochondrial activity, due to its conversion by the mitochondrial complex I of the electron transport chain (ETC) into the more reactive semiquinone (Bose et al., 2018). SFN preserved ETC functionality and mitochondria ultrastructure of cardiac cells from oxidative stress damage in Doxo-treated animal models (Singh et al., 2015; Bose et al., 2018).

Fibrosis and inflammation can contribute to heart stiffness and dysfunction. SFN prevented Doxo-induced cardiac fibrosis inhibiting cardiac collagen accumulation and contrasting the up-regulation of connective tissue growth factors induced by Doxo (Bai et al., 2017). Moreover, it decreased Doxo-induced inflammatory heart markers, such as plasminogen activator inhibitor-1 (Bai et al., 2017) and serum levels of IL-6 and TNF-α (tumor necrosis factor-α) (Bose et al., 2018).

Finally, SFN led to an increased survival rate in animals co-treated with SFN+Doxo compared to those treated with Doxo (85% reduction in rats and 90% reduction in mice in hazard of dying from Doxo exposure) (Singh et al., 2015; Bose et al., 2018). This evidence is mainly imputable to the preservation of heart functionality (measured by ejection fraction, fractional shortening, and stroke volume) mediated by SFN.

On the whole, *in vitro* mechanistic studies and *in vivo* results univocally outline SFN as a promising molecule to prevent Doxo-induced cardiotoxicity.

SFN AND CIS ASSOCIATION

SFN Enhances the Anticancer Efficacy of CIS

CIS is a platinum derivative used for both solid and liquid cancer treatment (Volarevic et al., 2019). Its anticancer activity is due to multiple mechanisms involving binding to genomic or mitochondrial DNA to generate DNA damage and interfering with DNA repair systems, eventually leading to activation of p53 and induction of apoptosis. CIS-induced DNA damage is also due to its ability to generate ROS (Ghosh, 2019). Thus, compounds able to increase ROS or DNA damage could enhance CIS anticancer effects.

Many studies reported that SFN synergizes with CIS in counteracting cancer development (**Figure 2**). SFN enhanced CIS-induced DNA damage and apoptosis in many cancer cell lines (Hunakova et al., 2014; Lan et al., 2017; Lee and Lee, 2017; Elkashty et al., 2018; Kan et al., 2018; Xu et al., 2019). In most of

CHEMOSENSITISATION

		Anticancer effects and molecular targets of the association	References
Human lung cancer cells (SFN 20μM; CIS 15-45μM)	=	= DNA damage	Di Pasqua et al., 2010
Human pancreatic and prostate cancer cells (SFN 5μM; CIS 7-28μM)	>	↑ apoptosis ↓ CSC-formation	Kallifaditis et al., 2011
Human ovarian cancer cells (SFN 2.5-20μM; CIS 5-25μM)	> <	↑ DNA damage, ↑ apoptosis (A2780) ↓ DNA damage, ↓ apoptosis (SKOV3)	Hunakova et al., 2014
Human ovarian cancer cells (SFN 2.5-10μM; CIS 2.5-20μM)	>	↑ p53, ↑ apoptosis	Kan et al., 2018
Human ovarian cancer cells (SFN 20μM; CIS 5-10μM)	=	↓ c-Myb	Tian et al., 2019
Human gastric cancer cells (SFN 10μM; CIS 2μM)	>	↑ miR124; ↓ IL6R, ↓ pSTAT3 ↓ CSC-formation	Wang et al., 2016
Human colon cancer cells (SFN 5-15μM; CIS 10μM)	>	↑ DNA damage	Lan et al., 2017
Human malignant mesothelioma cells (SFN 20μM; CIS 40μM)	>	↑ p53, ↑ apoptosis via intrinsic pathway	Lee and Lee, 2017
Human lung cancer cells (SFN 10μM; CIS 5μM)	>	↑ miR214, apoptosis ↓ CSC-formation	Li et al., 2017
Human cholangiocarcinoma cells (SFN 10μM; CIS 5μM)	>	= DNA damage ↑ apoptosis via intrinsic pathway	Rackauskas et al., 2017
Human head and neck cancer cells (SFN 3.5-7μM; CIS 0.5-2μM)	>	↑ apoptosis via intrinsic pathway	Elkashty et al., 2018
Spheroid of human epidermal squamous cell carcinoma (SFN 0.5, 5μM; CIS 0.5-1μM)	>	↑ apoptosis via intrinsic pathway	Kerr et al., 2018
Human breast cancer cells (nanoparticle formulation: SFN 10μM; CIS 20μM)	>	↑ DNA damage, ↑ p53, ↑ apoptosis via intrinsic pathway	Xu et al., 2019

>, <, = compared to CIS treatment

CHEMOSENSITISATION

	Anticancer effects of the association	References
BALB/c nu/nu mice bearing human lung cancer xenografts (SFN 4mg/kg; CIS 3mg/kg)	>	Li et al., 2017
NSG mice bearing human epidermal squamous (SFN 60mg/kg; CIS 25μmoles/dose)	>	Kerr et al., 2018
BALB/c nu/nu mice bearing human nasopharyngeal cancer xenografts (SFN 60mg/kg; CIS 3mg/kg)	>	Chen et al., 2019
BALB/c nu/nu mice bearing human breast or gastric cancer xenografts (nanoparticle formulation: SFN 0.59mg/kg; CIS 2mg/kg)	>	Xu et al., 2019

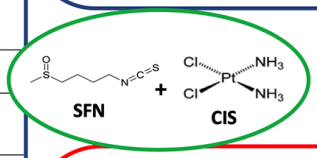

NEPHROPROTECTION

		Protection	References
Porcine renal epithelial cells (SFN 0.5-5μM; CIS 40μM)	Male Wistar rats (SFN 0.5mg/kg; CIS 7.5mg/kg)	Yes	Guerrero-Beltran et al., 2010a
Porcine renal epithelial cells (SFN 0.5-5μM; CIS 40μM)	Male Wistar rats (SFN 0.5mg/kg; CIS 7.5mg/kg)	Yes	Guerrero-Beltran et al., 2010b
	Male Wistar rats (SFN 0.5mg/kg; CIS 7.5mg/kg)	Yes	Guerrero-Beltran et al., 2012
Human embryonic kidney and human proximal tubule epithelial cells (SFN 5μM; CIS 5-80μM)		Yes	Atilano-Roque et al., 2016

FIGURE 2 | Chemosensitization and nephroprotection of sulforaphane (SFN) in association with cisplatin (CIS).

them apoptosis occurred *via* p53 and caspases activation. Few studies, however, deepened the mechanisms involved in those effects. The SFN's ability to inhibit DNA repair (Piberger et al., 2014) or to transiently depletes GSH (Pappa et al., 2007) represent two candidate mechanisms. In particular, GSH depletion lowered the inactivation/excretion of CIS that occurs mainly *via* conjugation with GSH or metallothioneins (Ghosh, 2019). Accordingly, a nanoparticle delivery system containing SFN plus CIS decreased GSH levels and enhanced the intracellular levels of CIS (Xu et al., 2019). Since GSH depletion deprives cells of one of the most important defenses against oxidative stress, a possible consequence could be an increase in ROS and an enhanced CIS-induced DNA damage. The role of ROS generation on the cytotoxicity of SFN+CIS was defined pre-treating cancer cells with N-acetylcysteine (NAC), a GSH precursor. NAC prevented ROS generation, activation of the mitochondrial apoptotic pathway as well as cell-cycle arrest and autophagy induced by SFN+CIS (Lee and Lee, 2017). Similarly, NAC abrogated the antitumor activity of SFN+CIS nanoparticles *in vivo* (Xu et al., 2019) (**Figure 2**).

Interestingly, SFN can increase the cytotoxicity of CIS also through mechanisms different from DNA damage. The association reduced the CIS-induced overexpression of antiapoptotic proteins such as Bcl2 (Rackauskas et al., 2017) (**Figure 2**), an event involved in the onset of chemoresistance (Galluzzi et al., 2012).

Another mechanism of CIS chemoresistance is the formation of cancer stem cells (CSC) (Wang et al., 2016). Both in *in vitro* and *in vivo* models, CIS-resistant cells overexpress β-catenin and c-Myc proteins, which are involved in CSC self-renewal (Li et al., 2017). CIS+SFN reduced the CSC population and inhibited their stem-like cell properties and viability in many cancer cells (Kallifaditisis et al., 2011; Wang et al., 2016; Li et al., 2017) (**Figure 2**). SFN reduced the activation of β-catenin/c-Myc pathway through the up-regulation of miR-214, a negative post-translational regulator of both c-Myc and β-catenin (Li et al., 2017). Through the up-regulation of one more miRNA, i.e., miR-124 targeting the IL-6 receptor gene (Xiao et al., 2015), SFN counteracted CIS-activation of IL-6/STAT3 pathway, which seems to be involved in CIS-induced expansion of CSC cells

(Wang et al., 2016). STAT3 signaling is also activated by c-Myb, a protein associated with CIS resistance and CSC self-renewal (Zhang et al., 2012). SFN reverted c-Myb-induced cancer cell proliferation and invasion and sensitized cells to CIS (Tian et al., 2019).

In summary, many reports disclose the ability of SFN to enhance CIS's anticancer activity and counteract chemoresistance, although there are some exceptions. As an example, SFN did not enhance CIS's cytotoxicity in a lung cancer cell line. Tubulin-binding drugs are widely used with CIS to enhance its cytotoxicity in non-small cell lung cancer. SFN, if compared with other isothiocyanates, weakly depletes β-tubulin levels (Di Pasqua et al., 2010). This evidence could explain its lack of activity in those cells. Besides, SFN exhibited a controversial role in two ovarian cancer cell lines: it synergized with CIS in A2780 cells and antagonized CIS effects in SKOV3 cells (Hunakova et al., 2014). A2780 cells have a weakly efficient Nrf2 pathway and cannot restore the depletion of GSH induced by SFN. Thus, the association significantly increased DNA damage and apoptosis compared to CIS alone. Conversely, SKOV3 cells have a highly efficient Nrf2 pathway. Thus, SFN-induced activation of the Nrf-2 pathway protected SKOV3 cells from the cytotoxicity of CIS instead of sensitizing them to CIS (Hunakova et al., 2014).

SFN Mitigates CIS-Induced Nephrotoxicity

CIS therapy causes nephrotoxicity in 30–40% of patients (Volarevic et al., 2019). The mechanism behind the onset of nephrotoxicity is particularly complex and involves multiple mechanisms, including ROS generation, mitochondrial dysfunction, apoptosis, necrosis, and autophagy of renal cells. Moreover, inflammation exacerbates these processes (Holditch et al., 2019).

ROS generation and mitochondrial dysfunction represent the earliest events in CIS-induced nephrotoxicity. SFN reduced CIS-induced ROS generation *in vitro*. It increased GSH pool and antioxidant enzyme activity, and reduced markers of nitrosative and oxidative stress. Accordingly, SFN ameliorated cellular, plasma, kidney, and liver oxidative status (Guerrero-Beltran et al., 2010a; Guerrero-Beltran et al., 2010b; Atilano-Roque et al., 2016) (**Figure 2**). Furthermore, SFN improved renal histopathology and physiological functions in rats treated with CIS (Guerrero-Beltran et al., 2010a; Guerrero-Beltran et al., 2010b). SFN antioxidant activity takes place through the Nrf2 pathway. Treatment with SFN before CIS exposure activated the Nrf2 pathway and its target genes (i.e., GCLC and NQO1) and protected from CIS-induced renal cell injury (Guerrero-Beltran et al., 2010a; Atilano-Roque et al., 2016). The inhibition of GCLC and NQO1 nullified nephroprotection (Guerrero-Beltran et al., 2010a). This finding clearly points out the close link between the SFN-protective effect and its ability to activate the Nrf2 pathway.

CIS accumulates in mitochondria (Dzamitika et al., 2006) and depletes GSH levels, thus increasing mitochondrial oxidative stress and damage to complex I (Guerrero-Beltran et al., 2010a). ROS exacerbate complex I damage and activate several pathways involved in apoptosis or inflammation (Sharma et al., 2009). SFN prevented CIS-induced alterations of mitochondrial functionality in rat kidney (Guerrero-Beltran et al., 2010a) and counteracted the pathways activated by ROS in CIS-induced kidney damage (Guerrero-Beltran et al., 2012). In particular, SFN increased pro-survival ERK (extracellular signal-regulated kinase) and antiapoptotic p38β mitogen-activated protein kinase, and decreased the proapoptotic Jun N-terminal kinase (JNK) and p38α pathways. SFN was also able to decrease TNF-α, nuclear factor kappa-light-chain-enhancer of activated B cells (NF-κB), adhesive molecule expression, and leukocytes and macrophage recruitment into renal tissue and reduce kidney inflammation (Guerrero-Beltran et al., 2012) (**Figure 2**).

These findings highlight the pivotal role of oxidative stress in CIS toxicity and the ability of SFN of counteracting these events through its antioxidant properties.

CONCLUSIONS

Pre-clinical existing data highlight that SFN enhances the anticancer activity of Doxo and CIS and counteracts the off-target toxicity through multiple mechanisms. In particular, SFN strongly activates the Nrf2 antioxidant signaling pathway. This evidence could have clinically relevant implications for cancer therapy as Nrf2 activation in cancer cells may contribute to the onset of either chemosensitisation or chemoresistance (Bai et al., 2016; Catanzaro et al., 2017). Most anticancer drugs amplify ROS levels in cancer cells over a threshold to induce cell death and tumor regression. Anthracyclines produce the highest levels of cellular ROS; alkylating drugs, platinum-based drugs, camptothecins, arsenic-based drugs, and topoisomerase inhibitors generate high levels of ROS; taxanes, Vinca alkaloids, nucleotide analogues, and antimetabolites induce lower levels of ROS (Yang H, et al., 2018). This means that the effect of SFN when used in association with anticancer therapy could be not easily predicted, and indeed, even with the two anticancer drugs included in our review, the effects of SFN are sometimes discordant, as reported above.

In addition, it is well known that cancer cells are not homogeneous. Reprogramming of cancer cells impacts on disease's progression and contributes to their heterogeneity (Milkovic et al., 2017). As an example, in later stages of cancer, Nrf2 and Keap1 are mutated and Nrf2 activity increased. This means that inhibitors of Nrf2 could be better than activators of Nrf2 in the later stages of the disease. Thus, cancer stage should be taken into account for the usage of specific Nrf2 activators or inhibitors during cancer therapy.

Of note, Nrf2 modulation was observed in women orally treated with a broccoli sprout preparation containing 200 μmol of SFN/g. In their breast tissues, increased NQO1 and HO-1 transcripts and NQO1 enzymatic activity have been found (Cornblatt et al., 2007). A phase-II clinical trial is actually recruiting patients with the aims to investigate the ability of SFN-rich broccoli sprout extracts to (i) enhance Doxo anticancer effects on women with breast cancer undergoing neoadjuvant chemotherapy, with no prior cardiac disease and who will receive Doxo without Her-2 receptor antagonists as part of their clinical care, (ii) protect from Doxo-associated cardiac dysfunction, and (iii) explore the role of Nrf2 in this association therapy (ClinicalTrial.gov identifier: NCT03934905, 2019). This interventional study will certainly contribute to define the role

of Nrf2 modulation in the efficacy and safety of SFN when associated with traditional anticancer therapies.

Concerning the safety profile of SFN in association with anticancer drugs, SFN prevented changes in animal body weight caused by either Doxo or CIS (Singh et al., 2015; Kerr et al., 2018; Chen et al., 2019). However, a recent study recorded hematic signs of possible myelosuppression and hepatotoxicity in animals exposed to CIS+SFN. Interestingly, these side effects became negligible when drugs were delivered in nanoparticles (Xu et al., 2019), a formulation improving the release of drugs in tumor cells. Thus, a controlled delivery system may enhance chemotherapy efficacy and reduce systemic toxicity of SFN+CIS.

Last but not least, the stability and bioavailability of SFN may influence its chemosensitizing/chemoprotective effects. Thus, the pharmacokinetics of SFN in association with anticancer drugs should be addressed to fully understand its clinical potential in the oncological field.

AUTHOR CONTRIBUTIONS

CC, FM, ET, and CF analyzed the scientific literature. CC, FM, and ET wrote the manuscript. CF designed the study and revised the manuscript.

REFERENCES

Agudelo, D., Bourassa, P., Berube, G., and Tajmir-Riahi, H. A. (2014). Intercalation of antitumor drug doxorubicin and its analogue by DNA duplex: structural features and biological implications. *Int. J. Biol. Macromol.* 66, 144–150. doi: 10.1016/j.ijbiomac.2014.02.028

Alimbetov, D., Askarova, S., Umbayev, B., Davis, T., and Kipling, D. (2018). Pharmacological targeting of cell cycle, apoptotic and cell adhesion sinaling pathways implicated in chemoresistance of cancer cells. *Int. J. Mol. Sci.* 19 (6), E1690. doi: 10.3390/ijms19061690

Angsutararux, P., Luanpitpong, S., and Issaragrisil, S. (2015). Chemotherapy-induced cardiotoxicity: overview of the roles of oxidative stress. *Oxid. Med. Cell Longev.* 2015, 795602. doi: 10.1155/2015/795602

Atilano-Roque, A., Wen, X., Aleksunes, L. M., and Joy, M. S. (2016). Nrf2 activators as potential modulators of injury in human kidney cells. *Toxicol. Rep.* 3, 153–159. doi: 10.1016/j.toxrep.2016.01.006

Bai, X., Chen, Y., Hou, X., Huang, M., and Jin, J. (2016). Emerging role of NRF2 in chemoresistance by regulating drug-metabolizing enzymes and efflux transporters. *Drug Metab. Rev.* 48 (4), 541–567. doi: 10.1080/03602532.2016.1197239

Bai, Y., Chen, Q., Sun, Y. P., Wang, X., Lv, L., Zhang, L. P., et al. (2017). Sulforaphane protection against the development of doxorubicin-induced chronic heart failure is associated with Nrf2 Upregulation. *Cardiovasc. Ther.* 35 (5), e12277. doi: 10.1111/1755-5922.12277

Bose, C., Awasthi, S., Sharma, R., Benes, H., Hauer-Jensen, M., Boerma, M., et al. (2018). Sulforaphane potentiates anticancer effects of doxorubicin and attenuates its cardiotoxicity in a breast cancer model. *PloS One* 13 (3), e0193918. doi: 10.1371/journal.pone.0193918

Briones-Herrera, A., Eugenio-Perez, D., Reyes-Ocampo, J. G., Rivera-Mancia, S., and Pedraza-Chaverri, J. (2018). New highlights on the health-improving effects of sulforaphane. *Food Funct.* 9 (5), 2589–2606. doi: 10.1039/c8fo00018b

Cao, Y., Eble, J. M., Moon, E., Yuan, H., Weitzel, D. H., Landon, C. D., et al. (2013). Tumor cells upregulate normoxic HIF-1α in response to doxorubicin. *Cancer Res.* 73 (20), 6230–6242. doi: 10.1158/0008-5472.CAN-12-1345

Catanzaro, E., Calcabrini, C., Turrini, E., Sestili, P., and Fimognari, C. (2017). Nrf2: a potential therapeutic target for naturally occurring anticancer drugs? *Expert Opin. Ther. Targets* 21 (8), 781–793. doi: 10.1080/14728222.2017.1351549

Chen, L., Chan, L. S., Lung, H. L., Yip, T. T. C., Ngan, R. K. C., Wong, J. W. C., et al. (2019). Crucifera sulforaphane (SFN) inhibits the growth of nasopharyngeal carcinoma through DNA methyltransferase 1 (DNMT1)/Wnt inhibitory factor 1 (WIF1) axis. *Phytomedicine* 63, 153058. doi: 10.1016/j.phymed.2019.153058

ClinicalTrials.gov Identifier: NCT03934905 (2019). *Protective Effects of the Nutritional Supplement Sulforaphane on Doxorubicin-Associated Cardiac Dysfunction*, [Online]. Available: https://clinicaltrials.gov/ct2/show/NCT03934905?term=sulforaphane&draw=2&rank=1 [Accessed 13/12/2019]..

Cornblatt, B. S., Ye, L., Dinkova-Kostova, A. T., Erb, M., Fahey, J. W., Singh, N. K., et al. (2007). Preclinical and clinical evaluation of sulforaphane for chemoprevention in the breast. *Carcinogenesis* 28 (7), 1485–1490. doi: 10.1093/carcin/bgm049

Di Pasqua, A. J., Hong, C., Wu, M. Y., McCracken, E., Wang, X., Mi, L., et al. (2010). Sensitization of non-small cell lung cancer cells to cisplatin by naturally occurring isothiocyanates. *Chem. Res. Toxicol.* 23 (8), 1307–1309. doi: 10.1021/tx100187f

Dzamitika, S., Salerno, M., Pereira-Maia, E., Le Moyec, L., and Garnier-Suillerot, A. (2006). Preferential energy- and potential-dependent accumulation of cisplatin-gutathione complexes in human cancer cell lines (GLC4 and K562): A likely role of mitochondria. *J. Bioenerg. Biomembr.* 38 (1), 11–21. doi: 10.1007/s10863-006-9001-x

Elkashty, O. A., Ashry, R., Elghanam, G. A., Pham, H. M., Su, X., Stegen, C., et al. (2018). Broccoli extract improves chemotherapeutic drug efficacy against head-neck squamous cell carcinomas. *Med. Oncol.* 35 (9), 124. doi: 10.1007/s12032-018-1186-4

Farzaei, M. H., Bahramsoltani, R., and Rahimi, R. (2016). Phytochemicals as Adjunctive with Conventional Anticancer Therapies. *Curr. Pharm. Des.* 22 (27), 4201–4218. doi: 10.2174/1381612822666160601100823

Fimognari, C., Nusse, M., Lenzi, M., Sciuscio, D., Cantelli-Forti, G., and Hrelia, P. (2006). Sulforaphane increases the efficacy of doxorubicin in mouse fibroblasts characterized by p53 mutations. *Mutat. Res.* 601 (1-2), 92–101. doi: 10.1016/j.mrfmmm.2006.06.001

Fimognari, C., Lenzi, M., Sciuscio, D., Cantelli-Forti, G., and Hrelia, P. (2007). Combination of doxorubicin and sulforaphane for reversing doxorubicin-resistant phenotype in mouse fibroblasts with p53Ser220 mutation. *Ann. N. Y. Acad. Sci.* 1095, 62–69. doi: 10.1196/annals.1397.008

Fimognari, C., Lenzi, M., Sestili, P., Turrini, E., Ferruzzi, L., Hrelia, P., et al. (2012). Sulforaphane potentiates RNA damage induced by different xenobiotics. *PloS One* 7 (4), e35267. doi: 10.1371/journal.pone.0035267

Galluzzi, L., Senovilla, L., Vitale, I., Michels, J., Martins, I., Kepp, O., et al. (2012). Molecular mechanisms of cisplatin resistance. *Oncogene* 31 (15), 1869–1883. doi: 10.1038/onc.2011.384

Ghosh, S. (2019). Cisplatin: The first metal based anticancer drug. *Bioorg. Chem.* 88, 102925. doi: 10.1016/j.bioorg.2019.102925

Guerrero-Beltran, C. E., Calderon-Oliver, M., Martinez-Abundis, E., Tapia, E., Zarco-Marquez, G., Zazueta, C., et al. (2010a). Protective effect of sulforaphane against cisplatin-induced mitochondrial alterations and impairment in the activity of NAD(P)H: quinone oxidoreductase 1 and gamma glutamyl cysteine ligase: studies in mitochondria isolated from rat kidney and in LLC-PK1 cells. *Toxicol. Lett.* 199 (1), 80–92. doi: 10.1016/j.toxlet.2010.08.009

Guerrero-Beltran, C. E., Calderon-Oliver, M., Tapia, E., Medina-Campos, O. N., Sanchez-Gonzalez, D. J., Martinez-Martinez, C. M., et al. (2010b). Sulforaphane protects against cisplatin-induced nephrotoxicity. *Toxicol. Lett.* 192 (3), 278–285. doi: 10.1016/j.toxlet.2009.11.007

Guerrero-Beltran, C. E., Mukhopadhyay, P., Horvath, B., Rajesh, M., Tapia, E., Garcia-Torres, I., et al. (2012). Sulforaphane, a natural constituent of broccoli, prevents cell death and inflammation in nephropathy. *J. Nutr. Biochem.* 23 (5), 494–500. doi: 10.1016/j.jnutbio.2011.02.004

Holditch, S. J., Brown, C. N., Lombardi, A. M., Nguyen, K. N., and Edelstein, C. L. (2019). Recent Advances in Models, Mechanisms, Biomarkers, and Interventions in Cisplatin-Induced Acute Kidney Injury. *Int. J. Mol. Sci.* 20 (12), E301. doi: 10.3390/ijms20123011

Hu, L., Miao, W., Loignon, M., Kandouz, M., and Batist, G. (2010). Putative chemopreventive molecules can increase Nrf2-regulated cell defense in some

human cancer cell lines, resulting in resistance to common cytotoxic therapies. *Cancer Chemother. Pharmacol.* 66 (3), 467–474. doi: 10.1007/s00280-009-1182-7

Hunakova, L., Gronesova, P., Horvathova, E., Chalupa, I., Cholujova, D., Duraj, J., et al. (2014). Modulation of cisplatin sensitivity in human ovarian carcinoma A2780 and SKOV3 cell lines by sulforaphane. *Toxicol. Lett.* 230 (3), 479–486. doi: 10.1016/j.toxlet.2014.08.018

Kallifatidis, G., Labsch, S., Rausch, V., Mattern, J., Gladkich, J., Moldenhauer, G., et al. (2011). Sulforaphane increases drug-mediated cytotoxicity toward cancer stem-like cells of pancreas and prostate. *Mol. Ther.* 19 (1), 188–195. doi: 10.1038/mt.2010.216

Kan, S. F., Wang, J., and Sun, G. X. (2018). Sulforaphane regulates apoptosis- and proliferation related signaling pathways and synergizes with cisplatin to suppress human ovarian cancer. *Int. J. Mol. Med.* 42 (5), 2447–2458. doi: 10.3892/ijmm.2018.3860

Karasawa, T., and Steyger, P. S. (2015). An integrated view of cisplatin-induced nephrotoxicity and ototoxicity. *Toxicol. Lett.* 237 (3), 219–227. doi: 10.1016/j.toxlet.2015.06.012

Kerr, C., Adhikary, G., Grun, D., George, N., and Eckert, R. L. (2018). Combination cisplatin and sulforaphane treatment reduces proliferation, invasion, and tumor formation in epidermal squamous cell carcinoma. *Mol. Carcinog.* 57 (1), 3–11. doi: 10.1002/mc.22714

Lan, H., Yuan, H., and Lin, C. (2017). Sulforaphane induces p53-deficient SW480 cell apoptosis via the ROS-MAPK signaling pathway. *Mol. Med. Rep.* 16 (5), 7796–7804. doi: 10.3892/mmr.2017.7558

Lee, Y. J., and Lee, S. H. (2017). Pro-oxidant activity of sulforaphane and cisplatin potentiates apoptosis and simultaneously promotes autophagy in malignant mesothelioma cells. *Mol. Med. Rep.* 16 (2), 2133–2141. doi: 10.3892/mmr.2017.6789

Li, B., Kim, D. S., Yadav, R. K., Kim, H. R., and Chae, H. J. (2015). Sulforaphane prevents doxorubicin-induced oxidative stress and cell death in rat H9c2 cells. *Int. J. Mol. Med.* 36 (1), 53–64. doi: 10.3892/ijmm.2015.2199

Li, Q. Q., Xie, Y. K., Wu, Y., Li, L. L., Liu, Y., Miao, X. B., et al. (2017). Sulforaphane inhibits cancer stem-like cell properties and cisplatin resistance through miR-214-mediated downregulation of c-MYC in non-small cell lung cancer. *Oncotarget* 8 (7), 12067–12080. doi: 10.18632/oncotarget.14512

McGowan, J. V., Chung, R., Maulik, A., Piotrowska, I., Walker, J. M., and Yellon, D. M. (2017). Anthracycline Chemotherapy and Cardiotoxicity. *Cardiovasc. Drugs Ther.* 31 (1), 63–75. doi: 10.1007/s10557-016-6711-0

Mielczarek, L., Krug, P., Mazur, M., Milczarek, M., Chilmonczyk, Z., and Wiktorska, K. (2019). In the triple-negative breast cancer MDA-MB-231 cell line, sulforaphane enhances the intracellular accumulation and anticancer action of doxorubicin encapsulated in liposomes. *Int. J. Pharm.* 558, 311–318. doi: 10.1016/j.ijpharm.2019.01.008

Milkovic, L., Zarkovic, N., and Saso, L. (2017). Controversy about pharmacological modulation of Nrf2 for cancer therapy. *Redox Biol.* 12, 727–732. doi: 10.1016/j.redox.2017.04.013

Muz, B., de la Puente, P., Azab, F., and Azab, A. K. (2015). The role of hypoxia in cancer progression, angiogenesis, metastasis, and resistance to therapy. *Hypoxia (Auckl)* 3, 83–92. doi: 10.2147/HP.S93413

Negrette-Guzman, M. (2019). Combinations of the antioxidants sulforaphane or curcumin and the conventional antineoplastics cisplatin or doxorubicin as prospects for anticancer chemotherapy. *Eur. J. Pharmacol.* 859, 172513. doi: 10.1016/j.ejphar.2019.172513

Pappa, G., Bartsch, H., and Gerhauser, C. (2007). Biphasic modulation of cell proliferation by sulforaphane at physiologically relevant exposure times in a human colon cancer cell line. *Mol. Nutr. Food Res.* 51 (8), 977–984. doi: 10.1002/mnfr.200700115

Pastorek, M., Simko, V., Takacova, M., Barathova, M., Bartosova, M., Hunakova, L., et al. (2015). Sulforaphane reduces molecular response to hypoxia in ovarian tumor cells independently of their resistance to chemotherapy. *Int. J. Oncol.* 47 (1), 51–60. doi: 10.3892/ijo.2015.2987

Piberger, A. L., Koberle, B., and Hartwig, A. (2014). The broccoli-born isothiocyanate sulforaphane impairs nucleotide excision repair: XPA as one potential target. *Arch. Toxicol.* 88 (3), 647–658. doi: 10.1007/s00204-013-1178-2

Rackauskas, R., Zhou, D., Uselis, S., Strupas, K., Herr, I., and Schemmer, P. (2017). Sulforaphane sensitizes human cholangiocarcinoma to cisplatin via the downregulation of anti-apoptotic proteins. *Oncol. Rep.* 37 (6), 3660–3666. doi: 10.3892/or.2017.5622

Rafiei, H., Asharafizadeh, M., and Ahmadi, Z. (2020). MicroRNAs as novel target of sulforaphane in cancer therapy: the beginning of a new tale? *Phytother. Res.*, 34 (4), 721–728. doi: 10.1002/ptr6572

Rizzo, V. L., Levine, C. B., and Wakshlag, J. J. (2017). The effects of sulforaphane on canine osteosarcoma proliferation and invasion. *Vet. Comp. Oncol.* 15 (3), 718–730. doi: 10.1111/vco.12212

Sestili, P., and Fimognari, C. (2015). Cytotoxic and Antitumor Activity of Sulforaphane: The Role of Reactive Oxygen Species. *BioMed. Res. Int.* 2015, 402386. doi: 10.1155/2015/402386

Sharma, L. K., Lu, J., and Bai, Y. (2009). Mitochondrial respiratory complex I: structure, function and implication in human diseases. *Curr. Med. Chem.* 16 (10), 1266–1277. doi: 10.2174/092986709787846578

Singh, P., Sharma, R., McElhanon, K., Allen, C. D., Megyesi, J. K., Benes, H., et al. (2015). Sulforaphane protects the heart from doxorubicin-induced toxicity. *Free Radic. Biol. Med.* 86, 90–101. doi: 10.1016/j.freeradbiomed.2015.05.028

Tafreshi, N. K., Lloyd, M. C., Bui, M. M., Gillies, R. J., and Morse, D. L. (2014). Carbonic anhydrase IX as an imaging and therapeutic target for tumors and metastases. *Subcell. Biochem.* 75, 221–254. doi: 10.1007/978-94-007-7359-2_12

Tian, M., Tian, D., Qiao, X., Li, J., and Zhang, L. (2019). Modulation of Myb-induced NF-kB -STAT3 signaling and resulting cisplatin resistance in ovarian cancer by dietary factors. *J. Cell Physiol.* 234 (11), 21126–21134. doi: 10.1002/jcp.28715

Tomlinson, L., Lu, Z. Q., Bentley, R. A., Colley, H. E., Murdoch, C., Webb, S. D., et al. (2019). Attenuation of doxorubicin-induced cardiotoxicity in a human in vitro cardiac model by the induction of the NRF-2 pathway. *BioMed. Pharmacother.* 112, 108637. doi: 10.1016/j.biopha.2019.108637

Volarevic, V., Djokovic, B., Jankovic, M. G., Harrell, C. R., Fellabaum, C., Djonov, V., et al. (2019). Molecular mechanisms of cisplatin-induced nephrotoxicity: a balance on the knife edge between renoprotection and tumor toxicity. *J. BioMed. Sci.* 26 (1), 25. doi: 10.1186/s12929-019-0518-9

Wang, X., Li, Y., Dai, Y., Liu, Q., Ning, S., Liu, J., et al. (2016). Sulforaphane improves chemotherapy efficacy by targeting cancer stem cell-like properties via the miR-124/IL-6R/STAT3 axis. *Sci. Rep.* 6, 36796. doi: 10.1038/srep36796

Xiao, Y., Wang, J., Yan, W., Zhou, Y., Chen, Y., Zhou, K., et al. (2015). Dysregulated miR-124 and miR-200 expression contribute to cholangiocyte proliferation in the cholestatic liver by targeting IL-6/STAT3 signalling. *J. Hepatol.* 62, 889–896. doi: 10.1016/j.jhep.2014.10.033

Xu, Y., Han, X., Li, Y., Min, H., Zhao, X., Zhang, Y., et al. (2019). Sulforaphane Mediates Glutathione Depletion via Polymeric Nanoparticles to Restore Cisplatin Chemosensitivity. *ACS Nano.* 13 (11), 13445–13455. doi: 10.1021/acsnano.9b07032

Yang, F., Wang, F., Liu, Y., Wang, S., Li, X., Huang, Y., et al. (2018). Sulforaphane induces autophagy by inhibition of HDAC6-mediated PTEN activation in triple negative breast cancer cells. *Life Sci.* 213, 149–157. doi: 10.1016/j.lfs.2018.10.034

Yang, H., Villani, R. M., Wang, H., Simpson, M. J., Roberts, M. S., Tang, M., et al. (2018). The role of cellular reactive oxygen species in cancer chemotherapy. *J. Exp. Clin. Cancer Res.* 37 (1), 266. doi: 10.1186/s13046-018-0909-x

Zanichelli, F., Capasso, S., Di Bernardo, G., Cipollaro, M., Pagnotta, E., Carteni, M., et al. (2012). Low concentrations of isothiocyanates protect mesenchymal stem cells from oxidative injuries, while high concentrations exacerbate DNA damage. *Apoptosis* 17 (9), 964–974. doi: 10.1007/s10495-012-0740-3

Zhang, J., Luo, N., Luo, Y., Peng, Z., Zhang, T., and Li, S. (2012). microRNA-150 inhibits human CD133-positive liver cancer stem cells through negative regulation of the transcription factor c-Myb. *Int. J. Oncol.* 40 (3), 747–756. doi: 10.3892/ijo.2011.1242

Conflict of Interest: The authors declare that the research was conducted in the absence of any commercial or financial relationships that could be construed as a potential conflict of interest.

frontiers in Pharmacology

ORIGINAL RESEARCH
published: 18 August 2020
doi: 10.3389/fphar.2020.01242

Antimutagenic and Chemopreventive Properties of 6-(Methylsulfinyl) Hexyl Isothiocyanate on TK6 Human Cells by Flow Cytometry

Veronica Cocchi, Patrizia Hrelia and Monia Lenzi*

Department of Pharmacy and Biotechnology, Alma Mater Studiorum University of Bologna, Bologna, Italy

6-(methylsulfinyl) hexyl isothiocyanate (6-MITC), is the main bioactive compound present in *Wasabia japonica* rhizome. Several scientific studies have shown that 6-MITC possesses interesting antimicrobial, anti-inflammatory, antiplatelet and antioxidant properties which therefore suggested us it could have an interesting chemopreventive potential. In a recent publication, we demonstrated, in two different leukemia cell lines, its ability to modulate several mechanisms supporting its antitumor activity. For this reason, we thought useful to continue the research, by investigating the potential antimutagenic activity of 6-MITC and thus better define its profile as a possible chemopreventive agent. 6-MITC antimutagenic effect against two known mutagenic agents: the clastogen Mitomycin C (MMC) and the aneuplodogen Vinblastine (VINB), was analyzed, in terms of micronuclei frequency decrease, after short- and long- time treatment on TK6 human cells, using a new automated protocol of the "*In Vitro* Mammalian Cell Micronucleous Test" by flow cytometry. The results showed a different behavior of the isothiocyante. In particular, 6-MITC was unable to counteract the MMC genotoxicity, but when it was associated with VINB a statistically significant decrease in the micronuclei frequency was registered. Overall, the results obtained suggest a potential antimutagenic activity of 6-MITC, in particular against the aneuploidogen agents. This ability, to inhibit or counteract the mutations at the cellular level has a great therapeutic value and it represents a mechanism through a chemopreventive agent can express its activity.

Keywords: 6-MITC, antimutagenesis, chemoprevention, micronuclei, flow cytometry, TK6

OPEN ACCESS

Edited by:
Katrin Sak,
NGO Praeventio, Estonia

Reviewed by:
Bakul Dhagat-Mehta,
University of Missouri, United States
Stefania Nobili,
University of Florence, Italy

****Correspondence:***
Veronica Cocchi
veronica.cocchi4@unibo.it

Specialty section:
This article was submitted to Pharmacology of Anti-Cancer Drugs, a section of the journal Frontiers in Pharmacology

Received: *20 December 2019*
Accepted: *29 July 2020*
Published: *18 August 2020*

Citation:
Cocchi V, Hrelia P and Lenzi M (2020) Antimutagenic and Chemopreventive Properties of 6-(Methylsulfinyl) Hexyl Isothiocyanate on TK6 Human Cells by Flow Cytometry. Front. Pharmacol. 11:1242. doi: 10.3389/fphar.2020.01242

INTRODUCTION

6-(Methylsulfinyl) hexil isothiocyanate (6-MITC) is the main bioactive compound present in *Wasabia japonica*, a plant belonging to the *Brassicaceae* family, also called "Japanese radish". A green paste with a particularly spicy taste is made from the rhizome of this plant, that is used in traditional Japanese cuisine and commonly known as Wasabi (Weil et al., 2004; Weil et al., 2005; Hsuan et al., 2016).

Isothiocyanates have long been considered by the scientific community, for the numerous pharmacological properties demonstrated (Melchini et al., 2013; Lenzi et al., 2014). Several scientific

studies have shown that 6-MITC in particular, possesses interesting antimicrobial (Hirokuni et al., 1998; Ko et al., 2016), anti-inflammatory (Uto et al., 2005; Uto et al., 2007; Uto et al., 2012), antiplatelet (Morimitsu et al., 2000) and antioxidant (Mizuno et al., 2011) properties.

These results suggested us a potential interest 6-MITC as a chemopreventive agent. In a recent publication, we therefore demonstrated, in two different leukemia cell lines (Jurkat and HL-60), its ability to modulate several mechanisms supporting its antitumor activity, such as the cyotodifferentiation and apoptosis induction or the cellular proliferation inhibition (Lenzi et al., 2017).

Beside the ability to interact with cellular and molecular targets, crucial in the development of cancer, also the study and the identification of compounds capable of counteracting the genotoxicity, it is recognized of great interest in the field of chemoprevention (Słoczyńska et al., 2010). In fact, if the mutation occurs in a somatic cell it could lead to premature aging, damage to the immune system and promote the development of chronic degenerative diseases, such as cancer (Basu, 2018).

Initially, the mutagenic activity of 6-MITC was evaluated both at short and long times, in order to exclude the mutagenicity of the compound under study, Subsequently, the research continued by analyzing the antimutagen potential of 6-MITC against two known mutagenic agents, characterized by different mechanism of action, *i.e* the clastogen Mitomycin C (MMC) and the aneuploidogen Vinblastine (VINB). For this purpose, we decided to use a new automated protocol of the Micronucleous (MN) Test by flow cytometry (FCM) (Lenzi et al., 2018; Lenzi et al., 2020).

Numerous genotoxicity tests are validated by OECD and some allow to highlight gene mutations, while other permit to show chromosomal aberrations (OECD Overview, 2014-2015). In this work, we select the "*In Vitro* Mammalian Cell Micronucleous Test", (OECD no. 487, 2016) because the MN represents a sensitive biomarker of both structural chromosomal damages, induced by clastogen agents and numeric chromosomal damages, induced by aneuploidogen agents (OECD Overview 2014-2015, 2017; Lenzi et al., 2020).

Among several cell lines (CHO, V79, CHL/IU, L5178Y and TK6) validated by the OECD guideline no. 487 that can be used to assess the genotoxicity of a xenobiotic, we selected TK6 cells (OECD no. 487, 2016). Our choice is based on the human and not tumorigenic origin of this cell line which better represents the possible effect on human beings. Moreover, since TK6 cells grow in suspension, they are particularly suitable for FCM (Lenzi et al., 2020).

MATERIALS AND METHODS

Reagents

Dimethyl sulfoxide (DMSO), Ethanol, Ethylenediaminetetraacetic acid (EDTA), Fetal Bovine Serum (FBS), L-Glutamine (L-GLU), Mitomycin C (MMC), Nonidet, Penicillin-Streptomycin solution (PS), Potassium Chloride, Potassium Dihydrogen Phosphate, Roswell Park Memorial Institute (RPMI) 1640 medium, Vinblastine (VINB),Water bpc grade, Sodium Chloride, Sodium Hydrogen Phosphate (all purchased from Sigma-Aldrich, St Louis, Missouri, USA), Guava Nexin Reagent, Guava ViaCount Reagent (all purchased from Luminex Corporation, Austin, Texas, USA), RNase A, SYTOX Green, 7-aminoactinomycinD (7-AAD) (all purchased from Thermo Fisher Scientific, Waltham, Massachusetts, USA).

6-MITC

6-MITC was purchased from Abcam, Cambridge, UK. The purity of ITC was >98%. The isothiocyanate was dissolved in DMSO up to 97.39mM stock solution and stored in the dark at −20°C. Increasing concentrations of 6-MITC from 0 to 64μM were tested. DMSO concentration was always in the range 0.05–1% in all the experimental conditions.

Cell Culture

TK6 human lymphoblast cells were purchased by Sigma-Aldrich (St. Louis, Missouri, USA) and were grown at 37°C and 5% CO_2 in RPMI-1640 supplemented with 10% FBS, 1% L-GLU and 1% PS. To maintain exponential growth, the cultures were divided every third day in fresh medium and the cell density did not exceed the critical value of $9x10^5$ cells/mL.

Treatments

Short-Term Treatment

Aliquot of $2.0x10^5$ of TK6 cells were treated with increasing concentrations of 6-MITC (0 to 64μM) and incubated for 3h followed by 23h of recovery in fresh medium, 26h total, corresponding to two replication cycles, in the presence or absence of MMC (400ng/mL) or VINB (25ng/mL) (co-treatment). We selected these concentrations on the basis of the literature (Sobol et al., 2012) and, as stated in the OECD guideline, we checked that cytotoxicity and cytostasis were lower than 55 ± 5% (OECD no. 487, 2016).

Long-Term Treatment

Aliquot of $2.0x10^5$ of TK6 cells were treated with increasing concentrations of 6-MITC (0 to 32μM) and incubated for 26h consecutive, corresponding to two replication cycles, in the presence or absence of MMC (200ng/mL) or VINB (6.25ng/mL) (co-treatment). We selected these concentrations on the basis of the literature (Sobol et al., 2012) and, as stated in the OECD guideline, we checked that cytotoxicity and cytostasis were lower than 55 ± 5% (OECD no. 487, 2016).

Flow Cytometry

All FCM analysis reported below were performed using a Guava easyCyte 5HT flow cytometer equipped with a class IIIb laser operating at 488 nm (Merck, Darmstadt, Germany).

Cytotoxicity and Cytostasis Analysis

In order to detect cytotoxicity and cytostasis the percentage of viable cells was evaluated by the Guava ViaCount Assay. Briefly,

cells were stained with Guava ViaCount Reagent (containing Propidium Iodide, PI) and analyzed by Guava ViaCount software.

In particular, to assess the cytotoxicity, the results obtained in the sample treated with different concentrations of 6-MITC were normalized on those obtained in the control cultures.

In parallel, the number of cells seeded at time 0 and that measured at the end of the treatment time, was used to check the correct replication in the control cultures and compare it to that measured in the treated cultures using the relative population doubling (RPD).

$$RPD = \frac{(No.\ of\ Population\ doublings\ in\ treated\ cultures)}{(No.\ of\ Population\ doublings\ in\ control\ cultures)} x100$$

Apoptosis Analysis

The percentage of apoptotic cells was evaluated by the Guava Nexin Assay. Briefly, the percentage of live, apoptotic and necrotic cells was assessed using the Guava Nexin Reagent (containing 7-AAD and Annexin-V-PE) and analyzed by Guava Nexin software.

The results obtained were expressed as apoptotic fold increase of treated cultures compared to control cultures and were used to select MNs test concentrations. In fact, it is necessary that the percentage of apoptotic cells measured in treated cultures is comparable to that present in the control cultures, in order to avoid possible false positives, due to the presence of apoptotic bodies.

Genotoxicity Analysis

The analysis of the MNs frequency was performed using an automated protocol by Lenzi et al. (2018). Briefly, after 3 or 26h from 6-MITC exposure, aliquots of $7x10^5$ cells were collected and stained with 7-AAD and SYTOX Green. The discrimination between nuclei and MNs was performed on the basis of the different size analyzed by Forward Scatter (FSC), and the different intensity of green fluorescence. For each sample the MNs frequency was measured on 10,000 nuclei derived from viable and proliferating cells on the basis of different red fluorescence. The results were expressed as MNs frequency fold increase in treated cultures compared to that present in the control cultures (**Figure 1**).

Statistical Analysis

All results were expressed as mean ± SEM of at least five independent experiments. For the statistical analysis of the viability, apoptosis and MNs we used the Analysis of Variance for paired data (repeated ANOVA), followed by Dunnett or Bonferroni as post-test. All the statistical analyses were performed using Prism Software 4.

RESULTS

Mutagenesis of 6-MITC

Short-Term Treatment (3h+23h)

In order to select the concentrations to be used in the following experiments, we, first, evaluated the cytotoxic and cytostatic potential of 6-MITC after 3h treatment followed by 23h of recovery in complete medium at different concentrations (0, 2, 4, 8, 16, 32, and 64μM). In fact, the OECD guideline no. 487 recommends proceeding to assess the genotoxicity of a xenobiotic, only if the highest concentration tested shows cytotoxicity and cytostasis at most equal to 55 ± 5% (OECD no. 487, 2016).

Figure 2 shows that the viability remains abundantly higher than the threshold (red line) required by the OECD guideline at all concentrations tested, except for the 6-MITC 64μM (**Figure 2A**).

At the same time, using RPD value, the cytostasis was checked. Similarly, to cytotoxicity, all concentrations tested, except the 6-MITC 64μM, respect the threshold (**Figure 2B**).

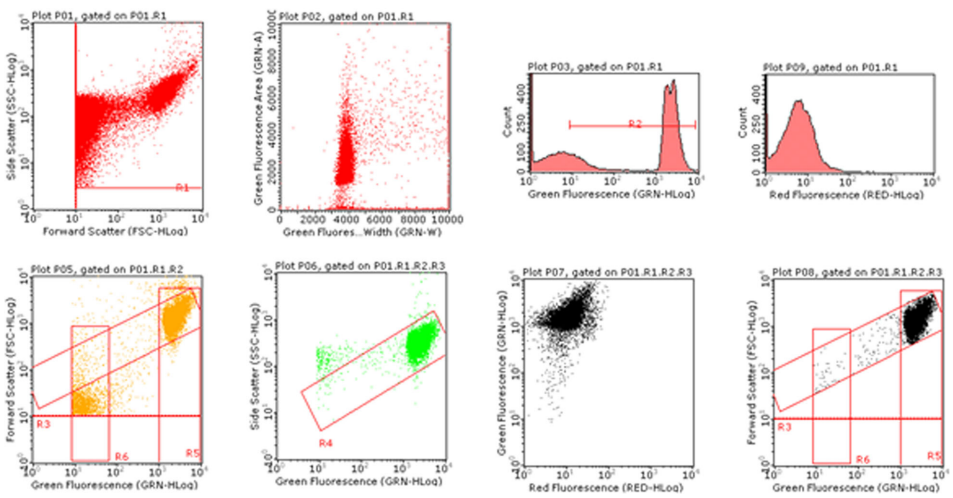

FIGURE 1 | Image of bivariate plots of nuclei and MNs analyzed by Guava Incyte software.

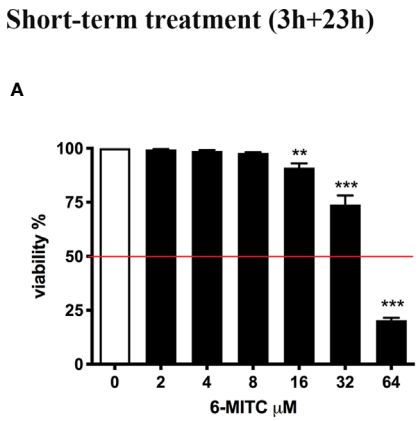

B

Treatment	RPD %
6-MITC 0 μM	100
6-MITC 2 μM	97.2±0.4
6-MITC 4 μM	98.5±0.2
6-MITC 8 μM	90.4±0.6
6-MITC 16 μM	82.2 ±0.7
6-MITC 32 μM	44.7 ±0.2
6-MITC 64 μM	8.6 ±0.3

FIGURE 2 | Effect of 6-MITC on cytotoxicity and cytostasis after short term treatment. Percentage of viability **(A)** and RPD **(B)** in TK6 cells treated with 6-MITC for 3h followed by 23h of recovery in complete medium. Each bar represents the mean ± SEM of five independent experiments. Data were analysed using repeated ANOVA followed by Dunnet post-test. **p < 0.01 *vs* 0; ***p < 0.001 *vs* 0.

Subsequently, the induction of apoptosis was evaluated as an alternative cell death mechanism, in order to avoid the possible confounding effect of apoptotic bodies with MNs. In particular, with respect to the control cultures, a similar apoptotic trend was detected a 2, 4 and 8μM, while a two and three-time increase was detected at 16 and 32μM, respectively (**Figure 3**).

Therefore, on the basis of the obtained results, 2 and 4μM concentrations were selected to be used to assess the potential genotoxicity induced by 6-MITC.

For this purpose, the MNs frequency was measured in control and treated cultures and compared with MMC 400ng/mL and VINB 25ng/mL, used as a positive control. As shown in **Figure 4** the MNs frequency increase registered in 6-MITC treated cultures was not statistically significant compared to the control cultures, while an increase equal to two and five time was detected in the MMC and VINB treated culture, respectively (**Figures 4A–C**).

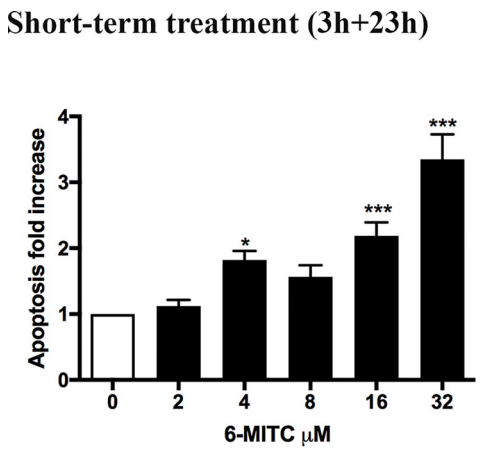

FIGURE 3 | Effect of 6-MITC on apoptosis after short term treatment. Apoptosis fold increase in TK6 cells treated with 6-MITC for 3h followed by 23h of recovery in complete medium. Each bar represents the mean ± SEM of five independent experiments. Data were analysed using repeated ANOVA followed by Dunnet post-test. *p < 0.05 *vs* 0; ***p < 0.001 *vs* 0.

Long-Term Treatment (26h)

In order to completely exclude the genotoxicity of a substance, the OECD guideline no. 487 suggests to check the effect also after a long-term treatment (OECD no. 487, 2016). For this reason, TK6 cells were treated with different concentrations of 6-MITC (0, 1, 2, 4, 8, 16μM) for 26h.

Similarly, to what described above for the short-time treatment, also in this case, initially were selected non-cytotoxic and non-cytostatic concentrations.

Figure 5 shows that the viability remains abundantly higher than the 50% (red line) for all concentrations tested (**Figure 5A**), while the RPD values respect the threshold at all concentrations tested, except the 16μM. In this case a cytostasis equal to 89.6% was observed and so a cell proliferation equal to 10.4% (**Figure 5B**). For this reason, the 16μM concentration was excluded from the apoptosis test.

Annexin V-PE/7-AAD double staining allowed to calculate the percentage of apoptotic cells. As shown in **Figure 6** only for the 6-MITC 8μM, compared to the control cultures, a population doubling was detected.

Therefore, on the basis of the obtained results, 1 and 2μM concentrations were selected to be used to assess the potential genotoxicity induced by 6-MITC.

As shown in **Figure 7** also in this case, analogously to the short-term treatment, 6-MITC not induced mutagenic activity. In fact, a MNs frequency statistically significant increase, was not registered in all 6-MITC treated cultures (compared to the control cultures), while a four- and five- time increase was detected for the mutagens MMC 200ng/ml and VINB 6.25ng/ml, respectively (**Figures 7A–C**).

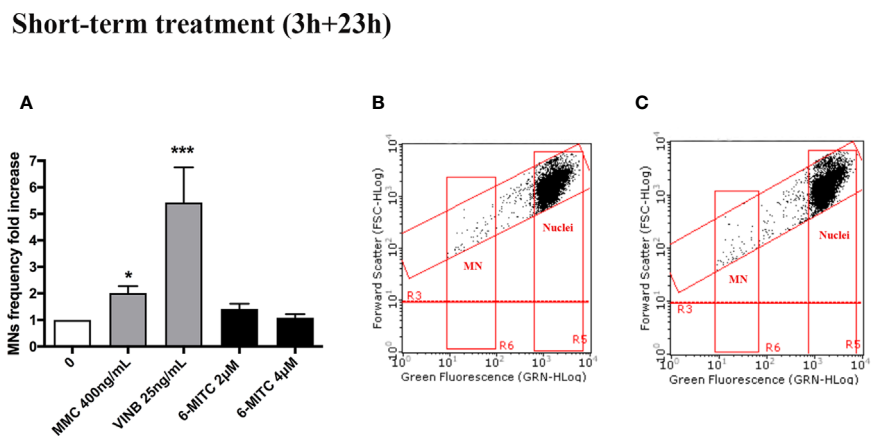

FIGURE 4 | Effect of 6-MITC on mutagenesis after short term treatment. MNs frequency fold increase **(A)** and dot plot obtained by FCM in the control cultures **(B)** and 6-MITC 4μM treated cultures **(C)** on TK6 cells after 3h treatment followed by 23h of recovery in complete medium. Each bar represents the mean ± SEM of five independent experiments. Data were analysed using repeated ANOVA followed by Bonferroni post-test. *p < 0.05 *vs* 0; ***P < 0.01 *vs* 0.

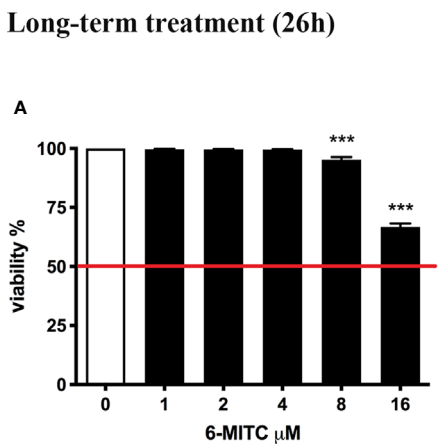

B

Treatment	RPD %
6-MITC 0 μM	100
6-MITC 1 μM	95.5±0.2
6-MITC 2 μM	95.6±0.4
6-MITC 4 μM	80.9±0.7
6-MITC 8 μM	55.2±0.9
6-MITC 16 μM	10.4±0.5

FIGURE 5 | Effect of 6-MITC on cytotocicity and cytostasis after long term treatment. Percentage of viability **(A)** and RPD **(B)** in TK6 cells treated with 6-MITC for 26h. Each bar represents the mean ± SEM of five independent experiments. Data were analysed using repeated ANOVA followed by Dunnet post-test. *** p < 0.001 *vs* 0.

Antimutagenesis of 6-MITC

Short-Term Treatment (3h+23h)

Once the non-mutagenicity of the isothiocyanate was demonstrated to both treatment conditions, the study continued evaluating the possible 6-MITC antimutagenic activity, against the known mutagens previously used as positive control (MMC and VINB), similarly after short- and long- term treatment.

A co-treatment of 3h, followed by 23h of recovery in complete medium, was performed and, also in this case, the cytotoxicity, cytostasis and apoptosis were checked, before proceeding with the genotoxicity analysis. As show in **Figure 8** cell viability (**Figures 8A, C**) and RPD value (**Figures 8B, D**) were abundantly above the threshold established by the OECD guideline no. 487 (**Figures 8A–D**).

An average apoptosis fold increase equal to three time in MMC +6-MITC associations treated cultures respect to the control cultures was observed (**Figure 9A**), while in VINB+6-MITC associations treated cultures an increase on average equal to two times respect to the control cultures was measured (**Figure 9B**).

Overall, the results obtained allowed to proceed with the MN test and to demonstrate the 6-MITC ability to counteract only the VINB mutagenic effect but not the MMC DNA-damage.

In particular, the MNs frequency increase in the MMC treated cultures in presence of 6-MITC 2μM was comparable than cultures treated with the only mutagen MMC, while the co-treatment MMC and 6-MITC 4μM shown a MNs frequency statistically significant increase (4.1 times *vs* 2.0 times in MMC) (**Figures 10A–C**). On the contrary, in the case of aneuploidogen VINB, a MNs frequency

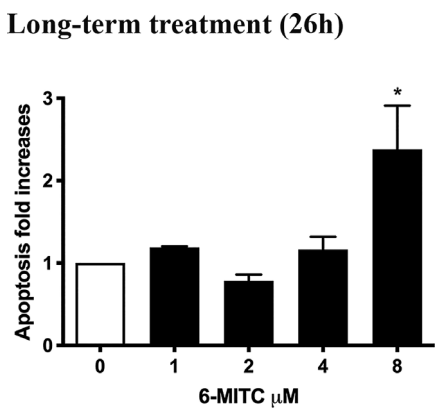

FIGURE 6 | Effect of 6-MITC on apoptosis after long term treatment. Apoptosis fold increase in TK6 cells treated with 6-MITC for 26h. Each bar represents the mean ± SEM of five independent experiments. Data were analysed using repeated ANOVA followed by Bonferroni post-test. *p < 0.05 *vs* 0.

decrease was observed for both 6-MITC associations tested with respect to cultures treated with the mutagen alone, which reaches statistical significance at the highest concentration tested (5.4 times *vs* 4.2 times) (**Figures 10D–F**).

Long-Term Treatment (26h)

The study was concluded by evaluating the antimutagenic activity of 6-MITC at 26h. Similarly, to the short-term treatment, cytotoxicity and cytostasis values respected the established threshold at all the conditions analyzed (**Figures 11A–D**).

Moreover, **Figure 12** show that the apoptosis fold increase reached a doubling in the cultures treated whit VINB alone and in presence of 6-MITC 1μM (**Figures 12A, B**).

Therefore, checked cytotoxicity, cytostasis and apoptosis, the study ended by evaluating the 6-MITC antimutagen activity, after 26h treatment. The MN test confirmed the results obtained at the short term treatment. Infact, also in this case, the association with MMC led to a statistically significant increase in MNs frequency at the highest concentration tested, compared to the treatment with the clastogen alone (3.8 times *vs* 5.5 times) (**Figures 13A–C**) whereas, the association with the VINB reduced in a statistically significant manner the MNs frequency respet to the treatment with aneuploidogen alone at both concentrations tested (2.3 times and 3.3 times *vs* 4.7 times) (**Figures 13D–F**).

DISCUSSION

According to our knowledge, no study has addressed the antigenotoxicity of 6-MITC, the main bioactive compound present on *W. japonica*, and very little information are available concerning the whole extract of this plant. In fact, bibliographic research, conducted on the main databases (*i.e.* PubMed from MEDLINE and Scopus from Elsevier) allowed us to identify only two publications. In particular, Kinae and collaborators demonstrated, using the Ames Test, the antimutagenic activity (in terms of gene mutations) of wasabi root, against the 2-amino-3,8-dimethylimidazo [4,5-f]quinoxaline, a well-known mutagen/carcinogen compound present in broiled fish and meat (Kinae et al., 2000).

More recently, the study conducted by Shimamura et al. documented, through Micronucleus Test and Alkaline Comet Assay, the inhibitory effect of Japanese horseradish, on the acrylamide formation and genotoxicity (Shimamura et al., 2017).

These evidences suggest us to verify if the proven *W. japonica* antimutagenic activity was attributable to the 6-MITC.

Despite Wasabi has long been used in traditional Japanese cuisine, it was initially checked the absence of 6-MITC mutagenicity. For this purpose, the non-cytotoxic and cytostatic doses, after short- and long- term treatment of TK6 cells, were defined. In fact, the OECD guideline no.487 recommends proceeding with the evaluation on genotoxicity, only if the treated

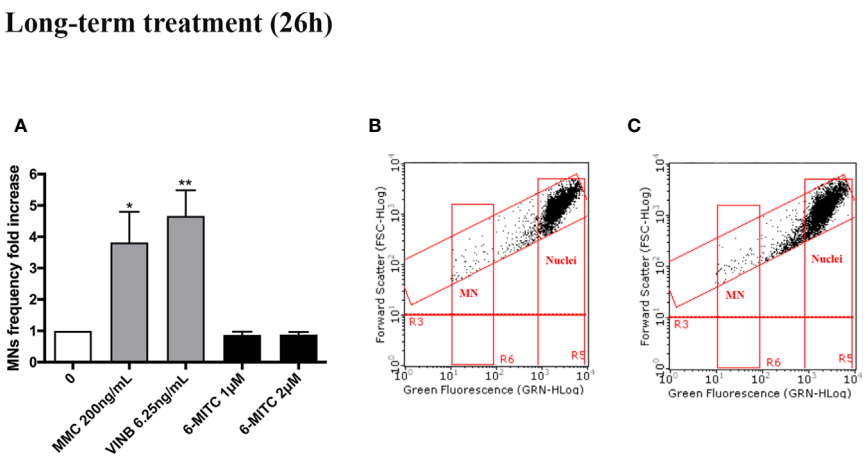

FIGURE 7 | Effect of 6-MITC on mutagenesis after long term treatment. MNs frequency fold increase **(A)** and dot plot obtained by FCM in the control cultures **(B)** and 6-MITC 2 μM treatment cultures **(C)** on TK6 cells after 26h of treatment. Each bar represents the mean ± SEM of five independent experiments. Data were analysed using repeated ANOVA followed by Bonferroni post-test. *p < 0.05 *vs* 0; **P < 0.01 *vs* 0.

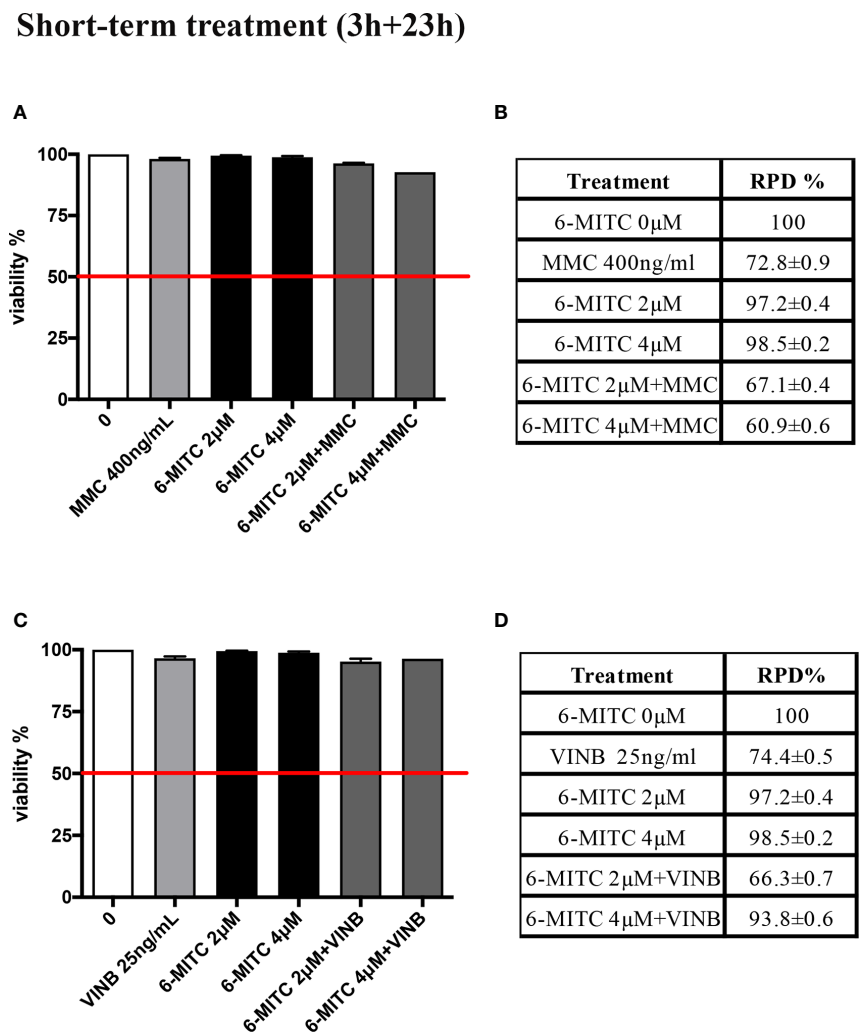

Treatment	RPD %
6-MITC 0μM	100
MMC 400ng/ml	72.8±0.9
6-MITC 2μM	97.2±0.4
6-MITC 4μM	98.5±0.2
6-MITC 2μM+MMC	67.1±0.4
6-MITC 4μM+MMC	60.9±0.6

Treatment	RPD%
6-MITC 0μM	100
VINB 25ng/ml	74.4±0.5
6-MITC 2μM	97.2±0.4
6-MITC 4μM	98.5±0.2
6-MITC 2μM+VINB	66.3±0.7
6-MITC 4μM+VINB	93.8±0.6

FIGURE 8 | Effect of 6-MITC on cytotoxicity and cytostasis after short term treatment Percentage of viability in TK6 cells treated with 6-MITC for 3h followed by 23h of recovery in complete medium in presence or absence of MMC 400ng/mL **(A)** or VINB 25ng/mL **(C)** and relative RPD values for MMC 400ng/mL **(B)** or VINB 25ng/mL **(D)**. Data represents the mean ± SEM of five independent experiments. Data were analysed using repeated ANOVA followed by Dunnet post-test.

population shows a viability and cell proliferation of at least 40% when compared to the control cultures (OECD no. 487, 2016).

At the same time, the induction of apoptosis was analyzed, as cell death alternative mechanism and in order to exclude false positive results, due to the possible confounding between apoptotic bodies and MNs by FCM. Overall, based on the results obtained, the concentrations to be used for the evaluation of mutagenicity were selected and, as can be easily predictable, 6-MITC did not show any mutagenic activity both after 3 and 26h treatment.

Subsequently, the study focused on the analysis of the isothiocyanate antimutagenic potential, against two known mutagenic agents: the clastogen MMC and the aneuploidogen VINB.

MMC is characterized by a complex mechanism of action, being able to generate monoalkylation or dialkylation products, and to form covalent cross-linking, between the DNA complementary strands. This interaction prevents strands separation, inhibits DNA replication and causes its break (Tomasz, 1995). Furthermore, MMC generates radical oxygen species such as O_2, H_2O_2, OH*, so the association with antioxidant molecules represent a possible approach to prevent DNA damage (Garcia et al., 2006; Unal et al., 2013). Since the antioxidant properties of wasabi have long been demonstrated (Morimitsu et al., 2002; Lee et al., 2010), it made sense to hypothesize that it was able to counteract the MMC genotoxicity. However, in the present research not only a protective effect was not observed, but even, when 6-MITC is associated with MMC, a statistically significant increase in the MNs frequency was registered. At the moment, exclusively on the basis of the results obtained, it's difficult to hypothesize a possible explanation of this increase. Certainly, the data must be checked on a greater number of mutagens, to verify if it is common to all clastogen agents or if it is peculiar of MMC.

On the contrary, the isothiocyanate has shown to counteract the mutagenic capacity of the aneuploidogen VINB, which acts at

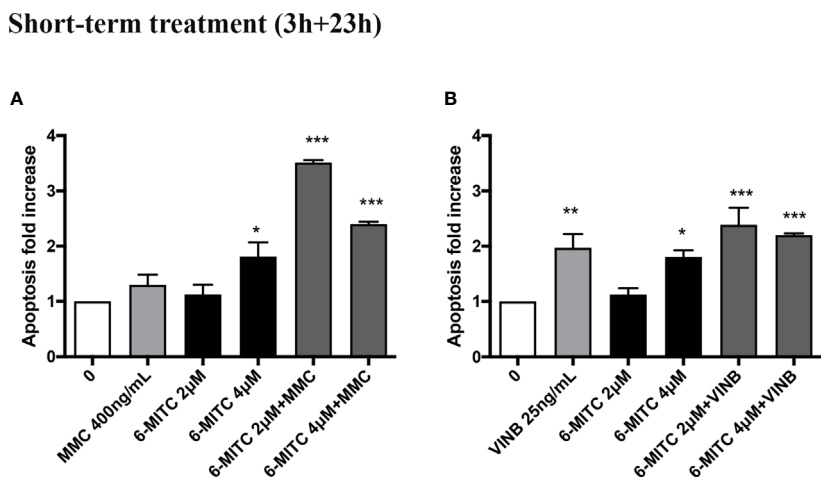

FIGURE 9 | Effect of 6-MITC on apoptosis after short term treatment. Apoptosis fold increase in TK6 cells treated with 6-MITC for 3h followed by 23h of recovery in complete medium in presence or absence of MMC 400ng/mL **(A)** or VINB 25ng/mL **(B)**. Each bar represents the mean ± SEM of five independent experiments. Data were analysed using repeated ANOVA followed by Dunnet post-test. *p < 0.05 *vs* 0; **p < 0.01 *vs* 0; ***p < 0.001 *vs* 0.

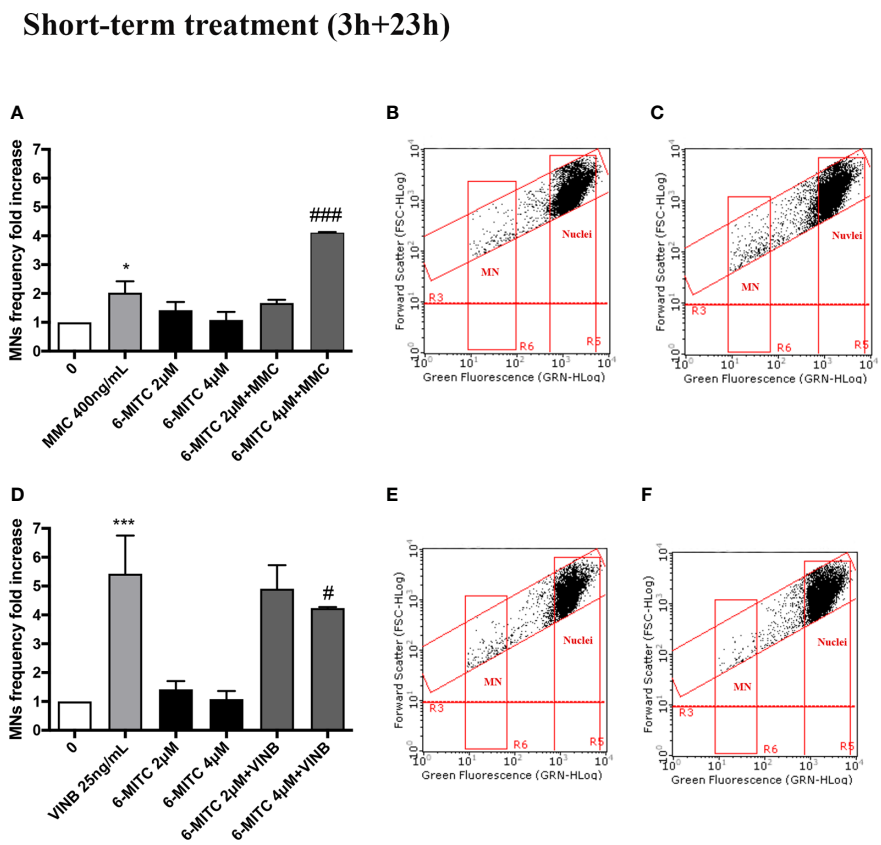

FIGURE 10 | Effect of 6-MITC on antimutagenesis after short term treatment. MNs frequency fold increase on TK6 cells treated for 3h with 6-MITC, followed by 23h of recovery in complete medium, in presence or absence of MMC 400ng/mL **(A)** or VINB 25ng/mL **(D)**. Dot plot obtained by FCM of MMC 400ng/mL **(B)**, MMC400ng/mL + 6-MITC 4μM **(C)**, VINB 25ng/mL **(E)** and VINB 25ng/mL + 6-MITC 4μM **(F)**. Each bar represents the mean ± SEM of five independent experiments. Data were analysed using repeated ANOVA followed by Dunnet or Bonfferoni post-test. *p < 0.05 *vs* 0; ***P < 0.001 *vs* 0. ###p < 0.001 *vs* MMC; #p < 0.05 *vs* VINB.

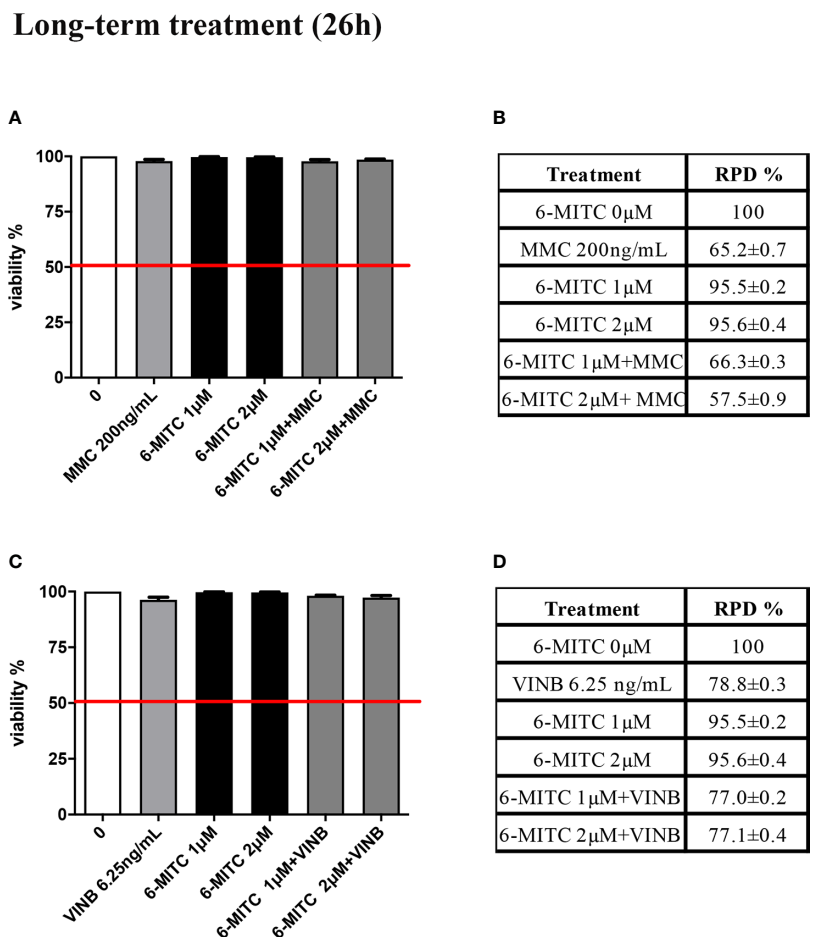

Treatment	RPD %
6-MITC 0μM	100
MMC 200ng/mL	65.2±0.7
6-MITC 1μM	95.5±0.2
6-MITC 2μM	95.6±0.4
6-MITC 1μM+MMC	66.3±0.3
6-MITC 2μM+ MMC	57.5±0.9

Treatment	RPD %
6-MITC 0μM	100
VINB 6.25 ng/mL	78.8±0.3
6-MITC 1μM	95.5±0.2
6-MITC 2μM	95.6±0.4
6-MITC 1μM+VINB	77.0±0.2
6-MITC 2μM+VINB	77.1±0.4

FIGURE 11 | Effect of 6-MITC on cytotocicity and cytostasis after long term treatment. Percentage of viable in TK6 cells treated with 6-MITC for 26h in presence or absence of MMC 200ng/mL **(A)** or VINB 6.25ng/mL **(C)** and relative RPD values for MMC 200ng/mL **(B)** or VINB 6.25ng/mL **(D)**. Each bar represents the mean ± SEM of five independent experiments. Data represents the mean ± SEM of five independent experiments Data were analysed using repeated ANOVA followed by Dunnet post-test.

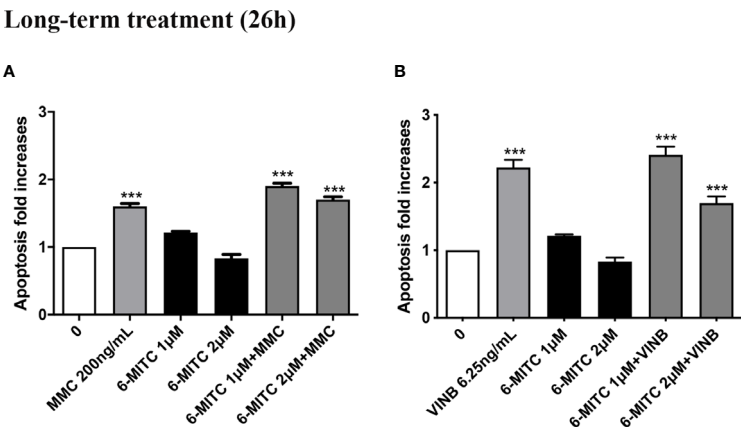

FIGURE 12 | Effect of 6-MITC on apoptosis after long term treatment. Apoptosis fold increase in TK6 cells treated with 6-MITC for 26h in presence or absence of MMC 200ng/mL **(A)** or VINB 6.25ng/mL **(B)**. Each bar represents the mean ± SEM of five independent experiments. Data were analysed using repeated ANOVA followed by Dunnet post-test. ***$p < 0.001$ vs 0.

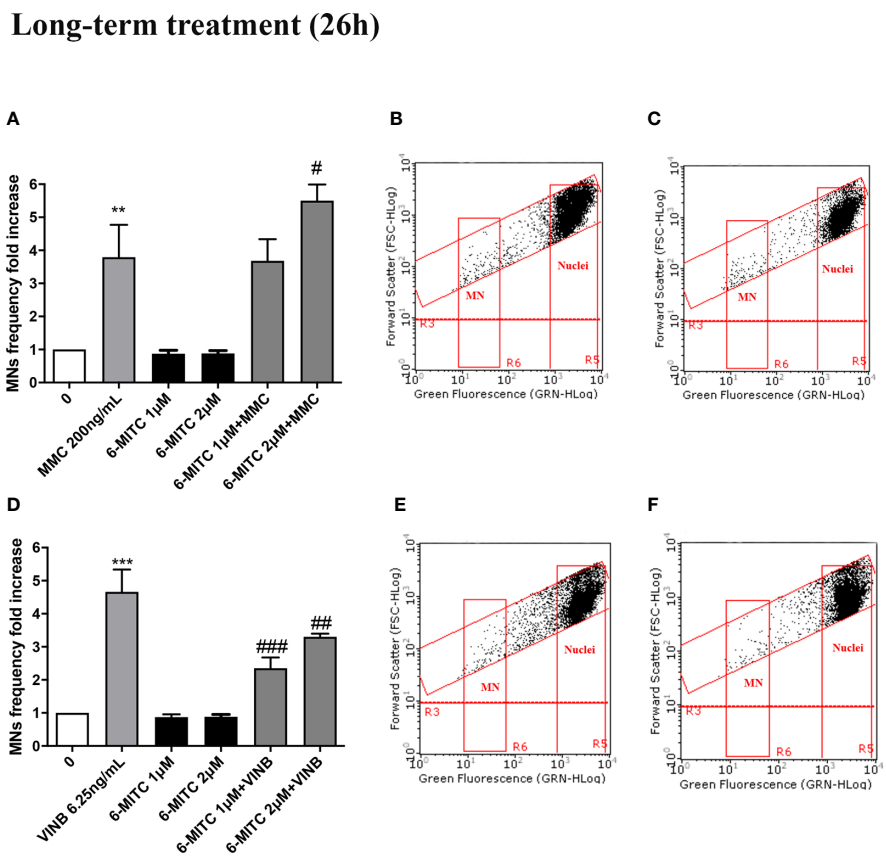

FIGURE 13 | Effect of 6-MITC on antimutagenesis after long term treatment. MNs frequency fold increase on TK6 cells treated for 26h with 6-MITC in presence or absence of MMC 200ng/mL **(A)** or VINB 6.25ng/mL **(D)**. Dot plot obtained by FCM of MMC 200ng/mL **(B)**, MMC 200ng/mL + 6-MITC 2μM **(C)**, VINB 6.25ng/mL **(E)** and VINB 6.25ng/mL + 6-MITC 2μM **(F)**. Each bar represents the mean ± SEM of five independent experiments. Data were analysed using repeated ANOVA followed by Dunnet or Bonfferoni post-test. $^{**}p < 0.01$ *vs* 0; $^{***}P < 0.001$ *vs* 0. $^{\#}p < 0.05$ *vs* MMC; $^{\#\#}p < 0.01$ *vs* VINB; $^{\#\#\#}p < 0.001$ *vs* VINB.

the level of cellular mitosis, by preventing tubulin polymerization and consequently, inhibiting the microtubules aggregation (Navarro et al., 1989).

The statistical analysis evidenced a significant decrease in the MNs frequency equal to about on half after the long treatment with 6 MITC 1μM concentration.

Overall, our work suggests to impute to 6-MITC an antimutagenic capacity. Our findings, are preliminary, since they are obtained against only two mutagens, but allow to highlight the possible mechanism underlying this activity.

In fact, from our data it seems that the isothiocyanate does not counteract the structural DNA damage, but rather the genomic DNA damage, highlighting the possibility that it acts on the mitotic spindle formation or at the chromosomal segregation time.

Alternatively, the co-treatment could suggest a direct extracellular interaction between the isothiacyanate and the mutagenic agent.

These hypothesis needs to be confirmed on a greater number of mutagens, but from the present research emerges an additional interesting biological potential of the 6-MITC. Indeed, the ability to inhibit or counteract the mutations at the cellular level has a great therapeutic value and it represents a less investigated mechanisms through which a chemopreventive agent can express its activity (Amkiss et al., 2013; Cristóbal-Luna et al., 2018). In conclusion, our work, in addition to the induction of apoptosis and the inhibition of cellular proliferation, previously demonstrated (Lenzi et al., 2017), better defines the chemopreventive profile of this interesting isothiocyanate.

DATA AVAILABILITY STATEMENT

The datasets generated for this study are available on request to the corresponding author.

AUTHOR CONTRIBUTIONS

PH and ML designed the project and supervised the experiments. VC performed the experiments and data analysis. VC writing—original draft preparation. VC, PH, and ML writing—review and editing. All authors contributed to the article and approved the submitted version.

REFERENCES

Amkiss, S., Dallouh, A., Idaomar, M., and Amkiss, B. (2013). Genotoxicity and anti-genotoxicity of fennel plant (Foeniculum vulgare Mill) fruit extracts using the somatic mutation and recombination test (SMART). *Afr. J. Food Sci.* 7 (8), 193–197. doi: 10.5897/AJFS13.0999

Basu, A. K. (2018). DNA Damage, Mutagenesis and Cancer. *Int. J. Mol. Sci.* 19 (4), pii: E970. doi: 10.3390/ijms19040970

Cristóbal-Luna, J. M., Álvarez-González, I., Madrigal-Bujaidar, E., and Chamorro-Cevallos, G. (2018). Grapefruit and its biomedical, antigenotoxic and chemopreventive properties. *Food Chem. Toxicol.* 112, 224–234. doi: 10.1016/j.fct.2017.12.038

Garcia, A. L., Filippi, S., Mosesso, P., Calavani, M., Nicolai, R., Mosconi, L., et al. (2006). The protective effect of L-carnitine in peripheral blood human lymphocytes exposed to oxidative agents. *Mutagenesis* 21, 21–27. doi: 10.1093/mutage/gei065

Hirokuni, T., Hisashi, K., Taketo, Y., and Taketo, A. (1998). Effects of synthetic hydroxy isothiocyanates on microbial systems. *Biosci. Biotechnol. Biochem.* 62 (3), 491–495. doi: 10.1271/bbb.62.491

Hsuan, S. W., Chyau, C. C., Hung, H. Y., Chen, J. H., and Chou, F. P. (2016). The induction of apoptosis and autophagy by Wasabia japonica extract in colon cancer. *Eur. J. Nutr.* 55 (2), 491–503. doi: 10.1007/s00394-015-0866-5

Kinae, N., Masuda, H., Shin, I. S., Furugori, M., and Shimoi, K. (2000). Functional properties of wasabi and horseradish. *Biofactors* 13 (1-4), 265–269. doi: 10.1002/biof.5520130140

Ko, M. O., Kim, M. B., and Lim, S. B. (2016). Relationship between Chemical Structure and Antimicrobial Activities of Isothiocyanates from Cruciferous Vegetables against Oral Pathogens. *J. Microbiol. Biotechnol.* 26 (12), 2036–2042. doi: 10.4014/jmb.1606.06008

Lee, Y. S., Yang, J. H., Bae, M. J., Yoo, W. K., Ye, S., Xue, C. C. L., et al. (2010). Antioxidant and anti-hypercholesterolemic activities of wasabia japonica. *Evid.-Based Complement. Alternat. Med.* 7 (4), 459–464. doi: 10.1093/ecam/nen038

Lenzi, M., Fimognari, C., and Hrelia, P. (2014). Sulforaphane as a promising molecule for fighting cancer. *Cancer Treat Res.* 159, 207–223. doi: 10.1007/978-3-642-38007-5_12

Lenzi, M., Cocchi, V., Malaguti, M., Barbalace, M. C., Marchionni, S., Hrelia, S., et al. (2017). 6-(Methylsulfonyl) hexyl isothiocyanate as potential chemopreventive agent: molecular and cellular profile in leukaemia cell lines. *Oncotarget* 8 (67), 111697–111714. doi: 10.18632/oncotarget.22902

Lenzi, M., Cocchi, V., and Hrelia, P. (2018). Flow cytometry vs optical microscopy in the evaluation of the genotoxic potential of xenobiotic compounds. *Cytometry B. Clin. Cytom.* 94 (5), 696–706. doi: 10.1002/cyto.b.21546

Lenzi, M., Cocchi, V., Cavazza, L., Bilel, S., Hrelia, P., and Marti, M. (2020). Genotoxic Properties of Synthetic Cannabinoids on TK6 Human Cells by Flow Cytometry. *Int. J. Mol. Sci.* 21 (3):1150. doi: 10.3390/ijms21031150

Melchini, A., Traka, M. H., Catania, S., Miceli, N., Taviano, M. F., Maimone, P., et al. (2013). Antiproliferative activity of the dietary isothiocyanate erucin, a bioactive compound from cruciferous vegetables, on human prostate cancer cells. *Nutr. Cancer.* 65 (1), 132–138. doi: 10.1080/01635581.2013.741747

Mizuno, K., Kume, T., Muto, C., Takada-Takatori, Y., Izumi, Y., Sugimoto, H., et al. (2011). Glutathione biosynthesis via activation of the nuclear factor E2-related factor 2 (Nrf2)-antioxidant-response element (ARE) pathway is essential for neuroprotective effects of sulforaphane and 6-(methylsulfinyl) hexyl isothiocyanate. *J. Pharmacol. Sci.* 115 (3), 320–328. doi: 10.1254/jphs.10257fp

Morimitsu, Y., Hayashi, K., Nakagawa, Y., Fujii, H., Horio, F., Uchida, K., et al. (2000). Antiplatelet and anticancer isothiocyanates in Japanese domestic horseradish, Wasabi. *Mech. Ageing Dev.* 116 (2-3), 125–134. doi: 10.1016/s0047-6374(00)00114-7

Morimitsu, Y., Nakagawa, Y., Hayashi, K., Fujii, H., Kumagai, T., Nakamura, Y., et al. (2002). A sulforaphane analogue that potently activates the Nrf2-dependent detoxification pathway. *J. Biol. Chem.* 277 (5), 3456–3463. doi: 10.1074/jbc.M110244200

Navarro, M., Bellmunt, J., Balañá, C., Colomer, R., Jolis, L., and del Campo, J. M. (1989). Mitomycin-C and-vinblastine-in advanced breast cancer. *Oncology* 46 (3), 137–142. doi: 10.1159/000226702

OECD Guideline for the Testing of Chemicals (2016). *Test No. 487: In vitro mammalian cell micronucleus test*. https://www.oecd.org/chemicalsafety/-test-no-487-in-vitromammalian-cell-micronucleus-test-9789264264861-en.htm

Overview of the Set of OECD Genetic Toxicology Test Guidelines and Updates Performed in 2014–2015 (2017). *Environment Directorate Joint Meeting of the Chemicals Committee and the Working Party on Chemicals, Pesticides and Biotechnology*. http://www.oecd.org/o_cialdocuments/publicdisplaydocumentpdf/?cote=ENV-JM-MONO(2016)33/rev1∓doclanguage=en

Shimamura, Y., Iio, M., Urahira, T., and Masuda, S. (2017). Inhibitory effects of Japanese horseradish (Wasabia japonica) on the formation and genotoxicity of a potent carcinogen, acrylamide. *J. Sci. Food Agric.* 97 (8), 2419–2425. doi: 10.1002/jsfa.8055

Słoczyńska, K., Pękala, E., Wajda, A., Węgrzyn, G., and Marona, H. (2010). Evaluation of mutagenic and antimutagenic properties of some bioactive xanthone derivatives using *Vibrio harveyi* test. *Lett. Appl. Microbiol.* 50 (3), 252–257. doi: 10.1111/j.1472-765X.2009.02781

Sobol, Z., Homiski, M., Dickinson, D. A., Spellman, R. A., Li, D., Scott, A., et al. (2012). Development and validation of an in vitro micronucleus assay platform in TK6 cells. *Mut. Res.* 746 (1), 29–34. doi: 10.1016/j.mrgentox.2012.02.005

Tomasz, M. (1995). Mitomycin C: small, fast and deadly (but very selective). *Chem. Biol.* 2 (9), 575–579. doi: 10.1016/1074-5521(95)90120-5

Unal, F., Taner, G., Yuzbasioglu, D., and Yilmaz, S. (2013). Antigenotoxic effect of lipoic acid against mitomycin-C in human lymphocyte cultures. *Cytotechnology* 65, 553–565. doi: 10.1007/s10616-012-9504-8

Uto, T., Fujii, M., and Hou, D.-X. (2005). 6-(Methylsulfinil) hexyl isothiocyanate suppresses inducible nitric oxide synthase expression through the inhibition of Janus kinase 2-mediated JNK pathway in lipopolysaccharide-activated murine macrophages. *Biochem. Pharmacol.* 70 (8), 1211–1221. doi: 10.1016/j.bcp.2005.07.011

Uto, T., Fujii, M., and Hou, D. X. (2007). Effects of 6-(methylsulfinyl)hexyl isothiocyanate on cyclooxygenase-2 expression induced by lipopolysaccharide, interferon-gamma and 12-O-tetradecanoylphorbol-13-acetate. *Oncol. Rep.* 17 (1), 233–238. doi: 10.3892/or.17.1.233

Uto, T., Hou, D.-X., Morinage, O., and Shoyama, Y. (2012). Molecular Mechanism Underlying Anti Inflammatory Actions of 6-(Methylsulfinyl) hexyl Isothiocyanate Derived from Wasabi (*Wasabia japonica*). *Adv. Pharmacol. Sci.* 2012, 614046. doi: 10.1155/2012/614046

Weil, M. J., Zhang, Y., and Nair, M. G. (2004). Colon cancer proliferating desulfosinigrin in wasabi (Wasabia japonica). *Nutr. Cancer.* 48 (2), 207–213. doi: 10.1207/s15327914nc480211

Weil, M. J., Zhang, Y., and Nair, M. G. (2005). Tumor cell proliferation and cyclooxygenase inhibitory constituents in horseradish (Armoracia rusticana) and Wasabi (Wasabia japonica). *J. Agric. Food Chem.* 53 (5), 1440–1444. doi: 10.1021/jf048264i

Conflict of Interest: The authors declare that the research was conducted in the absence of any commercial or financial relationships that could be construed as a potential conflict of interest.

frontiers in Pharmacology

REVIEW
published: 11 September 2020
doi: 10.3389/fphar.2020.01100

Therapeutic Applications of Human and Bovine Colostrum in the Treatment of Gastrointestinal Diseases and Distinctive Cancer Types: The Current Evidence

Siddhi Bagwe-Parab[1], Pratik Yadav[1], Ginpreet Kaur[1], Hardeep Singh Tuli[2]* and Harpal Singh Buttar[3]*

[1] Shobhaben Pratapbhai Patel School of Pharmacy and Technology Management, Shri Vile Parle Kelavani Mandals Narsee Monjee Institute of Management Studies, Mumbai, India, [2] Department of Biotechnology, Maharishi Markandeshwar (Deemed to be University), Mullana, Ambala, India, [3] Department of Pathology and Laboratory Medicine, Faculty of Medicine, University of Ottawa, Ottawa, ON, Canada

OPEN ACCESS

Edited by:
Lokesh Bhatt,
Dr. Bhanuben Nanavati College of Pharmacy, India

Reviewed by:
Mizuho Inagaki,
Gifu University, Japan
Saartjie Roux,
Nelson Mandela University, South Africa

***Correspondence:**
Ginpreet Kaur
Ginpreet.Kaur@nmims.edu
Hardeep Singh Tuli
hardeep.biotech@gmail.com

Specialty section:
This article was submitted to Pharmacology of Anti-Cancer Drugs, a section of the journal Frontiers in Pharmacology

Received: 27 January 2020
Accepted: 06 July 2020
Published: 11 September 2020

Citation:
Bagwe-Parab S, Yadav P, Kaur G, Tuli HS and Buttar HS (2020) Therapeutic Applications of Human and Bovine Colostrum in the Treatment of Gastrointestinal Diseases and Distinctive Cancer Types: The Current Evidence. Front. Pharmacol. 11:01100. doi: 10.3389/fphar.2020.01100

The incidence of gastrointestinal disorders (GID) and cancers is escalating all over the world. Limited consumption of colostrum by newborns not only weakens the immune system but also predisposes infants to microbial infections. Colostrum is nature's perfect food, sometimes referred to as the 'elixir of life'. Breast-fed infants have a lower incidence of GI tract infections than infants fed formula or cow's milk. As per WHO statistics, cancer is the most prevalent disease globally and causes 9.6 million deaths worldwide. The current strategies for treating cancer include chemotherapy, radiation, and surgery. However, chemotherapy and radiation exposure are usually associated with serious long-term side effects and deterioration in the quality of life (QOL) of patients. Furthermore, the hospitalization and medication costs for treating cancers are exorbitant and impose high economic burden on healthcare systems. People are desperately looking for cost-effective and affordable alternative therapies for treating GID and cancers. Therefore, there is an urgent need for clinically evaluating the anticancer compounds isolated from plants and animals. Such therapies would not only be economical and have fewer side effects, but also help to improve the QOL of cancer patients. Recently, bovine colostrum (BC) has caught the attention of many investigators to explore its anticancer potential in humans. BC impregnated dressings are highly effective in treating chronic wounds and diabetic foot ulcer. BC is rich in lactoferrin, a glycoprotein with strong antioxidant, anti-inflammatory, anti-cancer, and anti-microbial properties. Intravaginal application of BC tablets is effective in causing the regression of low-grade cervical intraepithelial neoplasia. The underlying mechanisms of BC at cellular, genetic, and molecular levels remain to be ascertained. Oral BC supplement is well-tolerated, but some people may experience problems such as flatulence and nausea. Well-designed, randomized, placebo-controlled, clinical trials are needed to access the therapeutic potential, long-term safety, and optimal doses of BC products. This review is aimed to highlight the anticancer potential of BC and its

components, and the therapeutic applications of BC supplements in treating gastrointestinal diseases in children and adults. We also discuss the health promotion benefits and therapeutic potential of BC nutraceuticals in reducing the incidence of non-communicable diseases.

Keywords: inflammatory bowel disease (IBD), anticancer therapy, antimicrobial activity, cervical intraepithelial neoplasia, proline-rich polypeptide, immunoglobulins, conjugated linoleic acid

INTRODUCTION

Role of Colostrum Against Gastrointestinal Disorders (GIDs)

Necrotizing enterocolitis and neonatal sepsis are the major gastrointestinal ailments in premature babies, newborns, and toddlers, especially those whose mothers are unable to provide colostrum. Breast-fed infants have a lower incidence of GI tract infections than infants fed with formula or cow's milk. GIDs can lead to stunted physical growth and neurodevelopment, retarded immune function, malabsorption of nutrients, and susceptibility to other diseases like allergies and asthma at an early age. In newborns, colostrum acts as a broad-spectrum antibacterial agent that protects against gut infections as well as contributes to physical growth, immune function, and development of the GI tract. In adults, colostrum promotes healing of the GI tract and protects against gut pathogens (bacteria, viruses, fungi, yeast, mold, etc.), and leaky gut syndrome. Mother's colostrum or first milk is significantly richer in biologically active peptides, anti-oxidants, anti-inflammation agents, and growth promoting factors that differ substantially from later milk (Bagwe et al., 2015; Buttar et al., 2017). According to Gensollen et al. (2016), some GIDs are caused by the compromised immune system in neonates. The intake of mother's colostrum lays the foundation for life-long immunity. In some cases, the neonate's immunity is compromised due to the lack of mother's colostrum or breast-feeding difficulty (Le Doare et al., 2018). Consequently, GID problems arise during adolescence or adulthood due to a deficient immune system. It is therefore imperative for neonates to consume colostrum for physical growth and proper development of the immune system, and to curb GID disorders later in life.

It has been suggested that bovine colostrum (BC) contains almost ninety bioactive components. These bioactive substances consist of immunoglobulins and growth factors, antibodies, higher levels of amino acids, oligosaccharides, antimicrobial compounds, and immune regulators like lactoferrin (Jacqmin, 2000). BC is also rich in vitamins and minerals. Colostrum provides nutrients in a highly concentrated low-volume form to the newborn. Due to its laxative properties, colostrum assists in the passage of baby's initial stools or meconium and helps to remove excess bilirubin from the infant's body to prevent jaundice (Buttar et al., 2017). Excess accumulation of bilirubin in the neonate can cause jaundice, anemia, liver cirrhosis, and Gilbert's syndrome (Maqbool, 1992; Crittenden et al., 2007; de Almeida and Draque, 2007). Research has shown that BC is 100-fold to 1,000-fold more potent than human colostrum. Thus, human infants can thrive very well by consuming infant- formula containing BC supplements that can provide passive immunity and growth factors needed for physical and gastrointestinal development. BC is an emerging nutraceutical and innovative therapeutic products being developed for children and adults.

Cancer

Cancer is the second leading cause of mortality and morbidity worldwide, behind only cardiovascular diseases (Siegel et al., 2016; Miller et al., 2019). Cancer is a collective name for a disease where the abnormal body cells divide in an uncontrollable fashion in a body part or organ, resulting in a tumor or carcinoma. Genetic, epigenetic, and environmental factors play an important role in the occurrence and progression of cancer. There are two types of cancer: benign or noninvasive and malignant or invasive. Malignant cancer cells can invade nearby tissues or organs and can also travel to distant places in the body through blood or the lymphatic system, and consequently form a new tumor far away from the original one. According to Seebacher et al. (2019), nearly 14.1 million people suffer from cancer, and about 9.6 million deaths were reported worldwide in 2018. From a mortality point of view, 1 out of 6 deaths are caused by cancer (Bray et al., 2018). The common types of cancers include: carcinoma, sarcoma, leukemia, lymphoma, melanoma, lung, colorectal, prostate, and breast cancer (Brandal and Heim, 2015; Linehan et al., 2016; Rosenberg et al., 2016; Tricoli et al., 2016; Bullinger et al., 2017; Etienne et al., 2017; Meurer et al., 2017; Rajyaguru et al., 2018; Miolo et al., 2019). The current strategies for cancer treatment consist of chemotherapy, radiotherapy, bone marrow transplants, and surgery. However, these therapies have drawbacks and limitations; for instance, radiation therapy causes indirect damage to surrounding tissues, and chemotherapy results in vital organ toxicity and also causes drug resistance, whereas surgical interventions may sometimes precipitate tumor recurrence (Formenti and Demaria, 2009; Taylor and Kirby, 2015; Vitetta et al., 2019). Recent trends in cancer treatment also include targeted drug delivery and immunotoxin therapy (Vitetta et al., 2019). Immunotoxin is a conjugated protein which blends a targeted conjugate with a toxin. These immunotoxins enter into the cancer cell through endocytosis and lead to cell death.

Stomach, colorectal, and lung cancer are common in both sexes, whereas liver and prostate cancer is common in men, and breast and cervical cancer occur in women. Currently, gastric

Abbreviations: BC, Bovine colostrum; CLA, Conjugated linolenic acid; GID, Gastrointestinal disorders; GIT, Gastrointestinal tract; IBD, Inflammatory bowel disease; NASH, Non-Alcoholic Steato Hepatitis; NK, Natural killer; NSAIDS = Non-steroidal anti-inflammatory drugs.

cancer is one of the serious diseases worldwide. According to global cancer statistics data, gastric cancer is the fourth most common cancer worldwide. Serious vital organ deleterious effects happen when gastric cancer is treated by chemotherapy (Rugge et al., 2015; Rathe et al., 2019). Therefore, there is an urgent need for the development of less toxic therapeutic agents for the prevention and cure of stomach cancer (Farziyan et al., 2016).

Role of BC for the Treatment of Cancer and Gastrointestinal Diseases (GIDs)

Colostrum or first milk is secreted by all female mammals, including women, during the first four days after parturition and is provided to their neonates during the initial 24-48 hours after birth (Bagwe et al., 2015; Agarwal and Gupta, 2016; Hyrslova et al., 2016; Jolly and Mascaro, 2016; Buttar et al., 2017). Colostrum is thick, sticky, yellowish liquid which not only provides nutrition and immunity but also gives protection against microbial infections. Almost all essential nutrients such as protein, fat, lactose, lactoferrin, immunoglobulins, vitamins and minerals, and growth factors are present in the colostrum in significantly higher concentrations than the regular mature milk (Shah, 2000). Colostrum creates life-long immunity in the newborn and helps in maturing the GI tract of babies. Whereas in adults, colostrum promotes healing of the GI tract and protects against gut pathogens (bacteria, viruses, fungi, yeast, mold, etc.), and leaky gut syndrome (Shah, 2000; Hurley and Theil, 2011; Osada et al., 2014; Wu Xiaoyun and Xiong Lin, 2015). The major bioactive components of bovine colostrum and their functions in children and adults are summarized in **Table 1**. BC acquired from cows and buffalo possess more immunoglobulins than human colostrum, and human infants could benefit by consuming BC (Ulfman et al., 2018). BC is usually regarded as safe in humans, whereas some people may experience nausea and flatulence initially, which declines over time. BC should not be given to individuals allergic to milk and milk products.

The central theme of this review is to address the potential benefits of colostrum nutrients in children and adults as well as the usefulness of BC components for the treatment of cancer and gastrointestinal disorders. As discussed earlier, the conventional cancer therapies include chemotherapy, radiotherapy, bone marrow transplant, and surgical interventions, but these therapies have drawbacks and limitations. Hence there is a need for cost-effective and safe novel therapies for the treatment of cancer. Limited numbers of clinical trials with BC have shown anticancer effects in different cancer types (Layman et al., 2018; França-Botelho, 2019). The anticancer effects of lactoferrin, proline rich polypeptides, conjugated linolenic acid (CLA), and alpha-lactalbumin are presented in **Table 2**. The nutrient profile of BC is markedly different from mature milk. The quantitative concentrations of the main constituents of cow colostrum and cow milk are depicted in **Table 3**. It can be seen from **Table 4** that the concentrations of lactoferrin, IgA, insulin like growth factor, growth hormone, and epidermal growth factor are markedly higher in human colostrum as opposed to bovine colostrum (Godhia and Patel, 2013, Bagwe et al., 2015).

TABLE 1 | Composition of bovine colostrum and functions in children and adults.

Components	Function	Reference
Vitamins (A, B1, B2, B6, B12, D, E) Minerals (Na, K, Ca, P, S, Mg, Mn, Zn, Cu, Fe) Amino acids and essential fatty acids	Promote health and growth of the infant.	(McGrath et al., 2016)
Immune factors Proline-rich polypeptide (PRP)	Regulate function of the thymus gland, and reduce oxidative stress.	(Stelwagen et al., 2009)
Immunoglobulins	IgG neutralizes toxins and microbes. IgA, IgD, IgE, and IgM destroy bacteria and are highly antiviral.	
Lactoferrin	Lactoferrin is an anti-viral, anti-inflammatory, and anti-bacterial iron-binding glycoprotein with potential therapeutic applications in cancer and HIV.	
Growth factors Growth hormone (GH) Platelet-derived growth factor (PDGF)	Stimulate DNA synthesis, enhance cell growth and tissue growth.	(Stelwagen et al., 2009)
Fat (6.7%) Protein (14.9%) Lactose (2.5%)		

N. B. Fat content in cow colostrum (6.7%) is higher than human colostrum (3–5%).
Protein content in cow colostrum (14.9%) is significantly greater than human colostrum (0.8–0.9%).
Lactose content in cow colostrum (2.5%) is significantly lower than human colostrum (6.9–7.2%).
[Source: (Bagwe et al., 2015; Buttar et al., 2017)]

ROLE OF HUMAN AND BOVINE COLOSTRUM IN THE MATURATION OF GI TRACT IN BABIES

Many researchers have shown that colostrum plays a critically significant role in the growth and maturity of the GI tract in infants. The nutrients in colostrum create a suitable environment - namely biochemical, physiological, morphological, functional, immunological, and antimicrobial - for the maturity of the gastrointestinal tract in new-born babies (Pluske, 2016). Recent studies performed on piglets, serving as a model for human infants, have suggested that the epidermal growth factor of BC is responsible for the growth and maturity of the GI tract in infants (Bedford et al., 2015). Another study in piglets also demonstrated the growth promoting effects of bovine lactoferrin in the stimulation of intestinal cell proliferation, increased crypt depth, and villus length. Lactoferrin is a glycoprotein with strong antioxidant, anti-inflammation, anti-cancer, and anti-microbial properties. Lactoferrin induces the stimulation of T-helper-1/T-helper-2 cytokine immune response and secretion of anti-inflammatory cytokines. It has been observed that lactoferrin can prevent gastric infections, necrotizing enterocolitis and late onset sepsis in children (Pammi and Abrams, 2015; Donovan, 2016; Pieper et al., 2016).

TABLE 2 | Important components of bovine colostrum: Functions and anticancer effects.

Component	Function	Anticancer Effect	Reference
Lactoferrin	Antibacterial, antiviral, antitumor	Gastric, lung, colorectal, breast	(Layman et al., 2018; França-Botelho, 2019)
Proline-rich polypeptides, Conjugated linolenic acid (CLA)	Promotion of T and NK cell activation	Ovaria, breast, rectal	
Alpha-lactalbumin	Antiviral, antitumor	Breast	

TABLE 3 | Main components of bovine colostrum and bovine milk: Amounts represented as per liter.

Component	Bovine colostrum (per liter)	Bovine milk (per liter)	Reference
IgG1	35-90 gram	0.30-0.40 gram	(Elfstrand et al., 2002)
IgG2	1.5-2 gram	0.03-0.08 gram	
IgA	3-6.5 gram	0.04-0.06 gram	(Bagwe et al., 2015)
IgM	3.8-6 gram	0.03-0.06 gram	(Buttar et al., 2017)
Lactoferrin	1.5-5 gram	0.1-0.3 gram	
Crude protein	41-140 gram	34 gram	
Growth hormone (GH)	<1μg	<0.03μg	
TNF-α	926 μg	3.3μg	

TABLE 4 | Comparison of human colostrum and bovine colostrum.

Component	Human colostrum (mg/ml)	Bovine colostrum (mg/ml)	Reference
Lactoferrin	700	100	(Godhia and Patel, 2013)
IgA	17.35	3.9	
IgG	0.43	47.6	(Bagwe et al., 2015)
IgM	1.59	4.2	
Insulin-like growth factor	18	10	
Growth hormone	41 ng/L	<0.03ng/L	
Epidermal growth factor	200 μg/L	30-50 μg/L	

APPLICATION OF BC IN TREATING INFLAMMATORY BOWEL DISEASE (IBD) AND NONALCOHOLIC STEATOHEPATITIS (NASH)

Inflammatory bowel diseases (IBDs) result from alterations in the systemic immune response and modulation of the gut immune system, which induce inflammation-mediated damage to the gastro-intestinal tract and injury to related organs. BC supplements have been used as an alternative therapy for the treatment of nonalcoholic steatohepatitis (NASH) and insulin resistance type 2 diabetes and colitis. Hyperimmune bovine colostrum is enriched with IgG and enhanced with glycosphingolipid immune adjuvants and anti-lipopolysaccharides. To determine the safety and efficacy of hyperimmune bovine colostrum (Imm124-E), Mizrahi et al. (2012) performed an open-label trial in ten patients diagnosed with insulin resistant type 2 diabetes and nonalcoholic steatohepatitis (NASH). Oral administration of Imm124-E at doses of 600 mg thrice daily (1800 mg/day) for 30 days improved type 2 diabetes and hyperlipidemia, and alleviated NASH through immunomodulatory action without any adverse effects. Oral administration of Imm124-E to mice ameliorated immune-mediated colitis induced by intra-colonic instillation of trinitrobenzene sulfonate. Imm124-E improved bowel histology and regeneration score, and decreased the extent of colitis damage in mice. This pathophysiological improvement was associated with the elevation of serum IL10, anti-inflammatory cytokine levels, CD4+, CD25+, and CD4+ Foxp3+ Tregs (Ya'acov et al., 2015). According to Ilan (2016), oral immune modulation therapies (e.g. nutraceuticals, functional foods, probiotics, prebiotics, polyunsaturated fatty acids, polyphenols, non-absorbable gut-associated adjuvuants, etc.) may be helpful to re-establish gut tolerance and to alter the gut immune system *via* the modulation of intestinal microbiota to treat autoimmune and inflammatory disorders like IBD.

APPLICATION OF BC SUPPLEMENTS IN TREATING CROHN'S DISEASE AND GUT INFECTIONS

Colostrum may be beneficial in chronic inflammatory diseases, such as various forms of arthritis, Crohn's disease, or inflammatory bowel disease (IBD). Crohn's or Celiac disease is an inflammatory bowel disease that causes abdominal pain and diarrhea (Sequeira et al., 2014). Non-steroidal anti-inflammatory drugs (NSAIDS) are often prescribed to reduce pain and abdominal cramps. However, chronic use of NSAIDS can cause peptic ulcers and alterations of gut microbiota, and the latter may induce leaky gut syndrome. BC possesses strong anti-inflammatory and anti-bacterial effects and can neutralize the lipopolysaccharides produced by gram negative bacteria (Rawal et al., 2008). BC reduces the expression of TNF-α in Caco-2 and HT29 cell lines as well as inhibits IL-8 expression and production of inflammatory cytokines, and consequently reduces gut inflammation. BC also decreases the adherence of invasive E. coli bacteria in human cell lines (Chae et al., 2017). Collectively, these findings suggest the promising therapeutic potential of BC in treating GI tract infections and inflammation-related IBD. Results of clinical and preclinical studies done with BC and dosage forms used for curing internal pathologies and external wounds are shown in **Table 5**.

ROLE OF BC AND COMPONENTS IN TREATING GUT DISEASES CAUSED BY MICROBIAL INFECTIONS

Generally, acute infectious diarrhea, immunodeficiency diarrhea, short bowel syndrome, IBD, etc. are treated with synthetic

TABLE 5 | Colostrum dosage forms used for treating internal pathologies and external wounds.

Types of Injuries	Colostrum dosage form	Number of patients enrolled in clinical trials (Male/Female)	Endpoints monitored	Effect observed	Dose and study duration	Reference
Gastrointestinal injury due to non-steroidal anti-inflammatory drugs	Colostrum powder in the form of tablets/capsules.	7 (7/0)	Intestinal permeability	IGF and TGF-β responsible for analgesic activity	125 ml t.i.d. for 7 days	(Playford et al., 2001)
Inflammation induced for HIV patients for infection in gastroesophageal tract.	Colostrum powder in the form of tablets/capsules or liquid colostrum.	87 (27/60)	Stool frequency; self-reported fatigue; $CD4^+$ count; body weight	Mucosal integrity, tissue repair, and antimicrobial actions	16 G b.i.d. for 4 weeks	(Kaducu et al., 2011)
Diabetes Delayed injury healing due to increase in blood glucose levels	Colostrum topical cream or colostrum powder in the form of tablets/ capsules.	18 (9/9)	Postprandial blood glucose; triglycerides; cholesterol; ketone bodies	Reduction of blood glucose, which starts wound healing problem in diabetic patients.	10 G daily	(Kim et al., 2009)
Repair of muscle, bone tissue, skin cartilage, and nerve cells.	Colostrum topical cream or colostrum powder in the form of tablets/ capsules	No clinical studies were done in humans; only *in vitro* cell line studies were done.	Increases the migration of WI38 fibroblasts	Nucleotides, epidermal growth factor, transforming growth factor, and IGF-1 promote wound healing and DNA, RNA damage repair.	10 G per 100 G of cream composition	(Takayama et al., 2001)
Ultraviolet B (UVB)-induced photo damage	Colostrum topical cream	Pre-clinical studies done on seven-week-old male Hos : HR-1 hairless mice.	Trans-epidermal water loss starts to increase.	Lactoferrin capable of preventing damage to the skin	10 G per 100 G of the cream composition	(Murata et al., 2014)
Infection with diarrhoeic *E. coli* in children	Colostrum powder in the form of tablets/capsules	27 (13/14)	Stool frequency; elimination of strainsexpressing virulence factors	Decrease stool frequency	21 G once daily for 14 days	(Huppertz et al., 1999)
Chronic pain syndrome	Colostrum powder in the form of tablets/capsules	4(2/2)	Flow cytometry; cytokine analysis;IGF-1; apoptosis	Apoptotic effect on monocytes	20 G once daily for 14 days	(Waaga-Gasser et al., 2009)
Inflammatory bowel disease (IBD)	Colostrum enemas	14(6/8)	Mild-to-moderate severe distal colitis (IBD), histological score was used for clinical assessment	Improvement in histological scores showed reduction of IBD symptoms.	100 ml of 10% BC solution enemas b.i.d	(Khan et al., 2002)

pharmaceuticals (Holtmann et al., 2017). The secondary infections in the GI tract and diarrhea in AIDS patients are also treated with drugs (Playford et al., 1999). A limited number of randomized, double-blind, and controlled studied have been done in children and adults to evaluate the efficacy of BC supplements for treating gut diseases caused by microbial infections. BC and its components were found to be effective against Gram negative and Gram positive bacteria and helped in treating gut infections and diarrhea. The dosages of BC supplements and bioactive ingredients used in preclinical and clinical studies for treating gastrointestinal diseases are summarized in **Table 6**.

ROLE OF LACTOFERRIN AND LACTALBUMIN IN CANCER THERAPY

Lactoferrin (LF) is an excellent immune modulator and anticancer agent and has a tissue regenerative capacity. It can also inhibit the production of inflammatory cytokines. Lactalbumin is present in whey and can markedly improve the immune response and enhance the synthesis of glutathione. It has been observed that lactoferrin and lactalbumin can induce apoptosis in cancerous cells (Teixeira et al., 2019). LF has been reported to elevate the level of caspase-1 and IL-18, and in turn reduce the metastatic foci in the intestine. LF-induced apoptotic activity of cytotoxic T and natural killer (NK) cells has also been observed. In addition, LF inhibits hepatic CYP1A2 enzyme, which is responsible for the activation of carcinogens (Tsuda et al., 2006). LF may be employed as a carrier for chemotherapeutic agents, especially for the treatment of brain tumors, due to its ability to cross the blood-brain barrier (Cutone et al. (2020). It therefore appears that LF and whey lactalbumin can be used as combination adjunct therapies with chemo- and radiotherapy for treating cancer. This approach would not only enhance the chemotherapeutic effectiveness of drugs, but also limit the use of chemo- and radiotherapy, resulting in reduced incidences of undesirable side effects observed in cancer patients.

IN VITRO EVALUATION OF THE ANTICANCER EFFECTS OF BC COMPONENTS USING DIFFERENT HUMAN CANCER CELL LINES

In vitro cell culture studies are used in selected cancer cell lines as a promising tool to determine the antiproliferative and cytotoxic effects of potential anticancer agents isolated from natural sources or synthesized in the laboratory. *In vitro* cell culture studies provide clues about the mechanism of action of anticancer agents toward cancer cells. Anti-cancer effects of lactoferrin were evaluated using MTT assay. The addition of lactoferrin in the culture medium inhibited the growth of cancer cell lines (MDA-MB-231 and MCF-7) (Sharma et al., 2019). Purified lactoferrin (2 mg/ml) retarded the growth of esophageal cancer cell lines (KYSE-30) and HEK cancer cell lines. The addition of 500 μg/ml of lactoferrin in the culture medium decreased the cell viability of KYSE-30 cancer cells by 80% after 62 hours' exposure. No effect was noted in the normal HEK cell line. Flow cytometry analysis suggested that lactoferrin induced apoptosis in KYSE-30 human esophagus cancer cell lines (Farziyan et al., 2016). The results of *in vitro* studies done to assess the anticancer properties of BC components (lactoferrin, liposomal bovine lactoferrin, bovine lactoperoxidase, lactoferrin nanoparticles, and conjugated linolenic acid) on different cancer cell lines (e.g., gastric, esophagus, colorectal, liver, lung, prostate, breast, ovarian) are summarized in **Table 7**.

IN VIVO ANTICANCER EFFECTS OF BC COMPONENTS IN ANIMAL MODELS AND HUMANS

Following the information obtained from *in vitro* studies, the next step involves preclinical investigations in appropriate animal models to assess the safety, efficacy, and toxicity of anticancer agents. Numerous anticancer studies with BC supplements and major components have been done on rodents. For instance, lactoferrin and conjugated linolenic acid (CLA) have been tested for treating colorectal, lung, and esophageal cancers in rats and mice. Reduction in colon tumor load and downregulation (**Figure 1**) in the expression of VEGF were observed in the preclinical studies (Tung et al., 2013; Sugihara et al., 2017). A limited number of clinical trials in a small number of patients have been performed in humans to understand the anticancer potential of BC components. Based on the promising anticancer effects of CLA in preclinical models, an open-label clinical study was done on 24 women diagnosed with breast cancer. CLA was given orally at doses of 7.5 G/day for 20 days. CLA was found to suppress the expression of fatty acid synthase (FASN) and lipoprotein lipase (LPL). The depressed activity of these biomarker enzymes indicates the suppression of breast tumor growth (McGowan et al., 2013). The results of another clinical trial suggested that CLA (3G/day) may be useful in rectal cancer patients undergoing chemoradiotherapy (Mohammadzadeh et al., 2013). The information obtained from preclinical and clinical effects of lactoferrin, liposomal lactoferrin, and CLA in different types of cancers is shown in **Table 8**.

INTRAVAGINAL APPLICATION OF BC TABLETS CAUSE SPONTANEOUS REGRESSION OF HPV-ASSOCIATED LOW-GRADE CERVICAL INTRAEPITHELIAL LESIONS IN WOMEN

Human papillomavirus (HPV) infection is the most common sexually transmitted disease in young people worldwide. Most infections are cleared by the immune system, but persistent infections may cause intraepithelial abnormalities in the infected cells that can develop into cancers of the cervix, vagina, vulva, anal canal, and penis. Immunotherapy is considered the most promising treatment for HPV-related pathologies. HPV vaccines have been developed to prevent

TABLE 6 | Pre-clinical and clinical applications of bovine colostrum in gastrointestinal diseases.

GI tract disease	Preclinical and clinical manifestations	Preclinical/Clinical studies					Reference
		Study Design	No. of patients enrolled in clinical trials (BC/placebo)	Endpoints observed	Effect	Dose	
Acute infectious diarrhea	Eliminate pathogen, improve the intestinal barrier function, inhibit bacterial translocation, and reduce disease severity	Double-blind randomized-controlled trial	160 children (80/80)	Investigated for bacterial/viral causes of diarrhea (*Salmonella, Shigella, E. coli, Campylobacter and Vibrio chole*ra; Rotavirus antigen in stool)	Lower frequency of vomiting and diarrhea	3G/sachet in 50 ml ordinary water	(Menchetti et al., 2016) (Barakat et al., 2020)
Helicobacter pylori infections	Inhibit the invasive capacity of pathogen bacteria, modulation of immune response, and favor mucosal repair	Randomized-controlled trial	C57BL/6 female mice subjected to 0.1 ml of 1×10(9) *H. pylori*	Bacterial load, gastric emptying time	Increased gastric emptying time (7.9 min)	0.1ml HNZ (hyperimmune bovine colostrum plus N-acetyl cysteine plus zinc)	(Rokka et al., 2008; Tran et al., 2010; Xu et al., 2015)
Immunodeficiency diarrhea	Reduced abdominal pain, diarrhea score, and fatigue, reduced daily stool frequency, and increased the body weight and body mass index	Randomized, single-blind trial	84 Adults (ColoPlus®/ placebo) (43/41)	Daily stool frequency, body weight, body mass index, and baseline $CD4^+$ count	Mean daily stool frequency (↓79%), self-reported fatigue (↓85%), mean $CD4^+$ count (↑14%)	50 G, twice daily	(Florén et al., 2006; Kaducu et al., 2011)
Short bowel syndrome (SBS)	Support intestinal development and function in newborn, and also enhance intestinal adaptation and functions	Randomized, double-blind, crossover, pilot study	9 children	Intestinal absorption of energy and wet weight	No improvement in the wet weight or intestinal absorption	20% of the children's basal fluid requirement (BFR)	(Ausholt et al., 2014; Støy et al., 2014; Shen et al., 2015)
Inflammatory bowel disease (IBD)	Reduced weight loss, decreased colon shortening, and improved the histologic severity of colon inflammation	Randomized-controlled trial	Six-week-old CD-1 mice	Clinical signs, histopathological characteristics, expression levels of toll-like receptor 4 (TLR4), pro- and anti-inflammatory cytokines, and microbial composition	↓TLR4 ($p < 0.01$), ↓Interleukin-1β (IL-1β; $p < 0.001$), ↓Interleukin-8 (IL-8; $p < 0.001$), and ↓Interleukin-10 (IL-10; $p < 0.001$)	100 mg of colostrum powder dissolved in 0.6 ml of physiological saline solution was given to each mouse	(Bellavia et al., 2014) (Menchetti et al., 2020)
Necrotizing enterocolitis (NEC)	Maturation of the digestive tract, balance gut microbiota, modulation of the intestinal immune system, and mucosal repair	Randomized-controlled trials	Four trials, 678 participants	Neonatal sepsis and necrotizing enterocolitis (NEC)	Late-onset sepsis (risk ratio (RR) 0.49, 95% confidence interval (CI) 0.32 to 0.73) NEC ≥ stage II RR 0.3 95% CI (0.12 to 0.76)	Oral lactoferrin 200mg/day	(Cairangzhuoma et al., 2013; Good et al., 2015);

TABLE 7 | Anticancer effects of bovine colostrum components on different cancer cell lines.

Component of bovine colostrum	Cancer type	Dose	Result	Reference
Lactoferrin	Gastric cancer (AGS human stomach carcinoma cell)	500 μg/ml	Caused 80% cytotoxicity in AGS cell line	(Amiri et al., 2015)
Lactoferrin	Human esophagus cancer cell (KYSE-30 esophageal squamous cell carcinoma)	500 μg/ml	Inhibited the development of azoxymethane (AOM)-induced aberrant crypt foci (ACF) by 53% and 80% after 20 and 62 h, respectively.	(Farziyan et al., 2016)
Liposomal bovine lactoferrin	Colorectal cancer (RKO and RCN-9 human CRC cells)	≥10 μg/ml	Significant inhibition of colon aberrant crypt foci growth occurred in the RKO and RCN-9 cells (P<0.01).	(Sugihara et al., 2017)
Bovine lactoperoxidase (LPO) and lactoferrin (LF) nanoparticles	Colorectal cancer (Caco-2), liver cancer (HepG-2), breast cancer (MCF-7), prostate cancer (PC-3).	315-1388 μg/ml	Ten-fold suppression in NF-kB expression in Caco-2, HepG-2, and MCF-7; four-fold downregulation of NF-κB mRNA level in PC-3 cell lines; 15-fold decrease in Bcl-2 levels, as compared to treatment with 5-flurouracil.	(Abu-Serie and El-Fakharany, 2017)
Lactoferrin	Lung cancer (human lung cancer cell line, A549)	0.9375-15 mg/ml	Decreased expression of *VEGF* mRNA and VEGF protein in a concentration-dependent manner.	(Tung et al., 2013)
Conjugated linolenic acid (CLA)	Ovarian cancer cells (SKOV-3 and A2780 cells)	7 μM CLA for 48 to 72 h	Nine-fold increase in autophagolysosomes, G1 cell cycle arrest in SKOV-3 and A2780 cell lines by downregulation of E2F1.	(Shahzad et al., 2018)
	Breast cancer cell line (MCF-7), colon cancer cell line (HT-29), (mouse fibroblast cell line Balb/3T3)	0.1-100 μg/ml	Reduced anti-apoptotic Bcl-2 expression	(Niezgoda et al., 2017)

TABLE 8 | Preclinical and clinical effects of bovine colostrum components on different cancer types in animals and humans.

Components of bovine colostrum	Cancer type	Dose	Preclinical/clinical study results	Reference
Liposomal Lactoferrin	Colorectal cancer (Thirty-six F344 male rats, 5-weeks-old, were used in the experiment).	1,000 mg/kg/day in drinking water	Approx. 43% reduction was observed in the colon tumor.	(Sugihara et al., 2017)
Lactoferrin	Lung cancer (12 transgenic mice)	300 mg/kg, 3 times a week.	Significantly decreased expression of hVEGF-A_{165} and suppressed the formation of tumor.	(Tung et al., 2013)
Conjugated linolenic acid (CLA)	Breast cancer (24 women)	7.5 G/day in the form of capsules for 20 days	Decrease in FAS and LPL enzymes which provide fatty acids for breast tumor growth.	(Kuemmerle et al., 2011; McGowan et al., 2013; Arab et al., 2016)
	Rectal cancer (33 human volunteers)	3G/day in the form of capsules for six weeks.	Significant changes occurred in TNF-α (P = 0.04), hsCRP (P = 0.03), and MMP-9 (P = 0.04)	(Mohammadzadeh et al., 2013)

HPV-associated cancer, external genital lesions, and genital warts (Bergman et al., 2019). In Italy, the immunomodulating action of BC was evaluated in an observational, multi-centre, pilot study, where 256 patients were enrolled with a history of low-grade cervical squamous intraepithelial lesions. At baseline, all patients were tested for cervical cytology (Pap smear), colposcopy, and targeted biopsy. BC-containing vaginal tablets (GINEDIE^{R}) were administered twice a week at bedtime for 24 weeks, without any other medication for the whole study period. The rates of regression were recorded histologically at the end of the study period. Overall regression rate with negative histology was 75.5% at the end of the 6 month follow-up period. The patients did not experience any adverse effects during the treatment. The authors concluded that, as opposed to a spontaneous regression period of 1-5 years, intravaginal topical application of BC significantly shortens the regression time of low-grade cervical intraepithelial lesions to half a year (Stefani et al., 2014).

CURRENT AND FUTURE DEVELOPMENTS OF BC NUTRACEUTICALS

In this review, we have attempted to summarize the nutraceutical health benefits of BC, and the therapeutic potential and effectiveness of marketed colostrum powder, capsules, and tablets for the treatment of various types of cancers and GI tract pathologies. BC is an emerging nutraceutical and innovative therapeutic products are being developed for children and adults. In future, BC products could be a boon in providing non-hazardous, cost-effective, and affordable alternative sources of natural remedies for treating different types of cancers, GIDs, and autoimmune disorders. However, there are several challenges and opportunities that need to be addressed. For instance, well-designed, placebo-controlled, and randomized clinical trials are needed to determine the long-term safety, effectiveness, and optimal doses of BC supplements. Some other aspects of BC nutraceuticals include the standardization

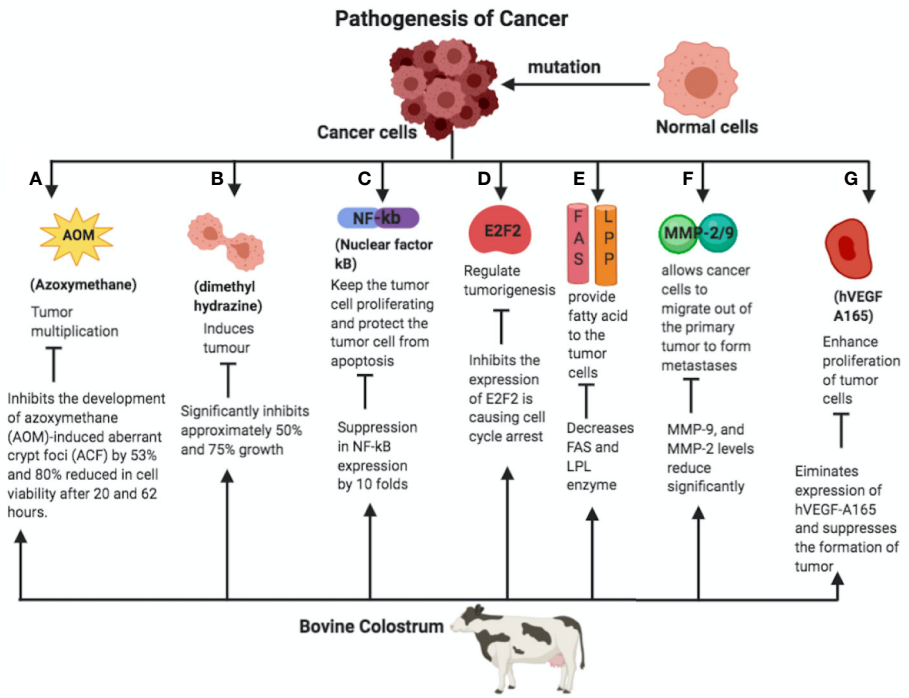

FIGURE 1 | A normal cell mutates into the cancer cell, which divides enormously and spreads across the surrounding tissues. The pathways responsible for initiation and metastasis of cancer and the role of bovine colostrum (BC) on the amelioration of the same is given as follows. **(A)** Azoxymethane is responsible for tumor multiplication and cancer cell development. BC inhibits the development if azoxymethane (AOM)-induced aberrant crypt foci (ACF), therefore reducing the cell viability. **(B)** BC inhibits the proliferation of tumor angiogenesis by dimethylhydrazine. **(C)** Nuclear factor-κB (NF-κB) is the transcription factor that is responsible for cancer cell growth, tumor formation, and tumor cell proliferation, and prevents tumor cells from apoptosis. BC suppresses NF-κB expression approximately by 10-fold. **(D)** E2F2 factor plays an important role in the tumorigenesis of the cancerous cells. BC inhibits expression of E2F2 factor and initiates cell cycle arrest. **(E)** BC inhibits the enzymes fatty acid synthetase (FAS) and lipoprotein lipase (LPL), which in turn inhibit neoplastic lipogenesis. **(F)** Matrix metalloproteinaise 2/9 (MMP-2/9) allows cancer cells to migrate out of the primary tumor to form metastases. BC supresses the levels of the MMP- 2/9. **(G)** BC inhibits the expression of Human Vascular Endothelial Growth Factor (hVEGF), which is responsible for proliferation of the cancer cells. AOM, Azoxymethane; ACF, Azoxymethane induced aberrant crypt foci; NF-κB, Nuclear factor Kappa B; E2Fi, E2F Transcription Factor 1; FAS, Fatty acid synthetase; LPL, Lipoprotein lipase; MMP, Matrix metalloproteinase; hVEGF, Human Vascular Endothelial Growth Factor.

of products originating from different breeds of cows and buffalo. In addition, good manufacturing practices and standardized techniques are required for making BC formulations, and possible adulteration of BC supplements with synthetic drugs and microbial contaminants, just to name a few. More basic research is needed to understand the mechanism of action of different components of BC for their anticancer and antidiabetic properties, and for curing wounds, gastrointestinal disorders, and inflammatory bowel diseases.

Nutraceuticals are defined as substances that provide physiological benefits and assist in improving overall health beyond basic nutritional functions and protect against non-communicable diseases. Generally, nutraceuticals consist of products isolated or purified from vegetables and fruits, colostrum supplements, and dairy products, and are sold as non-pharmacological, cost-effective, and affordable alternative therapies for the prevention and treatment of neurodegenerative and cardiovascular diseases, musculoskeletal abnormalities, diabetes, obesity, and some cancers. The influence of nutraceuticals, functional foods, natural health products, dietary supplements, and probiotics is often neglected by healthcare professionals and leading experts in the field of medicine. Nutraceuticals could be one of the biggest drivers for curing the global epidemic of chronic non-communicable diseases, including obesity, diabetes, cardiovascular diseases, and certain cancers. However, the evidence-based dietary advice is beset by poor quality science, a limited number of randomized, placebo-controlled studies, and unresolved controversy about the role of nutraceuticals in curing non-communicable diseases. Good manufacturing practices (GMPs) and high-quality control standards should be used for the manufacturing of BC nutraceuticals. Post-marketing surveillance should be conducted diligently for the tolerability of BC supplements and bioactive components. Dairy farmers should be encouraged to collect BC using sterile and hygienic conditions as much as possible.

Bovine colostrum is significantly rich in biologically active peptides, antioxidants, anti-inflammation agents, and growth promoting factors that differ substantially from later milk. The benefits of BC are well known in the health and disease of children and adults. As discussed earlier, BC is an emerging nutraceutical

and innovative therapeutic products that is being developed for children's formulas and for the treatment of non-communicable diseases. Hopefully, BC supplements will greatly contribute to curing different cancer types, diabetes, cardiovascular diseases, necrotizing enterocolitis, and inflammatory bowel disease or Crohn's disease, and autoimmune disorders. Understanding the biological roles of different BC ingredients is a major challenge for nutritionists and dieticians, basic researchers, and physicians.

BC can also mitigate a wide variety of bacterial, viral, fungal, and parasitic infections. BC impregnated dressings are non-allergic, safe, and promote wound-healing. Such dressings may be used as an adjunct for the management of deep wounds and burns. BC is richer in immunoglobulins than human colostrum and can be used in the treatment of immunodeficiency diseases and infections along with conventional medicines (Bagwe et al., 2015; Buttar et al., 2017). Our studies indicated that BC possesses strong antimicrobial activity against both Gram^{-tive} and Gram^{+tive} strains. The minimal inhibitory concentration (MIC) of colostrum was found to be 100 μg/ml against *E. coli, S. aureus, P. vulgaris, E. aerogenes, and S. typhi* (Yadav et al., 2016). It is possible that BC might have viricidal effects against the COVID-19 virus. Lactoferrin especially is well known for its anti-inflammation and anti-microbial properties. This hypothetical idea may be worth pursuing!

CONCLUSIONS

BC supplements have proven useful in the management of GIDs, such as acute infectious diarrhea, Helicobacter pylori infections, irritable bowel syndrome, inflammatory bowel disease (IBD), and different types of human cancer cell lines (e.g. esophagus, colorectal, lung, breast and ovarian cancer). The components of BC, such as lactoferrin, CLA, and alpha-lactalbumin, are useful in treating GI-related disorders and some cancer types. The oral consumption of BC can boost the immune system and improve the inflammatory condition of patients suffering from gastrointestinal disorders.

BC possesses strong antibacterial, antiviral, and antifungal properties, and has also exhibited antitumor actions in a limited number of *in vitro* and *in vivo* studies. Several components of BC have shown apoptosis in cancer cells and suppression in the growth of tumors. Also, NK cells are inhibited after BC exposure. While BC products are well tolerated, some patients allergic to dairy products may experience undesirable side effects. Overall, BC supplements can be safely used for the treatment of GIDs, autoimmune disorders, and different cancers. The clinical interactions of BC, if any, with orally administered prescription or over-the-counter drugs should be explored regarding the bioavailability and pharmacokinetics, and the possibility of such an interaction should be monitored in patients using synthetic drugs for co-morbid conditions.

AUTHOR CONTRIBUTIONS

GK, HS, and HT visualized the presented idea, contributed to manuscript writing, and supervised the project. SB-P and PY contributed to literature searches and to preparing the manuscript draft. GK and HS revised and approved the manuscript.

REFERENCES

Abu-Serie, M. M., and El-Fakharany, E. M. (2017). Efficiency of novel nanocombinations of bovine milk proteins (lactoperoxidase and lactoferrin) for combating different human cancer cell lines. *Sci. Rep.* 7, 1–2. doi: 10.1038/s41598-017-16962-6

Agarwal, P., and Gupta, R. (2016).A Review on Anticancer Property of Colostrum. *Res. Rev. - J. Med. Heal. Sci.* 5, 1–9.

Amiri, F., Moradian, F., and Rafiei, A. (2015). Anticancer effect of lactoferrin on Gastric Cancer Cell Line AGS. *rmm.mazums.ac.ir Res. Mol. Med.* 3, 11. doi: 10.7508/rmm.2015.02.002

Arab, A., Akbarian, S., Ghiyasvand, R., and Miraghajani, M. (2016). The effects of conjugated linoleic acids on breast cancer: A systematic review. *Adv. Biomed. Res.* 5, 115. doi: 10.4103/2277-9175.185573

Aunsholt, L., Jeppesen, P. B., Lund, P., Sangild, P. T., Ifaoui, I. B. R., Qvist, N., et al. (2014). Bovine colostrum to children with short bowel syndrome: a randomized, double-blind, crossover pilot study. *JPEN J. Parenter. Enteral Nutr.* 38, 99–106. doi: 10.1177/0148607112469630

Bagwe, S., Tharappel, L. J. P., Kaur, G., and Buttar, H. S. (2015). Bovine colostrum: An emerging nutraceutical. *J. Complement. Integr. Med.* 12, 175–185. doi: 10.1515/jcim-2014-0039

Barakat, S. H., Meheissen, M. A., Omar, O. M., and Elbana, D. A. (2020). Bovine Colostrum in the Treatment of Acute Diarrhea in Children: A Double-Blinded Randomized Controlled Trial. *J. Trop. Pediatr.* 66, 46–55. doi: 10.1093/tropej/fmz029

Bedford, A., Chen, T., Huynh, E., Zhu, C., Medeiros, S., Wey, D., et al. (2015). Epidermal growth factor containing culture supernatant enhances intestine development of early-weaned pigs in vivo: Potential mechanisms involved. *J. Biotechnol.* 196–197, 9–19. doi: 10.1016/j.jbiotec.2015.01.007

Bellavia, M., Rappa, F., Lo Bello, M., Brecchia, G., Tomasello, G., Leone, A., et al. (2014). Lactobacillus casei and bifidobacterium lactis supplementation reduces tissue damage of intestinal mucosa and liver after 2,4,6-trinitrobenzenesulfonic acid treatment in mice. *J. Biol. Regul. Homeost. Agents* 28, 251–261.

Bergman, H., Buckley, B. S., Villanueva, G., Petkovic, J., Garritty, C., Lutje, V., et al. (2019). Comparison of different human papillomavirus (HPV) vaccine types and dose schedules for prevention of HPV-related disease in females and males. *Cochrane Database Syst. Rev.* 2019, 1–154. doi: 10.1002/14651858.CD013479

Brandal, P., and Heim, S. (2015). "Tumors of the nervous system," in *Cancer Cytogenetics: Fourth Edition* (Hoboken, NJ, USA: John Wiley & Sons, Inc), 515–537. doi: 10.1002/9781118795569.ch20

Bray, F., Ferlay, J., Soerjomataram, I., Siegel, R. L., Torre, L. A., and Jemal, A. (2018). Global cancer statistics 2018: GLOBOCAN estimates of incidence and mortality worldwide for 36 cancers in 185 countries. *CA Cancer J. Clin.* 68, 394–424. doi: 10.3322/caac.21492

Bullinger, L., Döhner, K., and Dohner, H. (2017). Genomics of acute myeloid leukemia diagnosis and pathways. *J. Clin. Oncol.* 35, 934–946. doi: 10.1200/JCO.2016.71.2208

Buttar, H. S., Bagwe, S. M., Bhullar, S. K., and Kaur, G. (2017). Health Benefits of Bovine Colostrum in Children and Adults. *Dairy Hum. Health Dis. Across Lifespan* 12, 3–20. doi: 10.1016/b978-0-12-809868-4.00001-7

Cairangzhuoma, Yamamoto, M., Muranishi, H., Inagaki, M., Uchida, K., Yamashita, K., et al. (2013). Skimmed, Sterilized, and concentrated bovine late colostrum promotes both prevention and recovery from intestinal tissue damage in mice. *J. Dairy Sci.* 96, 1347–1355. doi: 10.3168/jds.2012-5701

Chae, A., Aitchison, A., Day, A. S., and Keenan, J. I. (2017). Bovine colostrum demonstrates anti-inflammatory and antibacterial activity in in vitro models of

intestinal inflammation and infection. *J. Funct. Foods* 28, 293–298. doi: 10.1016/j.jff.2016.11.016

Crittenden, R., Little, C., Georgiou, G., Forsyth, S., and Bennett, L. (2007). Cow's milk allergy: A complex disorder. in. *Aust. J. Dairy Technol.* 24, 62–71. doi: 10.1007/s00217-005-0178-8

Cutone, A., Rosa, L., Ianiro, G., Lepanto, M. S., Bonaccorsi di Patti, M. C., Valenti, P., et al. (2020). Lactoferrin's Anti-Cancer Properties: Safety, Selectivity, and Wide Range of Action. *Biomolecules* 10:456. doi: 10.3390/biom10030456

de Almeida, M. F. B., and Draque, C. M. (2007). Neonatal Jaundice and Breastfeeding. *Neoreviews* 8, e282–e288. doi: 10.1542/neo.8-7-e282

Donovan, S. M. (2016). The Role of Lactoferrin in Gastrointestinal and Immune Development and Function: A Preclinical Perspective. *J. Pediatr.* 173, S16–S28. doi: 10.1016/j.jpeds.2016.02.072

Elfstrand, L., Lindmark-Månsson, H., Paulsson, M., Nyberg, L., and Åkesson, B. (2002). Immunoglobulins, growth factors and growth hormone in bovine colostrum and the effects of processing. *Int. Dairy J.* 12, 879–887. doi: 10.1016/s0958-6946(02)00089-4

Etienne, G., Guilhot, J., Rea, D., Rigal-Huguet, F., Nicolini, F., Charbonnier, A., et al. (2017). Long-term follow-up of the French Stop Imatinib (STIM1) study in patients with chronic myeloid leukemia. *J. Clin. Oncol.* 35, 298–305. doi: 10.1200/JCO.2016.68.2914

Farziyan, M. A., Moradian, F., and Rafiei, A. R. (2016). Anticancer Effect of Bovine Lactoferrin on Human Esophagus Cancer Cell Line. *Res. Mol. Med.* 4, 18–23. doi: 10.7508/rmm.2016.01.003

Florén, C. H., Chinenye, S., Elfstrand, L., Hagman, C., and Ihse, I. (2006). ColoPlus, a new product based on bovine colostrum, alleviates HIV-associated diarrhoea. *Scand. J. Gastroenterol.* 41, 682–686. doi: 10.1080/00365520500380817

Formenti, S. C., and Demaria, S. (2009). Systemic effects of local radiotherapy. *Lancet Oncol.* 10, 718–726. doi: 10.1016/S1470-2045(09)70082-8

França-Botelho, A. (2019). Beneficial Components of Colostrum for Cancer Patients: A Mini-review Focused on Oxidative Aspects and Properties of Colostrinin. *Asian Oncol. Res. J.* 2 (1), 1–6.

Gensollen, T., Iyer, S. S., Kasper, D. L., and Blumberg, R. S. (2016). How colonization by microbiota in early life shapes the immune system. *Science* 352, 539–544. doi: 10.1126/science.aad9378

Godhia, M. L., and Patel, N. (2013). Colostrum - Its composition, benefits as a nutraceutical: A review. *Curr. Res. Nutr. Food Sci.* 1, 37–47. doi: 10.12944/CRNFSJ.1.1.04

Good, M., Sodhi, C. P., Egan, C. E., Afrazi, A., Jia, H., Yamaguchi, Y., et al. (2015). Breast milk protects against the development of necrotizing enterocolitis through inhibition of Toll-like receptor 4 in the intestinal epithelium via activation of the epidermal growth factor receptor. *Mucosal Immunol.* 8, 1166–1179. doi: 10.1038/mi.2015.30

Holtmann, G., Shah, A., and Morrison, M. (2017). Pathophysiology of Functional Gastrointestinal Disorders: A Holistic Overview. *Dig. Dis.* 35(Suppl 1), 5–13. doi: 10.1159/000485409

Huppertz, H.II, Rutkowski, S., Busch, D. H., Eisebit, R., Lissner, R., and Karch, H. (1999). Bovine colostrum ameliorates diarrhea in infection with diarrheagenic Escherichia coli, Shiga toxin-producing E. coli, and E. coli expressing intimin and hemolysin. *J. Pediatr. Gastroenterol. Nutr.* 29, 452–456. doi: 10.1097/00005176-199910000-00015

Hurley, W. L., and Theil, P. K. (2011). Perspectives on immunoglobulins in colostrum and milk. *Nutrients* 3, 442–474. doi: 10.3390/nu3040442

Hyrslova, I., Krausova, G., Bartova, J., Kolesar, L., and Curda, L. (2016). Goat and Bovine Colostrum as a Basis for New Probiotic Functional Foods and Dietary Supplements. *J. Microb. Biochem. Technol.* 08, 1948–5948. doi: 10.4172/1948-5948.1000262

Ilan, Y. (2016). Oral immune therapy: targeting the systemic immune system via the gut immune system for the treatment of inflammatory bowel disease. *Clin. Transl. Immunol.* 5, e60. doi: 10.1038/cti.2015.47

Jacqmin, S., Vleurick, L., Renaville, R., and Portetelle, D. (2000). Modulation of the biological action of bovine growth hormone by passive immunization in hypophysectomised rat. *Biotechnol. Agron. Société Environ. = Biotechnol. Agron. Soc Environ. [=BASE]* 3, 23–24.

Jolly, A., and Mascaro, M. (2016). Evaluation of Hyaluronic Acid in Cattle: Physiological Variations Related to Age, Periparturition and in Clinical Cases of Paratuberculosis. *J. Vet. Sci. Technol.* 7, 342–346. doi: 10.4172/2157-7579.1000342

Kaducu, F. O., Okia, S. A., Upenytho, G., Elfstrand, L., and Florén, C. H. (2011). Effect of bovine colostrum-based food supplement in the treatment of HIV-associated diarrhea in Northern Uganda: A randomized controlled trial. *Indian J. Gastroenterol.* 30, 270–276. doi: 10.1007/s12664-011-0146-0

Khan, Z., Macdonald, C., Wicks, A. C., Holt, M. P., Floyd, D., Ghosh, S., et al. (2002). Use of the "nutriceutical", bovine colostrum, for the treatment of distal colitis: Results from an initial study. *Aliment. Pharmacol. Ther.* 16, 1917–1922. doi: 10.1046/j.1365-2036.2002.01354.x

Kim, J. H., Jung, W. S., Choi, N. J., Kim, D. O., Shin, D. H., and Kim, Y. J. (2009). Health-promoting effects of bovine colostrum in Type 2 diabetic patients can reduce blood glucose, cholesterol, triglyceride and ketones. *J. Nutr. Biochem.* 20, 298–303. doi: 10.1016/j.jnutbio.2008.04.002

Kuemmerle, N. B., Rysman, E., Lombardo, P. S., Flanagan, A. J., Lipe, B. C., Wells, W. A., et al. (2011). Lipoprotein lipase links dietary fat to solid tumor cell proliferation. *Mol. Cancer Ther.* 10, 427–436. doi: 10.1158/1535-7163.MCT-10-0802

Layman, D. K., Lönnerdal, B., and Fernstrom, J. D. (2018). Applications for alpha-lactalbumin in human nutrition. *Nutr. Rev.* 76, 444–460. doi: 10.1093/nutrit/nuy004

Le Doare, K., Holder, B., Bassett, A., and Pannaraj, P. S. (2018). Mother's Milk: A Purposeful Contribution to the Development of the Infant Microbiota and Immunity. *Front. Immunol.* 9:361. doi: 10.3389/fimmu.2018.00361

Linehan, W. M., Spellman, P. T., Ricketts, C. J., Creighton, C. J., Fei, S. S., Davis, C., et al. (2016). Comprehensive Molecular Characterization of Papillary Renal-Cell Carcinoma. *N. Engl. J. Med.* 374, 135–145. doi: 10.1056/NEJMoa1505917

Maqbool, S. (1992). Jaundice in the newborn. *Specialist* 8, 71–83. doi: 10.5694/j.1326-5377.1957.tb60186.x

McGowan, M. M., Eisenberg, B. L., Lewis, L. D., Froehlich, H. M., Wells, W. A., Eastman, A., et al. (2013). A proof of principle clinical trial to determine whether conjugated linoleic acid modulates the lipogenic pathway in human breast cancer tissue. *Breast Cancer Res. Treat.* 138, 175–183. doi: 10.1007/s10549-013-2446-9

McGrath, B. A., Fox, P. F., McSweeney, P. L. H., and Kelly, A. L. (2016). Composition and properties of bovine colostrum: a review. *Dairy Sci. Technol.* 96, 133–158. doi: 10.1007/s13594-015-0258-x

Menchetti, L., Traina, G., Tomasello, G., Casagrande-Proietti, P., Leonardi, L., Barbato, O., et al. (2016). Potential benefits of colostrum in gastrointestinal diseases. *Front. Biosci. - Sch.* 8, 331–351. doi: 10.2741/s467

Menchetti, L., Curone, G., Filipescu, I. E., Barbato, O., Leonardi, L., Guelfi, G., et al. (2020). The Prophylactic Use of Bovine Colostrum in a Murine Model of TNBS-Induced Colitis. *Anim. (Basel)* 10, 492. doi: 10.3390/ani10030492

Meurer, M., Floquet, A., Italiano, A., Auriche, M., Mancini, J., Penel, N., et al. (2017). Undifferentiated endometrial sarcomas (UES): Results of a French sarcoma group (FSG) retrospective series of 52 patients (pts). *J. Clin. Oncol.* 35, e17109–e17109. doi: 10.1200/jco.2017.35.15_suppl.e17109

Miller, K. D., Nogueira, L., Mariotto, A. B., Rowland, J. H., Yabroff, K. R., Alfano, C. M., et al. (2019). Cancer treatment and survivorship statistics 2019. *CA. Cancer J. Clin.* 69, 363–385. doi: 10.3322/caac.21565

Miolo, G., Basile, D., Carretta, A., Santeufemia, D. A., Steffan, A., and Corona, G. (2019). The metabolomic scent of cancer disease progression in soft tissue sarcoma: A case report. *Int. J. Biol. Markers* 34, 205–209. doi: 10.1177/1724600818817316

Mizrahi, M., Shabat, Y., Ya'acov, A.B., Lalazar, G., Adar, T., Wong, V., et al. (2012). Alleviation of insulin resistance and liver damage by oral administration of Imm124-E is mediated by increased Tregs and associated with increased serum GLP-1 and adiponectin: Results of a phase I/II clinical trial in NASH. *J. Inflamm. Res.* 5, 141–150. doi: 10.2147/JIR.S35227

Mohammadzadeh, M., Faramarzi, E., Mahdavi, R., Nasirimotlagh, B., and Asghari Jafarabadi, M. (2013). Effect of conjugated linoleic acid supplementation on inflammatory factors and matrix metalloproteinase enzymes in rectal cancer patients undergoing chemoradiotherapy. *Integr. Cancer Ther.* 12, 496–502. doi: 10.1177/1534735413485417

Murata, M., Satoh, T., Wakabayashi, H., Yamauchi, K., Abe, F., and Nomura, Y. (2014). Oral administration of bovine lactoferrin attenuates ultraviolet B-induced skin photodamage in hairless mice. *J. Dairy Sci.* 97, 651–658. doi: 10.3168/jds.2013-7153

Niezgoda, N., Gliszczyńska, A., Kempińska, K., Wietrzyk, J., and Wawrzeńczyk, C. (2017). Synthesis and evaluation of cytotoxic activity of conjugated linoleic acid derivatives (esters, alcohols, and their acetates) toward cancer cell lines. *Eur. J. Lipid Sci. Technol.* 119:1600470. doi: 10.1002/ejlt.201600470

Osada, S. I., Yoshida, R., Kikuchi, I., Tsuruta, D., Ansai, S. I., Hashimoto, T., et al. (2014). Successful Treatment of Intravenous Immunoglobulins in a Patient with Intractable Epidermolysis Bullosa Acquisita with Autoantibodies to Type VII Collagen and Laminin Alpha-3. *J. Clin. Exp. Dermatol. Res.* 4, 1–3. doi: 10.4172/2155-9554.1000200

Pammi, M., and Abrams, S. A. (2015). Oral lactoferrin for the prevention of sepsis and necrotizing enterocolitis in preterm infants. *Cochrane Database Syst. Rev.* 2, CD007137. doi: 10.1002/14651858.CD007137.pub4

Pieper, R., Scharek-Tedin, L., Zetzsche, A., Röhe, I., Kröger, S., Vahjen, W., et al. (2016). Bovine milk–based formula leads to early maturation-like morphological, immunological, and functional changes in the jejunum of neonatal piglets. *J. Anim. Sci.* 94, 989–999. doi: 10.2527/jas.2015-9942

Playford, R. J., Floyd, D. N., Macdonald, C. E., Calnan, D. P., Adenekan, R. O., Johnson, W., et al. (1999). Bovine colostrum is a health food supplement which prevents NSAID induced gut damage. *Gut* 44, 653–658. doi: 10.1136/gut.44.5.653

Playford, R. J., Macdonald, C. E., Calnan, D. P., Floyd, D. N., Podas, T., Johnson, W., et al. (2001). Co-administration of the health food supplement, bovine colostrum, reduces the acute non-steroidal anti-inflammatory drug-induced increase in intestinal permeability. *Clin. Sci.* 100, 627–633. doi: 10.1042/CS20010015

Pluske, J. R. (2016). Invited review: Aspects of gastrointestinal tract growth and maturation in the pre- and postweaning period of pigs. *J. Anim. Sci.* 94, 399–411. doi: 10.2527/jas.2015-9767

Rajyaguru, D. J., Borgert, A. J., Smith, A. L., Thomes, R. M., Conway, P. D., Halfdanarson, T. R., et al. (2018). Radiofrequency Ablation Versus Stereotactic Body Radiotherapy for Localized Hepatocellular Carcinoma in Nonsurgically Managed Patients: Analysis of the National Cancer Database. *J. Clin. Oncol.* 36, 600–608. doi: 10.1200/JCO.2017.75.3228

Rathe, M., De Pietri, S., Wehner, P. S., Frandsen, T. L., Grell, K., Schmiegelow, K., et al. (2019). Bovine Colostrum Against Chemotherapy-Induced Gastrointestinal Toxicity in Children With Acute Lymphoblastic Leukemia: A Randomized, Double-Blind, Placebo-Controlled Trial. *J. Parenter. Enter. Nutr.* 44, 337–347. doi: 10.1002/jpen.1528

Rawal, P., Gupta, V., and Thapa, B. R. (2008). Role of colostrum in gastrointestinal infections. *Indian J. Pediatr.* 75, 917–921. doi: 10.1007/s12098-008-0192-5

Rokka, S., Myllykangas, S., and Joutsjoki, V. (2008). Effect of specific colostral antibodies and selected lactobacilli on the adhesion of Helicobacter pylori on AGS cells and the Helicobacter-induced IL-8 production. *Scand. J. Immunol.* 68, 280–286. doi: 10.1111/j.1365-3083.2008.02138.x

Rosenberg, J. E., Petrylak, D. P., Van Der Heijden, M. S., Necchi, A., O'Donnell, P. H., Loriot, Y., et al. (2016). PD-L1 expression, Cancer Genome Atlas (TCGA) subtype, and mutational load as independent predictors of response to atezolizumab (atezo) in metastatic urothelial carcinoma (mUC; IMvigor210). *IJCO* 34, 104–104. doi: 10.1200/JCO.2016.34.15_suppl.104

Rugge, M., Fassan, M., and Graham, D. Y. (2015). "Epidemiology of gastric cancer," in *Gastric Cancer: Principles and Practice*. (Cham, Switzerland: Springer International Publishing) 23–34. doi: 10.1007/978-3-319-15826-6_2

Seebacher, N. A., Stacy, A. E., Porter, G. M., and Merlot, A. M. (2019). Clinical development of targeted and immune based anti-cancer therapies. *J. Exp. Clin. Cancer Res.* 38, 156. doi: 10.1186/s13046-019-1094-2

Sequeira, E., Kaur, G., and Buttar, H. S. (2014). Celiac disease: Role of genetics and immunity and update on novel strategies for treatment. *Biomed. Rev.* 25, 45–58. doi: 10.14748/bmr.v25.1047

Shah, N. P. (2000). Effects of milk-derived bioactives: an overview. *Br. J. Nutr.* 84 (Suppl 1), S3–10. doi: 10.1017/s000711450000218x

Shahzad, M. M. K., Felder, M., Ludwig, K., Van Galder, H. R., Anderson, M. L., Kim, J., et al. (2018). Trans10,cis12 conjugated linoleic acid inhibits proliferation and migration of ovarian cancer cells by inducing ER stress, autophagy, and modulation of Src. *PLoS One* 13, e0189524. doi: 10.1371/journal.pone.0189524

Sharma, A., Shandilya, U. K., Sodhi, M., Mohanty, A. K., Jain, P., and Mukesh, M. (2019). Evaluation of Milk Colostrum Derived Lactoferrin of Sahiwal () and Karan Fries (Cross-Bred) Cows for Its Anti-Cancerous Potential. *Int. J. Mol. Sci.* 20, 6318. doi: 10.3390/ijms20246318

Shen, R. L., Thymann, T., Østergaard, M. V., Støy, A. C. F., Krych, Ł., Nielsen, D. S., et al. (2015). Early gradual feeding with bovine colostrum improves gut function and NEC resistance relative to infant formula in preterm pigs. *Am. J. Physiol. - Gastrointest. Liver Physiol.* 309, G310–G323. doi: 10.1152/ajpgi.00163.2015

Siegel, R. L., Miller, K. D., and Jemal, A. (2016). Cancer statistics 2016. *CA. Cancer J. Clin.* 66, 7–30. doi: 10.3322/caac.21332

Stefani, C., Liverani, C. A., Bianco, V., Penna, C., Guarnieri, T., Comparetto, C., et al. (2014). Spontaneous regression of low-grade cervical intraepithelial lesions is positively improved by topical bovine colostrum preparations (GINEDIE®). A multicentre, observational, italian pilot study. *Eur. Rev. Med. Pharmacol. Sci.* 18, 728–733.

Stelwagen, K., Carpenter, E., Haigh, B., Hodgkinson, A., and Wheeler, T. T. (2009). Immune components of bovine colostrum and milk. *J. Anim. Sci.* 87, 3–9. doi: 10.2527/jas.2008-1377

Støy, A. C. F., Heegaard, P. M. H., Thymann, T., Bjerre, M., Skovgaard, K., Boye, M., et al. (2014). Bovine colostrum improves intestinal function following formula-induced gut inflammation in preterm pigs. *Clin. Nutr.* 33, 322–329. doi: 10.1016/j.clnu.2013.05.013

Sugihara, Y., Zuo, X., Takata, T., Jin, S., Miyauti, M., Isikado, A., et al. (2017). Inhibition of DMH-DSS-induced colorectal cancer by liposomal bovine lactoferrin in rats. *Oncol. Lett.* 14, 5688–5694. doi: 10.3892/ol.2017.6976

Takayama, Y., Kitsunai, K., and Mizumachi, K. (2001). Factors in bovine colostrum that enhance the migration of human fibroblasts in type I collagen gels. *Biosci. Biotechnol. Biochem.* 65, 2776–2779. doi: 10.1271/bbb.65.2776

Taylor, C. W., and Kirby, A. M. (2015). Cardiac Side-effects From Breast Cancer Radiotherapy. *Clin. Oncol.* 27, 621–629. doi: 10.1016/j.clon.2015.06.007

Teixeira, F. J., Santos, H. O., Howell, S. L., and Pimentel, G. D. (2019). Whey protein in cancer therapy: A narrative review. *Pharmacol. Res.* 144, 245–256. doi: 10.1016/j.phrs.2019.04.019

Tran, C. D., Kritas, S., Campbell, M. A. F., Huynh, H. Q., Lee, S.-S., and Butler, R. N. (2010). Novel combination therapy for the eradication of Helicobacter pylori infection in a mouse model. *Scand. J. Gastroenterol.* 45, 1424–1430. doi: 10.3109/00365521.2010.506245

Tricoli, J. V., Blair, D. G., Anders, C. K., Bleyer, W. A., Boardman, L. A., Khan, J., et al. (2016). Biologic and clinical characteristics of adolescent and young adult cancers: Acute lymphoblastic leukemia, colorectal cancer, breast cancer, melanoma, and sarcoma. *Cancer* 122, 1017–1028. doi: 10.1002/cncr.29871

Tsuda, H., Fukamachi, K., Xu, J., Sekine, K., Ohkubo, S., Takasuka, N., et al. (2006). Prevention of carcinogenesis and cancer metastasis by bovine lactoferrin. *Proc. Jpn. Acad. Ser. B Phys. Biol. Sci.* 82, 208–215. doi: 10.2183/pjab.82.208

Tung, Y. T., Chen, H. L., Yen, C. C., Lee, P. Y., Tsai, H. C., Lin, M. F., et al. (2013). Bovine lactoferrin inhibits lung cancer growth through suppression of both inflammation and expression of vascular endothelial growth factor. *J. Dairy Sci.* 96, 2095–2106. doi: 10.3168/jds.2012-6153

Ulfman, L. H., Leusen, J. H. W., Savelkoul, H. F. J., Warner, J. O., and van Neerven, R. J. J. (2018). Effects of Bovine Immunoglobulins on Immune Function, Allergy, and Infection. *Front. Nutr.* 5:52. doi: 10.3389/fnut.2018.00052

Vitetta, E. S., Krolick, K. A., Miyama-Inaba, M., Cushley, W., and Uhr, J. W. (2019). "Immunotoxins: A New Approach to Cancer Therapy", in *Biotechnology and Biological Frontiers*, Ed. P. H. Abelson (Routledge), 73–85. doi: 10.4324/9780429050329-7

Waaga-Gasser, A. M., Gasser, M., Stock, M., Grimm, M., and Sprotte, G. (2009). Oral immunoglobulin induces mononuclear cell apoptosis in patients suffering from idiopathic chronic pain syndrome: Results from a pilot study. *Int. J. Clin. Pharmacol. Ther.* 47, 421–433. doi: 10.5414/CPP47421

Wu Xiaoyun, S. P. S., and Xiong Lin, D.x. (2015). The Influence of Heat Treatment in Liquid Whey at Various pH on Immunoglobulin G and Lactoferrin from Yak and Cows' Colostrum/Milk. *J. Food Process. Technol.* 6, 1–9. doi: 10.4172/2157-7110.1000503

Xu, M. L., Kim, H. J., Wi, G. R., and Kim, H. J. (2015). The effect of dietary bovine colostrum on respiratory syncytial virus infection and immune responses following the infection in the mouse. *J. Microbiol.* 53, 661–666. doi: 10.1007/s12275-015-5353-4

Yadav, R., Angolkar, T., Kaur, G., and Buttar, H. S. (2016). Antibacterial and Antiinflammatory Properties of Bovine Colostrum. *Recent Pat. Inflamm. Allergy Drug Discov.* 10, 49–53. doi: 10.2174/1872214810666160219163118

Ya'acov, A.B., Lichtenstein, Y., Zolotarov, L., and Ilan, Y. (2015). The gut microbiome as a target for regulatory T cell-based immunotherapy: Induction of regulatory lymphocytes by oral administration of anti-LPS enriched colostrum alleviates immune mediated colitis. *BMC Gastroenterol.* 15, 45–93. doi: 10.1186/s12876-015-0388-x

Conflict of Interest: The authors declare that the research was conducted in the absence of any commercial or financial relationships that could be construed as a potential conflict of interest.

Advantages of publishing in Frontiers

OPEN ACCESS
Articles are free to read for greatest visibility and readership

FAST PUBLICATION
Around 90 days from submission to decision

HIGH QUALITY PEER-REVIEW
Rigorous, collaborative, and constructive peer-review

TRANSPARENT PEER-REVIEW
Editors and reviewers acknowledged by name on published articles

Frontiers
Avenue du Tribunal-Fédéral 34
1005 Lausanne | Switzerland

Visit us: www.frontiersin.org
Contact us: frontiersin.org/about/contact

REPRODUCIBILITY OF RESEARCH
Support open data and methods to enhance research reproducibility

DIGITAL PUBLISHING
Articles designed for optimal readership across devices

FOLLOW US
@frontiersin

IMPACT METRICS
Advanced article metrics track visibility across digital media

EXTENSIVE PROMOTION
Marketing and promotion of impactful research

LOOP RESEARCH NETWORK
Our network increases your article's readership